GreenChem2000

4th Annual Green Chemistry and Engineering Conference Proceedings

Sustainable Technologies: From Research to Industrial Implementation

June 27-29, 2000

National Academy of Sciences

Washington, D.C.

Proceedings

4th Annual Green Chemistry & Engineering Conference

Sustainable Technologies: From Research to Industrial Implementation

June 27 - 29, 2000
Washington, D.C.

CONTENTS

4th Annual Chemistry and Engineering Conference
Sustainable Technologies: From Research to Industrial Implementation

PROCESS DESIGN II Page Number

BENIGN SYNTHESIS AND PROCESSING II Page Number

GREENER SOLVENTS II Page Number

4th Annual Green Chemistry &
Engineering Conference

Sustainable Technologies:
From Research to Industrial Implementation

June 27 - 29, 2000

CATALYSIS I

DEVELOPMENT OF A SELECTIVE HETEROGENEOUS CATALYST FOR USE IN SUPERCRITICAL DIOXIDE

Greg A. Snyder, Andrew R. Tadd, Mark R. Mason, and Martin A. Abraham
Department of Chemical and Environmental Engineering and Department of Chemistry,
The University of Toledo, Toledo, OH 43606

Abstract
The last decade has heralded a paradigm shift in society's view of industrial waste. Waste disposal is no longer a desirable option; rather, the use of green chemistry to minimize the formation of waste products is preferred [Anastas & Warner, 1998]. Environmental advances in the chemical industry must come from modifications in the processes rather than an end-of-pipe waste treatment. Our research embodies two precepts of green chemistry; the use of benign solvents, and the development of selective catalysts. We have been working towards the development of a selective heterogeneous catalyst for the hydroformylation of propylene in supercritical carbon dioxide. Rhodium supported on SiO_2 and rhodium supported on modified SiO_2 have been studied in a batch reactor at 100ºC and over a range of CO_2 pressures. This paper compares the effects of the catalytic support and metal precursor on reaction rate and selectivity towards the linear aldehyde. Detailed mechanistic studies using diffuse reflectance infrared spectroscopy in supercritical CO_2 reveal the presence of intermediates on the catalyst surface.

Introduction

The hydroformylation reaction produces greater than 3 billion pounds of aldehydes per year, with current technology employing a homogeneous rhodium or cobalt catalyst dissolved in either an organic or aqueous solvent. Because of the high cost of the metal catalyst, a significant effort must be made to recover the catalyst so that it can be recycled in the process. Catalyst losses, as well as the energy needed for catalyst recovery, represent two disadvantages of homogeneous catalysis. The use of a heterogeneous catalyst eliminates the need for catalyst recovery, but deactivation through catalyst leaching and lower selectivity represent technical obstacles to commercial utilization.

One of the principles of green chemistry is the elimination of organic solvents and their replacement with benign solvents. Recent experiments have shown that many reactions commercially accomplished with a liquid organic solvent may also be carried out in a supercritical fluid. For example, hydrogenation [Bertucco *et al.,* 1997] and propene hydroformylation [Guo & Akgerman, 1997; Koch & Leitner, 1998] have recently been demonstrated in supercritical CO_2 ($scCO_2$). Several research groups [Palo & Erkey, 1998, 1999; Koch & Leitner, 1998] have developed prototype homogeneous catalysts that are CO_2-soluble by the addition of perfluorinated chains to the catalytic ligands.

Rather than modifying the catalyst to increase its solubility in CO_2, our research has considered the development of a heterogeneous hydroformylation catalyst. Our development of a heterogeneous catalyst is based on the efforts of previous researchers to develop a heterogeneous hydroformylation catalyst. Numerous supported rhodium species have provided varying levels of activity and selectivity. $RhCl_3$ deposited on silica produces almost exclusively hydrogenation products [Balakos & Chuang, 1995], whereas $Rh_4(CO)_{12}$ deposited on silica gave 90% selectivity to aldehyde products [Shido, *et al.,* 1995]. $RhCl_3$ reduced with $NaBH_4$ [Lenarda, *et al.,* 1993] and platinum/tin [Homs, *et al.,* 1992] were also reported to provide active and selective catalysts. Rhodium carbonyl complexes supported on SiO_2 [Shido, *et al.,* 1995; Bando, *et al.* 1996] produced by reaction of tris(hydroxymethyl)phosphine with $Rh_4(CO)_{12}$ in dichloromethane were effective in promoting selectivity to the aldehyde product. High selectivity to the *n*-aldehyde was obtained when a rhodiurn triphenylphosphine complex was attached to a styrene-divinylbenzene copolymer [Yoneda, *et al.,* 1997]. $Rh_4(CO)_{12}$ supported on SiO_2 and modified SiO_2 [Hanaoka, *et al.,* 2000] showed varying reaction results.

Experimental

The hydroformylation reaction was carried out in the batch reactor system shown schematically in Figure 1, and described in more detail in Dharmidikhari and Abraham [2000]. The system was comprised of the batch reactor and an LDC Analytical 2396-89 high-pressure metering pump. We modified a 300 cm^3 Autoclave Engineers batch reactor by installing a basket apparatus on the rotating shaft; catalyst samples were placed in the basket at the beginning of each experimental run. The outlet from the reactor was connected to a flow restrictor that reduced the pressure at the sample collection point. Fluid exiting the reactor passed directly into an on-line HP 5890 gas chromatograph for detection of reaction products. The reactor and the reactor fittings were all rated to

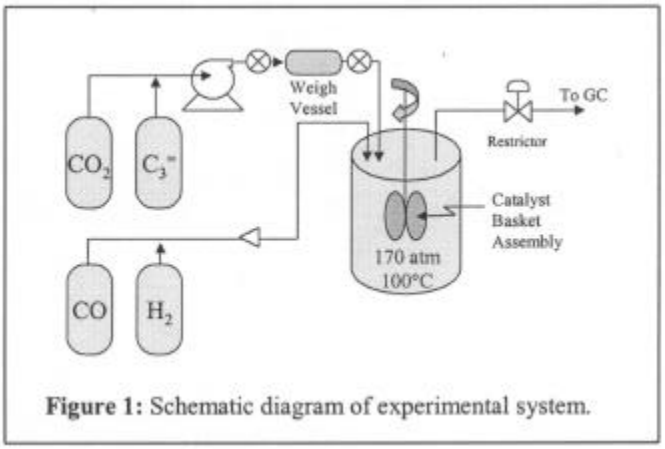

Figure 1: Schematic diagram of experimental system.

408 bar at 176 ºC and 295 bar at 400 ºC. A rupture disc (set point 340 bar) was used in the safety head assembly. The system was tested at the operating conditions before any run was carried out.

Hydrogen and carbon monoxide were added to the vessel based on the pressure required to obtain the desired molar quantities according to the Peng-Robinson equation of state. All experiments were conducted at approximately 0.7 mol/L of both CO and hydrogen, and approximately 0.55 mol/L propylene. In general, the gaseous reactants were added first, then propylene and CO_2 were pumped into the reactor using the high-pressure liquid pump via the weigh vessel.

Molar quantities of CO_2 and propylene were calculated by measuring the actual weight of material consumed from the weigh vessel. The reactor contents were then heated to 100ºC. Analysis of reaction samples obtained during the heat-up period generally revealed very low conversion and no formation of products.

The catalysts used in this study were prepared using the method of incipient wetness, starting from catalyst precursors dissolved in aqueous or organic solvents, as described in Table 1. The catalyst support was either purchased (Aldrich silica gel) or produced in our laboratory using standard procedures illustrated in Figure 2. A series of catalyst supports were prepared to test the hypothesis that support modifications would be effective in controlling the activity and selectivity of catalysts produced from these materials.

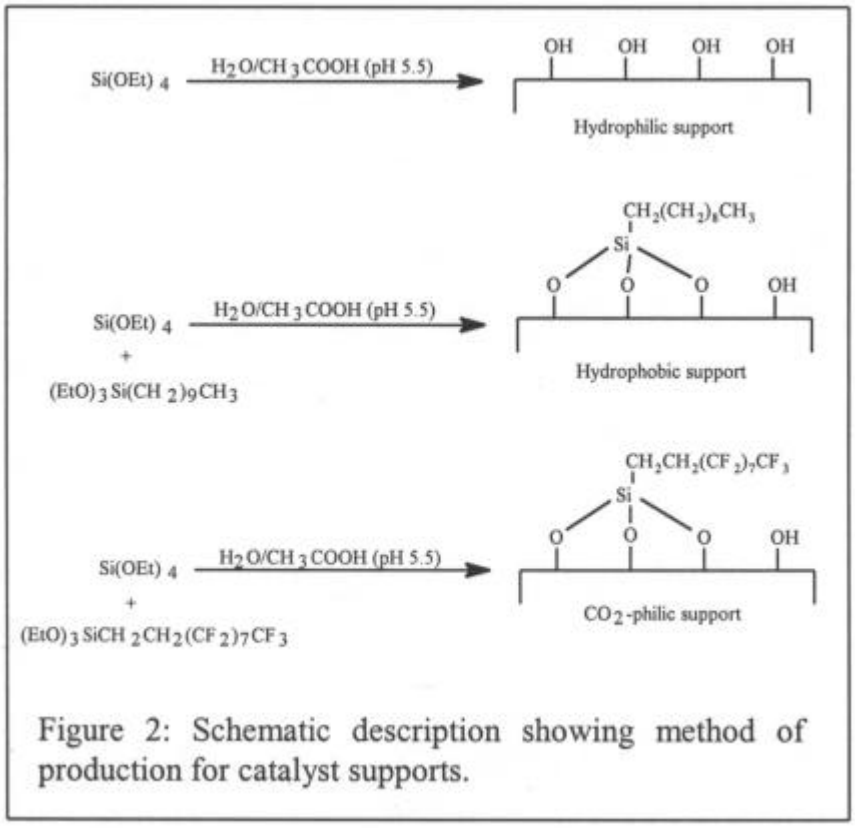

Figure 2: Schematic description showing method of production for catalyst supports.

Results

Catalyst performance has been monitored in terms of the initial reaction rate (based on the total amount of aldehyde obtained) and the average selectivity to the preferred linear butanal product. Table 1 indicates the effect of the catalyst support on performance. High surface area silica gel (Run 31) was purchased from Aldrich Chemical and can be considered a base-case situation. The initial rate of 0.053 mol/g Rh hr is comparable to other rhodium-catalyzed hydroformylation data [Balakos & Chuang, 1995; Hanoka *et al.*, 2000] but gave limited to no selectivity. SiO_2 produced in our laboratory had a low surface area. When used as a catalyst support, the rate was decreased by an order of magnitude (relative to the silica gel), although a slightly higher selectivity was observed. The hydrophobic support (Run 21) yielded a rate that was roughly one-half of that with the silica gel, but with a substantially higher selectivity. Use of a support modified with a highly fluorinated, CO_2-philic side chain gave a catalyst with very low activity (Run 30), although the highest selectivity was observed using this support.

Table 1. Summary of Experimental Conditions and Results

Run	Catalyst precursor	Support	Pressure (psig)	Solvent	Initial rate (mol/g Rh hr)	Average Selectivity
21	Rh(Acac)	$CH_3(CH_2)_9Si$	2500	CO_2	0.0245	4.20
30	Rh(Acac)	$CF_3(CF_2)_9Si$	2500	CO_2	0.0004	4.47
49	Rh(Acac)	SiO_2	2500	CO_2	0.0022	1.75
31	Rh(Acac)	Si gel	2500	CO_2	0.0530	1.28
34	Rh(Acac)	Si gel_2	2000	CO_2	0.0429	1.52
37	Rh(Acac)	Si gel	2000	Helium (CO_2 added)	0.0343	1.75
46	Rh(Acac)	$CH_3(CH_2)_9Si$	2500	Helium	0.0416	1.17

Our experiments indicate that modification of the support can be used to affect the catalyst performance. In the current case, we propose that the higher reaction rates obtained with the hydrophobic support can be attributed to the catalytic surface destabilizing the adsorption of the slightly polar reaction products. The fluorinated support always gave the lowest rate, presumably due to a competitive absorption of CO_2 with the reactants that does not occur on the other supports. While the catalysts produced from low surface area supports were not stable due to leaching of the rhodium from the surface, the porous silica gel provided a stable catalyst. Thus, we suggest that impregnating rhodium on a high surface area silica gel modified with hydrophobic side chains would produce a stable, active, and selective catalyst.

The effect of solvent density (pressure) on the performance of the catalyst prepared on silica gel is shown in Figure 3. Increasing the density (at constant concentration of reactants) led to an approximately linear increase in the reaction rate. In addition, the chemoselectivity (ratio of aldehyde to alcohol in the product) also increased as the solvent density was increased; extremely low yields of hydrogenation products were observed at elevated pressures. The regioselectivity decreased slightly as the density was increased, however, this variation was within the experimental error of the measurements and should be considered as only a preliminary indication of a possible trend. We have also attempted to determine if the effect of pressure was a result of the density of the system or the high concentration of CO_2. Runs 34 and 37 compare the results from two experiments at the same pressure but with a different solvent. The reaction rate was slightly slower when the reaction was performed in helium, but the selectivity was somewhat higher. However, comparison of runs 21 and 46 reveal the opposite result; a substantially lower rate was obtained with CO_2 as the solvent but much greater selectivity was observed. The differences in the observed solvent effect among these four catalysts may be attributable to interactions between the catalyst support and the solvent. It should also be noted that reactions performed in helium always yielded hydrogenation products, whereas those performed in CO_2 only gave hydrogenation products at low CO_2 density, clearly indicating that CO_2 plays a role in inhibiting the hydrogenation reaction.

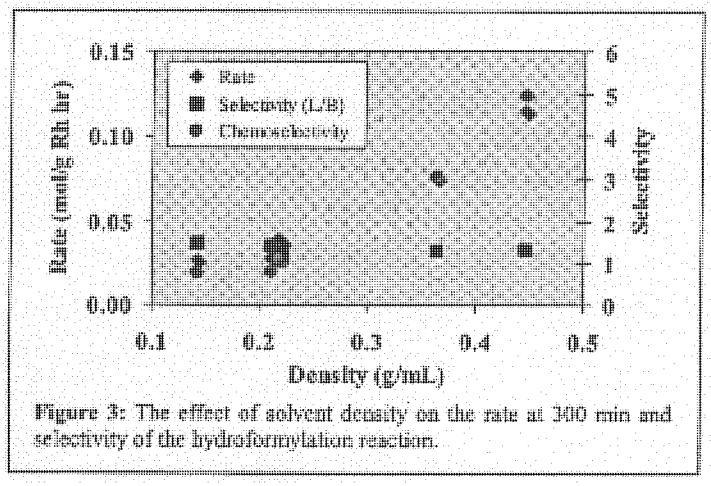

Figure 3: The effect of solvent density on the rate at 300 min and selectivity of the hydroformylation reaction.

Our experiments with multiple supports and solvents reveal that each has a role in the surface-catalyzed reaction. To learn more about the fundamental nature of these effects, we have also attempted to isolate reactive species on the surface by diffuse reflectance infrared spectroscopy. We have acquired an environmental cell capable of operating at pressures up to 1500 psia. Analysis of CO adsorption from helium and CO_2 at this pressure reveals differences in the nature of the adsorbed species. While the CO_2 adsorption from high pressure helium matches literature references, the adsorption from CO_2 is not consistent with known adsorption structures. Additional experiments for propylene have failed to yield any adsorbed species, regardless of the solvent. A

comparable result was observed for the aldehyde products. We believe that this result is consistent with our macroscopic observations on the effects of catalyst support and pressure. Additional experiments involving adsorption of propylene after CO adsorption are currently underway. These tests will allow us to understand more completely the interactions between the catalyst support and the solvent and their impact on the activity and selectivity of the catalyst.

Acknowledgments
This research was supported by the National Science Foundation/Lucent Technologies Foundation Industrial Ecology Research Fellowships program (NSF grant number BES-9873553).

References
Anastas, P.T.; Warner, J.C. **Green Chemistry: Theory and Practice,** Oxford University Press, New York (1998).
Balakos, M.W., S.S.C. Chuang, "Dynamic and LHHW Kinetic Analysis of Heterogeneous Catalytic Hydroformylation" *J. Catal,.,* **151**, 266 (1995).
Bando, K.K., Asakura, K., Arakawa, H., Isobe, K., Iwasawa, Y., "Surface Structures and Catalytic Hydroformylation Activities of Rh Dimers Attached on Various Inorganic Oxide Supports", *J. Phys. Chem.,* **100***,* 13636 (1996).
Bertucco, A., Cann, P., Devetta, L., Zwahlen, A.G. "Catalytic hydrogenation in supercritical CO_2: Kinetic measurements in a gradientless internal-recycle reactor" *Ind & Eng Chem Res.,* **36**, 2626 (1997).
Dharmidhikari, S., Abraham, M.A. "Rhodium supported on activated carbon as a heterogeneous catalyst for hydroformylation of propylene in supercritical carbon dioxide", *J. Supercritical Fluids,* (2000), accepted.
Guo, Y.; Akgerman, A., "Hydroformylation of propylene in supercritical carbon dioxide" *Ind. Eng. Chem. Res.,* **36**, 4581 (1997).
Hanoka, T., Arakawa, H., Matsuzaki, T., Sugi, Y., Abe, Y., "Ethylene hydroformylation and carbon monoxide hydrogenation over modified and unmodified silica supported rhodium catalysts", *Catalysis Today,* **58**, 271 (2000).
Horns, N., N. Clos, G. Muller, J. Sales, P. R. de la Piscina. "Supported Pt/Sn Complexes as Catalysts in the Hydroformylation of Olefins " *J.* Mol. *Catal.* **74**, 401, (1992).
Koch, D., Leitner, W. "Rhodium-catalyzed hydroformylation in supercritical carbon dioxide" *J. Am. Chem. Soc.* **120**, 13398, (1998).
Lenarda, M., Ganzerla, R., Storara, L., Zanom, R., "Vapor-phase propene hydroformylation catalyzed by the Rh/Al system on silica" *J. Mol. Catal.,* **79**(1-3), 243, (1993).
Palo, D., Erkey, C. "Homogeneous hydroformylation of 1-octene in supercritical carbon dioxide with $[RhH(CO)(P(p\text{-}CF_3C_6H_4)_3)_3]$" *Ind. Eng. Chem. Res.* **38**(5), 2163 (1999).
Shido, T., T. Okazaki, M. Ichikawa, "Rh-4 carbonyl clusters coordinated with tris(hydroxymethyl)phosphine grafted onto SiO_2 surfaces and structural control of active sites in gas-phase olefin hydroformylation reactions" *J. Catal.,* **157**, 436 (1995).
Yoneda, N., Nakagawa, Y., Mimami, T. "Hydroformylation catalyzed by immobilized rhodium complex to polymer support" *Catal. Today,* **36**, 357, (1997).

MOLECULE ASSEMBLY IN MICELLAR INTERFACE AND HIGH REGIOSELECTIVITY OF OLEFIN HYDROFORMYLATION

Xianjun Li*, Hua Chen, Yaozhong Li, Junru Chen, Puming Cheng
Department of Chemistry, Sichuan University, Chengdu, Sichuan 610064, China
*Corresponding author. Tel: +86-28-5412904; Fax: +86-28-5412904; E-mail: xianjunli@yahoo.com

Abstract
Long-chain olefin hydroformylation catalyzed by $RhCl(CO)(TPPTS)_2$ was studied in biphasic system containing TPPTS and cationic surfactant. A mechanism of synergistic effect of micelle and its interfacial electrostatic attraction with anionic rhodium active species was suggested. The micelle solubilization formed a transfer passageway of olefin from micelle core to its interface. Thus the reaction was dramatically accelerated. The

modification of the catalyst system by the addition of promoters could create a more favourable microcircumstance for molecule assembly in micelle interface. The novel combinatorial catalyst system exhibited high activity and very high regioselectivity in long chain olefin hydroformylation.

Introduction

Biphasic catalysis has attracted great attention in recent years. The advantages of replacement of organic solvent by water are the environmental benign, safety and better economical efficiency. There are a few examples of biphasic catalytic system using water soluble transition metal complexes containing TPPTS [P(*m*-$C_6H_4SO_3Na)_3$] and TPPMS [P($C_6H_5)_2$(*m*-$C_6H_4SO_3Na$)] as ligand with acceptable reaction rate and successful application in industrial production[1]. However, the very low solubility of most organic substrates in water makes the rate of their reactions too slow in biphasic catalysis. The long chain olefin hydroformylation is a typical example.

In order to accelerate the reaction rate and to increase the regioselectivity of hydroformylation a lot of efforts have been done. The studies can be divided two types. The first ones include the introduction of co-solvent[2], co-ligand[3], surfactant[4] and modified cyclodextrin[5] into the biphasic system containing Rh-TPPTS catalyst. Among these approaches the addition of surfactant is the most prospective. The second ones are the design and synthesis of novel water-soluble phosphine ligands, such as BISBIS and BINAS-Na[6], BISBIS and BINAP analogue[7], sulfonated Xantphos[8]. Although the properties of some novel ligands are superior to TPPTS in olefin hydroformylation, they are very expensive and their solubilities in water are lower than TPPTS. Therefore TPPTS is still the most wide application among all known water soluble phosphine ligands.

We studied the behaviors of cationic surfactant and the mechanism of interfacial reaction of long chain olefin hydroformylation in biphasic catalytic system containing $RhCI(CO)(TPPTS)_2$ and TPPTS in detail. Based on the knowledge a combinatorial rhodium catalyst system with high activity and very high regioselectivity in hydroformylation of long chain olefin could be prepared by the molecule assembly of micellar interface.

Results and Discussion

Effect of Different Surfactants

The studies on effect of different surfactants on 1-dodecene hydroformylation in biphasic catalytic system indicated that the reaction was inhibited with the addition of anionic surfactant. The addition of nonionic surfactant did not obviously enhance the reaction. Only the introduction of cationic surfactant could dramatically accelerate the hydroformylation. TOF reached to $375h^{-1}$ in the presence of CTAB(cetyltrimethylammonium bromide). The acceleration of cationic surfactant could be attributed to the synergistic effect of following two factors. One was the formation of micelle that was favorable for greatly increasing the interface between aqueous and organic phase. Another was the enrichment of rhodium catalyst in micellar interfacial layer. The micellar cationic end oriented to aqueous phase and formed a electrostatic field with positive charge at the micelle interface. It would attract rhodium anionic species, $HRh(CO)[P(m\text{-}C_6H_4SO_3)_3]_n^{3n-}$, to interfacial layer from aqueous solution. The measurements of rhodium concentration by ICP indicated that rhodium concentration in the interfacial layer was about 91 times higher than that in aqueous layer after end of the reaction.

Modification of Micellar Interfacial Layer

When a promoter with negative charge was introduced into the micellar solution and could insert the micelle, it would reduce the electrostatic repulsion of the cationic end and form a tighter micelle structure. This was favorable for the formation of linear aldehyde by means of linear alkyl-rhodium intermediate. The addition of SDS(sodium dodecyl sulfate), an anionic surfactant, exerted the effect in the modification of micellar structure. Therefore the regioselectivity of 1-dodecene hydroformylation increased obviously and the ratio of linear/branched aldehyde in the products rose from 7 to 18. The addition of TPPDS[P(C_6H_5)(*m*-$C_6H_4SO_3Na)_2$] exhibited more dramatical influence on the regioselectivity, although total phosphine concentration was constant only TPPTS was partly replaced by TPPDS. The results were shown in Fig. 1 and Fig. 2. In the former case a mixed micelle with tighter hydrophobic chain arrangement could form, but in latter case TPPDS could insert into the interfacial layer of micelle and make a crowded microcircumstance of hydroformylation. This would compel α-carbon atom of olefin bonding with rhodium and preferentially forming linear alkyl rhodium intermediate. Therefore the molecular assembly in micellar interfacial layer by the modification adding a suitable promotor could create a more favorable microcircumstance for the formation of linear aldehyde.

Effect of Hydrophilic Group and Olefin Chain Length

The structure of hydrophilic group in cationic surfactant would influence on molecule arrangement in micelle. When the hydrophilic end of cationic surfactant was small group, for example pyridinium and trimethylammonium group, the arrangement of molecular chain in micelle was tight. This would make a favorable microcircumstance for increasing the regioselectivity of olefin hydroformation as observed in the presence of cation surfactant CTAB, CPyB(cetylpyridinium bromide), TTAB(tetradecyltrimethylammonium bromide) and DTAB(dodecyltrimethylammonium bromide). The molar ratios of linear/branched aldehyde were as high as 26-32. In contrast, the large steric volume of hydrophilic end, for example dimethyl-phenyl group in TBAC, would make a loose arrangement of molecular chain and the distance between the hydrophobic chain in micelle could become wider. This caused the decrease of regioselectivity of 1-dodecene hydroformylation and the molar ratio of linear/branched aldehyde dropped from 26-32 to 8.4. The results indicated that the structure of micelle in the interfacial layer played a very important role in the control of regioselectivity.

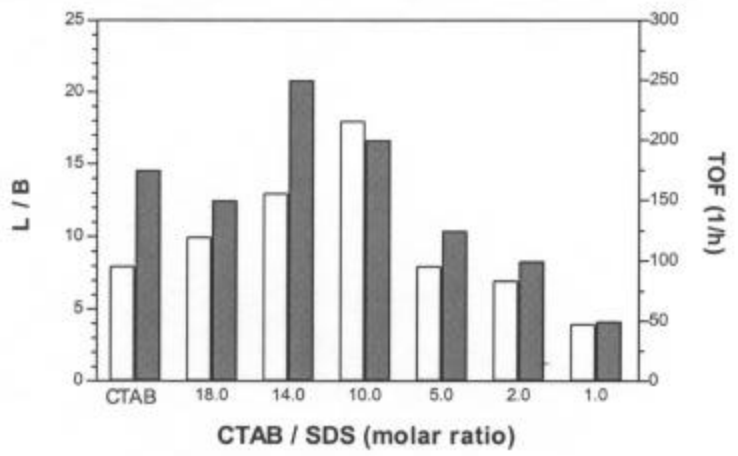

Figure 1. Effect of sodium dodecyl sulfate on 1-dodecene hydroformylation
Reaction conditions: [Rh]=6.7x10^{-3} mol/L, [TPPTS]/[Rb]=30, 1-dodecene: 13.5mmol, 0.6MPa (constant) :L/B, :TOF.

The effect of olefin chain length on the hydroformylation was studied in biphasic system containing TPPTS, TPPDS and CTAB. The results showed that as olefin chain length increased their reactivities decreased, but the ratios of linear/branched aldehyde in the products rose from 11 to 26. It suggested that probably there was a match relation between hydrophobic chain length of surfactant and the length of olefin chain. When both were matchable the regioselectivity of olefin hydroformylation would be very high.

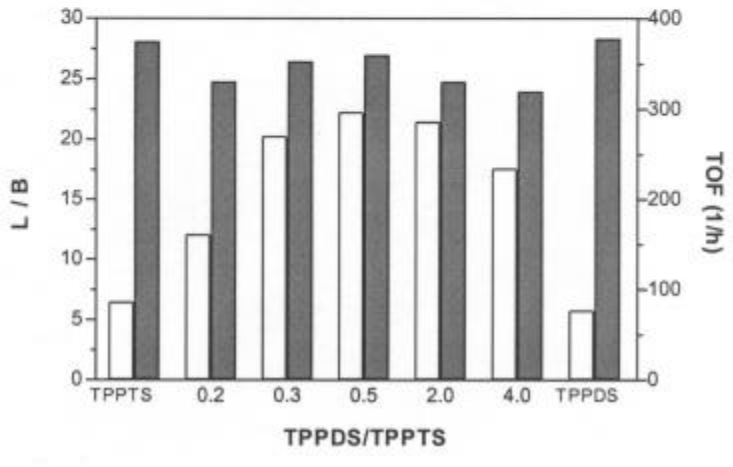

Figure 2. Effect of molar ratio of TPPDS toTPPTS on 1-dodecene hydroformylation.
Reaction conditions: [Rh]=1.0x10^{-3}mol/L, [CTAB]=5.53x10^{-3}mol/L, 1-dodecene:13.5mmol, H_2O:15ml, 100 , 1.5MPa(constant), :L/B, :TOF.

Conclusion

The acceleration of long-chain olefin hydroformylation in the presence of cationic surfactant was owing to the synergistic effect of olefin solubilization in micelle and its interfacial electrostatic field attraction with anionic rhodium active species, but the latter was key factor. The molecule assembly in the micellar interface between aqueous and organic phase could form a combinatorial catalyst system of high activity and high regioselectivity.

Acknowledgments

We thank the National Natural Science Foundation of China and the SINOPEC for the financial support.

References

1 . a) B. Cornils, W.F. Herrmann, R.W. Eckl, *J. Mol. Catal*. *A: Chemical*, **116**(1997)27; b) Cornils and E.G. Kuntz, *J. Organometallic Chem*., **502**(1995)177
2. P. Purwanto and H. Delmas, *Catal. Today*, **24**(1995)135
3. R.V. Chaudhri, B.M. Bhanagl, R.M. Dashpande and H. Delmas, *Nature*, **373**(1995)501
4. a) H. Chen, Y. Li, J. Chen, P. Cheng, Y. He and X. Li, *J. Mol. Catal. A: Chemical*, **149**(1999)1; b) M.J.H.

Russel, *Platinum Metals Rev*. **32**(1998)179; c) F.V. Vyve and A. Renken, *Catal. Today*, **48**(1999)237
5. a) E. Monflier, G. Fremy, Y Gastanet and A. Mortreux, *Angew. Chem. Int. Ed. Engl*. **34**(1995)2269; b) S. Tilloy, F. Bertoux, A. Mortreux and E. Monflier, *Catal. Today*, **48**(1999)245
6. W.A. Herrmann, C.W. Kohlpaintner, R.B. Manetsberger, H. Bahrmann, *J. Mol. Catal. A: Chemical*, **97**(1995)65
7. a) H. Ding, J. Kang, B.E. Hanson and C.W. Kolpaintner; *J. Mol. Catal. A: Chemical*, 124(1997)21; b) B.E. Hanson, H. Ding and C.W. Kohlpaintner, *Catal. Today*, **42**(1998)421
8. M.S. Goedheijt, Paul C.J. Kamer and Piet W.N.M. van Leeuwen, *J. Mol. Catal. A: Chemical*, **134**(1998)243

THE EFFECTS OF USING A HETEROGENEOUS ZNO CATALYST ON THE PERFORMANCE OF DIESEL ENGINES

Richard Wm. Tock, Professor, Quamrul Arefeen, Post Doctoral Research Associate,
and Harry W. Parker, Professor
Dept. of Chem. Engineering, Texas Tech University, P.O. Box 43121, Lubbock, TX 43121-3121

ABSTRACT
Micron sized particles of the mineral zinc oxide were suspended in commercial *tert*-butyl hydroperoxide (~50 ppm). This suspension was added to the diesel fuel (~0.2% by weight) used to fuel diesel trucks. Vehicle mileage was shown to increase on average by 20% and particulate emissions decreased by ~50%. Gaseous emissions of CO and hydrocarbons were also reduced substantially by ~30%, while the concentration of engine wear metals fell by ~20%. This paper explains why zinc oxide is a highly effective fuel borne catalyst even at these low concentrations. The paper also examines both the projected cost savings for the user and the projected positive benefits for the environment. This simple but fundamental approach to better combustion could make it possible for a majority of the internal combustion engines now in use to meet the emission goals established by the U.S. Congress and promulgated by the U.S. EPA.

INTRODUCTION
Resolution of the conflicts between engine efficiency and reduced emissions continues to be a critical issue for the scientific community and advocates for environmental responsibility. For example, diesel engines are among the most efficient of the internal combustion engines. However, because of elevated emissions of NO_x, CO, and particulate matter, diesel engines have also become synonymous with dirty engines and black smoke. Scientifically, this undesirable feature can be ascribed to high concentrations of particulate, carbonaceous matter in the exhaust, which must be reduced or eliminated. The question is how to do this?

The objective of this study was to investigate a potential solution that offers both improvement in engine performance and reductions in emissions from diesel engines. This approach is based on the utilization of fuel additives. While there are numerous additives being marketed, the additive used in this test was EnviroMax Diesel (EMD), a product of MAXMA L.C. of Lubbock, TX. The EMD additive consists of a combination of solid catalysts and organic peroxide as combustion promoters. The solid catalyst in EMD appears to stabilize the organic peroxide when the preferred combination is added to commercial diesel fuels. The presence of the organic peroxide in the fuel also creates an increase in the cetane rating of the diesel fuel. Elevated cetane levels are known to provide better road mileage and engine performance.

WORKING PRINCIPLE OF THE SOLID HETEROGENEOUS CATALYST
The solid micron-sized zinc oxide particles used in the EMD additive appear to promote better combustion within the engine's cylinders. When suspended in liquid diesel fuel, the zinc oxide particles are carried into the engine where they provide hot catalytic, refractory surfaces within the reaction zone during combustion. The reaction rates on the hot refractory surfaces are known to be an order of magnitude faster than the same reactions taking place solely in a homogeneous gas phase (Walker *et al*. 1923). Moreover, the high pressures, which are generated by the IC engine's compression stroke during ignition further enhances these adsorbed, phase combustion reactions. Since metal oxides and peroxides are used as the solid heterogeneous catalysts, the combustion reactions that occur on their surfaces have an additional supply of oxygen with the potential to push any

oxidation reactions closer to completion. The availability of this mineral oxygen lessens the potential for incomplete combustion reactions, which may occur during momentary depletions of gaseous oxygen created by any rapid thermal cracking of the fuel and poor mixing. Hence, the surface of the catalytic particle used in the EMD additive provides an environment that is potentially always oxygen rich. Furthermore, any elemental zinc, which may be created in a reducing atmosphere, is quickly oxidized back to the mineral oxide of zinc, because of the overall rich gaseous oxygen environment prevailing in the lean air-fuel mixture. Similarly, the zinc metal oxide compound decomposes quickly at the temperatures reached in the engine and reverts to the zinc oxide after having supplied with the additional oxygen from the excess air being fed to the combustion process.

EXPERIMENTAL PROCEDURE

With the EMD additive, micron sized particles of zinc oxide and peroxide can be introduced into the fuel with the help of carrier solvents. Use of the liquid organic peroxide as an additional carrier fluid was found to be beneficial since it also provided a boost to the cetane level of the diesel fuel and ultimately an increase in the road mileage of the vehicle. The organic peroxide used was commercial *tert*-butyl hydroperoxide (TBH) together with selected organic solvents such as methanol, ethanol, and V.M.&P. Several mixtures of different concentrations were prepared and tested to determine an optimum, compatible ratio of the heterogeneous catalyst with the solvents. Portions of the prepared suspensions were also sent to an independent laboratory for analysis. Twelve different fuel parameters such as cetane number, temperature-distillation curve, flash point, etc. were determined based on standard ASTM methods. The results were then compared with the same characteristics measured for the base fuel. However, the complete results regarding this optimum ratio of the heterogeneous catalysts and solvents will not be presented in this paper because they remain proprietary information of MAXMA L.C.

At the beginning of the experimental road tests, the fuel tanks of the vehicles were first filled with diesel fuel from a local service station. The odometer reading was recorded, and the trucks were driven for ~110 miles over roads in normal urban traffic. The trucks were then returned to the station for refueling. The amount of fuel needed to refill each tank was recorded and used to compute the baseline mileage (fuel consumption in mpg) for a given truck. The procedures required for exhaust gas analysis and collection of samples for studies on the particulate matter were then performed while the trucks were stationary. This approach allowed the baseline levels for all the parameters to be established as well. A measured quantity of the EMD fuel catalyst mixture (one ounce per five gallons of untreated fuel) was then added to the truck's fuel tanks. The vehicles were then driven for an additional ~110 miles following the previous driving pattern as closely as possible. Once again, the trucks were returned for refueling. The required amount of fuel needed to completely fill the tank after the road test was recorded and used to calculate the new mileage for each truck; this time for the combination of fuel with the EMD additive. Also, once again, the analyses of the exhaust gases and the particulate matter entrapment tests were performed in order to compare the effects from the use of EMD with the baseline values obtained for the exhaust emissions without the additive. A series of similar road tests was performed three or more times in order to assess experimental variations in the experiments and to detect chronological effects on the truck engines arising from continuous use of the additive with the fuel.

RESULTS AND DISCUSSION

Effects of Heterogeneous Catalysts on Engine Wear

To determine the fate of the catalyst particles, analyses were performed on the engine oil of one of the diesel trucks that used the additive. A commercial laboratory, Ek-Cel, performed the tests on the engine oil. Overall in this test, a 1995, International 8100 diesel truck was driven more than 28,000 miles covering a period of approximately seventy-five days. The lab analyses revealed that during this time period the wear nearly one half reduced metal concentrations in the engine oil. Iron, the major metal used in engine fabrication, was reduced in the engine oil from 170 down to 88 ppm. However, the concentration of zinc, a major component in the catalytic additive, increased from 444 ppm to 1544 ppm. Zinc is not considered to be a wear metal and is often part of the motor oil composition. All of the other four wear metals (Pb, Cu, Cr, or Al) showed significant decreases, while the other six non-wear metals either experienced slight increases or overall decreases. Figures I and 2 summarized the results of engine oil analysis for trace metals. These results suggest that the standard requirements for regular periodic maintenance may be reduced as a result of using the EMD additive.

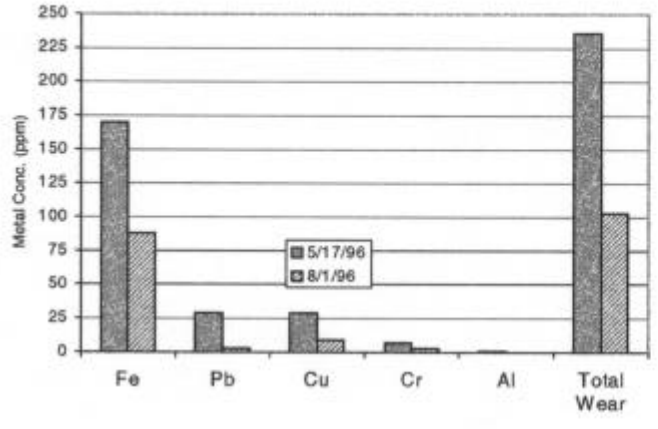

Figure 1. Conc. of wear metals in the engine oil

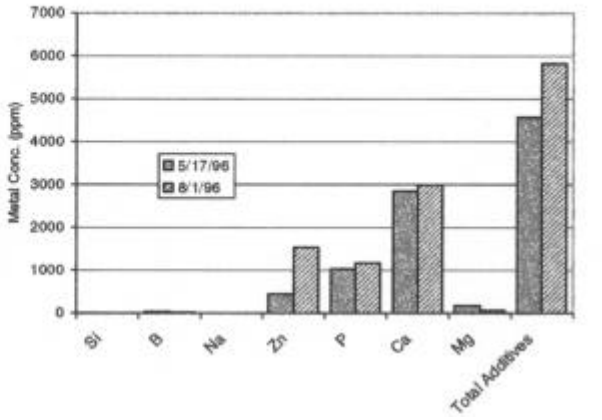

Figure 2. Conc. of contaminants/additive in the engine oil.

Core Labs in Houston, Texas, following ASTM D6078 guidelines also performed a lubricity test. The results of this test are presented in Figure 3. The smaller wear number with the use of the additive suggests greater lubricity between wear parts. The increased lubricity is consistent with the previous findings on wear metal concentration in engine oil, which showed a significant reduction of wear metal concentrations with the use of the additive. One of the reported problems with diesel fuels that exhibit naturally increased cetane levels is reduced lubricity. Because of this, highly refined diesels may tend to accelerate wear in fuel pumps and injectors if not modified. The use of EMD increases cetane without a decrease in lubricity.

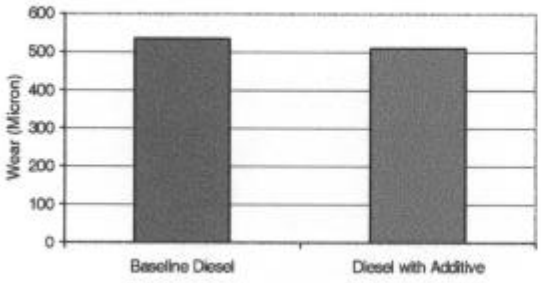

Figure 3. Effects of the additive on the lubricity.

Effects of Heterogeneous Catalysts on Fuel Efficiency

Diesel fuel treated with the additive was road tested with two different vehicles. In these mileage tests, the vehicles were first driven over urban roads with fuel obtained from a Shell service station. The same fuel was then treated with the heterogeneous additive at a level of 0.4 ounces per gallon of diesel fuel, which is equivalent to 11 ml of the additive per quart (1.06 liter) of fuel. During the road tests, the trucks did not carry cargo but were driven non-stop over a distance of 110 miles (117 km). The mileage achieved following the use of the additive was then compared with the mileage obtained with the base fuel. The increase in mileage varied from 14% to 32%. Tables 1 and 2 summarize the results of the road tests.

Table 1. Road performance for an International Diesel Truck with the additive.

Run	Miles	Gallons of diesel	MPG	Change	Conditions
1	110	12.93	8.507	--------	No additive (baseline)
2	110	9.81	11.213	32%	0.4 oz additive per gal.
3	110	10.08	10.913	28%	0.4 oz additive per gal.

Initial mileage: 37,574 miles.

A truck fleet operator used the additive in three of their trucks. Baseline records of each randomly selected vehicle were taken from past OBD computer records maintained by the company covering a time period of eighteen months. Only mileage improvement was investigated in these tests. Emission tests were neglected since they were not a concern of the trucking company at that time. These tests better reflect actual fleet practice, since the trucks were loaded and used on normal delivery routes in stop-and-go traffic. The results are presented in Table 4 as miles travel per gallon of fuel over a forty-two day span.

Table 2. Road performance for a GMC Diesel Truck with the additive.

Run	Miles	Gallons of diesel	MPG	Change	Conditions
1	110	13.24	8.308	--------	No additive (baseline)
2	110	10.58	10.397	25%	0.4 oz additive per gal.
3	110	11.58	9.499	14%	0.4 oz additive per gal.

Initial mileage: 59,163 miles.

Table 4. Mileage (MPG) data from three different trucks operated by a trucking company in Plainview, Texas.

Truck ID	4-949	7-821	7-825	Average*
Baseline	6.19	6.37	6.30	6.29
7/20/98	6.80	7.00	7.10	6.97
7/27/98	6.50	6.90		6.70
8/3/98	6.70	7.00	7.00	6.89
8/10/98	6.90	7.30	7.30	7.16
8/14/98	6.70	7.30	7.10	7.03
8/21/98	6.60		7.10	6.85
9/4/98	6.80	7.30	7.20	7.10
9/11/98	7.00	7.40	7.40	7.27

*Averages for all three vehicles.

CONCLUSIONS

It may be concluded from the experimental results that the use of the EMD additive has very little impact on the functional properties of the fuel. Most of the changes in fuel characteristics were for the better, especially with respect to those, which could affect cold weather start up. Like other additives available on the market, the optimum dosage for use of the heterogeneous EMD catalyst will depend on the base fuel. The test results have shown that, when EMD is used in low concentrations, the heterogeneous catalyst is compatible with the diesel fuel.

Experimental results also point out that apart from the obvious advantages of less emissions (Tock *et al*. 1999 and Tock *et al*. 2000) and increased mileage, the use of the additive may also ofter some non-obvious savings on maintenance of the vehicles. The use of fuel borne catalysts certainly offers potential economic savings for fleet operators and at the greater benefits for "green chemistry" in combustion process for IC engines.

REFERENCES

Tock, R.W., Arefeen, Q. and Sanders, K. (1999). "The Effects of Using a Heterogeneous Catalyst and a Chemical Combustion Promoter on Emissions from Diesel Engines", in World Refining, vol. 9, No. 2, March, 1999, pp 53-62.

Walker, W.H., Lewis, W.K., and McAdams, W.H. (1923). Principles of Chemical Engineering. McGraw-Hill, Inc., New York, NY, 193-206.

Tock, R.W., Arefeen, Q., and Sanders, K. (2000). "Improvements in the Performance of Heavy Diesel Engines with the Use of a Heterogeneous Catalyst and Chemical Combustion Promoter", Paper TE 007, AIChE Spring 2000 National Meeting, Atlanta, GA, March 2000.

4th Annual Green Chemistry &
Engineering Conference

Sustainable Technologies:
From Research to Industrial Implementation

June 27 - 29, 2000

DESIGNING SAFER CHEMICALS

AFFORDABLE COMPOSITES FROM RENEWABLE RESOURCES

R. P. Wool, S. N. Khot, J. J. LaScala, G. I. Williams, S. P. Bunker, W. Thielemans, J. Lu and S. S. Morye
Department of Chemical Engineering and ACRES Program, Center for Composite Materials,
University of Delaware, Newark DE 19716-3144

Abstract
Recent advances in soybean genetic engineering, natural fiber development and composite science offer significant opportunities for new improved materials from renewable resources which can be biodegradable and/or recyclable with enhanced support for global sustainability. Newly developed soy-based plastics and adhesive materials are being evaluated and tested by end-users and converters for high volume applications in agricultural equipment (tractors and farming machines), automotive (car and truck parts), civil (bridges and highway components), marine (pipes and offshore equipment), rail infrastructure (carriages, box cars and grain hoppers) and the construction industry (formaldehyde-free particle board, ceilings, and engineered lumber). Several examples are given for the synthesis, manufacturing and properties of both the neat soy-based resins and the glass, flax, lignin and hemp composites.

INTRODUCTION

The use of materials from renewable resources is becoming increasingly important as the world's leading industries and manufacturers seek to replace dwindling petrochemical-based feedstock with agricultural based materials. The quest for materials from renewable resources supports global sustainability and comes at a time when there is excess capacity in the Ag industry. Thus, the diversification into non-food uses addresses both an important global environmental issue and lends stability for an important segment of our economy. The materials utilization of Ag products has had to overcome many technical barriers which often resulted in products which were either non-competitive in either price or properties compared to petroleum based products. But now, genetic engineering is better understood and more sophisticated tools are available to fine-tune the design of natural molecules for optimum cost/performance in the finished product.

An interdisciplinary group of scientists in the Affordable Composites from Renewable Resources (ACRES) Program at the University of Delaware examined several hundred chemical pathways for the conversion of plant oils to high performance, inexpensive composites and plastics[1-4]. The chemical modification of the oil was done with regard to cost, manufacturability, method of cure and final material properties[5]. The fiber reinforced composite resins were suited to several manufacturing techniques including, Resin Transfer Molding (RTM), Vacuum Assisted Resin Transfer Molding (VARTM), Seeman's Composite Resin Infusion Manufacturing Process (SCRIMP), Atmospheric Pressure Molding (APM), Sheet Molding Compound (SMC), Bulk Molding Compound (BMC) Open Mold Casting, Spray-Up, Filament Winding Pultrusion, Fiber Placement, Prepreg Formation, Particle Board Manufacturing, Lamination and MDF manufacturing.

TRIGLYCERIDES AND SOYOIL

The liquid resins were derived from plant and animal oil triglycerides (see Table 1) by suitably functionalizing the triglyceride with chemical groups (epoxy, carboxyl, hydroxyl, vinyl, amine, etc.) that render it polymerizable. The triglyceride molecular structure is a combination of various triesters of fatty acids linked together with glycerol. The fatty acid residues are linear carboxylic acids containing from about 4 to about 30 carbon atoms, but usually from about 14 to about 22 carbons and from about zero to about 4, or usually from about 2 to 3 carbon-carbon double bonds. As obtained in nature, these double bonds are predominantly in the *cis* (Z) configuration and, in the case of polyunsaturated acids, not conjugated. The fatty acids derived from triglycerides include the following: Lauric (C12:0), i.e., 12 carbon atoms long containing zero C=C double bonds, Myristic (C14:0), Palmitic (C16:1), Stearic (C18:0), Oleic (C18:1), Linoleic (C18:2), Linolenic (C18:3), Arachidic (C20:0), Gadoleic

(C20:1), Behenic (C22:0) and Erucic (C22:1). The genetically engineered oils can have a very narrow distribution of molecular species and relatively few saturated fatty acid residues[6,7].

Table 1. Composition of Natural Fats and Oils

Oil	C/C=C	Canola	Corn	Linseed	Olive	Palm	Peanut	Safflower	Soy	Lard	Fish
Lauric	12:0					0.1				0.3	
Myristic	14:0	0.1				1.2		0.1	0.1	1.7	1.3
Palmitic	16:0	4.1	11.5	5.5	16.9	**46.8**	11.0	6.7	10.5	26.2	13.6
Stearic	18:0	1.8	2.2	3.5	2.7	3.8	2.3	2.7	3.2	13.5	1.4
Oleic	18:1	**60.9**	26.6	19.1	**61.9**	37.6	**51.0**	12.9	22.3	**42.9**	**23.5**
Linoleic	18:2	21.0	**58.7**	15.3	14.8	10.0	30.9	**77.5**	**54.5**	9.0	0.8
Lino-lenic	18:3	8.8	0.8	**56.6**	0.6				8.3	0.3	
Eicosanoic	20:0		0.2		0.4	0.2	0.7	0.5	0.2	0.2	
Eicosanoic	20:1				0.1	0.3		0.5	0.9	0.8	

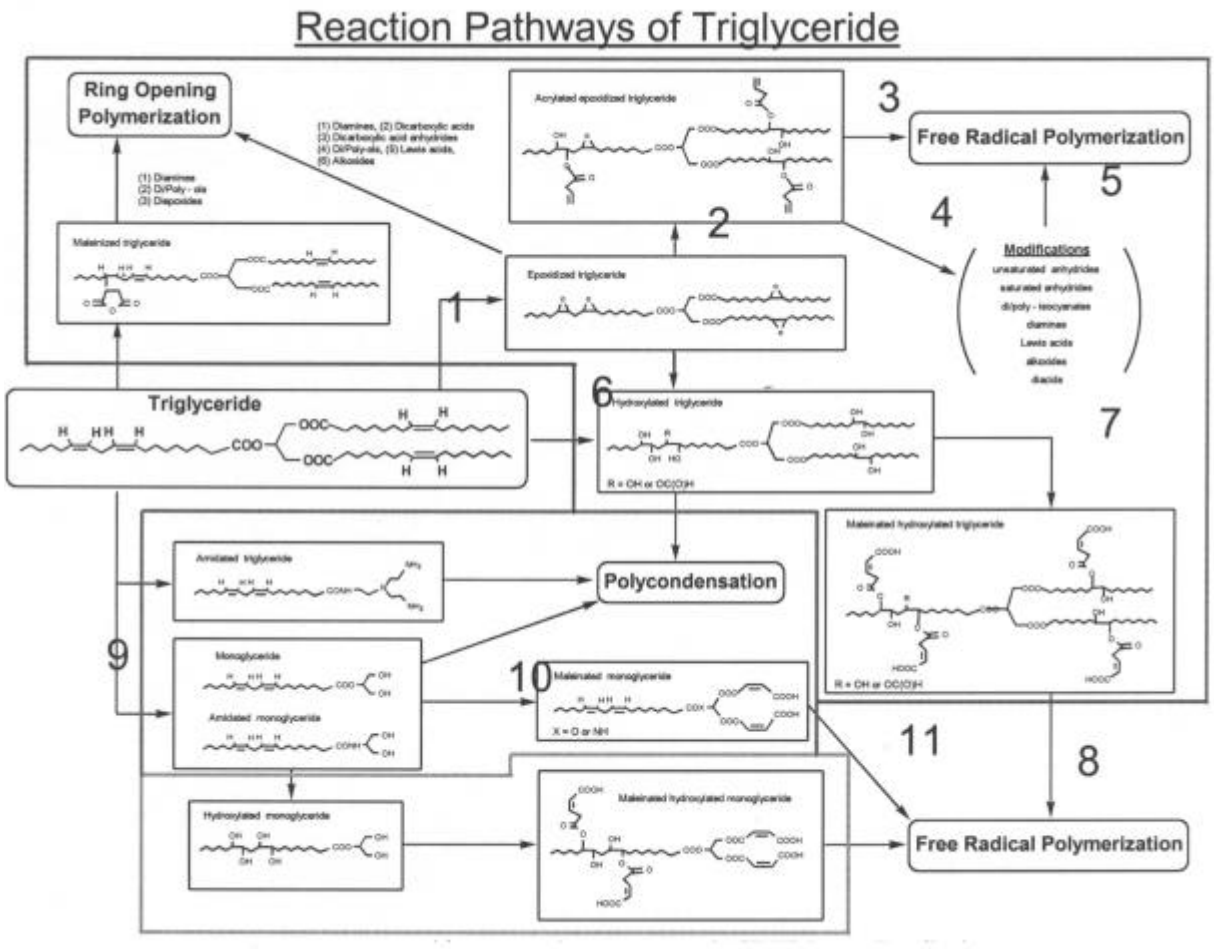

Figure 1. Conversion of triglycerides to reactive monomers (ACRES Patent Pending)

RESULTS AND APPLICATIONS

Resin Synthesis from Soybean Oil

The ACRES liquid resins were derived from plant and animal oil triglycerides by suitably functionalizing the triglyceride with chemical groups that render it polymerizable, as shown in Figure 1. About a dozen new soy-based resin systems were derived from chemically modified triglycerides which gave excellent properties (Patents Pending[5]). These included (i) semi epoxidized/hyroxylated oils, (ii) Maleinated half-esters of Hyroxylated oils, (iii) Maleinated Soy oil monoglyceride, (iv) acrylated maleinated soyoil, (v) and mixtures of the above with diols, diamines, diacids and other cross-linking agents. The triglyceride molecular structure (e.g., Fig 1, Path 1) is essentially that of a three arm-star where the length of the arms and the level of C=C unsaturation are the important structural variables.

Just prior to use, liquid molding resins are mixed with catalysts and accelerators that start and facilitate the cross-linking reaction. If the cross-linking reaction is of the addition type, such accelerators as cobalt naphtenate, aromatic tertiary amines, etc., and free radical initiators such as methyl ethyl ketone peroxide, benzoyl peroxide, cumyl hydroperoxide, etc., are added. The choice of initiators and accelerators depends on the reactivity of the polymer and the temperature and the time desired for the cure reaction. The soy-based resins, when injected into molds and reacted by free radical or condensation mechanisms, produced high modulus, high T_g, thermosetting composites matrices.

The new soy-based resins are estimated to be competitive and perhaps lower in cost than the lower end of current thermosetting resin systems. The pathways shown in Figure 1 provide the means to derive monomers which react to form linear, branched and cross-linked structures necessary for composite, elastomeric and adhesive materials.

Genetically Engineered and Model Oil Resins

A series of maleinized hydroxylated triglycerides derived respectively, from olive oil, safflower oil, soybean oil, high oleic genetically engineered soy oil and mixtures of soybean-olive oil, were prepared. The object of this study was to determine the role of C=C unsaturation in the triglyceride on the thermal and mechanical properties of the neat resin. The results (Table 2) indicate that significant improvements of mechanical and thermal properties can be obtained with control of the triglyceride structure and functionality. This work is in progress using genetically engineered oils[6,7].

Table 2. Properties of Maleinized Hydroxylated Plant Oils

Plant Oil	Number C=C Bonds/Triglyceride	T_g ºC	Hardness Shore D	Storage Modulus GPa Room Temp	Crosslink Density at 140 ºC mol/m^3	Functional Groups in Oil
Olive Oil	2.8	81	74.6	1.04	3952	1.23
Soy/Olive	3.7	91	77.4	1.31	4397	1.41
Soy Oil	4.6	102	82.6	1.64	4812	1.65
Safflower	5.1	117	84.3	1.9	5525	1.81

The structural versatility of the natural oil triglycerides allows the extent of chemical modification to be altered in a way that impacts on a range of properties to varying extents. For example, we can change the resin viscosity by reducing the level of hydroxylation to the extent needed for cross-linking reactions; additional hydroxylation does little for thermal or mechanical properties of the cured resin but alters the hydrophilicity and biodegradability[7]. These resins can also be partially cured or chealated with di-valent cations to obtain B-Staged resins suited for BMC and SMC applications.

Optimal molecular networks influencing the mechanical and thermal properties of the reacted resins are determined as a function of triglyceride structure, stoichiometry of reactants, triglyceride distribution function, chemical reactivity ratios and manufacturing conditions. The strength and durability is determined by vector percolation analysis of the optimal networks[8,9].

Composites from Soy-Based Resins

Four types of triglycerides typically make up a composite resin system, namely (a) sizing, (b) matrix, (c) rubber toughening, and (d) material modification. For natural fibers, or unsized glass or carbon, about 1% of the system consists of the sizing molecules. These have groups which allow them to bond both to the surface as well as to the matrix. A strong fiber-matrix interface bond is critical for high strength composites. The ability to apply the sizing *in situ*, offers considerable savings of time and cost, especially for all-natural composites which are intended to be low cost. The chemical modification on the sizing is chosen with respect to specific interactions on the natural fiber surface. The matrix consists of the dominant phase binding the fibers together in the composite and can be selected with respect to required material properties (hydrophilicity, biodegradability, flammability, dielectric, etc.). The rubber generating molecules (5-20%) can be made *in situ* or presythesized, depending on the manufacturing conditions. The rubber particles when used at the optimal concentration, impart considerable impact resistance to both the neat resin and the composite. Other triglycerides are chemically modified to tailor the optical, thermal, electrical and mechanical properties of the composite.

Typical properties of E-glass fiber filled resins (50% vol) gave tensile strengths of about 400 MPa (ASTM 3039-76), Young's Modulus of about 20 GPa and a fracture energy of about 50 kJ/m^2 (fracture mechanics collaboration with Professor Sri Bandypadhyay) which compare favorably with similar vinylester and polyester high performance composites (Tables 3 and 4). Excellent resistance to acid, alkali, hot and cold water were found for some of these high performance ACRES composites. Others were found to swell in hot water in a manner dependent on the amount of hydrophilic groups contained in the triglyceride structure and at least one resin exhibited rapid biodegradation in a soil burial test.

Table 3. Properties of Hydroxylated-Maleinized Soyoil and Commercial Vinyl Ester Composites

Property	Dow DK 411 C50 Fiber Glass Composite	Hydroxylated Soy Oil Fiber Glass Composite
Glass Fiber Content wt%	76	76
Tan Delta Peak ºC	128	128
Flex Modulus MSI	5.2	5.0
Flex Strength at Break KSI	118	97
Compression Strength KSI	42	29
Short Beam Shear Strength KSI	7.6	5.5

Table 4. Comparison of Soy-based and Commercial Vinyl Ester Fiber Glass Reinforced Composites

Materials	Testing Direction	Tensile Strength KSI ASTM D3039-76	Youngs's Modulus MSI ASTM D3039-76	Compressive Strength KSI ASTM D-3410-87	Compressive Modulus MSI ASTM D-3410-87
Soy/E-Glass (2 plies)	0º	67.2	3.6	43.9	3.6
Dow PC-100 VE/E-Glass	0º	66.5	3.45	61	3.4
Soy/E-Glass	90º	46.7	3.0	26.2	3.0
DowPC-100 VE/E-Glass	90º	47	2.55	49.2	2.6

Agricultural Equipment from Soybeans

The ACRES group in collaboration with John Deere and Company, Contemporary Products, Fibeco and Cara Plastics, designed several parts for agricultural equipment which are currently being field tested in the USA. These includethe Round Hay Baler Panel (shown in Fig 2[4b]), underhood tractor parts and the harvester rear wall

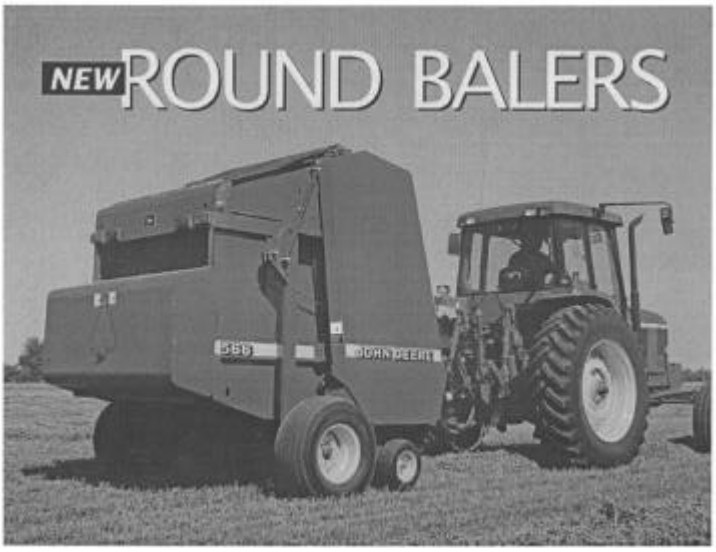

(exhibited at the Composite Fabricators Association meeting in Chicago, November 1999.

The durability and structural integrity of the ACRES composites fabricated by RTM, APM and Hand-Lay-Up processes are being evaluated. The soy-based composites have applicability to the automotive, trucking and transportation industry. When combined with natural fibers, the all-natural composites offer a new range of inexpensive environmentally friendly materials, as discussed in the next section.

Figure 2. Round Hay Bailer. The 8x3' Panel containing the name "John Deere" was made from the ACRES soy-based resin (Courtesy, John Deere, Moline, Illinois)

Natural Fiber Composites

The use of natural fibers with the natural oil resins described herein promises to give economical, potentially biodegradable or recyclable, engineering materials with a high level of vegetable-based raw materials[10-12]. Such materials have a low market cost, they are attractive with respect to global sustainability and should find commercial use as the composite industry becomes more environmentally responsible in the near future. The resins described can be modified by various additives to improve adhesion to these fibers, thereby significantly improving their physical properties and hydrolytic stability. Some of these resins can be used as sizing agents for the natural fibers by controlling the type of functional groups, e.g., by using hydrophilic hydroxylated oils, which contain sufficient vinyl reactive sites, e.g. by maleinization, to bond to the matrix, which by choice can be more hydrophobic than the sizing agent. Typically, the sizing agent concentration would be of the order of 1-2% by wt compared to the matrix. The resulting sizing provides a strong bond between the fibers and the matrix, which is essential to the manufacture of high performance composite materials. The composites thus formed have physical properties that compare favorably with the previously mentioned petroleum-based composite resins.

Tensile and flexural properties were obtained for resin transfer molded flax fibers (Durafiber Grade 2 supplied by Cargill) made by RTM using soy-based resins as the matrix[10,11]. The tensile strength at 34 wt% fiber was found to be about 30 MPa, flexural strength of 65 MPa with tensile moduli around 4-5 GPa. The tensile strength was dominated by the intrinsic strength of the fibers. Excellent bonding between the fibers and matrix was obtained using new soy-based sizing agents. The flax fibers broke in brittle fracture mode with little evidence for pullout or matrix debonding. When soy based sizing was used, a substantial increase in modulus was noted ca 6 GPa. These properties are superior to flax-polypropylene composites being evaluated by several automotive groups. Soy-based SMC materials made with flax fibers would be useful for the automotive industry and are being designed by the ACRES group.

Table 5. Water Absorption Data for Flax Fiber Composites

Flax Fiber 30% wt of Composite	Water Temperature	Immersion Time Hours	Weight Change %	Number of Samples Tested
Mesh-10 Shive	room	2	0.75	3
Mesh-10 Shive	Boiling	2	4.31	3
Grade-2 Fiber	room	2	1.27	3
Grade-2 Fiber	Boiling	2	5.43	3

Excellent inexpensive composites were made using natural fibers, such as hemp, straw, flax, jute and wood. The soy-based resins have a strong affinity for natural fibers and form an excellent fiber-matrix interface, as

determined by SEM analysis of fractured composites. Other abundantly available natural products such as lignin and starch can make substantial contributions to the composite properties by acting as toughening agents, improving the sizing, increasing adhesion between matrix, fillers and fibers, modifying the biodegradability, behaving as low profile additives, improving the antistatic properties and acting as reinforcement fillers.

Table 6. Hemp Composite Properties

Tensile Strength	Tensile Modulus	Toughness, K_{1c}	Fracture Energy	Density
35 MPa	4.4 GPa	3 MPa.m $^{1/2}$	2 KJ/m^2	1.104 g/cm^3

The tensile or flexural fracture stress σ, of composites with natural fibers can be determined by the vector percolation model of fracture[8,9] as

$$\sigma \sim [E(\phi)(1+\phi/\phi_c)]^{1/2}$$

where $E(\phi)$ is the composite modulus as a function of fiber volume fraction ϕ, and ϕ_c is a critical fiber fraction. This assumes that natural fibers have defects distributed along their length, whose concentration is proportional to ϕ. At a critical concentration $\phi = \phi_c$, the latter equation predicts that the composite becomes fragile. Since the composite stiffness $E(\phi)$ is typically an increasing function of ϕ, this relation predicts that in the linear approximation for $E(\phi)$, σ will attain a maximum value at ϕ. From Williams *et al*. work[10,11], $\phi_c \approx 35\%$, such that we expect $\phi_c \approx 70\%$. Elimination of such defects via sizing design, internal repair and healing processes (work in progress) would substantially increase the tensile properties of natural fiber composites.

These resins can be viewed as candidate replacements for phenol formaldehyde, urethane and other petroleum based binders in particle board, MDF and OFS board applications. The use of natural fibers with these compatible resins allows a double environmental impact of replacing wood with a more renewable resource such as flax or hemp, and petroleum oil with soyoil. Additionally, the new all-natural composites offer several alternatives for recycling and disposal of composites.

Ballistic Impact Resistance

High performance polymer composites based on aramid fibers, S-glass fibers and more recently gel spun polyethylene fibers are widely used in applications demanding protection from ballistic impact. These applications include personal armor and armor for equipment. The armor is designed with respect to the threat level, i.e., anticipated projectiles, type of ammunition and weapons, velocity of projectiles, etc. For very high velocity protection, an armor with a ceramic front plate and a polymer composite backing is selected. For personal protection where the weight of the armor is an important issue, fibers with a low density like aramid and gel spun polyethylene are commonly used. For equipment protection, on the other hand, S-glass fibers are used.

The ballistic impact of composites is measured in terms of the V50 parameter, which is defined as the velocity V, at which the probability of complete penetration of the target by the projectile is 50%. This involves firing a minimum of 6 shots on the target of which three are complete penetrations and three partial penetrations. The V50 is then given by the average of the six strike velocities. In the current study, ballistic impact resistance was determined on S-glass fiber reinforced soy-based resin panels 12x12x0.75 inch. The panels were made by SCRIMP at room temperature and cured at 110 ºC for 60 min. The composite consisted of 28 woven S-glass fabric layers. The composite was found to have a V50 of about 1,800 feet per second against 50 caliber (13.5 grams) blunt nosed fragment simulating projectiles, which is at least comparable if not better than epoxy and vinyl ester based composites. The composites were found to absorb the kinetic energy of the impacting projectiles by tensile failure of fibers, fiber pullout, delamination and shear between different layers in the composite.

When 0.75 inch thick ceramic tiles (Coors alumina) were placed on the soy-based composite, the ballistic impact V50 resistance improved to 3,100 ft/sec for 20 mm (53.75 g) projectiles. The role of a ceramic front face backed by a polymer composite back plate is to spread the impact energy over a larger area. The hard ceramic plate also deforms the projectile. On ballistic impact, the ceramic is shattered and it spreads the impact over a much larger area. The delocalized energy is then absorbed by the polymer composite back plate. This increases the amount of energy absorbed and therefore improves the ballistic performance. The enhanced impact resistance of soy based composites is also attributed to both the low temperature *beta* relaxation (similar to polycarbonate)

which occurs by virtue of the floppy nature of the triglyceride, coupled with the excellent frictional energy dissipation which the resin-fiber interface generates during impact. Low velocity impact tests have also been carried out on hybrid composites utilizing glass and flax fibers in the same composite in different ratios. The transverse impact is the most common in service loading mode in composites. In structural applications it could be an impact from a dropped tool, in aircraft applications it could be an impact from a bird and in aerospace applications it could be an impact from space debris.

When flax fibers were placed on the impact side of the composite plate with woven glass fibers on the back side, excellent impact resistance was obtained. This improved impact resistance also comes at a significant reduction in weight and cost[13]. These materials hold considerable promise for new and improved personal and vehicle armor at a reasonable cost.

Biodegradable Composites

Most of the composite resins shown in Figure 1 were found to be non-biodegradable, as required for the traditional long-life applications, but some were found to be biodegradable, as might be expected for materials made with triglycerides. The biodegradable composites could be useful in applications where the biodegradability is an important component of the materials performance in aquatic and terrestrial environments, or in municipal solid waste management where composting and landfill reclamation are considered to be important[14,15]. Compostable packaging and products which are disposed in the environment would particularly benefit from the new soy-based materials.

Adhesives and Elastomers

While the above topics concerned soy based thermosetting resins with high crosslink density (Mx ~ 100-200), the chemistry and triglyceride structure can be controlled to produce linear polymers of controlled molecular weight, branched polymers with controlled branch length and spacing, highly branched polymers, lightly cross-linked polymers and mixed systems with high crosslink density[16]. This allows the synthesis of a new generation of pressure sensitive adhesives, solid rocket propellants, elastomers, rubbers and low modulus composites.

Acknowledgments

The authors are grateful to the United Soybean Board, DuPont, the Delaware Transportation Institute, Hercules, the University of Delaware, John Deere, Westvaco and Cara Plastics for support of this research. Special thanks are offered to other members of the ACRES group, including Professor Selim Kusefoglu visiting on sabbatical from Bogazici University, Turkey; Professor Shri Bandypadhyay visiting on sabbatical from University of New South Wales, Australia; Professors P. Dhurjati (BioProcessing) and B. Lemieux (Genetic Engineering) Dr Guiseppe Palmese (CCM), Dr. Antonio Paesano (CCM); Christine Kellner, Ken Lo, Lisa Dietrich, and Kurt Sokol, all undergraduate research assistants, and Sunil Naik, CCM scientist at the University of Delaware.

References

1. ACRES Web Address: http://www.ccm.udel.edu/mission/programs/ACRES.html.
2. R.P. Wool, "Genetically Engineered Composites", Proceedings of the Sixth International Conference on Composites Engineering, June 27, 1999.
3. R. P. Wool, *Chemtech*, "Soy-Based Plastics, Resins and Adhesives", **44**, June, 1999.
4. a) The ACRES Group received the *Innovation in Real Materials* (IRM) Award, at the Innovation in Materials Conference, from the International Union of Materials Research Societies, Washington DC, July 21, 1998.
   b) Contemporary Products, in collaboration with the ACRES group, won the Technical Innovation ACE Award at the Composite Fabricators Association meeting in Orlando Florida in 1997, for the use of the ACRES soy-based resin in the John Deere Round Hay Baler door.
   c) Wool, R.P.; Kusefoglu, W.; Zhao, R.; Palmese, G.; Boyd, A.; Fisher, C.; Bandypadhyay, S.; Paesano, A.; Ranade, S.; Dhurjati, P.; Khot, S.; LaScala, J.; Williams, G.; Ligon, M.; Gibbons, K.; Wang, C.; Soultoukis, C.; Bryner, M.; Rhinehart, J.; and Robison, A., "Affordable Composites from Renewable Resources", Abstracts of Papers from The American Physical Society, 1998, Vol 216, pp
5. Wool, R.P., Kusefoglu S., Zhao, R., Palmese, G., and Khot, S: "High Modulus Polymers and Composites from Plant Oils", International Patent Publication Number WO 99/21900, May 6 1999; US Patent Approved April 16, 2000 (Patent Pending)
6. R.P. Woo *et al.*, "Affordable Genetically Engineered Soy-Based Composites, Resins and Adhesives," Proceedings of the 3rd Annual Green Chemistry and Engineering Conference, National Academy of Sciences, Washington D.C., June 30, 1999.
7. J.J. LaScala and R.P. Wool, paper submitted for publication.

8. Wool, R.P., "Adhesion at Polymer Interfaces; A Percolation Approach to Strength", Proceedings of the World Congress of Adhesion, WCARP-1, Germany, September 1998.
9. Wool, R. P. (1995). *Polymer Interfaces: Structure and Strength,* New York: Hanser/Gardner Press, 494 pages. ISBN 1-56990-133-3.
10. G.I. Williams and R.P. Wool, "Composites from Renewable Resources", Proceedings of the American Institute of Chemical Engineers 1998 Annual Meeting, Miami, FL; Nov. 19, 1998.
11. G.I. Williams and R.P. Wool, "Composites from Soyoil and Natural Fibers", *J. Applied Composites*, in press 1999.
12. Wool, R.P., Kusefoglu, S.K., Khot, S.N., Zhao, R., Palmese, G., Boyd, A., Williams, G. and LaScala, J., *Affordable Bioderived Plastics and Binders for the Composite Industry,* Proceedings of the Second European Panel Products Symposium, Bangor Wales, P233, October 21, 1998.
13. S.S. Morye and R.P. Wool, "Mechanical Properties of Glass/Flax Hybrid Composites Based on a Novel Modified Soy Oil Matrix Material", Polymer Composites, in press (2000).
14. Wool, R.P., *Perspectives on Standards Test Methods for Biodegradable Plastics,* Proceedings of International Workshop on Biodegradable Polymers, Osaka, Japan, November 1993. (p 250-258) in *Biodegradable Plastics and Polymers,* Y. Doi and K. Fukuda (Eds.), Elsevier Science, Amsterdam, (1994).
15. Wool, R.P. (1995). *The Science and Engineering of Polymer Composite Degradation,* (p. 138-152), *Degradable Polymers: Principles and Applications,* G. Scott and D. Gilead, (Eds.), Chapmann & Hall, London.
16. S.P. Bunker and R.P. Wool, Proceedings of the Oil Chemists Society, 2000.

FLUORINATED MATERIALS FOR HIGH SOLIDS/LOW VOC COATINGS

R. Thomas, R. Medsker, D. Woodland, B. Beers and R. Weinert
Omnova Solutions, Inc., 2990 Gilchrist Road, Akron, OH 44305-4489

ABSTRACT
A flexible, durable "dry erase" coating was prepared using a novel fluorinated prepolymer to impart the low surface tension component necessary for "dry erase" properties. The surface free energy was adjusted such that markers wet the surface, yet are removed easily after drying. During coating application, it was noticed that the solids level in the coating could be increased substantially (40 → 70 wt%) while maintaining excellent gloss, distinctness of image (DOI), dry erase performance and flow and leveling. The fluorine-modified polymer is an exceptional flow and leveling agent and responsible for the increased solids level or decreased VOC.

INTRODUCTION
Environmentally, there is a clear need to reduce the amount of volatile organic compounds (VOC) from the atmosphere. Solvent-borne coatings are a substantial contributor to VOC emissions. This is as much mandated by the cost to manufacture a finished article as it is by government regulations that continue to get more stringent. Therefore, lowering emission of VOCs is desirable from an economic and environmental perspective. However, lowering VOCs or raising solids levels in solvent-borne coatings can lead often to undesirable properties. For example, spraying of high solids coatings can be difficult due to a substantial increase in viscosity. Another example is the decrease in optical properties such as gloss and DOI observed often with low VOC/high solids coatings. A great deal of work is required from coatings manufacturers to deliver equal or even improved performance from high solids, low VOC coatings.

Omnova Solutions, Inc. manufactures and markets a dry erasable wall covering product under the MemErase™ trademark. A fluorinated prepolymer is incorporated into the coating to provide the dry erase properties. The presence of the fluorinated material lowers the surface free energy of the coating such that markers will wet the surface, but can be removed easily with standard board erasers. The fluorine-modified polymer chain segregates and is in excess at the coating surface. X-ray photoelectron spectroscopic measurements have demonstrated surfaces with 15-20 atomic % fluorine or a surface excess ≈ 100x. The surface excess of fluorinated material lowers the surface tension of the coating to an estimated value ≈ 25 mN/m.

During gravure application of this coating system in a manufacturing environment, it was demonstrated that the solids level of the coating could be increased from its typical value of 40 wt% to a value of 70 wt%. Furthermore,

it was observed that the coating applied at higher solids/lower VOC possessed superior properties to the lower solids version. The higher solids coating wet the substrate better and had higher gloss and DOI. In addition, the higher solids coating flow and level better than the lower solids version. While preparing a coating with better properties has immediate commercial value, an analysis of the entire coating operation yielded some unexpected environmental and economic benefits.

1) Reduced cost of raw materials as quantity of solvent per pound of dry coating is reduced.

2) Reduced solvent evolution per square yard of coated product since solvent loading is less. The value can be realized in several ways:

   a) Reduced cost of emission control if production rate remains the same (i.e., line speed is not increased).

   b) Improved equipment utilization (i.e., increased capacity) if line speed is increased to a point where emissions are equal to higher solvent formulations.

   c) Reduced labor cost per square yard of product produced if line speed is increased.

   d) Some blend of emission control cost reduction and equipment and labor cost reduction.

3) Reduced total coating per square yard of material if flow and leveling properties of higher solids coating allows for a more uniform surface coverage that can cover substrate at lesser thickness and give equal properties.

4) Possibility of substituting less regulated (either safety or environmental) solvents that may have a slower flash but because of smaller amounts used, may be able to be processed in existing equipment (i.e., maintain current line speed but still flash-off lower boiling solvent).

5) Improved environmental impact by producing a product that emits less VOC per square yard.

6) Improved indoor air quality (i.e., if line speed remains constant and current ventilation system is maintained, the amount of fugitive emissions is reduced).

In addition, it was easier to obtain better and more consistent cure conditions using the same lines speeds. The energy required to remove solvent was now being used to affect cure chemistry resulting in films with enhanced mechanical properties. This is very important for fast lines speeds. Furthermore, the incorporated fluorinated prepolymer was a better flow and leveling agent than many commercial silicone or fluorochemical agents added specifically for that task. Overall, the addition of the fluorinated prepolymer provided excellent flow and leveling to a higher solids coating.

SUMMARY

A fluorinated prepolymer was incorporated into a coating to prepare a dry erasable film. During application of this coating, many benefits were noticed and realized. A higher solids/lower VOC coating was obtained that provided superior properties compared to the lower solids version. An improvement in substrate wetting, gloss, DOI and flow and leveling were observed. In addition, there were a number of unexpected economic benefits found by using a higher solids coating on a manufacturing scale.

CORROSION CONTROL PACKAGING FILM PREPARED FROM A BIODEGRADABLE COMPOSTABLE RESIN

Christophe Chandler, Laboratory Director, Art Ahlbrecht, Vice President of Research & Development,
and Boris Miksic, President/CEO
Cortec Corporation, 4119 White Bear Parkway, St. Paul, MN 55110
Mrinal Bhattacharya, Professor
Department of Biosystems and Agricultural Engineering University of Minnesota,
212 BAE Building, St. Paul, MN 55108

ABSTRACT
Biodegradable packaging films useful in protecting metallic articles in corrosive atmospheres have been prepared and evaluated. Incorporating volatile corrosion inhibitors in film-forming biodegradable polyester resins improves the corrosion resistance of the films to equal conventional polyethylene packages. These new films not only pass the recently approved ATSM standard and the proposed CEN standard for biodegradability and compostability, but also provide a "green alternative" to polyethylene.

INTRODUCTION
Corrosion is a plight that anyone working with metals faces. Its impact on the United States economy has been documented to be about 4% of the Gross National Product. It was estimated that about one third of the cost of corrosion damage could be avoided. The avoidable costs were related to the failure to use the best corrosion prevention practices available.

There are several ways of combating corrosion. One method that is gaining wider acceptance is the use of vapor phase corrosion inhibitors. These chemical compounds combine their volatility at room temperature with their corrosion-inhibiting properties. VCI compounds can readily reach inaccessible crevices in metallic structures. Protective vapors disseminate within an enclosed space until equilibrium is reached. This equilibrium is determined by the partial vapor pressure of the VCI compound.

Volatile corrosion inhibitors (VCIs) were originally developed to protect boilers and piping systems of ships to be mothballed. Their effectiveness and ease of application attracted early users. Over the years, the field of usage has increased to cover electronics, packaging, process industries, reinforced concrete, coatings, and metalworking fluids.

VCI films based on polyethylene are used in numerous applications. These films are either recycled or disposed of in landfills. Due to a very limited amount of land space, several countries have enacted laws to severely reduce the disposal of plastic materials into landfills. An attractive alternative to using polyethylene is biodegradable resins. When placed in the right conditions, these resins will biodegrade into non-toxic compounds.

EXPERIMENTAL
A biodegradable VCI film using a polyester-based resin (poly (butylene) succinate and adipate) was prepared for this study. This polymer is stable in the atmosphere, but is biodegradable in compost, wet soil, fresh water, seawater and activated sludge.

Corrosion testing
There are several methods to measure the effectiveness of vapor phase corrosion inhibitors. One method that is used quite widely is the Vapor Inhibiting Ability (VIA) test method. It was developed to rapidly assess the protection offered by VCI compounds. The tested products can be powders, liquids or packaging products such as papers or plastic films. The test consists of placing a freshly polished carbon steel specimen in a 1-liter glass jar. The jar contains a measured amount of water blended with glycerin to control the relative humidity. A control sample is made of a jar containing only a steel specimen, while a test sample comprises of a jar with a steel specimen along with the VCI source (powder, liquid or packaging product). The VCI source never comes in contact with the metal specimen. After a conditioning period during which the VCI vapors are allowed to migrate from the source to the metallic specimens, the jars are placed in an oven set at an elevated temperature for a few hours. Once this time elapsed, the jars are placed at ambient temperature. The metal specimen is rapidly cooled leading to condensation due to the humid atmosphere. Effective VCI compounds provide protection in this environment, while the control specimen heavily corrodes. In this test method, a visible change in the surface finish, such as pitting or etching, is considered as corrosion. Stain alone does not constitute corrosion.

Biodegradation testing

The biodegradation of the VCI film was evaluated per ASTM D 5338 *(Determining Aerobic Biodegradation of Plastic Materials Under Controlled Composting Conditions).* The polymer samples were exposed to aerobic biodegradation by contact with composting material at 58ºC. The results were compared to the biodegradation rate of cellulose (positive control).

Chronic toxicity

Chronic toxicity was evaluated by performing seven-day static, renewal chronic toxicity tests. These chronic toxicity tests were carried out to identify whether exposure to the water extracts would potentially produce sub-lethal, long-term (chronic), adverse effects on aquatic organisms. A water extract was prepared following the procedures specified in ASTM D 5151-91 *(Standard Practice for Water Extraction of Residual Solids from Degraded Plastics for Toxicity Testing).* The test organisms were larval fathead minnows. The chronic screening toxicity tests were performed in accordance with methods specified by Weber *et al*. (1991). Chronic toxicity was determined to have occurred if the growth of test organisms in the extract exposure were significantly less than that of the control organisms.

DISCUSSION

Corrosion testing

The control metal specimen had heavy corrosion, while the metal specimens placed in the presence of the VCI film had no signs of corrosion.

Biodegradation

The amount of carbon from the VCI film converted to CO_2 during the test was 46-47% of the total carbon present in the sample.

The efficiency of CO_2 produced, when compared to the maximum theoretically calculated CO_2 that should have been produced, ranged from 92 to 128% for the sample. The carbon conversion efficiency for the positive control (cellulose) was 58%.

The weight loss for the film ranged from 36 to 51 %. The positive control (cellulose) had a weight loss of 100%.

Based on the carbon conversion and the overall weight loss, the polyester-based VCI film is considered to have good biodegradability.

Chronic toxicity

Mean percent survival of the larva fathead minnows exposed to control and extract solutions was 97.5% survival in both the control exposure and in the 100% extract exposure. Mean dry weight of fish exposed to the control and leachate exposures equaled 0.47 mg/fish for the lab control and 0.44 mg/fish for the 100% extract exposure. Based on these test results, the extract had no significant adverse effects on larval fathead minnows.

SUMMARY

A new generation of VCI film has been developed to address the disposal concerns that some of the polyethylene VCI films have. Corrosion and biodegradation testing demonstrated that these new films not only provide excellent corrosion protection, but also readily degrade when placed in composting conditions. Chronic toxicity testing also proved that these films have no detrimental effects on aquatic organisms.

STRATEGIC MATERIAL DESIGN ENABLES GREEN TECHNOLOGY FOR THE ENVIRONMENT

Shahab Siddigui, John R. Szwec, and Kariofilis Konstadinidis
Lucent Technologies, Inc., Bell Laboratories, 2000 Northeast Expressway, Norcross, GA 30071

ABSTRACT
Coloring of individual optical fibers is necessary for identification purposes in the finished cable. Organic solvent-based inks have typically been used for that; however, they pollute the environment with toxic and hazardous emissions. Recently use of organic solvent based inks posed a serious problem for us at the Lucent-Atlanta location. As more and more optical fibers were colored with solvent inks in recent times, the level of harmful emissions increased at the same time. Soon it reached the allowable annual emission limit for the location and caught the attention of local environmentalists, state legislators and regulators. However, Lucent Technologies Inc., as a corporation is strongly committed to protecting the environment as well as the health and safety of its workers and people in the community. To this end we have been proactively pursuing for a viable alternative for some time. Here we describe how we accomplished this strategic goal by implementing the state-of-the-art UV technology, which completely eliminated VOC and HAP emissions from the optical fiber coloring arena. We also describe how we championed the complex development of new UV curable materials for the specific application. Overall the UV system enabled a safe and clean 'green technology' for the environment while making quality products at reduced cost.

INTRODUCTION
Industrialization is certainly a boon to the society because that is what has brought about tremendous technological advancement for modern life comfort, convenience and human intelligence. Whether it is in the world of microelectronics, space aviation, telecommunication, photonics, plastics, or everyday consumer products, each respective industry makes its products or parts involving multiple processing steps and materials. While making the final product for beneficial use, we have been inadvertently hurting the environment by releasing harmful by-products into the surroundings, which sometimes goes unnoticed since some of them are invisible. Take the case of microelectronics, which makes high-speed chips for the interconnection technology. Here we still today use lead-soldering process for making circuit boards. Lead is undoubtedly harmful for the environment. Likewise, industries using coatings for protective and other useful purposes have been cumulatively polluting the environment over the years by releasing solvent to the environment. Solvent is an invisible by-product of solvent-borne coatings. Majority of solvents used in these coatings is now known to be deadly toxins. This is a huge price to pay for technological advancement considering the environment as well as the community in which we live is being threatened continuously as we make new products using potentially harmful precursors.

Most recently, however, the trend is rapidly changing.[1-3] Green revolution has taken a strong hold globally. This is a measure to keep the global environment safe and clean. Here in the United States, the movement started with the Clean Air Act (CAA) promulgation in 1970, in which the U. S. government gave authority to the Environmental Protection Agency (EPA) to set national air quality standards to protect against common pollutants. Since then the EPA, Occupational Health and Safety Administration (OSHA), state legislators, local environmental regulators and emerging environmental awareness clubs have been acting together to strictly regulate VOC (volatile organic compounds), HAP (hazardous air pollutants), ODC (ozone depleting chemicals) and other toxic emissions. Industries using solvent-based coatings in the past have now been obligated to take part in the green revolution by committing to new systems, which produce very little or no VOC and HAP emission. These novel alternatives are designed to ensure environmentally benign manufacturing as a step to safeguarding the environment and its people.

Both water-based and radiation (that is, Ultra Violet-UV and Electron Beam-EB) curable coating technologies have been equally hailed in this green revolution since each is deemed a befitting partner to combat the undesirable depletion of the environment by hazardous emission. Both technologies produce little or no harmful emission to the environment and thus, are being gradually proven-in as best available control technology (BACT) throughout the industry to replace solvent-based coatings and inks.

The manufacture of optical fiber involves use of protective polymeric coatings. It involves use of clear coatings in the outer layers to provide rigidity and handlability to the central glass core that transmits information. The outer-most layer that is built by applying another polymeric coating, however, is colored for identification purpose in the finished packaged ribbons and cables. Traditionally, clear UV coatings have long been used in the inner layers (primary and secondary coatings) while solvent-based pigmented coatings has been used in the

outer-most layer of optical fiber. Solvents used in these color coatings (inks) are considered not only VOC but also HAP. The optical fiber market has been experiencing an explosive growth for some time since there is an insatiable demand for its deployment in telecommunication for high-speed high bandwidth data, voice, and video and Internet connectivity. As the growth for fiber rose, so did the concomitant emission to the environment from using large volume of solvent-borne coatings in making fiber optic products. Naturally that is not good news for the environment!

Lucent Technologies, Inc., as a corporation is deeply committed to its people and the community for a safer and healthier environment. To that end, we have always been proactively working to drastically mitigate or eliminate emission of harmful components into the environment in all our manufacturing locations. In optical fiber manufacturing, for example, we made some strategic moves in recent years to increase fiber production capacity without jeopardizing the environment by pollution. Our business goal was to rapidly capture significant market share in the optical fiber business. One key strategy to achieve this was in the area of proper material selection for coloring optical fibers. Solvent-based inks became the biggest hurdles for manufacturing expansion because of accompanying increase in emission level beyond what is legislated by the state. They were replaced by just in time development of state-of-the-art UV curable inks, which do not produce any emission. Although the replacement was not straightforward because of complexity in material design and product performance issues, the final development of the UV technology was completed in 1997. Its immediate deployment in coloring optical fibers has certainly helped accomplish all critical corporate goals. This green manufacturing technology does not pollute the environment. At the same time, it makes product faster and in turn, cheaper because of higher throughput and better quality.

In this report, we briefly outline the UV technology and the design aspects of the novel UV curing materials as a strategic move in the right direction to herald green technology movement for rapidly making cleaner and better products while maintaining a safer environment.

RADIATION CURING AND UV TECHNOLOGY

In coatings terminology, curing refers to the conversion of a liquid into a solid system. Radiation (light) curing by electron beam (EB) and ultra violet (UV) technology has most recently been spurred by escalating costs of energy but most importantly by increasing concerns of damaging the environment by using solvent-based coatings. A solvent-based coating usually contains 70-80% solvent, which is totally released to the environment upon thermal drying/curing and is a complete waste of materials. The radiation curable coating, on the other hand is almost a 100% solid system, which means that upon curing by radiation (light) there is minimum or no loss of material into the environment. In that sense, it is truly an environmentally responsive system since it is not designed to harm the environment by invisible ingress of foreign compounds. In addition to emission control, the radiation curing technology provides unsurpassed product quality (better thermal stability, higher solvent and abrasion resistance, etc.) and higher processing speed. Truly, for all these reasons the radiation technology, notably the UV technology is now considered a big player in the green technology movement for the environment and the community.

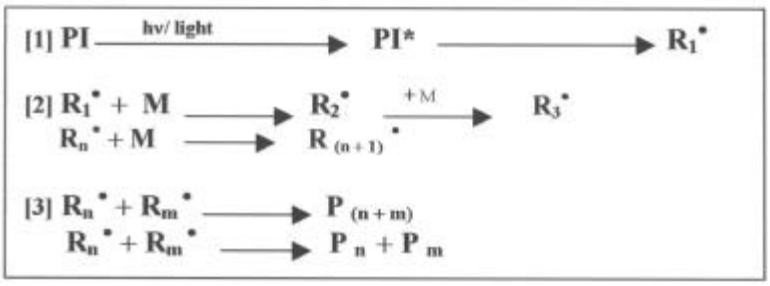

Traditionally, photo-polymers (light/radiation sensitive polymers) contain (1) monomers, (2) oligomers, (3) photoinitiators and (4) some additives. EB polymers/coatings do not contain photoinitiators, which cuts down material cost significantly. The reaction mechanism consists of three steps: initiation, propagation and termination (see Scheme 1 below).

Scheme 1. Photopolymerization Reaction Mechanism

Scheme 1 shows a free radical polymerization reaction pathway; however, UV reaction can also be initiated by photo-generated cations in an alternative mechanism involving separate chemistry. In the above initiation step, photoinitiator (PI) absorbs light to go to its excited state followed by subsequent reaction to generate a free radical. In the propagation step, this radical ($R_1^{\bullet}$) aids in the polymer chain growth by adding to the monomer (M) and oligomer. In the final step, termination of photopolymerization reaction occurs via recombination or

disproportionation reaction.

UV MATERIAL DESIGN CONSIDERATIONS

For development of optical fiber color coatings, we chose the UV technology since it is a mature, well-advanced and economic processing alternative compared to the EB technology today. Basically, we developed the UV radiation sensitive materials in close partnership with a world-class UV curable coating manufacturer. The UV ink does not contain any VOC or non-VOC component that can be easily emitted to the environment. Moreover, the absence of solvent in the ink eliminated fire hazards associated with most solvents. The fundamental material properties (e.g. color, viscosity, pigment dispersion quality, etc.) were quite easily formulated in this new pigmented set of color coatings. However, the big challenge was in matching some of the key material properties across twelve diverse colors to perform acceptably in the ribbon-packaged product. Two such characteristics that are diametrically opposite from design perspectives are low surface friction of colored fibers and certain level of interfacial adhesion of colored fiber to the matrix material, a polymeric material used to envelop multiple fibers (12 or more) in the ribbon structure. This turned out to be a very demanding requirement for the UV ink development program since an ink additive that is used to make the surface sleek normally affects ink/matrix adhesion adversely at the same time. That is, a sleeker ink surface would have lower than requisite ink/matrix adhesion (see Figure 1), which in turn negatively impacts ribbon performance characteristics.

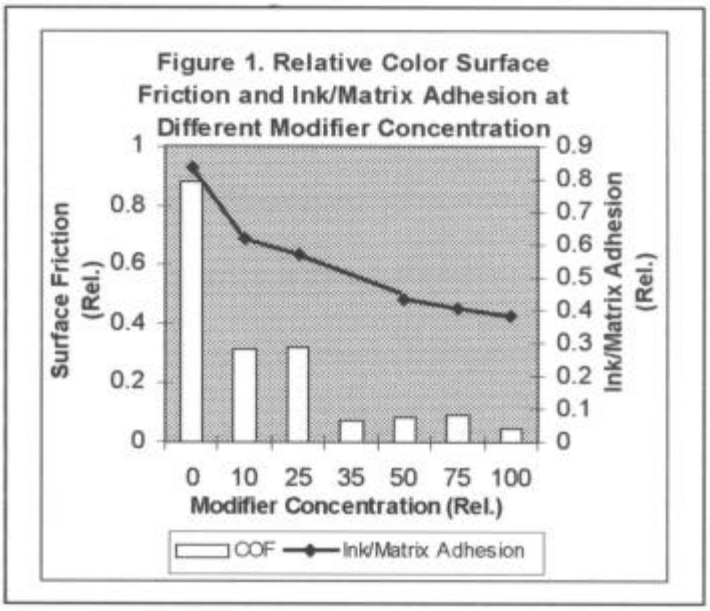

Adjustment of the two above mutually opposing characteristics needed optimization of the 'modifier level' concentration in the final UV ink formulation for all twelve colors. Additionally, a process window study was undertaken for seamless coloring operation and ribbon processing by statistical design of experiments.[4] At the end, the UV technology was successfully implemented in the Atlanta Optical Fiber manufacturing location for coloring fibers, which replaced the solvent-bearing inks system. This completely eliminated VOC and HAP emissions in the area thereby introducing a 'green technology' in the plant.

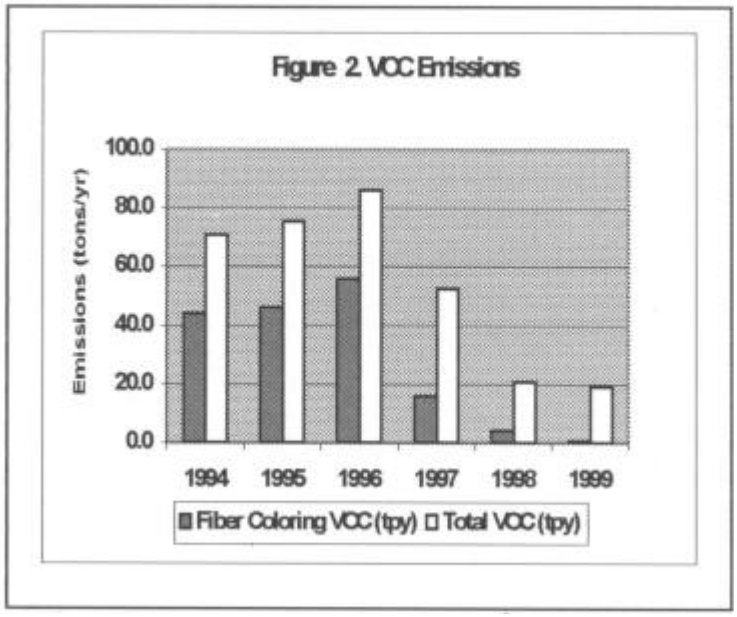

ENVIRONMENTAL AND OTHER BENEFITS

The introduction of new UV curing color-coating materials along with the emerging UV technology has recently placed Lucent-Atlanta facility in a strategically advantageous position. In 1997, the implementation of UV technology was begun which drastically reduced the level of VOC emission compared to preceding years (see Figure 2). In fact, the company came under scrutiny by the State of Georgia Environmental Protection Department (EPD) in 1994 to limit emission to the permissible 25 tons/year. At the same time, however, the manufacturing capacity needed to be scaled up because of a worldwide demand for optical fibers. In order to be in compliance with regulatory laws as well as support business growth, we acted proactively to propose a RACT (Reasonably Available Control Technology) plan to the State where we committed to fully develop the UV technology by 1996. The timely fulfillment of our commitment was highly significant since it provided a permanent solution to expanding

business without ever adding harmful emission to the environment. Note that the emission from color coatings area has been steadily declining since its gradual introduction in 1997. In 1999, the VOC emission from fiber coloring is almost negligible (see Figure 2).[5] In addition to environmental benefits, the UV technology has also improved the quality of our products. It makes them faster, better and hence, cheaper.

CONCLUSION

The strategic color coating material design involving UV technology provided significant achievements in a very short time. First and foremost, it made us as an important partner in the green revolution for a cleaner environment. It also helped us make very robust high-quality products with much higher throughput than ever before. Additionally, the green technology has vastly widened the business scope for unabated growth in manufacturing without ever polluting the environment at the same time. This is highly significant since it removes material and processing as formidable hurdles in business growth. The UV technology can potentially utilize 100% of materials without much material waste if proper processing technology is in place. This is where we are focused today globally- eliminate VOC emission and material waste entirely from manufacturing. To this end, Lucent-AtIanta facility was just awarded the ISO 14001 Certification in 1999 for its outstanding environmental management system. However, much work remains to be done ahead in the future. Achievements like implementation of new UV materials and establishment of ISO 14001 are just the opening volleys on our part in the struggle to win the green revolution. The work in progress is to continually "reduce, reuse and recyle" material for maintaining clean and safe environment for all living organisms on this planet while making useful products for the benefit of mankind in the twenty-first century.[6]

REFERENCES

1 . Susan Crum, "The Green Revolution: Electronics Manufacturing and the Environment" *Electronic Packaging and Production,* pp 20-24, April 2000.
2. "The Environment - A Cleaner Tomorrow Through Photonics", An overview by industry experts. *Photonics Spectra,* pp. 101-124, April 1998.
3. Barry Ritchie and Lester Bennington, "New Conformal Coatings Combine Protection with Environmental Safety", *SMT*, pp. 44-48, April 2000.
4. K. Konstadinidis, N.W. Sollenberger, S. Siddiqui, K.W. Jackson, J.M. Tumipseed, T.W. ALI, R.P. DeFabritis, C.R. Taylor, "UV Color Coatings and Matrix Material Design for Enhanced Fiber Optic Ribbon Products", Proceedings of the 46th International Wire and Cable Symposium, pp. 274-280, 1997.
5. M. Gaeth, Lucent Technologies Inc., provided data and the graph on the VOC emission.
6. Donald A. Carr, J.D., Chuca Meyer, Lawrence H. Keith, Robert E. Hall, Rhonda Harris, Stephen F. Gorden and Gregg A. Cooke, "Environmental Forecast for the 21st Century", *Environmental Protection*, pp. 14-28, January 2000.

4th Annual Green Chemistry &
Engineering Conference

Sustainable Technologies:
From Research to Industrial Implementation

June 27 - 29, 2000

BENIGN SYNTHESIS AND PROCESSING I

PRODUCING DIMETHYL CARBONATE FROM CO_2 AND METHANOL - A GREEN CHEMISTRY ALTERNATIVE TO PHOSGENE AS A CHEMICAL INTERMEDIATE

J. Yong Ryu, Sr. Scientist
CDTECH/CR&L, 10100 Bay Area Blvd, Pasadena, TX 77507
Abraham P. Gelbein
Consultant to CR&L, 3500 Pinetree Terrace, Falls Church, VA 22041

ABSTRACT

A cost-effective new process producing dimethyl carbonate (DMC) from methanol and urea in a single step has been developed. Ammonia is a co-product, which is recycled to a urea plant in commercial practice. The net result is synthesis of DMC from methanol and carbon dioxide. The technical achievement was accomplished by discovering a novel homogeneous organotin complex catalyst solvent system and by combining innovative reaction and separation technology. The process is economically superior and more environmentally friendly than the conventional technology. The commercial potential of the process has been evaluated by estimating capital and production cost for a large-scale plant, and comparing the results with current state-of-the-art practices.

EXECUTIVE SUMMARY

The new process pertains to the development of an environmentally friendly, raw material and energy efficient process for producing dimethyl carbonate (DMC) and ammonia from methanol and urea. Since urea is produced from carbon dioxide and ammonia, recycling the ammonia product from DMC production to urea production has the net effect of making carbon dioxide one of the primary raw materials rather than urea. The process is being developed by CDTECH and Chemical Research & Licensing Company (Pasadena, Texas) and is in the R&D stage. Two patents have been granted covering aspects of the process and the novel homogeneous catalyst[1]. DMC has also been identified as an environmentally friendly fuel oxygenate additive - a possible alternative to MTBE - but only if the price of production is significantly reduced.

Over the past several decades the chemical industry has been interested in finding economic alternatives to phosgene as a chemical intermediate to introduce carbonate functionality into molecules, for example, in the production of polycarbonates and polyurethanes. These products have multi-billion lb./yr. markets. The goal was to eliminate the use of a very hazardous material and the need to dispose of chloride containing waste streams. It has long been known that DMC could be used for this purpose but it wasn't until relatively recently that a technology was available to produce DMC at a cost that could justify its use in new polycarbonate plants. This technology is based on the reaction of methanol, carbon monoxide, and oxygen in the presence of a copper chloride catalyst[2]. However, the cost of production is still too high to encourage the replacement of phosgene in existing polycarbonate plants or the use of DMC in other applications such as solvent.

CDTECH's new process is a “green chemistry" approach to DMC. A prior art[3] exists but a practical process was never developed because of yield and separation problems. This chemistry has been known for some time[4]. In the new process, these problems are overcome through the discovering of a novel homogeneous catalyst, and employing innovative reaction and separation technology. The patented catalyst is dibutyltin dimethoxide complex with triethylene glycol dimethylether (triglyme). Triglyme is used as solvent for the reaction medium as well. Triglyme has low volatility under the reaction conditions and is a non-hazardous low volatility solvent that is readily contained in the reactor. DMC selectivity is enhanced by rapidly removing the DMC from the reaction zone. This has been accomplished by conducting the chemical reaction in a reaction-distillation environment under low pressure. Near stoichiometric yield of DMC has been demonstrated using methanol as the stripping vapor.

A process concept for the new process has been simulated and estimates of capital and production costs prepared for a range of commercial scale plants. The results indicate significant competitive advantages over the current state-of-the-art practice. The relatively low estimated sales price has the potential of greatly accelerating the phase out of phosgene use in polycarbonate manufacture as well as promoting the use of DMC as an economically acceptable and environmentally friendly fuel oxygen additive.

THE NEW PROCESS TECHNOLOGY PERTAINS TO AN ALTERNATIVE SYNTHETIC PATHWAY FOR GREEN CHEMISTRY

Dimethyl carbonate is currently produced from methanol, carbon monoxide and oxygen in the presence of a

cuprous chloride catalyst according to the following reaction stoichiometry:

$$2\ CH_3OH + CO + 0.5\ O_2 \rightarrow (CH_3O)_2CO + H_2O$$

Reaction conditions are ~125ºC and ~25 atm. Claimed (patent) selectivities are near 100% based on methanol converted and ~90% based on CO converted. By-products such as methyl chloride and dimethyl ether are produced as well as CO_2. The system is highly corrosive and requires careful design to avoid forming explosive mixtures. Spent catalyst is a hazardous waste.

The new technology produces DMC by reaction of methanol and urea in the presence of a novel organotin complex catalyst (dibutyltin dimethoxide-triglyme) according to the following reaction stoichiometry:

$$2\ CH_3OH + (NH_2)_2CO \leftrightarrow (CH_3O)_2CO + 2\ NH_3$$

Reaction conditions are ~180ºC and 7 atm. Demonstrated selectivities are near 100% based on methanol and urea converted. A small amount of methyl amine by-product is produced and recovered. The system is non-corrosive, does not involve the use of hazardous materials, and produces essentially no waste products. Integrating the DMC plant with a urea plant allows efficient recycle of the ammonia to urea production:

$$2\ NH_3 + CO_2 \rightarrow (NH_2)_2CO + H_2O$$

The net effect is a process for producing DMC from methanol and CO_2:

$$2\ CH_3OH + CO_2 \rightarrow (CH_3O)_2CO + H_2O$$

A process flow scheme was conceived and simulated using process simulation software. Material, energy balances, and equipment specifications were generated for plant capacities of 10-230 MM lb./yr. Based on this information factored battery limits and offsite capital costs were estimated. The material and energy balance data, unit prices for raw materials, utilities and labor, and factored capital related costs were used to prepare cost of production estimates. Results were compared with comparable values for the state-of-the-art commercial technology (ENIChem, Italy) described above. The comparison indicates a very significant advantage for the new process technology.

SIGNIFICANT ENVIRONMENTAL AND ECONOMICAL BENEFITS OF NEW PROCESS TO BOTH INDUSTRY AND SOCIETY

Most producers of polycarbonate (PC) in the world use phosgene (highly toxic gas) as the source of carbonate functionality in the polymer. The polymer can be formed directly via the reaction of bisphenol A with phosgene (solution polymerization) or indirectly by first forming diphenyl carbonate (DPC) from phosgene and phenol and then reacting the DPC with bisphenol A (melt polymerization). In both routes ~0.44 lbs. phosgene is consumed per lb. of polymer. The chlorine value in the phosgene is released as HCl and is generally captured as NaCl corresponding to ~0.52 lb. of salt per lb. of polymer. The magnitude of this waste stream on an industry wide basis can be appreciated when one considers that U.S. production of PC in 1998 was ~1 billion lbs./yr., global production was ~3 billion lbs./yr., and market growth is projected at 10%/yr through 2002.

DMC can replace phosgene in the production of DPC. Also the methanol generated in the process can be recycled to DMC production. The net effect is to make PC production a safer operation with greatly reduced emissions. At this time, however, the cost of DMC produced by the current state-of-the-art is limiting the commercial introduction of phosgene replacement with DMC. The lower cost of DMC produced via the nominated technology should accelerate this very desirable changeover.

As noted above the production of DMC via the new process uses CO_2 as a primary raw material. If DMC is used in PC manufacture, the amount of CO_2 incorporated into the polymer is 0.19 lb./lb. PC. This corresponds to consuming ~55 MM lb./yr. CO_2 for a typical 300 MM lb./yr. PC plant. It is understood, however, that in order to have impact on reducing "green house gases" this CO_2 (part of the CO_2 feed to the urea plant) would be sourced from a CO_2 rich stream that is ordinarily vented to the atmosphere (e.g., by-product CO_2 from a H_2 plant).

DMC has been investigated as a potential oxygenates additive in RFG[5]. It is readily biogradable, has a pleasant fruit-like smell, and a gasoline blending RON of 110-130. Further it has an oxygen content almost three times

that of MTBE (53 wt. % vs. 18 wt. %) so that on a weight basis only one third as much DMC is required to achieve the same oxygen level in RFG as MTBE. On a volume basis the differential is even higher. For example to meet a specification of 2.7 wt. % oxygen, a gallon of gasoline would have to contain 3.8 vol. % DMC compared to 15.7 vol. % MTBE. If MTBE were priced at 68¢/gal., the equivalent DMC price would be 32¢/lb. This price is well above the estimated product value (including a 30% return before tax) of DMC produced in an 1800 bbl/day plant based on the new process technology. DMC is the only effective additive for reducing particulate emissions for diesel fuel[6]. Therefore, assuming DMC is an acceptable alternative to MTBE from the regulatory perspective, it could be provided to the consumer at no additional cost.

SIGNIFICANT CONTRIBUTION OF THE NEW PROCESS TO CHEMICAL INDUSTRY

The new process is a "green chemistry" approach to DMC. Converting the known chemistry to successful commercial process requires identifying the key obstacles. The obstacles are high cost of DMC separation, undesired by-products and high cost of capital for a new plant. These obstacles are overcome by inventing the method carrying out the reaction in a single step under low pressure, discovering novel homogeneous catalyst, and putting together all the pieces to design a process scheme. The process is practically zero discharge into environment. All of these are translated into very low DMC production cost compared with the current state-of-art technology.

DMC from the new process is cost effective to warrant a number of applications in chemical raw material, solvent and fuel additive.

REFERENCES

1. US 5,902,894 (5/1999) and US 6,010,976 (1/2000)
2. EP 0 460 735 A2 (12/1991)
3. WO 95/17369 (6/1995)
4. P. Ball *et al*. *C_1 Mol. Chem*., **1**, 95, 1984 and ACS, Div. of Polymer Chemistry, Polymer Preprints, **25**, 272, 1984
5. M.A. Pacheco *et al*., *Energy & Fuel*, 1977, **11**, 2-29
6. US 4,891,049

ENVIRONMENTALLY BENIGN CARBAMATE SYNTHESIS

Steven S. C. Chuang, Yawu Chi, Pisanu Toochinda, Bei Chen and Mahesh V. Konduru
Department of Chemical Engineering, The University of Akron, Akron, OH 44325-3906

ABSTRACT

Carbonylation of nitrobenzene and aniline on supported metal catalysts through oxidative and reductive pathways provides an environmentally benign route for carbamate and isocyanate synthesis. Infrared studies suggest that both oxidative and reductive carbonylation proceed via the insertion of adsorbed CO into adsorbed nitrene which is formed from the reductive deoxygenation of nitrobenzene and oxidative dehydrogenation of aniline. Mechanistic studies show that the gas-liquid-solid catalyzed carbamate synthesis is limited by the low concentration of CO and oxygen in the liquid phase; gas-solid catalyzed carbamate synthesis is limited by the accumulation of products on the active sites of the catalysts. With appropriate catalysts, oxidative carbonylation can take place at significantly milder conditions than reductive carbonylation.

INTRODUCTION

The major goal of the environmentally benign chemical synthesis is to prevent pollution. Development of this synthesis technology, to a great extent, relies on innovation in design of synthesis pathways and their catalysts to bypass toxic feedstocks, combine process steps, increase selectivity and yields of products, and reduce energy use and risk at source. One notable research effort is the use of either oxidative or reductive carbonylation to replace the phosgene-amine reaction for isocyanate and carbamate synthesis.

Most carbonylation reactions have been carried out by homogeneous catalysis at pressures above 3.5 MPa[1]. Our objective is to develop a catalytic process for heterogeneous carbonylation at low pressure conditions,

eliminating the use of solvent and the catalyst recovery step. Figure 1 provides a schematic of the proposed mechanism which delineates the steps required for carbamate synthesis from carbonylation on the catalyst surface. In reductive carbonylation, the reaction begins with N-O bond dissociation for deoxygenation of nitrobenzene, CO insertion into adsorbed nitrene, dehydrogenation of alcohol to form alkoxide, and O-C bond formation between the carbonyl species and the alkoxide to form carbamate. In oxidative carbonylation, the reaction involves dehydrogenation of aniline and alcohols to produce the same type of adsorbates postulated for reductive carbonylation. The major roles of oxygen are to remove hydrogen from aniline and alcohol and to provide the thermodynamic driving force, allowing the oxidative carbonylation to occur at mild conditions.

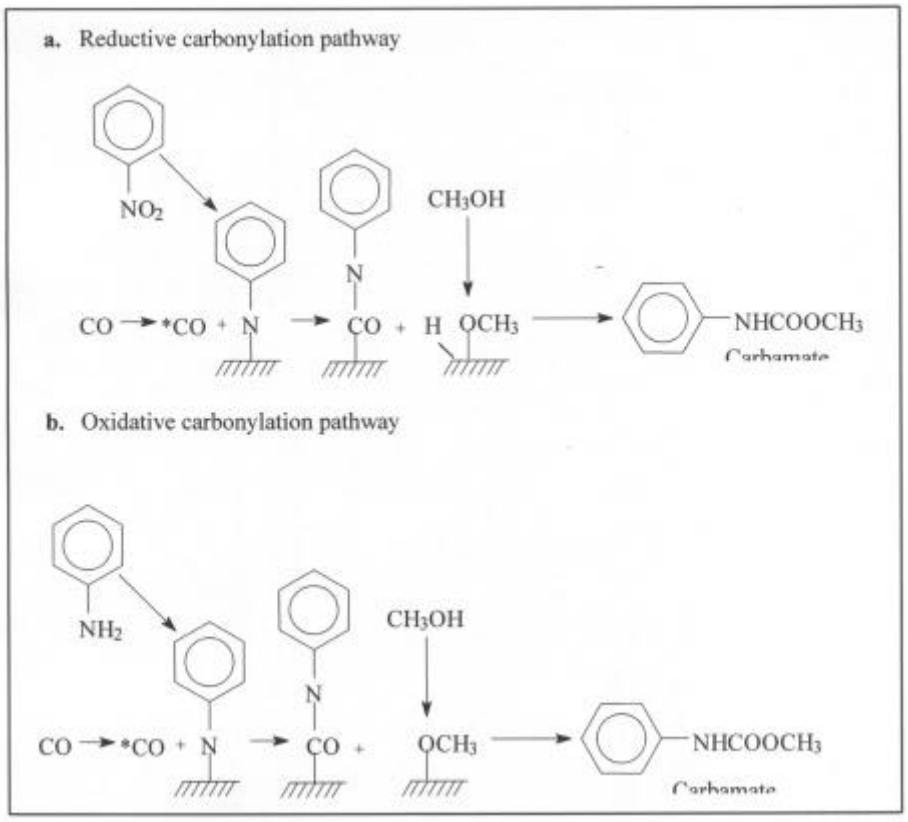

Figure 1. Reaction pathways during the carbonylation reactions

Carbamate can be selectively converted to isocyanate and vice versa. One distinct advantage of using carbamate as a precursor for investigating carbonylation is its low toxicity. Carbamate is also an important intermediate for chemical syntheses in agrichemistry and the pharmaceutical industry[2]. The present study was aimed at determining the reactivity of adsorbed CO for oxidative carbonylation of aniline with $CuCl_2$-$PdCl_2$/ZSM-5 at 0.101 MPa and 438 K (mild reaction conditions compared with those reported in literature).

EXPERIMENTAL

The $CuCl_2$-$PdCl_2$/ZSM-5 was prepared by the sequential impregnation of $PdCl_2$ onto the $CuCl_2$/ZSM-5 that was prepared by the incipient wetness impregnation of $CuCl_2$ into H-ZSM-5. The ratio of Cu to Pd was 1.4. The catalyst was dried in air at 298 K for 24 h.

A self-supporting disk of the catalyst weighing 25 mg was pressed by a hydraulic press at a pressure of 4000-4500 psi. The disk was placed in the IR beam path of the reactor cell[3]. The catalysts were exposed to 66 cm^3/min flow of CO/O_2 (CO/O_2=10) at the reaction temperature and the volatile organic reactants such as aniline and methanol were injected into the reactor with the aid of a liquid syringe through a septum present at the reactor inlet. IR spectra were collected at regular time intervals.

RESULTS AND DISCUSSION

IR spectra of $CuCl_2$-$PdCl_2$/ZSM-5 taken during the addition of CO (g) and 200 µl of aniline/methanol/NaI (17.1/79.3/3.6) at 438 K and 0.101 MPa is shown in Figure 2. Addition of the reactants led to the appearance of linear CO at 2082 cm^{-1} and 2051 cm^{-1}, N-H bending at 1615 and 1604 cm^{-1}, C=C aromatic stretch of the aromatic species at 1520 and 1506 cm^{-1}, C-H bending at 1453 cm^{-1}, methoxy (CH_3O^-) at 1347 cm^{-1}, and C-N stretching at 1266 cm^{-1}. Increase in reaction time from 3 to 10 min led to a decrease of all the adsorbed reactant species and formation of CO_2 (g) at 2363 and 2331 cm^{-1} as well as an increase in the C=O stretching (1765 cm^{-1}) and C-O stretching (1203 cm^{-1}) of the methyl phenyl carbamate species, suggesting that the carbamate species can be produced via the oxidative carbonylation of aniline at 0.101 MPa.

The rapid growth of the carbamate band in Fig. 2 demonstrates the high activity of $CuCl_2$-$PdCl_2$-NaI catalyst in oxidative car- bonylation. The excellent activity of $CuCl_2$-$PdCl_2$-NaI/ZSM-5 catalysts for oxidative carbonylation can be attributed to the high dehydrogenation activity of $CuCl_2$ and $PdCl_2$ and promoter effect of NaI. The redox cycle of $CuCl_2$ and $PdCl_2$ observed in Wacker catalysis[4] may play a role and remains to be investigated.

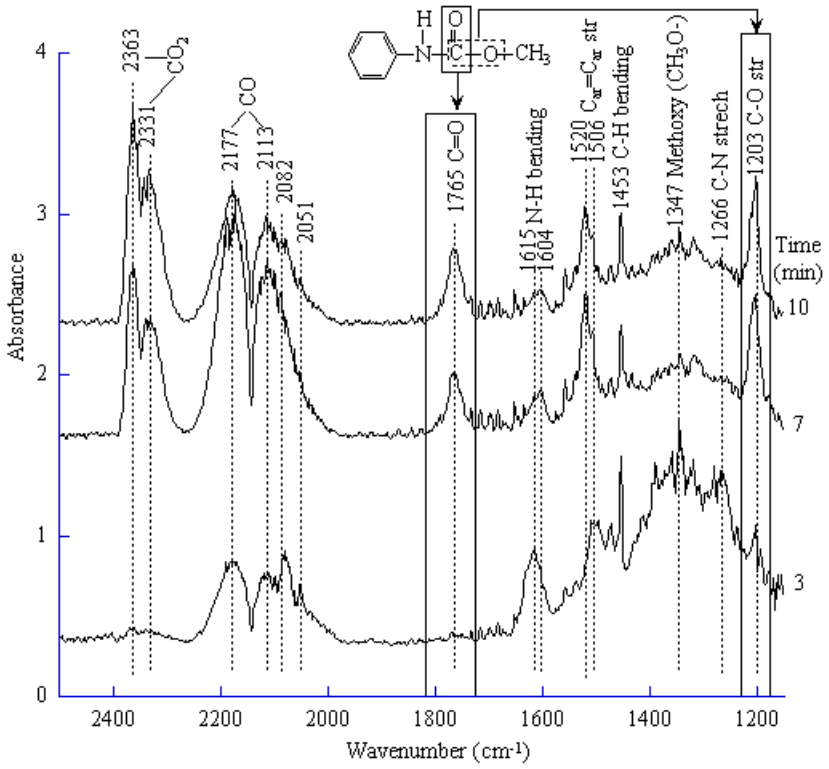

Figure 2. IR spectra during oxidative carbonylation on $CuCl_2$-$PdCl_2$/ZSM-5 at 438 K and 0.101 Mpa

CONCLUSION

This study demonstrates that adsorbed CO is involved in oxidative carbonylation on $CuCl_2$-$PdCl_2$-NaI catalysts to produce carbamate. Mechanistic studies show that the gas-liquid-solid catalyzed carbamate synthesis is limited by the low concentration of CO and oxygen in the liquid phase; gas-solid catalyzed carbamate synthesis is limited by the accumulation of products on the active sites of the catalysts. The reaction provides a potential route for an environmentally benign synthesis of isocyanate under mild reaction conditions. The absence of harmful organic solvents in this reaction process not only reduces the environmental risk but also eliminates the catalyst recovery step. The catalyst remained to be tested for a large number of analogous oxidative carbonylation reactions.

ACKNOWLDEGMENT

This work has been supported by the United States National Science Foundation under Grant CTS 9816954.

REFERENCES

1. Cenini, S., Pizzotti, M., and Crotti, C., "Metal Catalyzed Deoxygenation Reactions by Carbon Monoxide of Nitroso and Nitro Compounds" in Aspect of Homogeneous Catalysis: A Series of Advances, vol. 6, Ugo, R., Ed.; D. Reidel Publishing, Holland, 1988; pp 97-198.
2. Parshall, G.W., and Lyons, J.E., "Catalysis for Industrial Chemicals" in Advanced Heterogeneous Catalysts for Energy Applications; U.S. Department of Energy, 1994; Chapter 6.
3. Chuang, S.S.C., Brundage, M.A., Balakos, M., and Srinivas, G., *Appl. Spectrosc.* **49**, 1151 (1995).
4. Gates, B.C., Catalytic Chemistry, John Wiley & Sons, Inc., New York, 1992.

DEOXO-FLUOR™ REAGENT: A NEW BROAD-SPECTRUM DEOXOFLUORINATING AGENT WITH ENHANCED THERMAL STABILITY

G. S. Lal, Research Assoc., CSTC; G. P. Pez, Chief Scientist, CSTC;
F. M. Prozonic, Sr. Principal Research Chemist, Corporate Div.;
R. J. Pesaresi, Chemist, CSTC; H. Cheng, Sr. Principal Chemist, RES;
R. K. Agarwal Lead Engineer, CSTC; J. J. Hart, Pilot Plant Mgr., Specialty Gases R&D;
J. M. Schork, Research Mgr., Elec. Spec. Gases;
G. T. Saba, Business Mgr., Selective Fluorination;
G. B. Madhavan, Commercial Development Mgr., Selective Fluorination;
R. Taege, Fluorination Technology Manager, Packaged Gases Europe
Air Products and Chemicals, Inc., 7201 Hamilton Blvd., Allentown, PA 18195

ABSTRACT
The Deoxo-Fluor™ reagent [bis (2-methoxyethyl) aminosulfur trifluoride] $(CH_3OCH_2CH_2)_2NSF_3$), is effective for converting alcohols to alkyl fluorides, aldehydes/ketones to the corresponding gem-difluorides and carboxylic acids to their CF_3 derivatives. It is a thermally much more stable, broad spectrum alternative to the traditional dialkyl amino sulfur trifluoride (DAST) deoxofluorinating agents. Air Products and Chemicals, Inc. has successfully brought the Deoxo-Fluor reagent from discovery to commercial production; major pharmaceutical companies are currently using it in their new products developmental pipeline.

BACKGROUND/INTRODUCTION
Deoxofluorination chemistry has traditionally been performed using sulfur tetrafluoride, SF_4 or N,N-diethylamino-sulfur trifluoride, DAST (Et_2N-SF_3). Sulfur tetrafluoride is very effective for the conversion of ketones to gem-difluorides and of carboxylic acids to -CF_3 compounds, but as a gas with a toxicity that is about that of phosgene it is rarely used in research chemical laboratories. Being a liquid, the more easily handled DAST reagent is sufficiently reactive for C=O to CF_2 transformations and is most useful for alcohol to alkyl fluoride conversions for which SF_4 is usually not very selective. While it's been very popular among the research community DAST has not found commercial use at the large industrial scale, in view of its relatively high cost but mostly because of its thermal instability. It is well known that DAST can decompose violently upon heating to >90ºC; specific incidents of this have been reported and these have clearly discouraged its industrial use. We thus sought to find new deoxofluorination agents that would be as selectively reactive as DAST, but not carry the level of safety concerns that have precluded its use at a large industrial scale.

DISCOVERY OF THE DEOXO-FLUOR REAGENT
Our search for more stable aminosulfur trifluorides than DAST, was based on an intuitive reasoning guided by quantitative quantum mechanics calculations. One of the guiding theories was that of synthesizing R_2NSF_3 molecules wherein the R groups contain C-H linkages of minimal acidity - since these could react with the highly nucleophilic fluorines. The long process of discovery led to the identification of a number of new R_2N-SF_3 compositions with R = various phenyl and substituted phenyl groups, combinations of aryl and alkyl groups, which were more stable than DAST. In the end, the most stable new aminosulfur trifluoride was the bis(2-methoxyethyl)aminosulfur trifluoride:

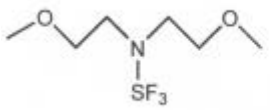

[Deoxo-Fluor™ Reagent (DF)]

THERMAL ANALYSIS STUDIES ON DF
A variety of calorimetric thermal analysis methods were used to screen and eventually conclusively demonstrate that the DF reagent has an acceptable level of thermal stability for industrial use.

The results of differential scanning calorimetry (DSC) studies displayed in Fig. 1 show that while both DAST and the Deoxo-Fluor reagent begin to decompose at about the same temperature (~140ºC), DAST releases more heat and does so far more rapidly. Data derived from isothermal heat evolution measurements are displayed in Fig. 2 which shows heat flow versus time for samples of DAST and the Deoxo-Fluor reagent, contained in a Setaram C80 calorimeter. At 90ºC DAST is completely decomposed in a few hours with a high rate of heat release. For DF however, the time to maximum reaction at 90ºC is 25 hours and the heat flow is substantially

less (~67mW vs 160mW). The much greater stability of DF vs DAST is also seen by the corresponding data at 80ºC. In accelerated rate calorimetry experiments the sample is heated in a small test cell and temperature and pressure are measured as it undergoes exothermic runaway reaction with self-heating, at close to adiabatic conditions. Self-heating is seen at a slightly lower temperature for DF than for DAST (100ºC vs 85ºC), but the rate of heat generation is about an order of magnitude greater for DAST at any temperature. More significant in terms of explosion danger, the rate of gas generation by DF and hence pressure buildup is about an order of magnitude less than is seen with DAST.

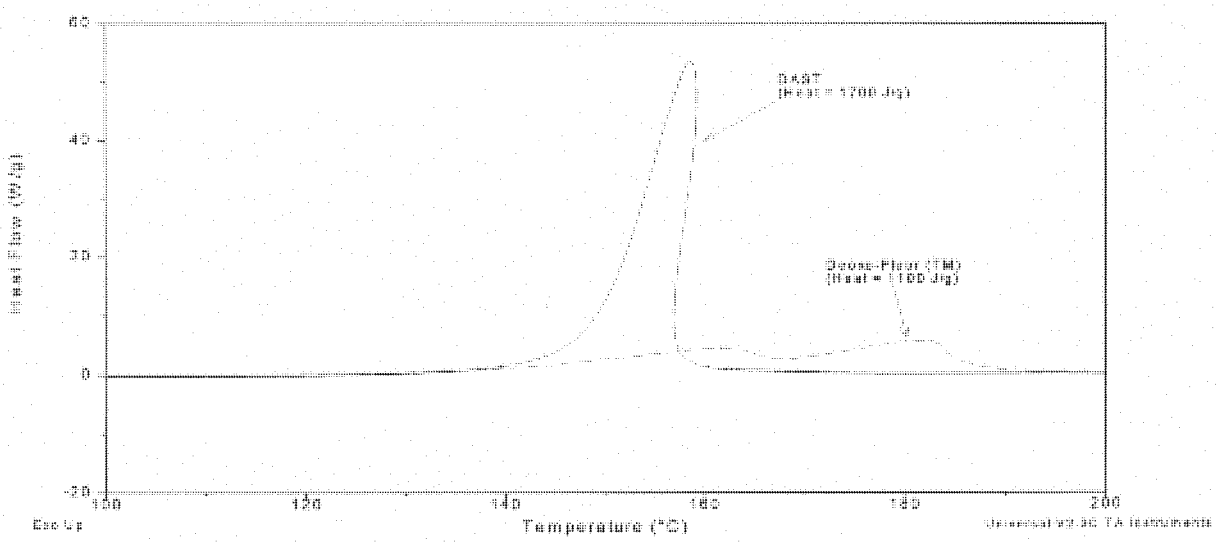

Figure 1. DSC data for DAST and Deoxo-Fluor reagents.

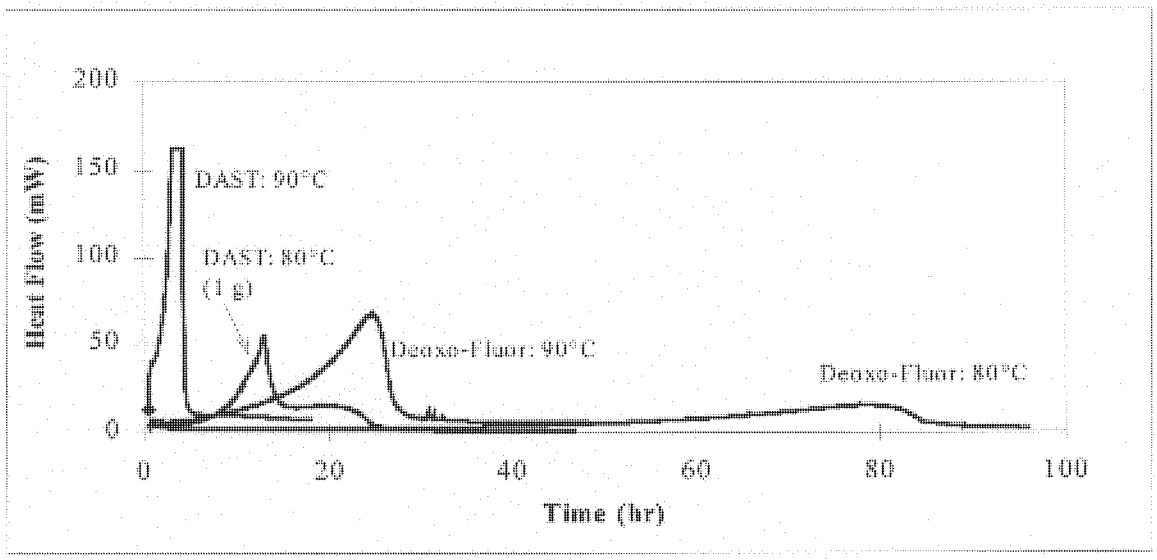

Figure 2. Isothermal calorimetry data for DAST and Deoxo-Fluor reagents.

FLUORINATION REACTIONS WITH THE DEOXO-FLUOR REAGENT

Alcohols

Alcohols are readily converted to alkyl fluorides at room temperature or lower; excellent to moderate yields were obtained with a variety of structurally diverse substrates. In reactions with some alcohols, better yields were obtained with DF than with DAST. For example, under the same reaction conditions, fluorination of cyclooctanol afforded an 85% yield of cyclooctyl fluoride with DF and only a 70% yield with DAST. Some of the more

interesting examples dealing with the fluorination of the anomeric hydroxyl of sugar molecules are shown below:

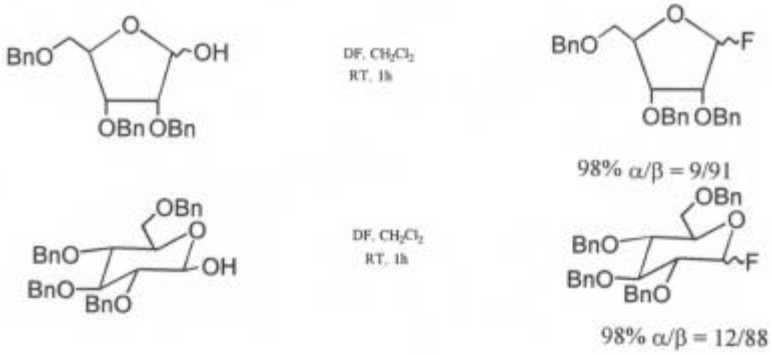

Aldehydes and Ketones

The fluorination of several structurally different aldehydes and ketones was readily accomplished. Thus 4-*t*-butylcyclohexanone, afforded a mixture of 1-*t*-butyl-4,4-difluorocyclohexane and 4-*t*-butyl-1-fluoro-1-cyclohexene (5.25:1 ratio), while at the same conditions, DAST gave a 2.03:1 ratio of the required difluoride to vinyl fluoride. Good yields of the gem-difluoride were also obtained on reaction of DF with the straight chain ketone, 3-phenoxy-2-propanone, the keto-ester, ethyl benzoylformate and the electron-deficient ketone, acetophenone. The latter reaction was done at 85ºC, which was only possible because of the improved thermal stability of our reagent.

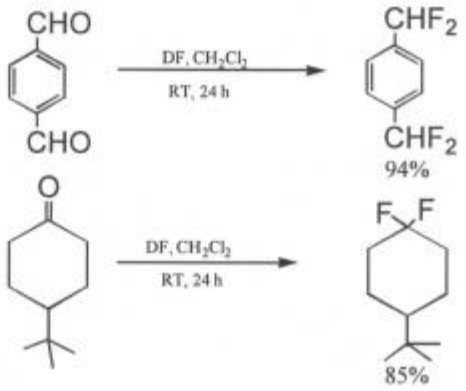

Carboxylic acids

The DF reagent can be used for the synthesis of trifluoromethylsubstituted aromatic and aliphatic compounds from the corresponding carboxylic acid or acid chloride. There is a facile initial conversion to the carbonyl fluoride and then the mono-fluoro product is heated in the neat Deoxo-Fluor reagent at 85ºC to obtain the trifluoromethyl derivative. In this conversion, the greater thermal stability of DF is again exploited for the fluorination of relatively unreactive compounds.

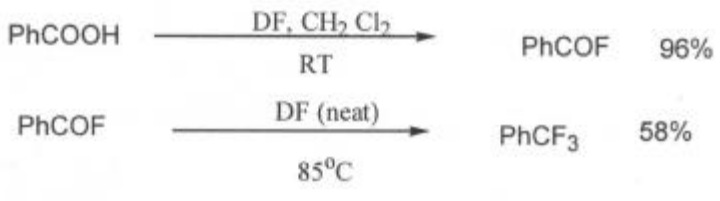

AN ENVIRONMENTALLY BENIGN PROCESS FOR FRIEDEL-CRAFTS ACYLATION[1]

Martin A. Walker, Assistant Professor
Department of Environmental and Health Sciences
Michael S. Balshi, former student
Department of Environmental and Health Sciences*
Adele J. Lauster, former student
Department of Environmental and Health Sciences*, 337 College Hill, Johnson, VT 05656
Patrick M. Birmingham, former student
Department of Chemistry, College of the Holy Cross*, 1 College Hill, Worcester, MA 01610
* Former address

ABSTRACT
We have developed a new method for Friedel-Crafts acylation of aromatic substrates with carboxylic acids, using a metal trifluoromethanesulfonate catalyst[2]. The reaction is driven to completion (over several days) by the azeotropic removal of water. A wide variety of carboxylic acids may be used to acylate even weakly activated aromatic substrates in good yield, without the need to synthesize or use hazardous acid chlorides. Unlike aluminum chloride (the traditional "catalyst"), our catalyst is not toxic, water sensitive or corrosive, it is wholly reusable, and it may be used (in catalytic amounts) either as a solid or an aqueous solution. The work up is extremely simple, and yields a "crude" product which often requires no further purification. Only a small amount of aqueous sodium bicarbonate is produced, instead of the large quantity of strongly acidic waste generated when aluminum chloride is used.

INTRODUCTION
Friedel-Crafts acylation (Scheme 1) is an important industrial process, used for the preparation of a variety of pharmaceuticals, agrochemicals, and other chemical products.

Scheme 1. Friedel-Crafts acylation.

R cannot be a deactivating group
X = halogen, OCOR' or OH

Its utility centers around the fact that it is one of only a very few ways of forming a new carbon-carbon bond onto an aromatic ring. Currently, the most widely-used method has three serious drawbacks:

(a) The carboxylic acid needs to be converted first (in a separate step) to a reactive and corrosive derivative, the carboxylic acid chloride. This requires the use of hazardous reagents such as thionyl chloride.
(b) The catalyst used (anhydrous $AlCl_3$) is a water-sensitive, corrosive solid, which causes severe problems in waste streams, since aqueous neutralization of it results in a gelatinous mass. These waste streams have to be disposed of as acidic waste, adding significantly to the commercial cost and the environmental impact.
(c) The aluminum chloride catalyst forms a stable complex with the product, so that a full molar equivalent of catalyst (often more) is required AND the product can only be recovered by destruction of the catalyst (i.e., the catalyst cannot be reused). Both of these factors add significantly to the cost of operating the process.

Attempts have been made to overcome these problems, with only partial success. Use of catalytic quantities of a corrosive protic acid (HF[3], H_2SO_4 [4] or CF_3SO_3H[5], all difficult to recycle) allows the carboxylic acid to be used. Another process[6] from the carboxylic acid utilizes full molar amounts of $(CF_3CO)_2O$ to form a reactive mixed

anhydride *in situ*, but highly corrosive materials ($(CF_3CO)_2O$, P_4O_{10}) are still involved. Recyclable, non-toxic catalysts such as metal trifluoromethanesulfonate (triflate) salts have been used[7], but always with a hazardous acid chloride or acid anhydride which entails an extra step. Such procedures also require drying of the catalyst *in vacuo* at 200ºC before re-use. Addition of certain metal salts[8] makes it possible to recycle $AlCl_3$, but this does not affect the hazardous nature of the catalyst or avoid use of the acid chloride as a second step.

The goal of this work was to design a process that addresses all three of the present problems, yet remains suitable for large scale manufacturing. The process described below allows aryl ketones to be prepared in one step from carboxylic acids using only a catalytic amount of a reusable catalyst which is both non-toxic and non-corrosive.

RESULTS AND DISCUSSION

In our procedure, an aromatic substrate is reacted with a carboxylic acid in the presence of a hydrated metal trifluoromethanesulfonate (triflate) salt, with azeotropic removal of water to drive the reaction. Toluene is both an effective substrate and a solvent for more activated substrates (e.g. anisole), though alternative solvents such as chlorobenzene may be used. The catalyst may be added as a solid or as an aqueous solution. After a simple workup, the crude product is essentially pure, except for small amounts of the *ortho* acylation product; if need be, the product may be further purified by recrystallization.

In a typical example, hydrated cerium (III) trifluoromethanesulfate (3.23 g) and *para*-toluic acid (1.36 g, 10 mmol) were refluxed together in toluene (125 mL), with azeotropic removal of water (Dean-Stark trap). After 100 hours reaction time, the mixture was cooled and extracted with 3 x 25 mL water (to recover the catalyst). The organic phase was then washed with 2 x 25 mL 8% $NaHCO_3$ solution, dried over Na_2SO_4, then stripped to dryness *in vacuo* to give 4,4'-dimethylbenzophenone (1.65 g, 79 % yield) which was essentially pure (M.P. 84.5-86.5ºC and by NMR). The aqueous extracts (excluding $NaHCO_3$) may then be used directly as the catalyst for a fresh reaction, without further workup.

Variation of catalyst

A wide variety of metal triflates were tested, with triflates of the lighter lanthanides generally being the catalysts of choice (Table 1). In work by other authors, scandium and ytterbium(III) salts are often the more effective recyclable catalysts, but these were always used under anhydrous conditions (unlike in our work, where water is necessarily present). In(III) and Bi(III) triflates could not easily be recycled because of hydrolysis.

Addition of triflic acid to the mixture (as an activator[6a]) had no noticeable effect. Cerium (III) *p*-toluenesulfonate was completely ineffective as a catalyst.

Table 1. Variation of catalyst in acylation of toluene.

Metal triflate	Sc	Y		In	La	Ce		Pr		Dy		Er	Yb		Bi	Th	
Carboxylic acid	T	T	B	T	T	T	B	T	B	T	B	B	T	B	T	T	B
% yield of crude ketone	7	17	20	60 *	16	28	26†	31	77	32	94	12	20	17	47 *	45 *	11

* Product was impure † Believed to be low due to physical losses during isolation

All catalysts were used as the M(III) triflate (M = metal), except for $Th(OTf)_4$. Reactions used either a **168 h reflux with benzoic acid** (B), or a **24 h reflux with *p*-toluic acid** (T), in reaction with toluene.

Although 0.6 molar equivalents of catalyst (if assumed dry) were used in the above experiments, smaller amounts may be used. For example, a yield of 73% was obtained from toluene and benzoic acid (after 144 h), using only 0.06 molar equivalents $Ce(OTf)_3$.

Scope and limitations of the reaction

Even weakly activated aromatics such as toluene are acylated in good yield; more highly activated compounds such as anisole or indole react smoothly in refluxing toluene. However, non-activated substrates such as benzene gave little or no reaction. A variety of carboxylic acids are effective acylating agents, including many aliphatic acids (which fail in some alternative procedures), as shown in Table 3 below. One notable exception occurs with a strong electron withdrawing group conjugated to the carboxyl group, e.g., in *p*-nitrobenzoic acid,

where acylation only occurs in low yield.

Table 3. Variation of reaction substrate.

Aromatic substrate	Carboxylic acid	Catalyst	Rxn. Time (h)	% Yield crude ketone
Benzene	*p*-anisic acid	$Ce(OTf)_3$	168	1*
Anisole	*p*-toluic acid	$Ce(OTf)_3$	48	88
Anisole	*p*-anisic acid	$Dy(OTf)_3$	168	92
Anisole	2-methylbutanoic acid	$Dy(OTf)_3$	24	44
Indole	benzoic acid	$Ce(OTf)_3$	168	60
Toluene	*p*-toluic acid	$Ce(OTf)_3$	100	79
Toluene	*p*-anisic acid	$Ce(OTf)_3$	168	63
Toluene	*p*-nitrobenzoic acid	$Dy(OTf)_3$	24	2*
Toluene	*m*-nitrobenzoic acid	$Dy(OTf)_3$	168	39
Toluene	Cyclohexanecarboxylic acid	$Ce(OTf)_3$	168	61

• Impure product

SUMMARY

The new Friedel-Crafts acylation method is applicable to both weakly and strongly activated aromatic substrates, and a variety of aromatic and carboxylic acids. Good yields of aryl ketones may be obtained directly from the carboxylic acid in one step, using a process which totally avoids the use of hazardous reagents.

ACKNOWLEDGEMENTS

College of the Holy Cross, Brandeis University and Johnson State College, for use of facilities and for funding. I would like also to thank Dr. James B. Hendrickson (Brandeis University) for his support and encouragement.

REFERENCES

1. A US patent application 09/454,083 (1999) has been filed, to College of the Holy Cross, Worcester, MA.
2. A patent using a related (though different) procedure has recently been published. See Jpn. Kokai Tokkyo Koho JP 10 87,549 (1998), to Kao Corp., Japan.
3. US Patent 4,894,482, to Hoechst Celanese Corp., Sommerville, NJ.
4. For example, see March, J., *"Advanced Organic Chemistry",* John Wiley & Sons, New York.
5. US Patent 5,041,616, to Eastman Kodak Co., Rochester, NY.
6. Smyth, T. P.; Corby, B. W. *Org. Proc. Res. Dev.* **1997**, *1,* 264-267.
7. (a) Hf triflate: Kobayashi, S.; Iwamoto, S. *Tetrahedron Letters* **1998***, 39,* 4697-4700.
   (b) Ln triflates: Kobayashi, S., *et al*. J *Chem. Soc. Chemical Communications* **1993***,* 1157-1158.
   (c) Bi triflate: Desmurs, J. R., *et al*. *Tetrahedron Letters* **1997***, 38,* 8871-8874.
8. US Patent 5,859,302, to Albemarle Corp., Richmond, VA.

4th Annual Green Chemistry &
Engineering Conference

Sustainable Technologies:
From Research to Industrial Implementation

June 27 - 29, 2000

GREENER SOLVENTS I

SOLVENT DESIGN UNDER VARYING ENVIRONMENTAL REQUIREMENTS

H. Cabezas and P. F. Harten
National Risk Management Research Laboratory, U.S. Environmental Protection Agency,
26 West Martin Luther King Drive, Cincinnati, OH 45268
R. Zhao
Postdoctoral Research Fellow, Oak Ridge Institute for Science and Education
M. Li
Postdoctoral Research Associate, National Research Council
M. R. Green
Technical Database Services, Inc., 330 West 58th Street, New York, NY 10019

ABSTRACT
There is currently a great need to replace many solvents that are commonly used by industry and the public, but whose continued use entails a number of human health and environmental risks. One issue hampering solvent replacement is the general thought that replacement, particularly for environmental reasons, can involve severe compromises on solvent technical performance. Using the Program for Assisting the Replacement of Industrial Solvents, Version 2 or PARIS II developed by the authors under a Cooperative Research and Development Agreement or CRADA, we demonstrate that, in fact, replacements can be designed for pure solvents and solvent mixtures that are as effective as the solvents they replace while possessing superior environmental properties. This is shown to be the case regardless of whether the solvent is being designed to minimize human toxicity, ecological toxicity, or any other environmental effect. These conclusions are supported with examples of pure and mixture solvent replacements.

INTRODUCTION
Solvents are used in nearly every industry for products or processes. In the United States alone, the sale of solvents represents a $3 billion per year market, and solvent use stands at about 11 billion pounds per year. Interest in solvent substitution has received tremendous attention recently with increasing awareness of the consequences of pollution and growing environmental and health concerns. There are two basic strategies for eliminating undesired solvents from use: (1) develop new technologies which do not use solvents and (2) substitute new and better solvents for those currently used. New technologies always require new processes and new equipment. Thus, solvent substitution is often more attractive because this approach can use existing processes and equipment with minor modification. Solvent substitution, however, is technically complicated because substitute solvents must satisfy specifications with regard to effectiveness, operability, cost, safety, environmental impacts, and health concerns. Finding successful substitute solvents is, therefore, often difficult. Traditionally, substitute solvents have been found using individual experience and basic physical chemistry. More recently, computer-based tools have become available which greatly simplify the task and expand on the possibilities. Computer tools are important because they make it possible to custom design substitute solvents for specific needs and requirements. Using computer aided methods, a skilled chemist or engineer can literally design and screen thousands of possible solvents in an hour. The PARIS software (Cabezas *et al*., 1999; Zhao and Cabezas, 1998) used in this paper is one of these tools. Several other tools including the Computer Aided Molecular Design software (Gani and Brignole, 1981; Gani *et al*., 1991) and Synapse (Joback and Stephanopoulos, 1989; Joback, 1994) are also available.

PARIS II SOLVENT DESIGN SOFTWARE
The PARIS II software designs replacement solvents by matching: (1) solvent operational and safety properties, (2) solvent environmental properties, and (3) solvent function properties. PARIS II looks for pure chemicals or chemical mixtures that have properties as close as possible to those of the solvent being replaced. Details of the PARIS II software are beyond the scope of this paper and are given elsewhere (Cabezas *et al*., 1999). The solvent operational properties are: molecular mass, liquid density, boiling temperature, vapor pressure, surface tension, viscosity, and thermal conductivity. These refer to use of the solvent in a given process or operation. The safety property is the flash point. The solvent environmental properties are: an air index and an environmental index. The solvent function properties are the activity coefficients at infinite dilution (γ_i^{∞}) in the solvent being replaced and the candidate substitute solvent for six different chemicals: ethanol, diethyl ether, acetone, water, octane, and benzene. These represent six different chemical families, and their activity coefficients characterize the non-idealities, i.e., the molecular interactions between each chemical family and the solvent.

The calculation methods for solvent operational and safety properties are from the literature and they are

documented elsewhere (Zhao and Cabezas, 1998). The environmental index is calculated from a database of potential environmental impact scores (Young and Cabezas, 1999) covering 1600+ chemicals and eight environmental impact categories: human toxicity by ingestion, human toxicity by dermal/inhalation exposure, ecological aquatic toxicity, ecological terrestrial toxicity, photochemical oxidation, acidification, stratospheric ozone depletion, and global warming. The environmental index for a chemical mixture is calculated from,

$$\psi_m = \sum_i \sum_j W_i \alpha_j \psi_{i,j}^S \qquad (1)$$

where y_m is the environmental index of mixture m in units of potential environmental impact per kilogram, W_i is the mass fraction of chemical i, a_j is the user adjusted relative weight (0-10) of environmental impact category j, $\psi_{i,j}^S$ is the potential environmental impact score of chemical i in category j from the aforementioned database, and where the summation over i is taken over chemicals and the summation over j is taken over environmental impact categories. For a single chemical this reduces to $\psi_i = \sum_j \alpha_j \psi_{i,j}^S$. The air index for a chemical mixture is calculated from,

$$\psi_m^{air} = \frac{\sum_i \sum_j x_i \gamma_i P_i^v M_i \alpha_j \psi_{i,j}^S}{P \sum_i x_i M_i} \qquad (2)$$

where ψ_m^{air} is the air index for chemical mixture m in units of potential environmental impact per kilogram, x_i is the mole fraction, γ_i is the activity coefficient, P_i^v is the vapor pressure, M_i is the molecular mass, P is the operating pressure and the other symbols have the previously assigned meaning. For a single chemical this reduces to $\psi_i^{air} = P_i^v \psi_i / P$.

METHYL ETHYL KETONE SUBSTITUTES

Mixture replacements for methyl ethyl ketone were designed under the following six different cases: (1) neglecting all environmental considerations for which the replacement is 78% methyl isopropyl ketone and 22% acetone, (2) considering only human toxicity (α_j = 5 for human toxicity by ingestion and human toxicity by inhalation/dermal exposure and α_j= 0 for all other categories) for which the replacement is 72% ethyl acetate, 22% 2-pentanone, and 6% methanol, (3) considering only ecological toxicity (α_j = 5 for ecological aquatic toxicity and ecological terrestrial toxicity and α_j = 0 for all other categories) for which the replacement is 73% 2-pentanone and 27% acetone, (4) considering only regional environmental effects (α_j = 5 for acidification and photochemical oxidation and α_j = 0 for all other categories) for which the replacement is 78% methyl isopropyl ketone and 22% acetone, (5) considering only global environmental effects (α_j = 5 for stratospheric ozone depletion and global warming and α_j = 0 for all other categories) for which the replacement is 78% methyl isopropyl ketone and 22% acetone, and (6) considering all categories (α_j = 5 for all eight potential environmental impact categories) for which the replacement is 73% 2-pentanone and 27% acetone. Tables 1 and 2 below give the properties of methyl ethyl ketone and the six substitute solvents designed under the six cases outlined above. The properties of the substitute solvents were designed to be within a ±20% bracket around the properties of methyl ethyl ketone. The substitute solvents should, therefore, closely mimic the properties and behavior of methyl ethyl ketone, and one would expect them to be very close to being "drop-in" replacements for methyl ethyl ketone.

SUMMARY

The most important conclusion from this work is that it demonstrates through the example of replacing methyl ethyl ketone, that one can design replacement solvents that are about equal in terms of technical effectiveness regardless of environmental requirements. For instance, the substitute solvent that was designed without regard to environmental concerns (Case I) has properties and, therefore, performance that is as similar to methyl ethyl ketone as the substitute solvent designed considering all environmental constraints (Case 6). For that matter, all of the replacements (Cases 1 to 6) have properties similar to those of methyl ethyl ketone (Tables 1 and 2). One should note, however, that the environmental indexes of all of the substitutes (last two rows of Table 1) are lower than those of methyl ethyl ketone under all six solvent design cases. These are, therefore, substitute solvents that appear to be technically similar but environmentally better than methyl ethyl ketone when used under similar conditions and for similar purposes.

Table 1. Operational and safety properties of methyl ethyl ketone and substitute solvents designed under six different environmental constraints at 25ºC and 1 ATM.

Environmental Considerations	**MEK Base Case**	**None Case 1**	**Human Toxicity Case 2**	**Ecologic Toxicity Case 3**	**Regional Case 4**	**Global Case 5**	**All Case 6**
Molecular Mass (kg/kmol)	72.1	77.7	79.3	76.3	77.7	77.7	76.3
Liquid Density (kg/m^3)	800	801	866	799	801	801	799
Boiling Temperature (K)	353	350	345	351	350	350	351
Vapor Pressure (kPa)	12.3	14.3	14.8	14.0	14.3	14.3	14
Surface Tension (kg/s^2)	0.0240	0.0243	0.0232	0.0236	0.0243	0.0243	0.0236
Viscosity X 10^4 (kg/m-s)	3.96	3.92	4.28	4.13	3.92	3.92	4.13
Thermal Conductivity (J/m-s-K)	0.145	0.146	0.147	0.147	0.146	0.146	0.147
Flash Point (K)	267	268	273	271	268	268	271
Air Index Substitute/MEK	N/A	N/A	.04/.08	.04/.08	0/0	0.1/0.6	0.2/0.8
Env. Index Substitute/MEK	N/A	N/A	0.4/0.7	0.4/0.7	0/0	0.4/5	1/6

Table 2. Activity coefficients at infinite dilution of six representative chemicals in MEK and in substitute solvents designed under six different environmental constraints at 25ºC and 1 ATM.

Environmental Considerations	**MEK**	**None**	**Human Toxicity**	**Ecologic Toxicity**	**Regional**	**Global**	**All**
Activity Coefficients	**Base Case**	**Case 1**	**Case 2**	**Case 3**	**Case 4**	**Case 5**	**Case 6**
Ethanol	2.24	2.27	2.12	2.26	2.27	2.27	2.26
Diethyl Ether	1.46	1.37	1.22	1.39	1.37	1.37	1.39
Acetone	1.01	N/A	1.00	N/A	N/A	N/A	N/A
Water	7.38	7.94	6.95	7.79	7.94	7.94	7.79
Octane	5.26	4.60	4.81	4.75	4.60	4.60	4.75
Benzene	1.32	1.24	1.29	1.26	1.24	1.24	1.26

REFERENCES
Zhao, R. and H. Cabezas, "Molecular Thermodynamics in the Design of Substitute Solvents," invited paper, *Ind. & Eng. Chem. Res*., **27**, 3268 (1998).
Cabezas, H., R. Zhao, J.C. Bare, and S.R. Nishtala, "Designing Environmentally Benign Solvent Substitutes," In *Tools and Methods for Pollution Prevention,* S.K. Sikdar and U. Diwekar Eds., Kluwer Academic Publishers, Dordrecht, The Netherlands, 317 (1999).
Gani, R., and E. A. Brignole, "Molecular Design of Solvents for Liquid Extraction Based on UNIFAC," *Fluid Phase Equil.,* **13**, 331 (1983).
Gani, R., B. Nielsen, and A. Fredenslund, "Group Contribution Approach to Computer-Aided Molecular Design," *AIChE J,* **37**, 1318 (1991).
Joback, K.G., and G. Stephanopoulos, "Designing Molecules Possessing Desired Physical Property Values," In *Proceedings of the Third International Conference on Foundations of Computer-Aided Process Design,* CACHE Corp., **11**, 631 (1989).
Joback, K.G., "Solvent Substitution For Pollution Prevention," In *Pollution Prevention Via Process and Product Modifications,* E.L. Gaden, Ed., AlChE Symposium Series, Vol. 90, American Institute of Chemical Engineers, New York, 98 (1994).
Young, D.M.., and Cabezas, H., "Designing Sustainable Processes with Simulation: The WAR Algorithm," invited paper, *Comp. & Chem. Eng*., **23**, 1477 (1999).

CHEMICAL AND PHYSICAL CHARACTERISTICS OF ROOM TEMPERATURE IONIC LIQUIDS AND THE ASSOCIATED IMPLICATIONS FOR THEIR USE AS SOLVENT ALTERNATIVES

Ann E. Visser, Richard P. Swatloski, W. Matthew Reichert,
Heather D. Willauer, Jonathan G. Huddleston and Robin D. Rogers
Department of Chemistry and Center for Green Manufacturing,
The University of Alabama, Tuscaloosa, AL 35487

ABSTRACT
Room Temperature Ionic Liquids (RTIL) have received significant attention due to their remarkable solvent-like properties including low volatility, water and air stability, and high thermal stability. Exciting results utilizing RTIL as alternatives to volatile organic compounds (VOCs) have encouraged methods to control changes in their chemical and physical properties. The numerous combinations of cations and anions ensures that the properties of RTIL can be fine-tuned to meet the requirements for use in virtually any process. This presentation will discuss the characteristics of various RTIL with regard to structural changes in both the constituent cation and anion.

INTRODUCTION
An inherent difficulty associated with any industrial manufacturing process is the production of waste, albeit in the gaseous, liquid, or solid form. In the past few decades, the chemical industry has come under intense scrutiny for their contributions towards environmental pollution. As a result, the public interpretation of the chemical industry has shifted from that of a source of life-enhancing products towards a more disheartened view, one in which many perceive the industry as a major contributor towards air, land, and water pollution. To regulate waste management issues and problems, a profusion of environmental regulations has enforced stringent controls on the emission, discharge, and disposal of chemicals associated with manufacturing processes.

To remedy this situation, eliminating the source of the problem presents an alternative to the traditional treatment “at the end of the pipe,” or after the problem occurs. Such a shift in the approach to environmental problems represents a new paradigm of pollution prevention. The crux of the new paradigm is the development of alternative means for producing a desired product, focusing on “Green Chemistry” and reducing environmental risk by reducing hazards associated with particular manufacturing processes.[1] These issues are central towards Technology Vision 2020 and the opportunity for new chemical and engineering technologies for enhanced separations.[2]

Many separations are carried out using a traditional liquid/liquid scheme, typically involving an organic solvent and an aqueous phase. The biphasic technique has several benefits including a wide range of different organic

phases and extractants that can be used, in addition to the rapid kinetics and favorable stripping mechanics that have been reported.[3,4] Nevertheless, the traditional organic solvents are often toxic and flammable, owing to the high costs and increased safety measures associated with these systems. Contrary to metallic melts such as NaCl at 800 °C, RTIL are a class of ionic compounds composed of large, hydrophobic organic cations (Figure 1) and one of a variety of anions that together melt at or below ambient temperatures. The utility of certain RTIL has been demonstrated in a variety of separations since there are several RTIL that have solvent characteristics suitable for their incorporation in place of traditional VOCs in liquid/liquid separations.[5,6] For a series of solutes, we have shown that their affinity for the RTIL phase increases in correlation with the solute's 1-octanol/water log P value. As solvents, RTIL are highly solvating which makes them suitable for catalysis and synthesis, hence their designation as 'alternative reaction media.'[7-9]

Figure 1. The generic 1-alkyl-3-methylimidazolium cation

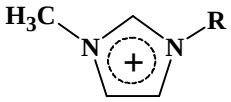

where $[C_4mim]^+$ (R = $CH_3CH_2CH_2CH_2$)
$[C_6mim]^+$ (R = $CH_3CH_2CH_2CH_2CH_2CH_2$)
$[C_8mim]^+$ (R = $CH_3CH_2CH_2CH_2CH_2CH_2CH_2CH_2$)

While the C_4, C_6, or C_8 derivatives of the $[C_nmim]^+$ cation (Figure 1) in combination with the PF_6^- anion produces RTIL which are well-suited towards forming biphasic systems in contact with aqueous phases, recent publications have examined how variations in the cation and anion affect the chemical and physical properties of the resulting RTIL. For instance, changing the alkyl chain length on the 1-alkyl-3-methylimidazolium cation dramatically affects the melting point for a series of PF_6^- or BF_4^- RTIL.[10]

Similarly, using different anions (e.g., PF_6^-, BF_4^-, $N(CF_3SO_2)_2^-$, Cl^-, Br^-, or I^-) have a distinct impact on the properties of the RTIL.[11,12] An important effect of different anions is the water miscibility of the resulting RTIL; 1-alkyl-3-methylimidazolium salts of PF_6^- are water immiscible, BF_4^- salts are water miscible depending on alkyl chain length, and tetrahaloaluminate salts are moisture sensitive. Fluorinated anions such as $N(CF_3SO_2)_2^-$ impart hydrophobicity and some desirable physical properties despite their increased expense.

The RTIL considered as solvent alternatives for liquid/liquid separations are free from the difficulties involved in the use of the haloaluminate (e.g., $[C_nmim][AlCl_4]$) RTIL.[7] In the same manner as traditional organic solvents in contact with water, the RTIL phase contains varying amounts of water, a property largely attributable to the hydrophobicity of the anion as shown in Table 1.

Table 1. Water content of water equilibrated and dried RTIL

Ionic Liquid	Water Content (ppm, water equilibrated)	Water content (ppm, dried*)
$[C_4mim][TF_2N]$	3280	474
$[C_4mim][PF_6]$	11700	309
$[C_4mim][BF_4]$	19600	4530
$[C_4mim][Cl]$	Miscible	2200
$[C_4mim][I]$	Miscible	1870
$[C_6mim][PF_6]$	8837	560
$[C_6mim][Cl]$	Miscible	1130
$[C_8mim][PF_6]$	6666	537
$[C_8mim][Cl]$	Miscible	1690

*Each RTIL was dried under vacuum at 70 °C for 4 hours. Water content measured by Karl-Fisher titration.

In total, there are millions of RTIL that can be produced through simple variations in the cation and anion. In light of such a vast selection, understanding the physical and chemical properties for these compounds is of paramount importance towards understanding their solvent behavior or for designing a RTIL for a specific

application. Several properties (e.g., density, viscosity, and liquidus range) have a direct influence on the engineering aspects of their applications. These properties are important for engineering concerns such as rates of liquid/liquid phase separation, mass transfer, and power requirements of mixing.[13] Refractive index and dielectric permittivity may be important in determining the solvation of charged species through their relationship to polarity and polarizability. Overall, new solvents are aimed at attaining the properties of ideal solvents. To that extent, important chemical properties would include a non-toxic and non-flammable nature, both important contributors towards their implementation as more environmentally friendly solvent alternatives. Others include a high capacity for the solute, a high selectivity of the solute, and compatibility with the solute, all key factors towards their implementation in a reaction process.

Our current research demonstrates an early stage in a rapidly developing field of separation science, but clearly shows the versatility and promise for the facilitated incorporation of RTIL into many separation schemes. From the green chemistry standpoint, the chemical and physical properties of RTIL warrant their further study and exploration. As a class of neoteric solvents, RTIL have established their utility as solvent replacements for traditional solvents in liquid/liquid separations.

ACKNOWLEDGEMENTS
This work was supported by funding from the Division of Chemical Sciences, Office of Basic Energy Sciences, Office of Energy Research, U. S. Department of Energy (Grant No. DE-FG02-96ER14673) and the PG Research Foundation.

REFERENCES

1. P.T. Anastas and J.C. Warner, *Green Chemistry: Theory and Practice,* Oxford University Press, New York, 1998.
2. Adler, S., Beaver, E., Bryan, P., Rogers, J. E. L., Robinson, S., and Russomanno, C. Vision 2020: 1998 Separations Roadmap. 1998. Center for Waste Reduction Technologies (AIChE) and U.S. Dept. of Energy, Office of Industrial Technology.
3. T.C. Lo, M.H.I. Baird and C. Hanson, *Handbook of Solvent Extraction,* Wiley-Interscience, New York, 1983.
4. J. Rydberg, C. Musikas and G.R. Choppin, *Principles and Practices of Solvent Extraction,* Marcel Dekker, New York, 1992.
5. J.G. Huddleston, H.D. Willauer, R.P. Swatloski, A.E. Visser and R.D. Rogers, *Chem. Commun.*, 1998, 1765.
6. A.E. Visser, R.P. Swatloski and R.D. Rogers, *Green Chem.*, 2000, **1**, 1.
7. C.L. Hussey, *Pure and Appl. Chem.*, 1988, **60**, 1763.
8. T. Welton, *Chem. Rev.*, 1999, **99**, 2071.
9. J.S. Wilkes, J.A. Levisky, R.A. Wilson and C.L. Hussey, *Inorg. Chem.*, 1982, **21**, 1263.
10. J.D. Holbrey and K.R. Seddon, *Clean Prod. and Proc.*, 1999, 223.
11. P. Bonhote, A.-P. Dias, N. Papageogiou, K. Kalyanasundaram and M. Gratzel, *Inorg. Chem.*, 1996, **35**, 1168.
12. P.A.Z. Suarez, S. Einloft, J.E.L. Dullius, R.F. de Souza and J. Dupont, *J. Chim. Phys.*, 1998, **95**, 1626.
13. Y. Marcus, *Chem. Rev.*, 1993, 416.

ETHYL LACTATE: A GREEN SOLVENT FOR MAGNETIC TAPE COATING

Sarah M. Nikles, Meihua Piao, Alan M. Lane and David E. Nikles
Center for Materials for Information Technology, The University of Alabama, Tuscaloosa, AL 35487-0209
dnikles@mint.ua.edu

Introduction

The magnetic tape industry uses solvent-based magnetic inks in their tape coating processes. The solvents include 2-butanone (MEK), cyclohexanone, 4-methyl-2-pentanone (MIBK), tetrahydrofuran (THF), and toluene. MEK, MIBK and toluene are hazardous air pollutants that cause photochemical smog and ground level ozone. In state-of-the-art coating operations, the solvents are captured on a carbon adsorber, stripped, purified and recycled. The coating operations use the best pollution prevention practices and meet EPA regulations; however, the three world-class magnetic tape manufacturing sites in The State of Alabama released 1.78 million pounds of

MEK and toluene in 1997.[1]

Our continuing interest in preventing air pollution in magnetic tape manufacture has led us to examine the possibility of using ethyl lactate as the solvent in the magnetic inks. We were inspired by a presentation by R. Datta entitled "Lactate Esters for Green Solvents-Process Technology Advances" at the 3rd Annual Green Chemistry and Engineering Conference[2]. Ethyl lactate is non-toxic, indeed it is a FDA approved food additive. If released to the environment, it quickly biodegrades. It is not an air pollutant. In this paper we demonstrate the possibility of replacing the HAP's used in magnetic tape manufacture with ethyl lactate. We also consider the economics of using ethyl lactate in the coating process.

Magnetic Dispersions

Magnetic dispersions contain magnetic particles dispersed in organic solvents. A polyvinylchloride wetting binder is used as a dispersing aid, either MR-110 from Nippon Xenon or UCARMAG from Union Carbide. The binders contain carboxylate or sulfonate functional groups that chemisorb to the particle surface. The adsorbed polymer layer provides a steric barrier that separates the particles, thereby stabilizing the dispersion. The dispersions also contain a thermoplastic polyurethane that, after cross-linking with a polyisocyanate, gives the coating its requisite mechanical properties. Modem magnetic tape formulations use either Estane from BFGoorich or Morthane from Morton International.

The first consideration was to replace all the solvents with ethyl lactate, a "fully green" solvent system. Unfortunately neither the polyvinylchloride wetting binder, MR-110, nor the thermoplastic polyurethane, Morthane CA-271, was soluble in ethyl lactate. However, both were soluble in a 50/50 (wt/wt) mixture of ethyl lactate and tetrahydrofuran. Tetrahydrofuran is not a HAP and is commonly used in as a solvent in magnetic inks. Therefore, we prepared a "partially green" formulation, where the solvent was a 50/50 mixture of ethyl lactate and THF, Table 1. MR-110 2.50 g was dissolved in 15.14 g THF and then the solution was diluted with 15.06 g ethyl lactate. Morthane CA-271 was dissolved in 15.52 g THF with shaking overnight. The next day the solution was diluted with 15.03 g ethyl lactate. Both polymer solutions were homogeneous mixtures. The MR-110 solution was mixed with 20.01 g of videotape grade cobalt-modified _-Fe_2O_3 particles (Pferrcio 3570 from ISK Magnetics). The heterogeneous mixture was poured in an Eiger "Mini 50" bead mill. THF (7.53 g) and ethyl lactate (7.52 g) were added and the mixture was milled for an hour using glass beads as the milling media. After milling for one hour, the Morthane solution was added and milling continued for another 30 minutes. The dispersion was then pumped into a glass jar. Magnetic coatings were cast onto polyester base film using a 6 mil Garner blade in a hand draw-down apparatus that passed the wet coating through an orienting magnetic field. The coatings were dried overnight at 65ºC in a convection oven.

Table 1. Partially Green Formulation.

Ingredient	Amount (g)
Pferrico 3570	20.01
MR-110	2.50
Morthane CA-271	2.51
Tetrahydrofuran	38.19
Ethyl Lactate	37.69

The rheolgical properties for the magnetic dispersions were measured on a Haake RS-100 oscillating shear rheometer. In Fig. 1a are plots of elastic modulus (G') and viscous modulus (G") as a function of frequency. The rheological properties of magnetic dispersions are dominated by magnetic attraction forces between the particles. This gives the dispersions a high elasticity. The values of G' and G" for the dispersion containing ethyl lactate are similar to those for conventional videotape dispersions. The dispersion also displayed a shear-thinning behavior, similar to that observed for conventional dispersions.

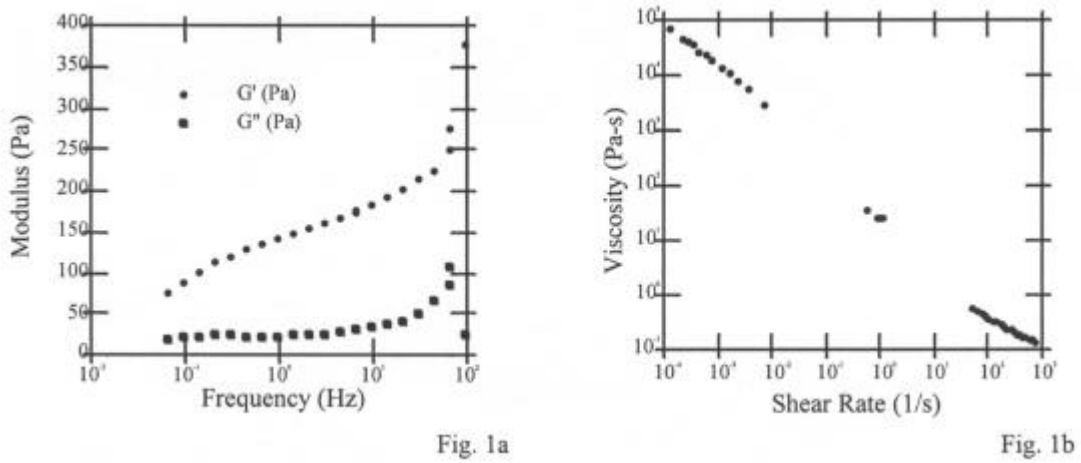

Figure 1. Rheological properties of the magnetic dispersion containing ethyl lactate. Figure 1a. Frequency dependence of the elastic modulus (G') and the viscous modulus, G". Figure 1b. Shear rate dependence of the viscosity.

The magnetic properties of the dried tape samples were determined by measuring a hysteresis curve on a DMS model 880 vibrating sample magnetometer (Figure 2). The squareness and coercivity of the curve were quite similar to that for conventional videotape. Clearly, magnetic dispersions can be prepared with 50/50 THF/ethyl lactate and these dispersions give tape with adequate magnetic properties.

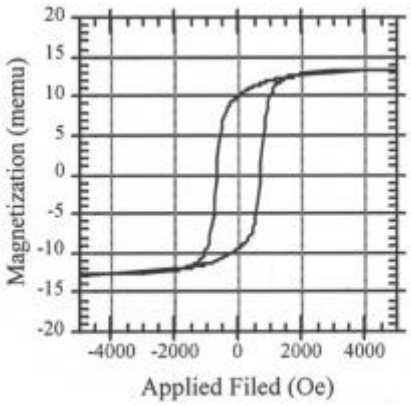

Figure 2. Magnetic hysteresis curve for the tape sample cast from the dispersion containing ethyl lactate. The curve was measured in the direction parallel to the particle orientation.

Economics

With the demonstration that magnetic tape can be cast from dispersions containing ethyl lactate, the next consideration becomes the economics of the process. We have reported an hourly materials consumption costs for a videotape coating line using conventional, solvent-based tape dispersion.[3] In Table 2 is a comparison of the hourly materials costs for a conventional coating process, a partially green coating process, and a fully green coating process. The conventional process consumes $2,000 of materials per hour. The partially green process, where the solvents are 50/50 THF and ethyl lactate, consumes $2,800 of materials per hour, a 40% increase. The increase is due to the higher cost of ethyl lactate ($0.85/lb), relative to MEK and toluene. The partially green process also uses THF, a more expensive solvent. The fully green process (only ethyl lactate), consumed $2,400 of materials per hour, only a 20% increase over the conventional process. In order for the fully green process to be competitive, the price of ethyl lactate must be cut in half.

Energy Consumption

Another consideration is the hourly energy consumption. In Table 3 is a comparison of the hourly energy consumption and costs for the three different cases. Although ethyl lactate has a lower enthalpy of vaporization than the other solvents, the energy cost savings enjoyed by the fully green process are small relative to the materials costs.

References

1. Environmental Protection Agency, Toxics Release Inventory.
2. Datta, R.; Henry, M.; Tsai, S.P.; Halpern, Y.; Frank, J.R. *Proc. 3rd Ann. Green Chemistry and Engineering Conference,* **1999,** Washington, DC.
3. Cheng, S.; Fan, H.; Gogineni, N.; Jacobs, B.; Jefcoat, I.A.; Lane, A.M.; Nikles, D.E. *Waste Management* 1995, **15**(4), 257-264.

Table 2. Comparison of the hourly materials consumption and materials costs.

	Conventional		Partially Green		Fully Green	
Material	Amount	Cost	Amount	Cost	Amount	Cost
Pferrico 3570	200.8	$973.88	200.8	$973.88	200.8	$973.88
Carbon Black	4.01	$13.63	4.01	$13.63	4.01	$13.63
Alumina	12.1	$68.85	12.1	$68.85	12.1	$68.85
UCARMAG-536	22.6	$99.67	22.6	$99.67	22.6	$99.67
Morthane CA-271	27.6	$240.40	27.6	$240.40	27.6	$240.40
Mondur CB-701	5.03	$26.06	5.03	$26.06	5.03	$26.06
Butyl Stearate	2.51	$3.26	2.51	$3.26	2.51	$3.26
Stearic Acid	2.51	$2.54	2.51	$2.54	2.51	$2.54
THF	129	$365.07	320	$905.60		
MEK	258	$162.02				
Toluene	254	$67.31				
Ethyl Lactate			321	$500.76	641	$999.96
Total		$2,023		$2,835		$2,428

Table 3. Comparison of energy consumption and cost per hour.

Solvent	Amount (kg/h)	DH_{vap} (kJ/kg)	Energy Use (kJ/h)	Cost ($/h)*
Conventional				
THF	129	480	61920	1.05
MEK	258	473	122034	2.06
Toluene	254	426	108204	1.83
			292158	4.94
Partially Green				
THF	320	480	153600	2.60
Ethyl Lactate	321	419	134499	2.28
			288099	4.87
Fully Green				
Ethyl Lactate	641	419	268579	4.54

* Assuming an energy cost of 6.09¢ per kilowatt hour.

BIPHASIC CATALYSIS APPROACHES IN DENSE PHASE CARBON DIOXIDE

Gunilla B. Jacobson
CST-12, MS E537
Michael B. Abrams, Fuchen Liu, John G. Watkin, R. Tom Baker and William Tumas
CST-18, MS J514
Los Alamos National Laboratory, Los Alamos, NM 87545

ABSTRACT
We demonstrate, for the first time, that water/supercritical carbon dioxide (w/c) emulsions can be used for biphasic homogeneous catalysis and lead to a phase-separable system with facile separations yet higher reactivities than conventional biphasic catalytic systems using water and organic solvents. Through preliminary kinetic investigations, we demonstrate significant improvements in reaction rate upon emulsion formation using three different surfactants for the hydrogenation of 1-alkenes catalyzed by water-soluble rhodium-phosphine complexes. After reaction, the emulsion can be broken by simply decreasing the pressure to effect product separation. Catalyst recycle has also been demonstrated.

INTRODUCTION
The difficulty of catalyst separation and recovery continues to create economic and environmental barriers to the broader industrial application of homogeneous catalysts for chemical transformations, despite the remarkable activity and selectivity attainable through sophisticated ligand design in these systems. A number of approaches termed biphasic catalysis have been advanced where a soluble catalyst is immobilized in one liquid phase (often aqueous) and the substrates and products are isolated in a separate immiscible phase.[1] The concept of aqueous biphasic catalysis was advanced over 20 years ago[2] and a number of reactions and water-soluble catalysts have been reported.[3] While rates can be high for volatile or slightly water-soluble reactants *(i.e.* the commercially practiced hydroformylation of propene[4]), these systems have found limited use for more hydrophobic *(i.e.* most organic) substrates, because of lower reaction rates due to mass transfer limitations across the interface.

We will present a new aqueous biphasic homogeneous catalysis system that uses only water and environmentally benign supercritical carbon dioxide (CO_2) along with emulsion forming surfactants, which are active at the water/CO_2 interface.[5] The recent development of surfactants capable of forming emulsions and microemulsions of H_2O and CO_2 has led to micellar systems that are good solvents for both hydrophilic and hydrophobic species.[6] We have been examining catalytic reactions using water-soluble catalysts and lipophilic substrates in these emulsion systems. A high pressure variable-volume-view-cell is charged with an aqueous phase containing the catalyst, a surfactant, the reactants in the CO_2 phase. The system is pressurized and heated while recirculating the fluids with a pump, forming the emulsion. After reaction, the emulsion can be broken by simply decreasing the pressure to effect product separation and catalyst recycle.

For example, we have found that the rates and conversions of the hydrogenation of long chain alkenes using water soluble rhodium-phosphine complexes are significantly higher in water/CO_2 emulsions than in two-phase water/CO_2 or water/toluene mixtures.[7] Preliminary results on hydrophobic alkenes may suggest that the reaction occurs at the interface rather than in the bulk water phase. These high reaction rates are likely due to a combination of higher hydrogen concentration due to miscibility in the CO_2 phase and increased interfacial surface area by emulsion formation. This concept should be applicable to a wide range of catalytic processes, particularly those involving gaseous reagents (e.g. H_2, CO, O_2), including hydroformylation and other carbonylations, oxidations and reductions.

SUMMARY
We have found a new biphasic catalysis system that capitalizes on the unique and controllable phase properties of water/supercritical CO_2 emulsions and allows for both catalyst recycle and enhanced reaction rates. Supercritical CO_2 is unique in allowing for emulsion formation followed by efficient phase separation. Activity for even highly hydrophobic substrates is significantly higher than conventional aqueous biphasic systems. We believe the key advantages of our system are 1) miscibility of gaseous reactants, *e.g*. H_2, 2) high interfacial surface area due to emulsion formation, 3) the ability to break emulsions by pressure decrease for efficient phase separation (simplifying product recovery and catalyst recycle), and 4) low interfacial tension between water and CO_2.

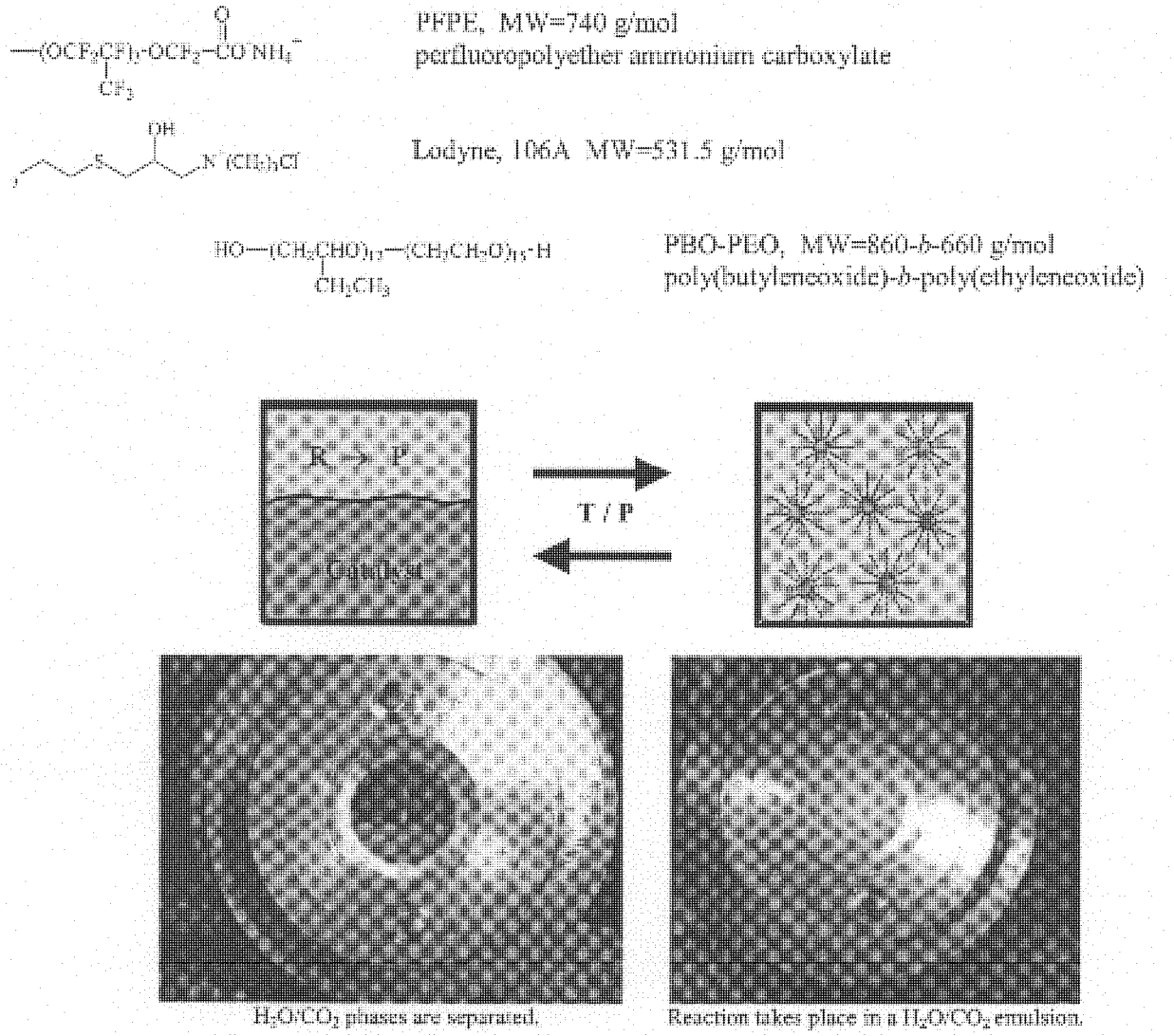

ACKNOWLEDGMENT

This work was supported by the US Department of Energy through a Laboratory Directed Research and Development (LDRD) grant. G. B. Jacobson acknowledges the Swedish Research Council for Engineering Sciences for postdoctoral fellowship support.

REFERENCES

1. A recent issue of *Catal. Today*, 1998 **42**(2) was devoted to biphasic homogeneous catalysis.
2. Herrmann, W.A.; Kohlpaintner, C.W., *Angew. Chem. Int. Ed. Engl*. 1993, **32**, 1524-1544.
3. Cornils, B.; Herrmann, W.A., Aqueous-Phase Organometallic Catalysis, Wiley-VCH, Weinheim, Germany, 1998.
4. Kuntz, E.G. *Chemtech*, 1987, **17**, 570.
5. Johnston, K.P.; Harrison, K.L.; Clarke, M.J.; Howdle, S.M.; Heitz, M.P.; Bright, F.V.; Carlier, C.; Randolph, T.W., *Science*, 1996, **271**, 624-626.
6. a) Jacobson, G.B.; Lee, Jr., C.T.; Johnston, K.P., Organic synthesis in water/carbon dioxide microemulsions. *J. Org. Chem*., 1999, **64**, 1201-1206.
   b) Jacobson, G.B.; Lee, Jr., C.T.; daRocha, S.R.P.; Johnston, K.P., Organic synthesis in water/carbon dioxide emulsions. *J. Org. Chem*., 1999, **64**, 1207-1210.
7. Jacobson, G.B.; Lee, Jr., C.T.; Johnston, K.P.; Tumas, W., Biphasic Catalysis in Water/Carbon Dioxide Emulsions, *J. Am. Chem. Soc*. 1999; **121**(50); 11902-11903.

4th Annual Green Chemistry &
Engineering Conference

Sustainable Technologies:
From Research to Industrial Implementation

June 27 - 29, 2000

BIO-BASED SYNTHESIS AND PROCESSING I

GREEN BIOSYNTHESIS OF POLYHYDROXYALKANOATES: ENGINEERING OF CYANOBACTERIA FOR BIOPOLYMER PRODUCTION

Gaspar Taroncher-Oldenburg, Ph.D., Ryan T. Gill, Ph.D. and Gregory Stephanopoulos, Ph.D.
Dept. of Chemical Engineering, Massachusetts Institute of Technology, Cambridge, MA 02139

Abstract
Cyanobacteria have been proposed as a viable alternative for the efficient production of polyhydroxyalkanoates from atmospheric CO_2 while using solar radiation as the energy source. Studies on the physiological function of the polymer in these organisms provide the necessary background for the rational design and engineering of new strains with modified regulatory circuits resulting in enhanced product formation. Studies on the model organism *Synechocystis* sp. PCC6803 are presented to illustrate this approach, and some of the economic and energetic implications of cyanobacterium based polymer production are discussed.

Introduction
Polyhydroxyalkanoates (PHAs) are naturally occurring, biodegradable polyoxoesters with properties that range from elastomers to thermoplastics. PHAs are accumulated by a range of microorganisms that includes autotrophic as well as heterotrophic species (Doi, 1990). Heterotrophic organisms biosynthesize PHAs from organic carbon precursors provided in the growth medium; autotrophic organisms are able to derive all the carbon needed for PHA production from atmospheric CO_2. Autotrophic organisms, and in particular those deriving their energy from solar radiation via photosynthesis, i.e., the photoautotrophs, have attracted great interest for the mass production of PHAs because they do not require the addition of expensive precursors to the culture medium and thus reduce production costs (Poirier, Nawrath & Somerville, 1995) (Fig. 1). Two approaches have been proposed to exploit the advantages of photoautotrophic organisms for PHA production (Steinbüchel & Füchtenbusch, 1998). The first method consists of expressing the PHA biosynthetic pathway genes from bacteria in crop plants. An alternative approach consists of enhancing native PHA production in photosynthetic bacteria through the optimization of growth conditions for high PHA yields, or, through the overexpression of key regulatory genes in the PHA biosynthetic pathway. Efforts to implement PHA production in plants have been partially successful (Slater *et al.,* 1999). The disadvantages of these systems are the slow growth rates of plants, the low yield of PHAs, due to the competing carbon demand for structural purposes, and the complexity of polymer extraction from plant tissues. Alternatively, the use of aquatic, photosynthetic bacteria circumvents some of the preceding problems: their growth rates are higher, they have no support structures and their downstream processing is simpler. For the purpose of PHA production, the best studied group of photoautotrophic organisms is that of the cyanobacteria. In this communication we report studies on the genetics and physiology of PHA production by the model organism *Synechocystis* sp. PCC6803 (from here on referred to as *Synechocystis)* and discuss aspects related to its potential implementation.

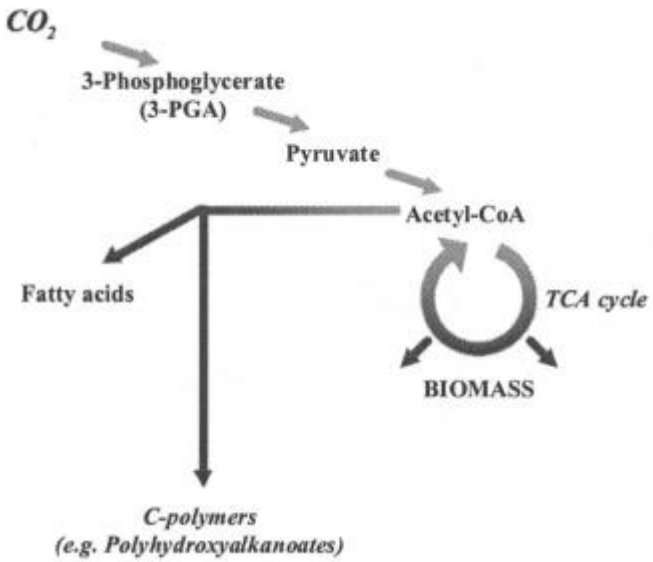

Figure 1. Photosynthesis derived Polyhydroxyalkanoate production in cyanobacteria.

PHA biosynthesis in cyanobacteria
Cyanobacteria produce PHAs photosynthetically from CO_2. Several species of cyanobacteria have been reported to accumulate PHAs, including unicellular, filamentous and nitrogen fixing species (Stal, 1992). The most common PHA in cyanobacteria is poly(3-hydroxybutyrate) (PHB), followed by poly(3-hydroxyvalerate) (PHV) and the copolymer of the preceding PHAs, P(HB-*co*-HV). Only recently have the first genes coding for the PHA biosynthetic pathway in these organisms been identified in the model organism *Synechocystis* (Hein, Tran & Steinbüchel, 1998; Taroncher-Oldenburg, Nishina & Stephanopoulos, 2000). Three enzymes are required for the biosynthesis of PHAs: a β-ketothiolase *($phaA_{Syn}$)* that catalyzes the Claisen-type condensation of two acyl-CoA precursors, an acetoacyl-CoA reductase *($phaB_{Syn}$)* and the PHA synthase *($pha(E)C_{Syn}$)* responsible for the

polymerization (Fig. 2). The availability of the entire genome sequence of *Synechocystis* facilitated the identification of the genes. These genes are organized in two clusters, one containing the two subunits of the type III, heterodimeric PHA synthase and the other one comprising the β-ketothiolase and acetoacyl-CoA reductase. Issues of regulation and coregulation of these genes are currently under investigation in our laboratory.

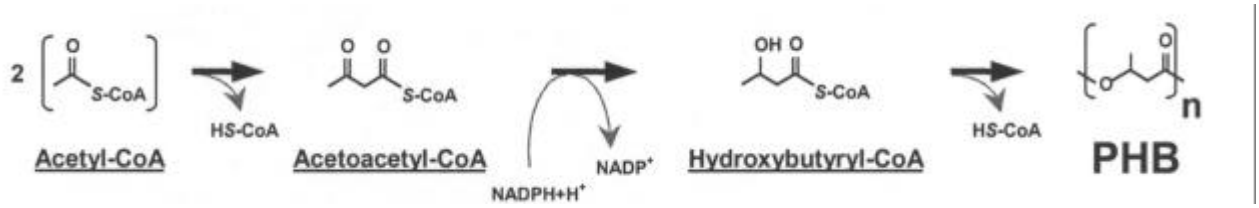

Figure 2. The PHA blosynthetic pathway showing the formation of poly(3-hydroxybutyrate) (PHB)

Prior to the identification of the first cyanobacterial PHA biosynthesis genes, and in an attempt to develop microalgal systems for the biological conversion of CO_2 to PHAs, two strains of *Synechococcus* sp. had been transformed with the genes from *Alcaligenes eutrophus* (Miyasaka *et al.,* 1998; Suzuki *et al.,* 1996). The PHA yields obtained in the transformed strains on the basis of dry cell weight (DCW) were ca. 17%. These levels are similar to those reported for wild type *Synechocystis* grown under nitrogen deficiency (Hein *et al., 1998).* Recent studies with *Synechocystis* in our laboratory have shown that these levels can be further enhanced to reach 35-40% DCW accumulation under proper nutrient starvation conditions (GTO & GS, unpublished data). These results raise the issues of regulation of PHA production and function of the polymer in cyanobacteria. PHA biosynthesis in bacteria is closely related to periods of physiological stress for the cells (Stal, *1992,* GTO, unpublished data). Predictability and control of these stress factors is a critical component in the implementation of industrial, cyanobacterial PHA production.

Metabolic engineering of cyanobacteria

Over the past 50 years, the manipulation of biochemical pathways to improve the production efficiency of specific compounds has been extensively applied in many different species. With the more recent expansion over the last 20 years of the field of genetic engineering, such improvements began to be obtained by the targeted modification of metabolic pathways rather than by random mutation and selection of transformed organisms (Stephanopoulos, 1999). This goal requires a good understanding of cellular metabolism, including the factors controlling metabolic fluxes and their distribution among competing pathways, in order to amplify the product forming pathways relative to those leading to side products. Metabolic engineering thus focuses on the modification of metabolic pathways in order to optimize product formation while maintaining optimal cellular properties. Recently, the principles of metabolic engineering have been successfully applied to improve the production of specific carotenoids in bacteria and cyanobacteria (Farmer & Liao, 2000; Lagarde, Beuf & Vermaas, 2000).

We are using a new approach to the optimization of PHA biosynthesis consisting in combining two systemic methods to study substrate channeling toward the end product in *Synechocystis.* First, we determine genetic activity of genes related to PHA production in the organism via expression profile analysis on partial or whole genome DNA microarrays (DNA chips). In parallel to this, we also determine substrate allocation and distribution in the cells through metabolic flux analysis (MFA). The combination of these two techniques provides a powerful means of identifying critical points in the metabolic network whose modification can lead to improved product formation.

Energetic and economic considerations

The application of microalgal systems to the production of commodity chemicals is still in its infancy. The high production costs of industrial microalgal systems currently precludes the use of microalgae as sources of commodity products, because these can be produced inexpensively and on a vast scale in crop plants or heterotrophic bacterial fermentors (Lorenz & Cysewski, 2000). The current estimated direct cost of producing microalgae is US$5-20 (kg dry weight)$^{-1}$. This calculation does not include extraction and processing of the final product, PHA. Optimistic figures for a heterotrophic PHA production process with an optimized recovery process and at a production scale of one million tonnes per year is US$3-4 kg^{-1}. In contrast, current market prices of synthetic commodity polymers such as polypropylene, polyethylene and polystyrene are US$0.62-0.96 kg^{-1} (Steinbüchel & Füchten- busch, 1998). Clearly, improvements in the production process have to be implemented for a cost

effective production of PHAs.

A second hurdle for the implementation of microalgal based 'green' manufacturing processes is similar to that encountered by other microbiological fermentation processes. Possibly the main thrust in studying and optimizing processes such as PHA production is their potential to be applied to the sequestration of carbon dioxide from stack and flue gases, effluent purification and the production of biodegradable polyesters. Economic considerations such as the ones outlined above are important, but in addition, the design of production systems has to balance a basic energy equation: the amount of energy used (electricity or other forms of power) to produce the biodegradable plastics can not be higher than the amount of energy used for the production of other synthetic polymers (Gerngross, 1999).

Metabolic engineering of cyanobacteria, improvement of their yield through new growth technologies and the optimization of downstream processing PHAs are the three areas in which this group of organisms shows a great potential. The techniques for metabolic engineering in cyanobacteria are in place and improvement in PHA accumulation to the range of 60-70% of the cell's dry weight should be attainable through a combination of genetic engineering and manipulation of growth conditions. Further work is needed in the areas of downstream processing and growth optimization. The maximum biomass yields reported in the literature are around 10 g l^{-1} for cyanobacteria grown under experimental conditions in closed photobioreactors. Higher yields are easily attainable if factors such as self-shading and gas transport, including the availability of carbon dioxide, are addressed in the context of large scale, closed and contamination-less photobioreactors.

Summary

Microalgal systems, and in particular cyanobacterial systems, show a great potential for the "green" production of PHAs. Issues remaining to be addressed are all included in the area of optimization of the different aspects of their industrial application. Manipulation of cellular yields through metabolic engineering are a significant part of this process and recent advances in the field of biological system control studies with the availability of the entire genomes of certain organisms of interest, are rapidly moving this field forward.

References

Doi, Y. (1990). *Microbial polyesters.* VCH Publishers.

Farmer, W. R. & Liao, J.C. (2000). Improving lycopene production in *Escherichia coli* by engineering metabolic control. *Nature Biotechnol. .*

Gerngross, T.U. (1999). Can biotechnology move us toward a sustainable society? *Nature* **17***,* 541-4.

Hein, S., Tran, H. & Steinbüchel, A. (1998). *Synechocystis* sp. PCC6803 possesses a two-component polyhydroxyalkanoic acid synthase similar to that of anoxygenic purple sulfur bacteria. *Arch. Microbial.* **170***,* 162-170,

Lagarde, D., Beuf, L. & Vermaas, W. (2000). Increased production *of* zeaxanthin and other pigments by application *of* genetic engineering techniques to *Synechocystis* sp. strains PCC 6803. *Appl. Environ. Microbiol.* **66***,* 64-72.

Lorenz, R.T. & Cysewski, G.R. (2000). Commercial potential for *Haematococcus* microalgae as a natural source of astaxanthin. *Trends Biotechnol.* **18***,* 160-7.

Miyasaka, H., Nakano, H., Akiyama, H., Kanai, S. & Hirano, M. (1998). Production of PHA (polyhydroxyalkanoate) by genetically engineered marine cyanobacterium. In *Advances in chemical conversions for mitigating carbon dioxide,* vol. 114. *Studies in surface science and catalysis* (ed. T. Inui, M. Anpo, S. Yanagida and T. Yamaguchi), pp. 237-42. Elsevier Science.

Poirier, Y., Nawrath, C. & Somerville, C. (1995). Production of polyhydroxyalkanoates, a family of biodegradable plastics and elastomers, in bacteria and plants. *Biotechnology* **13***,* 142-50.

Slater, S., Mitsky, T.A., Houmial, K.L., Hao, M., Reiser, S. E., Taylor, N.B., Tran, M., Valentin, H.E., Rodriguez, D.J., Stone, D.A., Padgette, S.R., Kishore, G. & Gruys, K.J. (1999). Metabolic engineering of *Arabidopsis* and *Brassica* for poly(3-hydroxybutyrate-*co*-3-hydroxyvalerate) copolymer production. *Nature Biotechnology 17,* 1011-16.

Stal, L.J. (1992). Poly(hydroxyalkanoate) in cyanobacteria - An overview. *FEMS Microbiol. Rev.* **103***,* 169-80.

Steinbüchel, A. & Füchtenbusch, B. (1998). Bacterial and other biological systems for polyester production. *Trends Biotechnol.* **16***,* 419-27.

Stephanopoulos, G. (1999). Metabolic fluxes and metabolic engineering. *Met. Eng.* **1***, 1 -10.*

Suzuki, T., Miyake, M., Tokiwa, Y., Saegusa, H., Saito, T. & Asada, Y. (1996). A recombinant cyanobacterium that accumulates poly-(hydroxybutyrate). *Biotechnol. Lett.* **18***,* 1047-50.

Taroncher-Oldenburg, G., Nishina, K. & Stephanopoulos, G. (2000). Identification and analysis of the polyhydroxyalkanoate specific β-ketothiolase and acetoacetyl-CoA reductase genes in the cyanobacteriurn *Synechocystis* sp. PCC6803.

RESEARCH DIRECTIONS TO SUPPORT THE EMERGENCE OF A NEW BIOCOMMODITY INDUSTRY

Charles E. Wyman, Professor of Engineering
Thayer School of Engineering, Dartmouth College, 8000 Cummings Hall, Hanover, NH 03755

ABSTRACT
Substantial progress has been made in advancing technology for conversion of cellulosic biomass into ethanol, and several companies are striving to build the first commercial bioethanol plants. Success by one or more of these companies will be a vital first step toward the emergence of a much broader biocommodity industry with major environmental, economic, and strategic benefits. The challenges for raising large amounts of capital are immense for unproven technologies, and strengthening our fundamental understanding of the unit operations for biological biomass processing will speed the rate of application and reduce costs for advanced technologies. In addition, for biomass processing to realize its potential, more attention must be focused on development of advanced hemicellulose and cellulose hydrolysis approaches that promise large cost reductions. Improved knowledge grounded in fundamental principles will accelerate such vital improvements and lead to a wide range of biocommodity products.

INTRODUCTION
A wide range of fuels and commodity chemicals can be biologically derived from low cost and abundant cellulosic biomass materials such as agricultural residues, forestry wastes, substantial portions of municipal solid waste, and dedicated herbaceous and woody crops[1,2]. The application of biotechnology to produce such low cost, high volume products can be termed biocommodity engineering, a very distinct endeavor from the application of biotechnology to healthcare[3], and biocommodity products could provide unparalleled environmental, economic, and strategic benefits. For example, production of ethanol from biomass, termed bioethanol, could reduce carbon dioxide emissions by 90% and more and play a powerful role in reducing greenhouse gas emissions[4]. This impact is enhanced even more if excess electricity is exported[5]. Furthermore, biomass is the only sustainable route to production of organic fuels such as ethanol as well as organic chemicals such as succinic acid[6]. Biomass processing also offers a promising approach for disposing of solid wastes that are becoming more challenging to deal with in an environmentally acceptable manner[7]. Thus, it is vital to develop low cost technology for making fuels and commodity chemicals from biomass and commercialize it rapidly to realize these and many other important benefits.

BIOMASS CONVERSION TO COMMODITY PRODUCTS
Biomass has a complex structure[8]. About 40 to 50% of the material on a dry weight basis is cellulose, a chain of covalently bonded glucose molecules. Approximately another 25 to 35% of dry biomass is hemicellulose, also a sugar polymer but usually made up of five different sugars (arabinose, galactose, glucose, mannose, and xylose) with smaller amounts of some other constituents such as acetic acid. In addition, while cellulose is mostly crystalline, hemicellulose is amorphous. Both cellulose and hemicellulose can be broken down or hydrolyzed by acids (e.g., sulfuric) or enzymes (e.g., cellulases for cellulose) to release the sugars in these long chains. The remainder of biomass is mostly lignin with generally smaller amounts of minerals, oils, and other compounds often loosely termed extractives.

Enzymatically based routes for producing biocommodity products from biomass promise substantial cost reductions that would make the technology competitive with fossil-based fuel production[7,9,10]. In one configuration, the enzymatic conversion process begins with size reduction and dilute acid hydrolysis of hemicellulose (pretreatment) to fermentable sugars to open up the biomass structure and expose the cellulose fraction for hydrolysis by enzymes. A small portion of the pretreated substrate is then used for production of cellulase enzymes that are combined with the bulk of the pretreated solids to released glucose. Fermentative organisms convert this glucose and the sugars extracted from the hemicellulose during pretreatment to ethanol or other products. These are then recovered from the fermentation broth while the residual solids containing primarily lignin can be used as boiler

fuel to meet the heat and electricity needs for the process with any surplus exported or converted into chemicals.

BIOETHANOL COMMERCIALIZATION AND CHALLENGES

Because far more attention has been focused on development of bioethanol technology than other biocommodity products, this paper will build from information available for bioethanol[8]. However, most of the key process steps are common to all biocommodity products, and the conclusions for bioethanol experience are applicable to other biocommodity products[2].

The projected cost of producing bioethanol has been reduced from about $4.60/gallon in 1979 to only about $1.18/gallon now, a value competitive with the price of corn ethanol[7,9]. The drop in processing costs can be attributed to two classes of advancements: reductions in the cost of breaking down carbohydrate polymers into sugars and development of technology to ferment all five sugars in biomass to ethanol with high yields. The former, termed "overcoming the recalcitrance of biomass," resulted from improvements in pretreatment to recover hemicellulose sugars with better yields and enhance cellulose digestibility to glucose, development of better cellulase enzymes, and combining enzymatic hydrolysis and fermentation steps to improve the rates, yields, and concentrations of ethanol production. Fermentation of all five sugars at high yields, a critical step to achieving low costs, first came to fruition with the genetic engineering of various common bacteria and was recognized by the award of US patent 5,000,000 [11,12].

Several companies are working to commercialize bioethanol production technology in the United States including Arkenol, BC International, HAFTA, Masada, and SWAN Biomass. BC International is working with a team of engineers and contractors to retrofit a former molasses and then grain ethanol plant in Jennings, Louisiana to make about 23 million gallons of bioethanol per year from sugar cane bagasse and other wastes abundant in that area. The process is based on the unique five sugar fermentation technology described in patent 5,000,000 and related patents to which BC International has exclusive rights. Although the details of the process are confidential, it relies on hydrolysis of hemicellulose to fermentable sugars followed by breakdown of the cellulose fraction to glucose for conversion to bioethanol. BC International is developing another project with rice growers, community leaders, and others in Gridley, California to produce bioethanol from rice straw and wood wastes.

It is important to appreciate that the cost of implementing new technology is more expensive for a first plant than for the next. This can be pictured in terms of a series of concentric circles layered around a core. The core represents the cost of the technology itself, and the adjacent ring represents normal contingencies associated with applying any technology. The sum of the two can be thought of as the true cost for a particular technology that won't change over time. However, for new technology, an additional cost ring is added to provide a safety margin for first plants to compensate for possible poorer performance than projected from scale-up data. Another ring represents extra equipment that is included to insure operation and compensate for design data deficiencies. A fourth ring accounts for additional contingencies that are applied to account for unexpected delays and costs that could result for first-of-a-kind technology. Although the costs associated with the performance, equipment, and extra contingency rings will drop exponentially for a given technology with each application due to a learning curve effect, the total of these rings can significantly increase the project costs for the first plant and jeopardize commercialization. In fact, these extra costs can make new technology more expensive to apply than established technology even though the cost of the core technology is much less for the advanced approach. The high cost associated with these extra cost rings can trap new technology in the "Valley of Death," terminating introduction of seemingly low cost processes.

OPPORTUNITIES TO REDUCE BIOCOMMODITY PROCESSING COSTS

It has been shown that biomass at about $40/ton is competitive in costs with oil at $6/barrel on a weight basis or at $12.70/barrel on an energy content basis[3]. Thus, the primary challenge in making biocommodity products competitive is in reducing the cost of processing biomass. Furthermore, no fundamental barriers prevent biomass processing from being competitive[13], and scenarios have been defined that can realize bioethanol costs of only about $0.50/gallon for advanced technology or about $0.34/gallon for the best possible technology performance[10]. The primary conclusions from these studies are that advanced pretreatment technologies must be devised to reduce chemical and energy costs and that cellulase production and cellulose and hemicellulose sugar utilization must be consolidated and simplified. Both of these advances, and not just one, are essential to be competitive.

THE IMPORTANCE OF APPLIED FUNDAMENTAL RESEARCH

An approach that deserves more attention in the emerging biocommodity engineering field is improvement in our

fundamental understanding of biological conversion systems. Better knowledge would allow us to design processes with much greater confidence, reducing extra equipment, performance margins, and other contingencies that drive up costs. Such information would allow us to project performance for commercial processes more reliably from bench or limited pilot plant operations and lower the number of experiments and scale-up demonstration steps that delay projects and increase costs. The result would reduce uncertainty and risk, thereby speeding technology applications and dropping scale-up costs by bridging the “Valley of Death" with better information. Interpreting performance based on fundamental principles and models and accurately accounting for process chemistry and energy flows are examples of this approach.

Better knowledge of pretreatment and biological processing steps would also feed improvements in these vital technologies. Although substantial progress has been realized, it is becoming more and more difficult and expensive to reduce costs further by traditional trial-and-error approaches. If we clearly understand what limits systems now, we could use this new knowledge to devise better technologies. Donald Stokes recently labeled the approach in which we seek to improve our understanding of fundamentals in light of its application as "Pasteur's Quadrant"[14].

SUMMARY

Biocommodity engineering, the production of low cost, high volume fuels, chemicals, and materials through the application of modern biotechnology and bioprocessing, provides impressive environmental, economic, and strategic benefits. Biocommodity processing is particularly powerful in its potential to virtually eliminate greenhouse gas emissions and in the truly unique path to sustainable production of organic fuels and chemicals. Impressive progress has been made in advancing technology for bioethanol production from low cost sources of biomass so that it is competitive in the fuel blending market. Consequently, commercialization of the first bioethanol processes is now underway, and once implemented, these projects will reduce costs some through a learning curve. Even lower costs and much greater impact can be realized if both pretreatment and biological steps are substantially improved. However, it is very challenging to develop low cost advanced biocommodity technologies and overcome uncertainty that could terminate its application in the Valley of Death. A focus on improving our knowledge of fundamentals with an eye to its application would enhance our ability to achieve low cost biomass processing and to scale up processes with confidence, realizing a once-in-a-lifetime opportunity to gain unparalleled environ-mental, economic, and strategic benefits.

ACKNOWLEDGMENT

I would like to thank the Thayer School of Engineering at Dartmouth College for their support in developing the ideas presented and the sponsors of this meeting for making it possible to attend.

REFERENCES

1. Dale, B.E.; Artzen, C.E., eds. 1999. "Biobased Industrial Products: Research and Commercialization Priorities," National Research Council, Washington.
2. Wyman, C.E.; Goodman, B.J. 1993. *Applied Biochemistry Biotechnology* **39/40**:41.
3. Lynd, L.R.; Wyman, C.E.; Gerngross, T.U. 1999. *Biotechnology Progress.*
4. Tyson, K.S. 1993. NREL/TP-463-4950, DE94000227. Golden, CO: National Renewable Energy Laboratory, November.
5. Wyman, C.E. 1994. *Applied Biochemistry Biotechnology* **45/46:** 897-915.
6. Lynd, L.R. 1997. Personal communication.
7. Wyman, C.E. 1999. *Annual Review of Energy and the Environment* **24**: 189-226.
8. Wyman, C.E., ed. 1996. "Handbook on Bioethanol: Production and Utilization." *Applied Energy Technology Series,* Taylor & Francis, Washington, 424 pp.
9. Hinman, N.D.; Schell, D.J.; Riley, C.J.; Bergeron, P.W.; Walter, P.J. 1992. *Applied Biochemistry Biotechnology* **34/35**:639-49.
10. Lynd, L.R.; Elander, R.T.; Wyman, C.E. 1996. *Applied Biochemistry Biotechnology* **57/58**:741-61.
11. Ingram, L.O.; Conway, T.; Alterthum, F. 1991. US Patent 5,000,000, March 19.
12. Ingram, L.O.; Conway, T.; Clark, D.P.; Sewell, G.W.; Preston, J.F. 1987. *Applied Environmental Microbiology* **53**: 2420-5.
13. Wyman, C.E. 1995. In "Enzymatic Degradation of Insoluble Carbohydrates," ACS Symposium Series 618, Saddler, J.N.; Penner, M.H., ed, American Chemical Society, Washington, pp. 272-290.
14. Stokes, D.E. 1997. “Pasteur's Quadrant." Brookings Institution Press, Washington, 180 pp.

SYNTHESIS OF NEW CHIRAL BUILDING BLOCKS FROM LEVOGLUCOSENONE

Zbigniew J. Witczak, Associate Professor
Department of Pharmaceutical Sciences, School of Pharmacy, Wilkes University, Wilkes-Barre, PA 18766

ABSTRACT
New developments of functionalized chiral building blocks from convenient cellulose derived pyrolysis product (levoglucosenone) are presented.

INTRODUCTION

Industrial production of this convenient chiral building block from waste cellulosic materials, such as newsprint, paper-mill sludge or any waste paper could solve some environmental problems, classifying it as green chemistry. Indeed, environmental protection, for as simple a reason as preventing the accumulation of waste paper and its conversion into value-added products, could be an alternative goal as well. The raw carbohydrate material for functionalization into useful building blocks must be economically feasible and cost effective, hence the use of waste cellulosic materials. Laboratory production of levoglucosenone as depicted is well defined[1] in contrast to the industrial small-scale process[2].

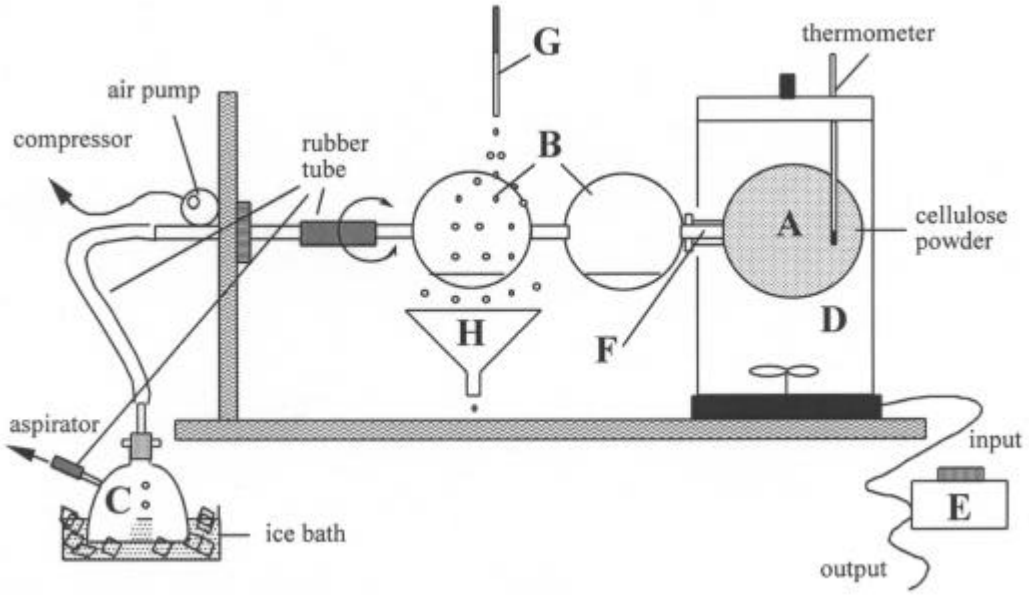

A) *Apparatus*-The apparatus is shown in Fig. 1. **A** is a 1-L round bottom flask packing with ca. 500 g of prepared cellulose powder, that is connected to **B**. **B** is a 500 mL two-bulb trap, the other end being connected through a rubber tubing (8 cm) to a hemi-rotary metal tubing equipped with air-pump. **C** is a 500 mL ice-trap connected to an aspirator. **D** is an air-bath (Aldrich; Z10, 0463-3) with a thermometer, and connected to a voltage regulator **E**.

The chemical character and high reactivity of the conjugate system of this chiral synthon warrants the easy and stereoselective functionalizations at C-4, C-3, C-2 , and C-6. These positions are extremely important for the functionalization and introduction of important functional groups such -NH_2, -SH, OR. Such a possibility of stereoselective introduction of the new group in one simple step constitutes an enormous advantage over other more complicated and multiple step approaches. (+) Diastereoisomer of levoglucosenone was first synthesized in our laboratory[3] and could be an ideal precursor for L-series of functionalized analogs and rare sugars.

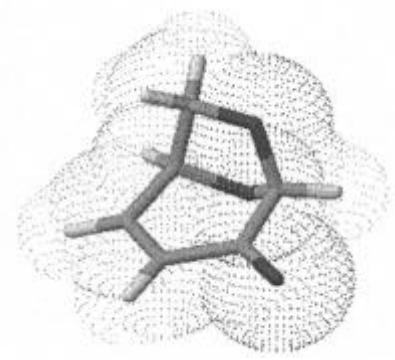

In order to synthesize these new analogs functionalized at strategically important positions such as C-4, C-3, C-2 and C-6, the specific approach can be drawn.

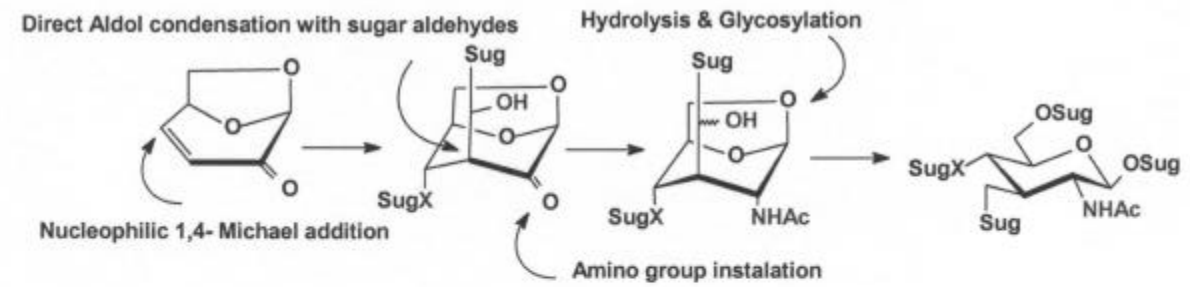

Other single functionalization through established set of reactions[4-6] can also be used for the purpose of extension of functionality or addition of additional chiral center as well.

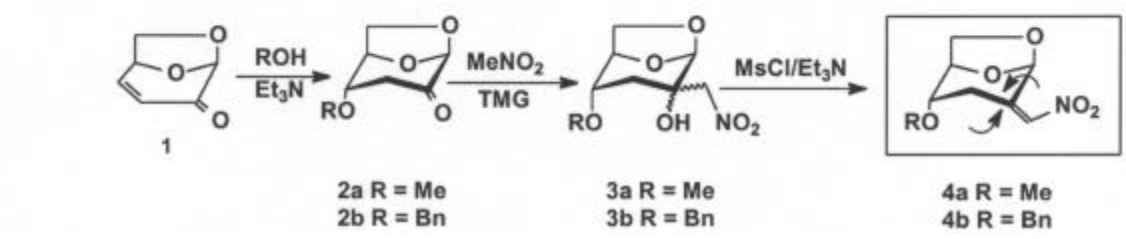

This specific functionalization produces a new family of nitroenones, as chiral building blocks highly suitable for further manipulation and introduction of a variety of additional groups through simple type Michael addition approach. This particular type approach is stereoselective with the formation of only one type of adduct as it is controlled by the steric hindrance of the bulky 1,6-anhydro bridge. Both nitroenones are convenient starting chiral building blocks for the synthesis of biologically important thio-sugars, including especially rare (1-3)-thiodisaccharides produced in highly stereoselective approaches.

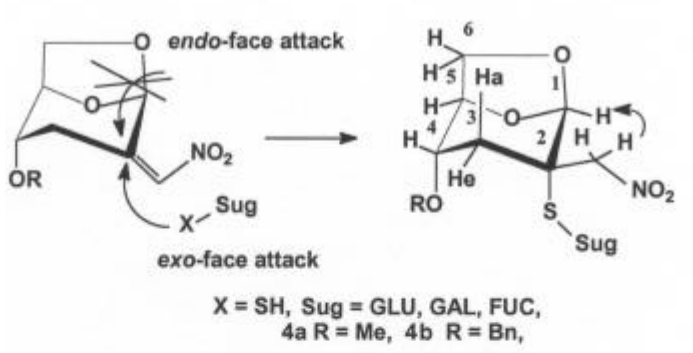

The deprotection and additional functionalization of the strategically important nitro group at C-2 constitutes new and stereoselective approach to this class of thio- and aminothiosugars.

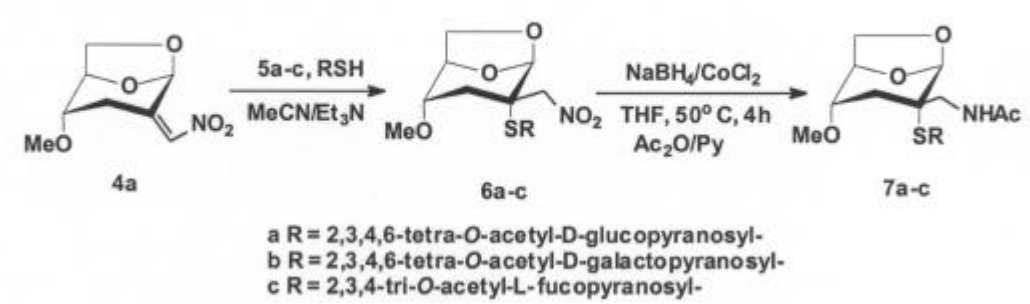

SUMMARY

The variety of methods for the functionalization of this classical building block provides a number of attractive

stereoselective approaches to various classes of optically active derivatives of particular interest, including sulphur and nitrogen heterocycles as well as rare carbohydrates.

Despite the low level of chemical industry interest, levoglucosenone chemistry will be one of the frontiers in carbohydrate chemistry, especially in the area of small molecules and complex oligosaccharides of medicinal interests.

Additionally, an environmental issue of the utilization of waste cellulosic material and waste biomass products should be considered as an alternative green chemistry application to the production of many value-added products based on levoglucosenone. The combinatorial utilization of carbohydrate scaffolds based on levoglucosenone functionalization will also constitute an attractive and relatively cheap starting material.

This rich selection of potential approaches, combined with further developments of new procedures and modern reagents, create an enormous opportunity for the field to be the frontier for many years to come.

REFERENCES

1. For reviews see; *Levoglucosenone and Levoglucosans Chemistry and Applications* Witczak, Z.J. Ed. ATL Press Science Publishers; Mt Prospect, IL **1994;** Witczak, Z.J. in *Studies in Natural Products Chemistry,* Atta-Ur-Rahman, Ed. Vol. 14, Elsevier Science Publishers, Amsterdam, **1993;** pp. 267-282*;* Miftakhov, M.S.; Valeev, F.A.; Gaisina, I.N. *Uspekhi Khimi,* **1994,** *63,* 922*.*
2. Levoglucosenone is produced by: Yuki Gosei Kogyo Co. Ltd.
3. Witczak, Z.J.; Mielguj, R. *Synlett,* **1996,** 108*.*
4. Witczak, Z.J.; Sun, J.; Mielguj, R. *Bioorg Med Chem Lett* **1995,** *5*, 2169*.*
5. Witczak, Z.J.; Chhabra, R.; Chen, H.; Xie, *Q. Carbohydrate Res.,* **1997,** *301*, 167*.*
6. Witczak, Z.J.; Chhabra, R.; Chojnacki, J. *Tetrahedron Lett.* **1997,** *38*, 2215*.*
7. Witczak, Z.J.; Chen, H.; Kaplon, P. *Tetrahedron: Asymmetry,* **2000***, 11,* 519*.*

4th Annual Green Chemistry &
Engineering Conference

Sustainable Technologies:
From Research to Industrial Implementation

June 27 - 29, 2000

PROCESS DESIGN I

IS THE PRODUCTION OF MICROBIAL POLYMERS (PHAS) A GOOD IDEA? A LIFE CYCLE AND ENERGY PERSPECTIVE

Tillman U. Gerngross
Biochemical Engineering Program, Dartmouth College, Hanover, NH 03755

ABSTRACT
We have conducted two life cycle analysis on the production of PHAs: (1) by fermentation from corn, and (2) in genetically modified corn. Both studies suggest that making PHAs from renewable resources, using current energy usage patterns, has an overall negative environmental impact when compared to the production of conventional polymers such as polystyrene or polyethylene. We further argue that biodegradability has potential environmental tradeoffs and offer a life cycle view of possible alternatives.

INTRODUCTION
The sustainability of a society based on finite fossil resources is the subject of ongoing scientific and political debate. One aspect of this debate, besides exploring alternative energy sources, is the challenge to provide chemical commodities (fuels, lubricants, adhesives, solvents, paints and materials etc.) to an advanced consumer society, without depleting non-renewable resources.

An approach, that has recently gained popularity, advocates the use of biological (fermentation) processes to produce chemical commodities from agricultural feedstocks. Fueled by advances in the area of metabolic engineering an array of products ranging from polymers to polymer intermediates and industrial dyes can now be produced by fermentation. With numerous such biological approaches currently being considered, it appears timely to analyze whether the proposed processes have the intended effect of sparing nonrenewable resources and benefiting the environment. Fermentation based processes offer intuitive advantages such as aqueous processing environments, non-toxic waste and most importantly the use of renewable, non fossil feedstocks. However, in most cases these benefits have not been critically weighed against an overall inventory of materials and energy required, to produce a given product. To close this gap we offer a side by side comparison of a biological versus a conventional petrochemical plastic manufacturing process to illustrate the complexity of choices confronting society and the commodity biotechnology industry in the years to come.

Much has been made of the disadvantages and environmental shortcomings of traditional, fossil oil based polymers used in the packaging industry (i.e. Polyethylene, Polypropylene and Polystyrene (PS)). While offering good material properties at a low price the environmental impact and manufacture of these polymers has traditionally been viewed with reservation. As a result much effort has been dedicated to the effort of developing alternative polymers that are both (1) biodegradable and (2) sustainable in their production. Of these alternatives, polyhydroxy alkanoic acids (PHAs) have been one of the leading candidates to replace conventional petrochemical based polymeric materials on a large scale. PHAs can be made entirely from an agricultural sugar source such as dextrose and besides showing good material properties offer the benefit of biodegradability. Hence replacing traditional polymers used in the packaging industry is viewed by many as a desirable and environmentally sound approach.

However, numerous factors contribute to the environmental impact of a given product. Very often an environmental burden is caused by the manufacture of a given product and only to a minor extent by its ultimate use. Hence a "cradle to grave" analysis, which incorporates manufacturing practices, and disposal becomes the benchmark for assessing the environmental impact of a given product. Accordingly we will try to make reasonable assumptions of a large scale industrial PHA fermentation and compare the energy and raw material requirements of such a process with current refining and polymerization practices. We also attempt to quantify the impact of various alternative biological polymer production systems, such as polylactic acid (PLA) and PHAs derived from transgenic plants. Finally an overall systems analysis attempts to rate competing polymer production technologies on the basis of their expected environmental footprint. Three metrics are used to assess environmental impact: (1) resource depletion, (2) net greenhouse gas emissions, and (3) eutrophication.

SUMMARY
Biological polymers have been promoted as the "green" answer to conventional plastic manufacturing. A "cradle to grave" analysis of these products however cast doubt on the premise that these polymers offer environmental benefits. While chemicals and fuels made from renewable resources have the potential to be more benign to the

environment, our current studies suggest that they may also have the opposite effect and in fact deplete more fossil resources. Full life cycle assessments are thus recommended prior to committing societal resources to developing these technologies.

STUDY ON UNSTEADY STATE OXIDATION OF *N*-BUTANE TO MALEIC ANHYDRIDE TO DEVELOP A CLEANER TECHNOLOGY*

Cheng-Yue Li, Xiao-Feng Huang, Biao-Hua Chen, Hui Liu, Dong-Hai Yang

College of Chemical Engineering, Beijing University of Chemical Technology
Beijing 100029, P.R.China

INTRODUCTION

Up to date, the partial oxidation of *n*-butane to maleic anhydride (MA) over vanadium phosphorus oxide (VPO) catalyst is still an unique alkane selective oxidation reaction industrialized. This reaction system has been studied extensively in recent years in consideration of its practical significance and representative of reaction mechanism. Contractor *et al*.[1-3] proposed a new unsteady-state reaction mode to synthesize maleic anhydride from *n*-butane, by spatial separation of *n*-butane oxidation and VPO catalyst re-oxidation in a CFB reactor system and demonstrated its advantages over the traditional technologies in reducing the emission of CO_2 and saving feedstock. As an alternative way, temporal separation of selective oxidation of *n*-butane and catalyst re-oxidation in fixed-bed reactors with different scales was systematically investigated and obvious improvements in selectivity and yield were observed. Moreover, transient reaction kinetics of *n*-butane oxidation to maleic anhydride was also studied, using weight gain measurements in a TGA unit and on-line MS/GC measurements. The models based on the transient reaction kinetics and developed for the fixed-bed reactors with different scales can predicate the data obtained in transient response experiments and/or forced periodic operation of the reactors.

EXPERIMENTAL

A domestic commercial VPO catalyst was adopted and two types of experiments were undertaken in this study. First, the performances of fixed-bed reactors with different scales under unsteady-state operation by periodic composition modulation or both composition and temperature modulation were investigated. These experiments were respectively carried out in a fixed-bed micro reactor with a stainless steel tube of 9.5mm O.D. and 250mm length, packed with about 0.6g of 40/60 mesh catalyst diluted with quartz sands in its reaction section, and in a tubular fixed-bed reactor with single tube of 25.4mm O.D. and 1.2m length, packed with cylindrical pellets of VPO catalyst (6x6mm) diluted with ceramic beads in the middle section. An on-line mass spectrometer and a series of two on-line gas chromatograph systems were used to measure the composition of the effluent. Next, reaction network structure and transient reaction kinetics were respectively investigated in a fixed-bed micro reactor by a series of transient response measurements with on-line MS/GC and in a TGA unit by temperature programmed oxidation and weight gain measurements.

RESULTS AND DISCUSSION

Figure 1 shows the weight response on temperature ramping of the fresh VPO catalyst crushed in flowing mixture of 21(vol)% O_2 and He balanced. Initially, the sample loses water adsorbed and weight decreases up to 280 ºC. Obvious weight increase after about 500 ºC suggests that a temperature of at least 500 ºC is needed for catalyst re-oxidation process to proceed rapidly and forced periodic operation by both composition and temperature modulation probably may lead to improved time-average performances of the reactor.

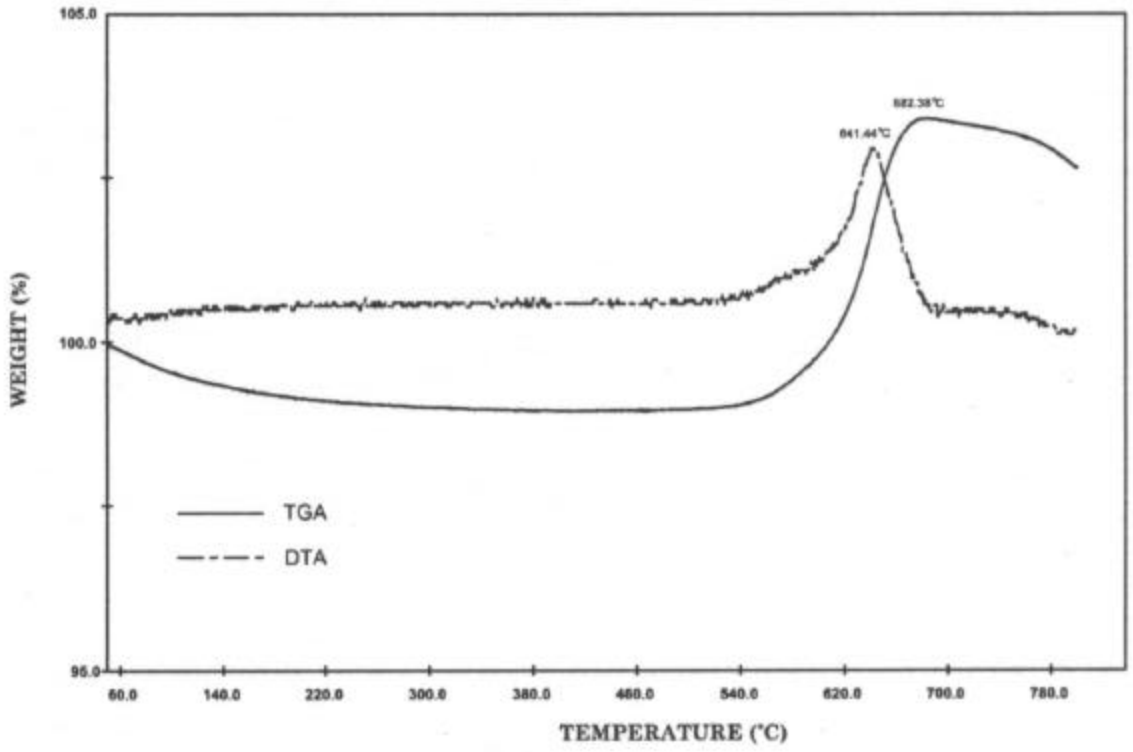

Figure 1. TGA and DTA curves as the functions of temperature in 21 % O_2+He

Table 1 summarizes some experimental results on the performances of the fixed-bed micro reactor under steady state, periodic composition modulation and periodic modulations of both composition and temperature.

Table 1. Performance comparison of the fixed-bed micro reactor under different operation modes

Operation	T_{ROX} (ºC)	T_{SOX}C)	C_B (%)	S_{MA} (%)	Y_{MA} (%)
SS1	416	416	56.5	63.5	35.9
SS2	416	416	88.1	65.5	57.7
USS1 (CM.)	416	416	73	70.7	51.6
USS2 (C&T M.)	560	416	89.8	67.4	60.5

SS1 : Steady state, 3% C_4H_{10}+15% O_2 + He; SS2 : Steady state, 1.5% C_4H_{10} + 20% O_2 + He; USS1 : Composition Modulation(C M), 3%C_4H_{10} + 15% O_2 + He (5mins) / 21% O_2 + He (5mins); USS2: Composition and Temperature Modulation (C&T M), 3%C_4H_{10} + 15% O_2 + He (5mins) / 21% O_2 + He (5mins).

The data listed in Table 1 show that the yield of MA under composition modulation decreases as the conversion of *n*-butane is considerably reduced, even though the selectivity is improved while periodic modulation of both composition and temperature (raising re-oxidation temperature of the catalyst) can improve the yield of maleic anhydride. It means that the re-oxidation of the catalyst at about 416 ºC is so slow that this step is certainly rate-controlling. Similar experimental results, as shown is Table 2, were also found in a tubular fixed-bed reactor packed with cylindrical pellets of commercial VPO catalyst.

The final rank in Table 2 represents the experimental results in respect to an optimal condition coming from an orthogonal experiment design of four factors and three levels. For a specified oxygen-containing feed gas, selective oxidation temperature (T_{SOX}), re-oxidation temperature of the catalyst (T_{ROX}), period duration (τ_p) and cycling split (C_S) were considered as the most important influence factors on the time-average performances. Obviously, raising the regeneration temperature of the catalyst increases the rate of rate-controlling step, the diffusion of lattice oxygen in the bulk phase of the catalyst.

Table 2. Performance comparison of the tubular fixed-bed reactor under different operation modes

Operation	T_{ROX}(ºC)	T_{SOX}(ºC)	τ_p (min)	C_B (%)	S_{MA} (%)	Y_{MA} (%)
SS	410	410		82.6	61.6	50.9
USS1 (C M.)	400	400	4	68.9	69.9	48
USS2 (C M.)	400	400	6	68.6	73	50
USS3 (C&T M.)	530	405	4	89	76.3	67.9

SS : Steady state, 1.5% C_4H_{10} + 20% O_2 + N_2; USS: Composition (and Temperature) Modulation, 3% C_4H_{10} +15% O_2 + N_2 / 21% O_2 + N_2.

TRANSIENT KINETICS AND MODELING

Based on prior investigations, weight gain measurements in a TGA unit and a series of transient response measurements to step change in feed composition were carried out. It is concluded that surface lattice oxygen and the oxygen adsorbed on the surface are responsible respectively for selective oxidation to MA and the formations of CO_X. Besides the following surface re-oxidation steps of the catalyst can be presented,

$$O_2 + 2(S) \rightarrow 2O(S) \quad (1)$$

$$O(S) + (L) \rightleftharpoons O(L) + (S) \quad (2)$$

a set of gradual selective oxidation reactions to MA can be devised as follows:

$$C_4H_{10} + O(L) \not\rightarrow C_4H_8(L) + H_2O \quad (3.a)$$

$$C_4H_8(L) + O(L) \rightarrow C_4H_6(L) + H_2O + (L) \quad (3.b)$$

$$C_4H_6(L) + O(L) \rightarrow C_4H_6O(L) + (L) \quad (3.c)$$

$$C_4H_6O(L) + O(L) \rightarrow C_4H_4O(L) + H_2O + (L) \quad (3.d)$$

$$C_4H_4O(L) + 3\ O(L) \rightarrow C_4H_2O_3(L) + H_2O + 3\ (L) \quad (3.e)$$

$$C_4H_2O_3(L) \rightleftharpoons C_4H_2O_3 + (L) \quad (4)$$

It is well known that the initial oxidation rate of 1-butene is several tens times higher than that of *n*-butane[4], so (3.a) is considered to be rate-controlling step of selective oxidation reaction. Correspondingly, a set of formation reactions of CO_X can be approximately written as follows:

$$C_4H_{10} + 9\ O(s) \rightarrow 4CO + 5\ H_2O + 9(s) \quad (5)$$

$$C_4H_{10} + 13\ O(S) \rightarrow 4CO_2 + 5\ H_2O + 13(S) \quad (6)$$

$$C_4H_2O_3(L) + 2\ O(S) \rightarrow 4\ CO + H_2O + (L) + 2(S) \quad (7)$$

$$C_4H_2O_3(L) + 6\ O(S) \rightarrow 4\ CO_2 + H_2O + (L) + 6(S) \quad (8)$$

The following basic assumptions are adopted to simplify further the descriptions of the reaction and transport processes in the fixed-bed micro reactor:

(1) The rates of the reactions (5)-(8) can be expressed as the rates of their controlling steps, the first steps;

(2) Must take account of the diffusion of the lattice oxygen in the bulk phase of the catalyst and its rate is considered to be directly proportional to the difference between θ_L and θ_B, the coverage of lattice oxygen on surface and in bulk phase, respectively;

(3) The axial dispersion in the catalyst bed is negligible and a one-dimensional plug-flow model for the fixed-bed

micro reactor can be adopted.

Therefore, a set of partial differential equations with corresponding initial and boundary conditions, as a transient model of the fixed-bed micro reactor used and including the kinetic parameters of all elementary processes involved in, can be induced.

A part of data coming from transient response experiments was used to estimate these transient kinetic parameters, while else was used to test the model by comparing the model predictions to corresponding transient responses. It is noticed that the model predictions are in good agreement with the experimental data obtained with on-line GC measurements except stronger overshoot in simulation. However, the trends of the model predictions to transient response curves are in very good agreement with the on-line MS measurements, qualitatively.

This set of transient kinetic parameters was also successfully adopted to predicate time-average performances of fixed-bed micro reactor operated under periodic composition modulation or periodic modulations of both composition and temperature, to simulate rough the performances of a CFB system with a riser and a fluidized bed regenerator.

SUMMARY

(1) The results coming from experimental investigation show that periodic modulations of both composition and temperature can improve time-average performances of fixed-bed reactors. With a 1:0.4 cycle split and period of 4 minutes, re-oxidation of the catalyst at 530 ºC and selective oxidation at 405 ºC, the yield of maleic anhydride for a single-tube fixed-bed reactor was improved 11.4% than that operated under steady-state conditions with the same time-average flow of *n*-butane.

(2) Transient reaction-diffusion kinetics of the VPO catalyst adopted in this work was studied and the values of corresponding kinetic parameters were estimated.

(3) Based on the transient kinetics mentioned above, the models for the fixed-bed reactors involved in the work were developed and the predictions to transient responses and time-average performances of these reactors are in good agreement with the experimental data.

(4) Transient kinetic model of the catalyst has also been adopted to develop a rough model of CFB reactor system and to perform parametric analysis for this type of reactor system.

REFERENCES

1. Contractor, R.M.; Bergna, H.E.; Horowitz, H.S.; Blackstone, C.M.; Chowdhry, U.; Sleight, A.W., *Stud. Surf. Sci. Catal.,* 1987, **38**, 645
2. Contractor, R.M.; Garnett, D.I.; Horowitz, H.S.; Bergna, H.E.; Patience, G.S.; Schwartz, J.T.; Sisler, G.M., In *New development in selective oxidation II,* eds V.C. Corberan and S.V. Bellon, Elsevier, Amsterdam, 1994, p233
3. Contactor, R.M., *Chem. Eng. Sci.,* 1999, **54**, 5627
4. Cavani, F.; Trifiro, F., *ChemTech,* 1994, **18**(4), 18

*Financially supported by the National Natural Science Foundation of China under grant No. 29792073-3.

CARBON DIOXIDE-INDUCED PLASTICIZATION OF POLYMER MELTS: RHEOLOGY AND RHEOMETER DESIGN

Joseph R. Royer
Graduate Student in Chemical Engineering
Saad A. Khan
Associate Professor of Chemical Engineering
Department of Chemical Engineering, North Carolina State University, Campus Box 7905, Raleigh, NC 27695
Joseph M. DeSimone
William R. Kenan Jr., Distinguished Professor of Chemistry at UNC-CH and Chemical Engineering at NC State,
Director, NSF S&T Center for Environmentally Responsible Solvents and Processes
Department of Chemistry, University of North Carolina at Chapel Hill,
Venable and Kenan Laboratories, CB#3290, Chapel Hill, NC 27599

ABSTRACT
One of the most utilized techniques for modifying a polymer's physical properties is plasticization. Unfortunately, plasticizers used in industry today usually are difficult to remove from the product and permanently alter their properties. Supercritical carbon dioxide has been shown to be highly soluble in many polymer melts, and to be an effective plasticizer that is easily removed. Our study involves the construction of two high pressure rheometers to study the steady shear properties of various polymer systems with dissolved carbon dioxide. The results reveal viscosity reductions of polymer melts of greater than 50%, when exposed to liquid and supercritical carbon dioxide. The effects of polymer structure, molecular weight, temperature, and carbon dioxide concentration on viscosity reduction are examined.

INTRODUCTION
One of the most utilized techniques for modifying a polymer's physical properties is plasticization. Unfortunately, plasticizers used in most industries today are difficult to remove from a product or permanently alter the polymer's properties. This is undesirable in many applications. Finding methods to selectively manipulate the concentration of a plasticizer in a polymer matrix and remove them from the final product is essential. Supercritical carbon dioxide ($scCO_2$) has been shown to be highly soluble in many polymer melts, an effective plasticizer, and can be easily removed. Our study involves construction of a high pressure extrusion slit die rheometer to study the steady shear properties of various polymer systems with dissolved carbon dioxide. The rheometer was tested to ensure that fully developed, one-phase flow was obtained. The results reveal reduction in the viscosity of the polymer melts of greater than 50%, when exposed to liquid and supercritical carbon dioxide. The effects of polymer structure, molecular weight, temperature, and CO_2 concentration on viscosity reduction are examined. Classical viscoelastic scaling has been used to reduce the rheological data to a set of master curves. The scaling information has been used to further quantify effects of CO_2 on the polymers free volume, as well as towards the development of a rheological equation of state for the polymer/CO_2 systems.

VISCOSITY REDUCTION
Experimental measurements of viscosity for all 3 polystyrene and 2 poly(vinylidene fluoride) commercial polymer resins were conducted and a representative curve is shown in Figure 1 for Styron-685D at CO_2 concentrations of 0, 2, 3, and 4 wt% at 200ºC. The viscosity data is shown as apparent viscosity versus apparent shear rate, and the points are all taken at different pressure conditions. The average pressure during each individual measurement is indicated to give an example of the conditions during measurement. After the addition of CO_2 to the polymer melt the general shape of the viscosity versus shear rate curve is maintained. The effect of increasing CO_2 concentration simply shifts the viscosity curve to the left, thereby decreasing the viscosity at a given shear rate. This trend in viscosity has been observed not only for the addition of CO_2 but for many different plasticizer systems. By using viscoelastic modeling the effects of CO_2 concentration and pressure are scaled by their effects on T_g allowing a predictive model for CO_2 plasticization to be developed.

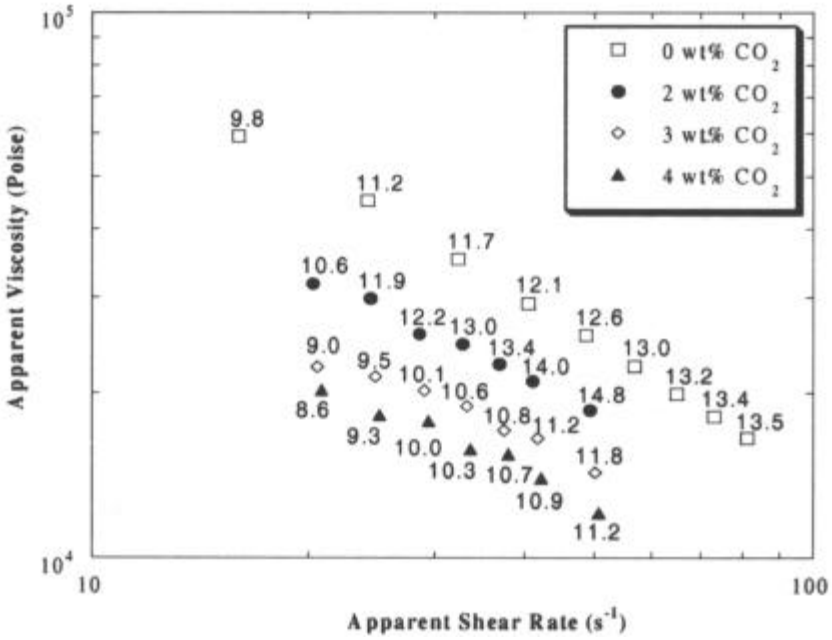

Figure 1. Viscosity reduction of Styron-685D at 200ºC, pressures are given in MPa.

VISCOELASTIC MODELING

The depression of T_g with the addition of CO_2 and other diluents has been widely reported for many polymer systems. Chow has proposed the following explicit expression based on both classical and statistical thermodynamics that predicts the T_g of polymer-diluent mixtures:

$$\ln\left(\frac{T_{g,mix}}{T_g}\right) = \Psi\{(1-\theta)\ln(1-\theta) + \theta\ln\theta\} \quad (1)$$

$$\theta = \frac{M_p}{zM_d}\frac{\omega}{1-\omega} \quad (2)$$

$$\Psi = \frac{zR}{M_p\Delta C_{p,Tg}} \quad (3)$$

Here $T_{g,mix}$ is the glass transition temperature of the diluent-polymer mixture, ω is the weight fraction of diluent, z is a lattice coordination number for the polymer repeat unit, $\Delta C_{p,Tg}$ is the change in heat capacity associated with the glass transition temperature and M_p and M_d are the molecular weights of the monomer and diluent, respectively. This equation has been shown to be an effective estimate of polymer T_g depression with various diluents including carbon dioxide up to a weight fraction of approximately 12%.

Substitution of the $T_{g,mix}$ for T_g in the WLF equation introduces the effects of CO_2 concentration on the free volume of the melt. By modifying the definition of free volume as suggested by Ferry and Stratton the effects of pressure on free volume can also be include as follows:

$$f = f_g + \alpha\left(T - T_{g,mix} - \frac{\beta}{\alpha}P\right) \quad (4)$$

Where β is the isothermal compressibility of the polymer melt. This free volume expression suggests that the effects of CO_2 concentration and pressure can be directly incorporated as shifts in T_g of the polymer solution.

To describe the effects of T_g depression by CO_2 addition and of T_g elevation due to pressure on the viscosity of the polymer melt; the free volume expression can be combined with the Doolittle model. If f_g is held constant and independent of CO_2 concentration and pressure, a set of shifting equations analogous to the WLF equation for temperature can be derived to determine the effects of pressure CO_2 concentration on the undiluted polymer melt viscosity. Using this theory, a priori prediction of viscosity shift factors for temperature, concentration, and pressure can be determined. Therefore, the viscosity reduction of polymer systems plasticized by $scCO_2$ can be predicted from the physical properties of the polymer melt and the rheology of the unplasticized polymer at atmospheric pressure. An example of a predicted master curve for the Styron-658D system is shown in Figure 2.

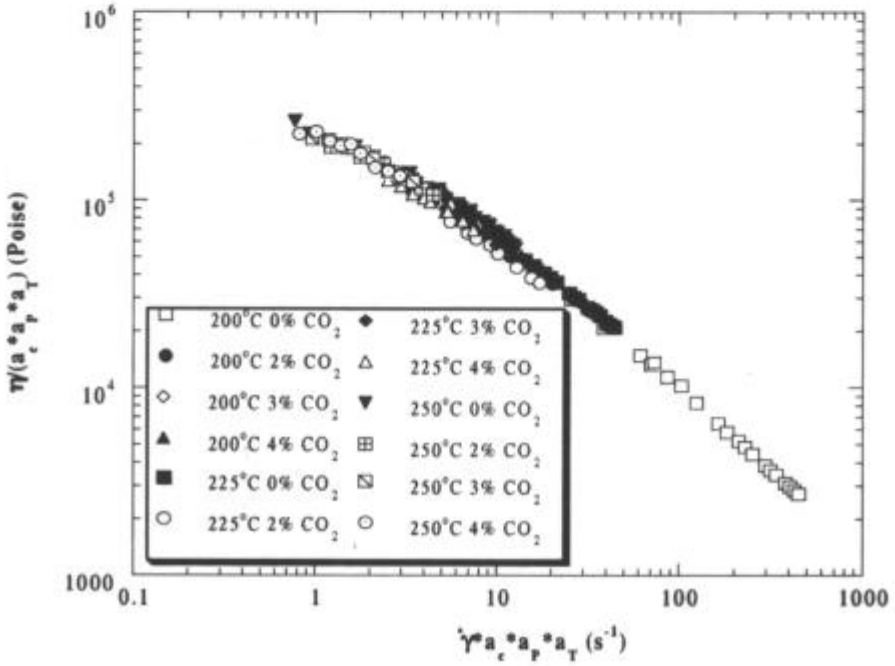

SUMMARY

Experimental measurements of viscosity as a function of shear rate, pressure, temperature and CO_2 concentration were conducted for various commercial polymer resins using an extrusion slit die rheometer. CO_2 was shown to be an excellent plasticizer for polystyrene, lowering the viscosity of the polymer melt by 25-80% depending on pressure, temperature and CO_2 concentration.

Figure 2. Master curve predicting the effects of CO_2 concentration and pressure on PS rheology.

Using existing theories for viscoelastic scaling of polymer melts and the prediction of T_g depression by a diluent, a free volume model was developed to predict the effects of CO_2 on melt rheology. The free volume model depends only on material parameters of the polymer melt which are available in the existing literature for most polymer melts or can be easily measured from the polymer resin under atmospheric conditions in the absence of CO_2. The combination of classical viscoelastic scaling and free volume theory with thermodynamic models to predict the depression of T_g by diluents could thus serve as a predictive tool to quantify the viscosity reduction of polymer melts due to plasticization by CO_2 or other diluents.

ACKNOWLEDGMENTS

This material is based upon work supported in part by the STC Program of the National Science Foundation under Agreement No. CHE-9876674. The authors also gratefully acknowledge support from the Kenan Center for the Utilization of Carbon Dioxide in Manufacturing at North Carolina State University and the University of North Carolina at Chapel Hill, and the Office of Naval Research award number N00014-98-1-0157.

4th Annual Green Chemistry &
Engineering Conference

Sustainable Technologies:
From Research to Industrial Implementation

June 27 - 29, 2000

CATALYSIS II

EFFECTS OF LIGAND MODIFICATION ON HOMOGENEOUS HYDROFORMYLATION OF OLEFINS IN SUPERCRITICAL CARBON DIOXIDE

C. Erkey
Department of Chemical Engineering, Environmental Engineering Program,
University of Connecticut, Storrs, CT 06269

INTRODUCTION

Homogeneous catalysis by soluble transition metal complexes offers many advantages over heterogeneous catalysis such as milder reaction conditions, higher activities and selectivities and better control of operating conditions. Such superior performance arises from the ability of transition metals to complex with a wide variety of ligands in a number of geometries and to easily change from one oxidation state to another. Even though heterogeneous catalysts dominate the industrial scene today (~85% of all existing catalytic processes), the importance and market share of homogeneous catalysts are growing at a very fast pace. This growth is being fueled by a combination of factors:

1. environmental and economic pressures for cleaner processes
2. growth in specialty and fine chemicals
3. scientific advances in organometallic chemistry

and is expected to continue in the coming decade.

A major drawback for homogeneous catalysis lies in the difficulty of catalyst recovery and recycling. Many of the homogeneous catalysts are complexes of expensive metals, and some of the ligands used can be manufactured only by long and tedious syntheses. Therefore, the costs associated with their recovery is a very important factor in the economics of a process. Only a small minority of organometallic reactions have so far cleared the hurdles for use on an industrial scale due to lack of effective methods for catalyst recovery and recycle. Catalyst recovery is still a very active research area and the number of methods currently under investigation in many laboratories around the world are numerous. Some of these include membrane separations, heterogenizing homogeneous catalysts by anchoring them to polymeric supports, supported aqueous and liquid phase catalysis, fluorous and aqueous biphasic catalysis. Using supercritical carbon dioxide ($scCO_2$) as a solvent may have great advantages in catalyst recovery. The solubility of solutes in $scCO_2$ are strong functions of temperature and pressure in the vicinity of the critical point. Therefore, the catalyst, products and reactants can possibly be separated in an efficient manner through temperature and/or pressure programming.

Unfortunately, conventional homogeneous catalysts have very low solubilities in $scCO_2$ having a detrimental effect on activity. This problem can be overcome by incorporating fluorous groups into conventional catalysts. We synthesized several fluoroalkyl- or fluoroalkoxy-substituted arylphosphines and demonstrated their use in the rhodium-catalyzed homogeneous hydroformylation of 1-octene in $scCO_2$.

Hydroformylation of olefins is one of the largest applications of homogeneous catalysis. Over 6 million tons of aldehydes are produced annually by the homogeneous catalytic hydroformylation of olefins. This reaction involves the formation of branched or linear aldehydes by the addition of H_2 and CO to a double bond. The linear aldehydes are the preferred products and the selectivity in such reactions is usually expressed in terms of *n:iso* ratio, which is the ratio of the linear aldehyde to the branched aldehyde. The catalysts generally employed are of the form $H_xM_y(CO)_zL_n$; the two transition metals utilized are rhodium and cobalt and the most commonly utilized ligands are phosphines (PR_3 where R = C_6H_5 or *n*-C_4H_9). Production of C_4 aldehydes from hydroformylation of propene is dominated by rhodium based catalysts whereas higher aldehydes are produced mainly by cobalt catalysts. Since rhodium is about 1000 times more active than cobalt, processes based on Rh catalysts operate at significantly lower temperatures and pressures than processes based on Co catalysts. Therefore, substantial savings in operating and capital costs can be achieved if hydroformylation of higher olefins is conducted using Rh based catalysts.

RESULTS

Figure 1 shows the concentration versus time data for the hydroformylation of 1-octene in $scCO_2$. All reactions were conducted at identical conditions, as described in the figure caption. Each reaction proceeded smoothly, producing both normal and branched C_9 aldehydes. When $[3,5\text{-}(CF_3)_2C_6H_3]_3P$ was the phosphine, approximately 1 % conversion to C_8 species resulted, but experiments employing the remaining phosphines in Figure 1 showed no detectable isom-erization or hydrogenation. Table 1 lists the initial rates and selectivities observed for the

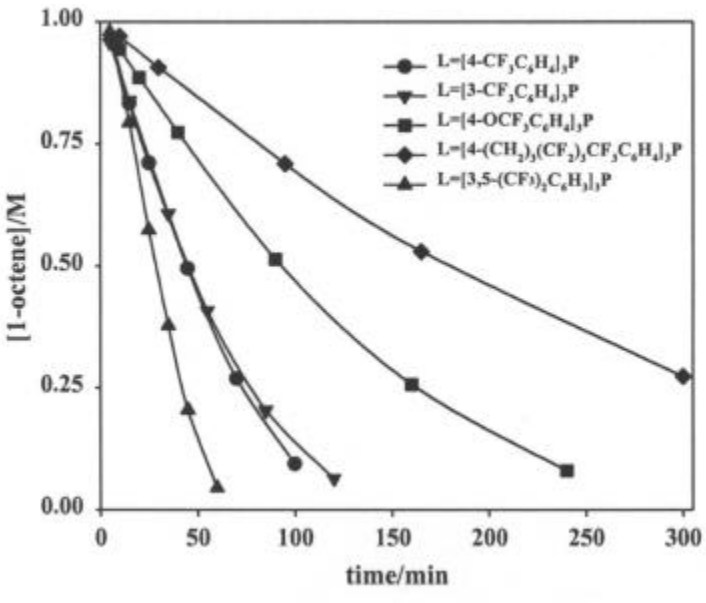

various ligands under standard reaction conditions. Initial rates were calculated from the linear portion of each rate curve by estimating the slope in mol dm^{-3} s^{-1}. The selectivities listed are those measured at the end of each experiment, (between 90 and 98 percent conversion). Among the various catalyst systems, the initial rates of reaction differ more than five-fold between the slowest and the fastest.

Figure 1. Hydroformylation of 1-octene with $Rh(CO)_2acac$/L : P = 273 atm, T = 50 ºC, $[1\text{-octene}]_0$ = 0.95 M, $[H_2]_0 = [CO]_0$ = 1.1 M, [Rh] = 1.27 mM, [P]/[Rh] = 3.0.

Table 1. Hydroformylation of 1-octene in $scCO_2$ using $Rh(CO)_2(acac)$ and various fluorinated phosphine ligands

Ligand	10^6 x Initial Rate[a] mol dm^{-3} s^{-1}	Selectivity (*n:iso* ratio)	$\nu(CO)$[b] cm^{-1}	θ degrees
$[3,5\text{-}(CF_3)_2C_6H_3]_3P$	263	3.02	1996	160
$(4\text{-}CF_3C_6H_4)_3P$	188	3.29	1950	145
$(3\text{-}CF_3C_6H_4)_3P$	185	3.13	1950	153
$(4\text{-}CF_3OC_6H_4)_3P$	94.8	2.99	1934	145
$[4\text{-}F(CF_2)_4(CH_2)_3C_6H_4]_3P$	51.2	3.09	1,921	145

[a] Standard conditions: T = 50 ºC, P = 273 atm, V = 54 mL, $[substrate]_0$ = 1.0 M, [Rh] = 1.2 mM, [P]/[Rh] = 3.0, $[CO]_0 = [H_2]_0$ = 1.1 M. [b] For $HRh(CO)L_3$.

This fact alone speaks of the significant effects phosphine ligands have on the nature of the catalytic species. It is well known that fluorine has a very strong electron-withdrawing effect on the phosphine, causing the phosphorous lone pair to become less basic, and leading to a significant decrease in the electron density at the metal center. The trend of activity observed among the five phosphines of Figure 1 indicates that less basic phosphines lead to more active hydroformylation catalysts. Syntheses of the various catalysts in $scCO_2$ were performed for the purpose of measuring the NMR and FTIR values listed in Table 2. These NMR measurements on the catalysts shed further light on the fundamental difference between the substituted phosphines and triphenylphosphine (PPh_3).

The most recognizable feature of the ^1H NMR spectrum of the complex $HRh(CO)L_3$ is a quartet at $\delta \approx -9.8$ corresponding to the rhodium hydride. The quartet arises from coupling of the hydride with the three equivalent phosphorous nuclei of the complex. For PPh_3, this quartet is only observed at low temperatures, where the phosphine exchange rate is reduced enough to allow resolution of the quartet. For phosphines $(4\text{-}CF_3C_6H_4)_3P$, $(3\text{-}CF_3C_6H_4)_3P$, and $(4\text{-}CF_3OC_6H_4)_3P$, the quartet is well resolved at 30 ºC, indicating a much slower exchange rate for the fluoroalkyl-substituted phosphines than for the more basic PPh_3. However, the quartet is not resolved for the complex formed from $[4\text{-}F(CF_2)_4(CH_2)_3C_6H_4]_3P$, indicating a similarity to PPh_3.

Table 2. Properties of various fluorinated phosphine ligands and their complexes with rhodium as $HRh(CO)L_3$

Ligand	Free	Complexed as $HRh(CO)L_3$					
	$\delta(^{31}P)$ ppm	$\delta(^{31}P)$ ppm	J(Rh-P) Hz	$\delta(^{1}H)$ ppm	^{3}J(H-P) Hz	ν(Rh-H) cm^{-1}	ν(CO) cm^{-1}
$(C_6H_5)_3P$	-6	39.8	155	-9.7	14	2040	1923
$(4\text{-}CF_3C_6H_4)_3P$ **3**	-6.3	40.2	156	-9.9	14	2038	1950
$(3\text{-}CF_3C_6H_4)_3P$ **4**	-5.4	42.9	156	-9.7	14	2025	1950
$[3,5\text{-}(CF_3)_2C_6H_3]_3P$ **5**	-4.4	59	194	-10.1	15	2040	1963
$(4\text{-}CF_3OC_6H_4)_3P$ **6**	-8.9	37.2	155	-9.9	14	2016	1934
$[4\text{-}F(CF_2)_4(CH_2)_3C_6H_4]_3P$ **8**	-8.1	37.4	153	-9.7	[f]	1969	1921

It can be seen from Figure 2 that the rate of hydroformylation correlates very well with the value of ν(CO) for the various catalysts, showing a linear dependence. The IR stretching frequency of metal carbonyls is a sensitive indicator of electron density at the metal center, yielding a relative measure of the amount of π-backbonding from an occupied metal d-orbital to the empty π^*-orbital of the carbonyl. The trend in ν(CO) corresponds well with the amount and proximity of the electron withdrawing fluoroalkyl or fluoro-alkoxy groups of the phosphines, with **5** having the greatest effect and **8** having the least effect relative to the value for PPh_3. The phosphines **3** and **4** show identical electronic behavior, and almost identical activity/selectivity behavior, while **5**, with a much higher ν(CO) value also has a significantly higher activity. The ability of oxygen and methylene groups to insulate against the electron-withdrawing effects of the fluoroalkyl moieties can be seen for phosphines **6** and **8**, where significant decreases in ν(CO) are accompanied by 50% and 70% decreases in activity, respectively. While these spacers are effective insulators they actually de- crease the catalytic activity relative to "non-insulated" phosphines. Surprisingly, steric differences among the phosphines have very little if any effect on the activity or selectivity of the cata-lyst. Phosphines **3** and **4**, which are electronically identical but sterically dif- ferent (θ_3 = 145º, θ_4 = 153º) exhibit the quite similar activities and selectivities. Furthermore, and quite surprisingly, phosphine **5** (θ_5 = 160º) showed no improved selectivity, despite a significant increase in cone angle over phosphine **3**.

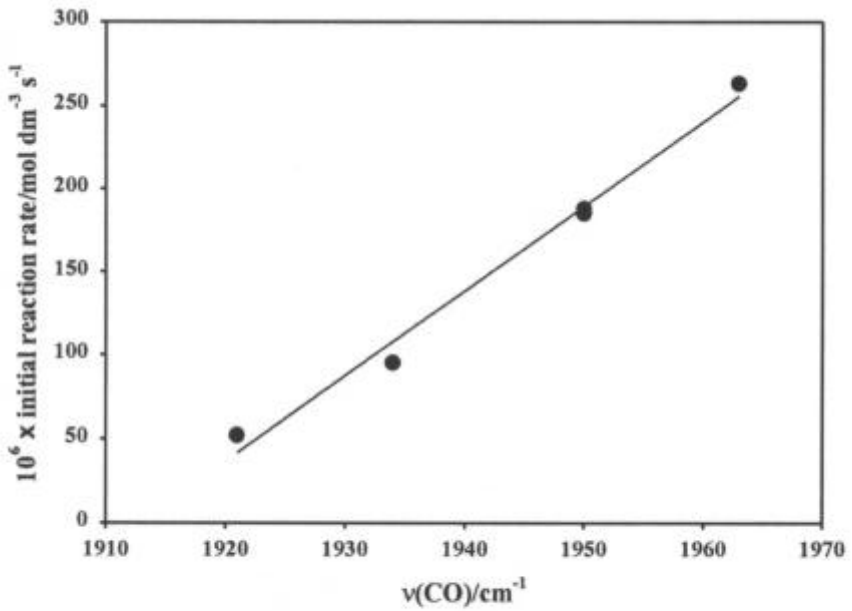

Figure 2. Effect of ν(CO) on Reaction Rate

CONCLUSION

A wide variety of novel fluorinated phosphine ligands were synthesized. Rhodium complexes of these ligands exhibit high solubility in $scCO_2$ and efficiently catalyze hydroformylation of olefins in $scCO_2$. The promising results demonstrate the potential of utilizing $scCO_2$ as a medium for carrying out homogeneous catalytic reactions.

EPOXIDATION OF PROPYLENE ON TITANIUM-SILICA CATALYSTS MODIFICATION WITH POLYMERIC SURFACTANTS

Zhong Tang, Director
Laboratory of Catalysis
Shengcheng Pan, Yangyu Feng
Institute of Jinling Petrochemical Company, SINOPEC, Nanjing, 210046, China
Xinwen Guo, Xiangsheng Wang
Laboratory of Comprehensive Utilization of Carbonaceous Resources,
Dalian University of Technology, Dalian, 116012, China
Enze Min
Member of the Chinese Academy of Sciences,
Research Institute of Petroleum Processing, SINOPEC, Beijing, 100083, China

ABSTRACT
Titanium-silica catalysts prepared by different methods have been used to epoxide propylene by hydrogen peroxide. Experiments were conducted in a fixed-bed reactor, and the optimum operation conditions were determined preliminary through the testing of the effects of reaction temperature, pressure of system, etc. The data indicate that a significant portion of the product is produced by heterogenous reactions occurring in the active sites on the catalyst with both isolated framework titanium and the secondary formed between the surface of zeolite crystal particle and adhesives. The hydrogen peroxide efficiencies approached 98% and the selectivity to propylene oxide is about 96.5% for the catalysts used in this study. The activity and selectivity for epoxidation increased when the catalyst was modified with polymeric surfactants.

INTRODUCTION
Epoxidated olefins are important commercially and are used in great quantities as intermediates in the manufacture of urethanes, glycols, surfactants, plasticizers, and the like. However, processes availabe to the art for the epoxidation of olefins are becoming less and less suitable because they are subject to ecology restrictions while also being uneconomical.

Hydrogen peroxide is a useful reactant because of its nature as a non-polluting oxidizing agent. However, its reactivity as epoxidizing agent in regard to unactivated olefins is low and requires the presence of an activating agent to produce, *in situ*, a more active percompound. There have been proposed various epoxidation processes using, for example, peracids such as performic, peracetic or perpropionic acid, however, because of the instability of epoxides in an acid medium, such processes are particularly difficult to use.

For more than a decade, titanium silicate molecular sieve, TS-1[1], having the medium pore MFI topology has been used as an efficient, clean, and selective oxidation catalyst under liquid phase heterogeneous reaction conditions in the presence of dilute hydrogen peroxide[2-3]. It is well known that the high performance of titanium silicalites is due to the presence of isolated framework titanium. However, the TS-1 catalyst designed to catalyze a certain type of reaction has some special characteristics. For examples: TS-1 for phenol hydroxylation is treated with solution of NH_4Ac, TS-1 for ammoxidation of cyclohexanone is treated with a solution of H_2O_2 and H_2SO_4 and that for epoxidation of olefins is usually treated with weak base, in order to obtain high activity and selectivity. Consideration of the size of substrates and the stability of products, one can image that the properties of TS-1 catalyst for a certain reaction are different. Here we describe the epoxidation of propylene with H_2O_2 catalyzed by TS-1 prepared under different condition.

SUMMARY
Titanium hydroperoxide is the proposed intermediate generated *in situ* when titanium silicates come in contact with dilute aqueous hydrogen peroxide. This intermediate attacks olefinic double bonds, with the formation of epoxides and/or glycols.

Effect of template
TS-1 is usually synthesized by using tetrapropylammonium hydroxide (TPAOH) solution, which acts as the structure-directing agent and provides the alkalinity necessary for the crystallization of the zeolite. Recently, some researchers[4-6] reported that TS-1 was able to prepare with some template else. Table 1 shows the epoxidation properties on TS-1 prepared under different template. When TPAOH as the base, addition of small amount

of TEA can improve the selectivity to propylene oxide. When TPABr as the template, and different organic amines as the base, some synthesized TS-1 are also satisfactory in the epoxidation of propylene.

Table 1. Epoxidation of propylene on TS-1 prepared with different template

Samples	Template	*X* (mol)	*U* (mol)	*S* (mol)
TS-1	TPAOH	100	97.0	100
TST-1	TPAOH+TEAOH	99.5	97.3	100
TSB-1	TPABr+TEAOH	99.5	96.2	99.2
TSB-2	TPABr+Diethylamine	98.1	92.6	100
TSB-3	TPABr+NH_3•H_2O	91.0	85.5	99.0

X — the conversion of H_2O_2; *U* — the utilization of H_2O_2; *S* — the selectivity to propylene oxide.
Condition: Slurry reactor, reaction temperature 333K, reaction time 90 min, pressure of system 0.8 MPa, 1.0 g of catalyst, 31.6 ml of methanol, 7.8 ml of 27.5% H_2O_2 aqueous solution.

Epoxidation performance of modified TS-1 in fixed-bed reactor

Besides the properties of catalysts, manufacturers are concerned with the process and economics. Supported catalysts can be used in a fixed-bed reactor, in which makes it possible to realize continuous production. Sample P-1 was prepared by pelleting. Sample C-1, C-2 was prepared by coating respectively. Polyvinyl alcohol (PVA) was dissolved in water, pure TS-1 zeolite was added under agitating, then the mixture was coated over SiO_2 ball support by spray. Poly-2-vinyl anthraquinone (PVAQ) was dissolved in aromatics, other steps are the same as the above. Sample E-1, E-2, E-3 was prepared by extruding respectively.

The catalytic properties of the samples were studied in a fixed-bed reactor in which loaded about 4 gram catalytic (including the weight of promoter and support). Results are listed in Table 2, which shows that the catalysts modified with polymeric surfactants (PVA, PVAQ) have high conversion of H_2O_2 and selectivity to propylene oxide.

Table 2. Epoxidation of propylene on TS-1 modified with polymeric surfactants

Samples	Molding	Promoter	*X* (mol)	*U* (mol)	*S* (mol)
P-1	Pelleting	-	92.3	95.0	95.3
C-1	Coating	PVA	95.1	96.3	97.6
C-2	Coating	PVAQ	99.0	96.2	98.3
E-1	Extruding	SiO_2	94.0	90.5	90.3
E-2	Extruding	PVA	97.0	96.5	96.3
E-3	Extruding	PVAQ	99.4	97.0	97.2

X — the conversion of H_2O_2; *U* — the utilization of H_2O_2; *S* — the selectivity to propylene oxide.
Condition: Fixed-bed reactor, temperature 323K, the pressure of system 2.5 MPa, liquid space velocity (propylene) $2.5h^{-1}$, catalyst 4 g, ratio of methanol to 27.5% H_2O_2 (v) 6: 1.

Effect of reaction condition

The experiments show that the reaction temperature and the pressure of system are important factors of epoxidation. 323K, 2.5Mpa is suitable for this system, and the other reaction conditions are also worth being studied further.

Table 3. Effect of reaction condition to the epoxidation of propylene on E-3

Run time /h	Temperature /K	Pressure /Mpa	*X* /Mol	*U* /Mol	*S* /Mol
48	313	2.5	95.1	94.5	100
48	318	2.5	96.5	95.8	100
24	323	2.0	98.2	95.2	99.1
24	323	2.5	99.4	96.5	98.5
150	323	3.0	99.5	97.0	96.2
48	333	2.5	100	92.3	89.5

X — the conversion of H_2O_2; *U* — the utilization of H_2O_2; *S* — the selectivity to propylene oxide.
Condition: Fixed-bed reactor, liquid space velocity (propylene) $2.5h^{-1}$, catalyst (sample E-3) 4g, ratio of methanol to 27.5% H_2O_2 (v) 6: 1.

CONCLUSION

Titanium silicalite synthesized by mixture template possess high performance in epoxidation of propylene. Fixed-bed catalysts modified with polymeric surfactants have high conversion of H_2O_2 and selectivity to propylene oxide in continuous reactor. The reaction condition is important to obtain the better results of epoxidation of propylene.

ACKNOWLEDGMENTS

Financial support by the National Natural Science Foundation of China (project 29792071) and SINOPEC is gratefully acknowledged.

REFERENCES

1. M. Taramasso, G. Perego, B. Notari, US Pat. 4 410 501 (1983)
2. M.G. Clerici, P. Ingallina, *J. Catal*. **140** (1993), 71
3. B. Notari, *Stud. Surf Sci. Catal*. **60** (1991), 343
4. X.S. Wang and X. W. Guo, *Catal. Today* **50** (1999), 177
5. Q.H. Xia, Z. Gao, CN Pat. 9 111 650 (1995)
6. A. Tuel, *Stud. Surf Sci. Catal*. **105** (1997), 261
7. M.G. Clerici, G. Bellussi, U. Romano, *J. Catal*. **129** (1991), 159
8. U. Romano, A. Esposito, F. Maspero, *et al*. *Stud. Surf. Sci. Catal*. **55** (1990), 33
9. C. Neri, B. Anfossi, A. Esposito, *et al*. US Pat. 4 833 260 (1989)

THERMAL AND PHOTOCHEMICAL OXIDATION OF CYCLOHEXANE IN BAY

R. G. Larsen, A. R. Leone, V. H. Grassian, S. C. Larsen
Department of Chemistry, University of Iowa, Iowa City, IA 52242

ABSTRACT

The kinetics of the thermal and photochemical oxidation of cyclohexane in BaY were investigated using *ex situ* GC product analysis and *in situ* solid state NMR spectroscopy. The results show that cyclohexyl hydroperoxide, cyclohexanone and cyclohexanol are the main products of the thermal and photochemical oxidation of cyclohexane in BaY. Large kinetic isotope effects were observed with deuterated cyclohexane for both the thermal and photochemical reactions.

INTRODUCTION

The oxidation of cyclohexane to cyclohexanone and cyclohexanol is an important industrial process for the synthesis of nylon-6 and nylon-6,6. Current liquid phase methods for the oxidation of cyclohexane are run under conditions of low conversion to prevent overoxidation of the desired products.[1,2] Thus, it would be desirable to have a process for cyclohexane oxidation that is selective at high conversion. Frei and coworkers have shown that the selective oxidation of cyclohexane to cyclohexanone occurs under thermal and photochemical conditions in cation-exchanged zeolites, such as NaY.[3] A reaction mechanism (shown below) involving an initial charge transfer complex, [(cyclohexane)$^+$ O_2^-] was proposed by Frei and coworkers.[4,5] The charge transfer complex is thought to be stabilized by the exchangeable cation in the zeolite. Frei and coworkers illustrated that many different hydrocarbons can be selectively oxidized in cation-exchanged zeolites by an analogous mechanism.[5,6] In related work, we have shown that a series of 1-alkenes (propene, 1-butene and 1-pentene) as well as aromatics such as *p*-xylene and toluene can be photooxidized in other zeolites, such as ZSM-5 and Beta.[7,8] Similarly, Vanoppen and coworkers also studied thermal cyclohexane oxidation reactions in cation-exchanged Y zeolites, such as CaY, SrY, BaY and NaY.[9,10] Based on the observed trend in reactivity of CaY>SrY>BaY>NaY, Vanoppen and coworkers concluded that the mechanism proposed by Frei involving the formation of an alkane-oxygen charge transfer complex may also be responsible for the thermal chemistry.[10]

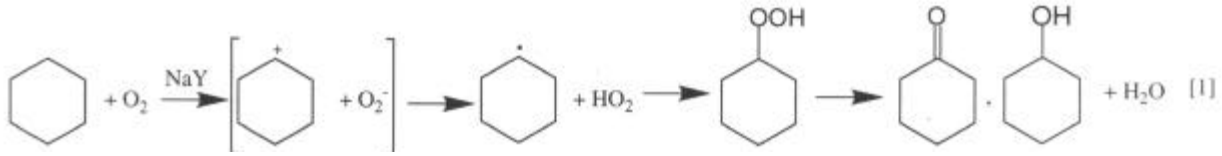

The objective of the current study was to examine the kinetics of the thermal and photochemical oxidation of cyclohexane using *ex situ* gas chromatography (GC) for product analysis. Although there are now several studies that support the hypothesis that the electric field at cation sites in zeolites facilitates the excitation of a O_2•hydrocarbon charge transfer, the evidence also suggests that the overall forward reaction is not the sole governing factor.[5] For example, if the charge transfer state were the sole determinate of the ability of the reaction to proceed, the reaction threshold would be expected to be linearly related to the ionization potential of the hydrocarbon. However, a nonlinear relationship was observed by Frei and coworkers and has been attributed to differences in reaction quantum efficiencies.[11] These changes in quantum efficiencies could be due to a kinetic competition between an electron transfer back reaction and the proton transfer between the cation radical and superoxide ion in the charge transfer state. Recent solution phase studies of photoinitiated electron-transfer reactions involving the formation of alkylbenzene cation radicals have shown that a deuterium isotope effect results when the rate of deprotonation is competitive with the rate of back electron transfer.[12-14] Kinetic isotope effects between 1.5 and 5.6 have been observed depending on the alkylbenzene and donor molecule used.[12-14] Specifically, the impact of the proton transfer rate on the oxidation process was examined in this study. Kinetic isotope studies with deuterated cyclohexane were used to determine whether or not the proton transfer step enters into the overall quantum efficiency. In addition, complementary solid state magic angle spinning nuclear magnetic resonance (MAS NMR) experiments were conducted to assess *in situ* product distributions.

EXPERIMENTAL SECTION

BaY was prepared from NaY (Aldrich) by standard ion-exchange procedures at 90 ºC using an aqueous 0.5 M $BaCl_2$ solution. The elemental composition of Al, Si and Ba was determined by inductively coupled plasma/atomic emission spectroscopy (ICP/AES). The Si/Al and cation/Al ratios for BaY were 2.4 and 0.33, respectively. Zeolites were activated in vials by heating on a vacuum rack to 300 ºC overnight to remove adsorbed water. The activated samples contained in vials were then placed in a glove bag filled with oxygen. The sample vials were capped, removed from the glove bag and the desired amount of cyclohexane was added to the vial through the septum in the cap. Then, the samples were either heated in a forced air oven for thermal reactions or irradiated with a 500 Watt mercury lamp (Oriel Corp.) for photochemical reactions. A broadband long pass filter was placed in front of the lamp for visible light excitation (Oriel Corp. filter 59472, %T = 0 at 400 nm). After the reactions were completed, the products were extracted from the zeolite in acetonitrile. The product distribution was determined by GC or GC/MS with an FID detector and a 5% phenyl/95% methylpolysiloxane capillary column. For NMR experiments, a Chemagnetics double-channel 7.5 mm pencil magic angle spinning (MAS) probe was used to spin the sample at ~5.0 kHz at the magic angle. Cross polarization (CP) with high power proton decoupling was used for ^{13}C NMR signal acquisition with the following parameters: CP, contact time 2.0 ms, recycle delay 2.0 s. 90 degree pulse length 5.1 µsec. All of the chemical shifts for ^{13}C are reported

relative to TMS. The data were acquired using a 300 MHz Bruker MSL NMR spectrometer.

RESULTS AND DISCUSSION

Preliminary results from our laboratory suggest that BaY is effective for the thermal oxidation of cyclohexane. Typical conversions of ~60% are achieved at 95ºC and the selectivity for cylcohexane to cyclohexyl hydroperoxide, cyclohexanone and cyclohexanol is ~95%. Using 1:1 mixtures of normal and perdeuterated cyclohexane, kinetic studies of the thermal and photochemical oxidation of cyclohexane in BaY were conducted with *ex situ* product analysis using GC. In every case examined, the measured ratio of protonated to deuterated reaction products, at low overall conversion, showed a pronounced isotope effect. For photochemical oxidation of cyclohexane in BaY, perdeuterated cyclohexane was found to be approximately 15 times less likely to react than normal cyclohexane. For thermal oxidation of cyclohexane, the observed isotope effect was temperature dependent and resulted in product ratios (normal to perdeuterated) of 14 and 9 at 40ºC and 77ºC, respectively. Since the secondary isotope effects are relatively small in these systems (total effect for α and 4β is ~1.4), these results indicate substantial primary isotope effects of 10 and 6.4, respectively. These results are interpreted as an indication that the rate of deprotonation is competitive with the rate of back electron transfer.[12-15]

The studies described above are *ex situ* studies in which the products and reactants were extracted from the zeolite with acetonitrile for analysis by gas chromatography (GC). The primary problem with the extraction method is that an accurate representation of the product composition in the zeolite pores may not be obtained. For example, not all of the products may be extracted from the zeolite or reactive products or intermediates may continue to react in solution. For this reason, solid state MAS NMR experiments were initiated. We have obtained a preliminary solid state MAS NMR spectrum using unlabeled cyclohexane. ^{13}C is the only isotope of carbon that possesses a nuclear spin and its natural abundance is 1.1%. A sample of cyclohexane, BaY and oxygen was prepared and was heated at 85ºC for 1 hour. After signal averaging for approximately 10 hrs, the ^{13}C NMR spectrum (cross polarization with proton decoupling) shown in Figure 1 was obtained. Several products are observed in the zeolite. Cyclohexanone, cyclohexanol and cyclohexyl hydroperoxide are easily identified by peaks at 231 ppm (C=O), 74 ppm (C-OH) and 89 ppm (COOH), respectively.[16] Substantial overlap in the ring carbon region of the spectrum (~25-33 ppm) makes interpretation of this region of the spectrum difficult. These results suggest that further NMR experiments would be valuable for determining the product distributions for products adsorbed in the zeolite pores.

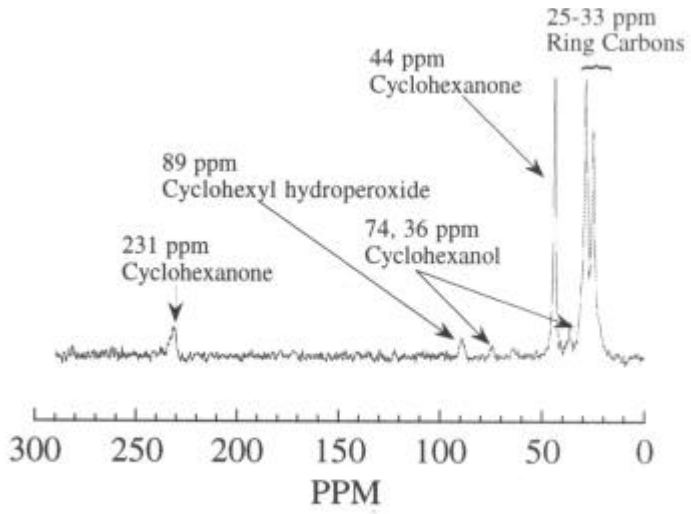

Figure 1. ^{13}C CP MAS NMR experiment with ^{1}H decoupling of BaY with cyclohexane and oxygen, heated at 85 ºC for 1 hr.

SUMMARY

The thermal and photochemical oxidation of cyclohexane was investigated using a combination of *ex situ* GC and solid state MAS NMR for product analysis. The kinetics of the cyclohexane oxidation reaction were examined using *ex situ* GC for product analysis. Cyclohexyl hydroperoxide, cyclohexanone and cyclohexanol were produced in BaY at 95ºC at ~60% cyclohexane conversion with a combined selectivity of ~95%. Substantial kinetic isotope effects were observed for both thermal and photochemical oxidation reactions indicating that the proton transfer step is the rate-determining step and is competitive with the back electron transfer. Solid state MAS NMR was introduced as an *in situ* method for monitoring product distributions and reaction kinetics.

ACKNOWLEDGMENTS

The research described in this article has been funded by the Environmental Protection Agency through grant number R825304-01-0 to SCL and VHG.

REFERENCES

1. Sheldon, R. *The Chemistry of Peroxides;* Wiley: New York, 1983.

2. Parshall, G.W.; Ittel, S.D. *Homogeneous Catalysis;* 2nd ed.; Wiley: New York, 1992.
3. Sun, H.; Blatter, F.; Frei, H. *Selective oxidation of small hydrocarbons by O_2 in zeolites with visible light;* Sun, H.; Blatter, F.; Frei, H., Ed.: New Orleans. 1996.
4. Sun, H.; Blatter, F.; Frei, H. *J. Am. Chem. Soc.* **1996**, 118, 6873-6879.
5. Blatter, F.; Sun, H.; Vasenkov; Frei, H. *Catalysis Today* **1998**, *41,* 297-309.
6. Frei, H.; Blatter, F.; Sun, H. *Chemtech 1996,* 24-30.
7. Myli, K.B.; Larsen, S.C.; Grassian, V.H. *Catal. Lett.* **1997**, *48,* 199-202.
8. Xiang, Y.; Larsen, S.C.; Grassian, V.H. *J. Am. Chem. Soc.* **1999**, *121,* 5063-5072.
9. Vanoppen, D.L.; DeVos, D.E.; Jacobs, P.A. *J. Catal.* **1998**, *177,* 22-28.
10. Vanoppen, D.L.; DeVos, D.E.; Jacobs, P.A. *Stud. Surf. Sci. Catal.* **1996**, *10-5,* 1045-1051.
11. Blatter, F.; Frei, H. *J. Am. Chem. Soc.* **1994**, *116,* 1812 -1820.
12. Fujita, M.; Ishida, A.; Takamuku, S.; Fukuzumi, S. *J. Am. Chem. Soc.* **1996**, *118,* 8566-8574.
13. Bockman, T.M.; Hubig, S.M.; Kochi, J.K. *J. Am. Chem. Soc.* **1998**, *120,* 2826-2830.
14. Lewis, F.D.; Petisce, J.R. *Tetrahedron* **1986**, *42,* 6207-6217.
15. Dixon, R.E.; Streitweiser, A.J. *J. Org. Chem.* **1992**, *57,* 6125-6128.
16. Barton, D.H.R.; Csuhai, E.; Doller, D.; Balavoine, G. *J. Chem. Soc., Chem. Commun.* **1990**, 1787-1789.

SYNTHESIS, CHARACTERIZATION AND CATALYTIC PROPERTIES OF TS/TiO_2 NANO-STRUCTURED COMPOSITE MATERIALS

Xiang-sheng Wang, Xin-wen Guo, Yi-hua Zhang and Hong-lin Wang
Laboratory of Comprehensive Utilization of Carbonaceous
Resources, Dalian University of Technology, Dalian 116012, P.R, China

ABSTRACT
TS/TiO_2 nano-structured composite materials were synthesized by adding TiO_2 moiety to the synthetic gel containing tetra-propylammonium bromide (TPABr). TEM, ^{13}C CP/MAS NMR, XRD, UV-Vis and UV-Raman techniques were used to characterize the material. The results show that this material is composed of three parts: nano-structured ZSM-5 rnolecular sieves (about 50nm), TiO_2 moiety and TiO_2 dispersed on the molecular sieve. During the synthesis of the composite material, only self-made amorphous TiO_2 can be used as the moiety. The amount of the TiO_2 moiety affects greatly on the specific surface area and pore structure of TS/TiO_2 composite material but has minor effect on the catalytic properties. The effect of calcination temperature on the catalytic properties of TS/TiO_2 composite material is very great, only TS/TiO_2 composite material calcined at above 500ºC shows high selectivity of PO and utilization of H_2O_2 in the epoxidation of propylene with dilute H_2O_2.

Keywords: TS/TiO_2 nano-structured composite material; TiO_2 moiety; epoxidation of propylene; Propylene oxide.

INTRODUCTION
Titanium silicalite (TS-1) is one kind of heteroatom molecular sieve synthesized by Taramasso and his coworkers in 1983[1]. It was found to be an efficient catalyst for the oxygenation of a variety of organic compounds with aqueous hydrogen peroxide as oxidant. Examples of catalyzed reactions include the hydroxylation of phenol, the epoxidation of olefins and the amoxidation of cyclohexanone[2]. Because of no pollution and by-product in the process catalyzed by TS-1, it is thought to be "green catalyst". Since then, many investigations on the synthesis of TS-1 were made[3-4]. Recently, one kind of large TS-1 whose crystal size is about 30 μm was synthesized through adding 30 μm of TiO_2 particle to the synthetic gel[5]. While in our lab, by adopting self-made amorphous TiO_2 as the moiety adding to the synthetic gel, a kind of TS/TiO_2 composite material was synthesized. In this communication, the characterization and the catalytic properties of this material were investigated in detail.

EXPERIMENTAL
In a typical synthesis process, $TiCl_4$ dissolved in the isopropyl alcohol was used as titanium source; silica sol (30%, QINGDAO Chemical Plant) was used as silica source. An amorphous Titania was added to the gel to make the mixture with the following composition: SiO_2 : TiO_2 : TPABr : NH_4OH : H_2O = 1 : 0.2 ~ 2.0 : 0.05 ~ 0.2 : 2 ~ 4 : 40 ~ 60. The mixture was transferred to a stainless steel autoclave and crystallized at 170-180ºC for 3-5

day under stirring (300rpm). The solid was dried overnight at 110 ºC and calcined at 540ºC for 5h.

X-ray diffraction patterns of the samples were obtained on a shimadzu XD-3A diffractometer using the CuK_a radiation; IR spectra of the samples were taken using KBr as pellets on a Nicolet-5DX FTIR spectrometer. MAS NMR Spectra were obtained on a Bruker DRX-400 NMR Spectrometer using MAS BBO probe head. High resolute TEM photographs were obtained by a JEM-1200EX microscopy. The specific surface areas were determined by nitrogen physisorption using an AUTOSORB-1 micromeritics instrument.

The epoxidation reaction of propylene was carried out in a 200ml stainless steel autoclave equipped with a stirrer. Typically 0.4g of catalyst, 20g of methanol, 2g of aqueous H_2O_2 solution (30%wt) were charged into the reactor. The reaction was carried out at 60ºC under pressure of propylene (0.4MPa). Samples were periodically taken and analyzed by iodometric titration and gas Chromatography (GC) using a capillary column (30m X 0.25mm) containing PEG 20M as the stationary phase. GC analyses were performed on a SF 1102 instrument (SHANGHAI) equipped with a flame ionization detector.

RESULTS AND DISCUSSION

Characterization of the TS/TiO_2 composite materials

In the similar synthetic condition, using TPABr as the template and NH_3 • H2O, *n*-butylamine, hexanediamine, methylamine, ethylamine or diethyleneamine as the base, without adding the rnoiety titania, a highly crystallized TS-1 can be obtained. These TS-1 samples usually have a crystal size of several microns. While in our lab, adding self-made amorphous Titania, the resultant materials have nano-scale particles and high activity. In the following passage, several techniques were used to characterize TS/TiO_2 composite materials (the molar ratio of moiety TiO_2 to SiO_2 in the gel is 1 :1).

X-ray powder patterns of the as-synthesized material exhibits triple peaks in the 2 θ range from 23 to 25 degree, which indicated the existence of zeolite with MFI structure in the composite material, XRD patterns of the calcined sample shows a new and wide peak at about 25 ~ 26 degree (2 θ), which reveals that the moiety TiO_2 is converted to anatase and highly dispersed in the sample after calcined at 540ºC.

^{13}C CP/MAS NMR spectrum of the as-synthesized material shows that the TPA^+ cations are occluded in the channels of zeolite, the splitting of the C_3 peak reveals that the methyl end groups of the TPA cations are enclosed in two kinds of channels of the ZSM-5 crystalline structure.

UV-Vis Spectrum of the as-synthesized composite material exhibits one peak at 240 ~ 260nm, no peak at 210 ~ 220nm, which is attributed to tetra-coordination titanium species. The peak at 240 ~ 260nm is generally thought to be highly dispersed titania in amorphous Si-O tetrahedron or extra framework titania in the titanium silicalite[6-7]. It can be seen that the titanium species in the composite material do not exist in the form of tetra-coordination, but in the form of high dispersion. From our analysis, these titanium species have two features: high dispersion and low structure tension from zeolite crystal. So it can be concluded that the titanium species in the composite material is highly dispersed extra-framework titanium species existing in zeolite defect structure.

TEM photograph of the composite material shows that there are a lot of 50nm particles in the material. Ultraviolet resonance Raman spectroscopy was thought to be the direct method to distinguish framework titanium from extra-framework titanium species[12]. UV-Raman spectrum of the composite material does not have any peaks at 1125cm^{-1}; this shows that there is no tetra-coordination titanium species in the material.

From the results of characterization, it can be concluded that, the TS/TiO_2 composite material is composed of three parts: nano-structured ZSM-5 molecular sieve, TiO_2 moiety and TiO_2 highly dispersed in the defect structure of MFI structure zeolite.

Catalytic properties of TS/TiO_2 composite material

Effect of the amount of TiO_2 moiety

During the synthesis of TS/TiO_2 composite material, commercial TiO_2 (anatase or rutile) can not be used to act as the moiety. Only using self-made TiO_2 with specific surface area as the moiety, can the as-synthesized TS/TiO_2 composite material exhibit high catalytic properties.

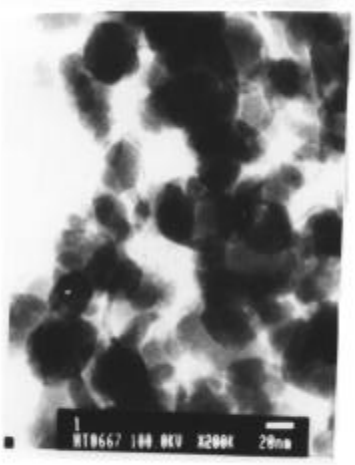

Figure 1. TEM photograph of TS/TiO_2 composite material

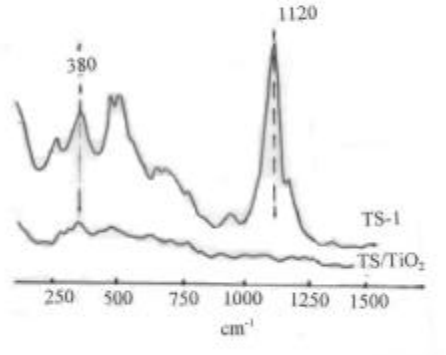

Figure 2. UV-Raman spectra of Ts/TiO_2 composite material and TS-1

Table 1 lists the specific surface area and epoxidation properties of TS/TiO_2 composite materials with different ratios of TiO_2 moiety to SiO_2 in the gel. It can be seen that, with the increase in the amount of TiO_2 moiety, the specific surface area of TS/TiO_2 composite materials decreases drastically. This is because, the specific surface area of TiO_2 moiety after calcined at 540 ºC is about $80m^2/g$, so, when the amount of the TiO_2 moiety in the TS/TiO_2 composite material increases, the specific surface area of the composite material will decrease. The average pore diameter of the composite material is 5.6 Å, which is similar to that of molecular sieve with MFI structure. In addition, there are about 4.5 Å of micropore and 1.0nm ~ 1.4nm of mesopore. From Table 1, it is seen that all the samples have high activity in the epoxidation of propylene. Although with the increase in the amount of TiO_2 moiety, catalytic properties decrease slightly.

Table 1. Specific surface area and propylene epoxidation properties of TS/TiO_2 composite materials

sample	Moiety/ SiO_2	specific surface area (m^2/g)	XH_2O_2%	Spo%	UH_2O_2%
1	0.2	284.7	93.6	93.6	98.7
2	0.4	207.1	94.9	92.2	93.4
3	1.0	132.6	96.6	89.8	94.4
4	1.5	141.7	89.3	92.3	96.1
5	2.0	111.7	82.7	91.7	92.3

Effect of calcined temperature

Table 2 lists the propylene epoxidation properties of TS/TiO_2 composite materials calcined at different temperatures. From Table 2, it can be seen that the powder of TS/TiO_2 composite material has little activity, only a lot of H_2O_2 is decomposed. With the increase in the calcined temperature, the conversion and the utilization of H_2O_2 and the selectivity of propylene oxide increase. When the calcined temperature is above 600ºC, the conversion of H_2O_2 decreases slightly.

From XRD spectra of TS/TiO_2 composite materials calcined at different temperatures, it can be seen that the spectrum of TS/TiO_2 composite material calcined at 300ºC exhibits two peaks at $2\theta = 25.4º$ and 37.9º, and with the increase in the calcined temperature, the intensities of the two peaks increase. This shows that TS/TiO_2 composite material calcined at high temperature contains large amount of anatase. Generally, anatase existing in the TS-1 will improve the decomposition of H_2O_2 and restrain epoxidation of propylene. Before TS/TiO_2 composite material is calcined, it contains a large amount of amorphous TiO_2, TS/TiO_2 composite material does not show any activity, only improves the decomposition. After calcined, the amorphous TiO_2 in the TS/TiO_2 composite material was converted into anatase or rutile, at this time, TS/TiO_2 composite material shows high activity and selectivity.

Table 2. Epoxidation of propylene with H_2O_2 over TS/TiO_2 materials calcined at different temperatures

Calcined temperature(ºC)	X_{H2O2}(%)	Spo(%)	U_{H2O2}(%)
powder	77.7	0	0
200	50.8	62.0	29.9
300	72.5	54.3	47.0
400	90.1	55.5	96.0
500	91.1	82.2	100
600	91.1	88.7	94.0
800	86.8	91.8	97.1

From the above result, it presents an interesting idea, TS/TiO_2 composite material shows high selectivity in the epoxidation of propylene and high utilization of H_2O_2 in the presence of a lot of extra-framework titanium species. This shows that some extra-framework titanium also acts as the active center.

CONCLUSION

TS/TiO_2 nano-structured composite materials were synthesized using TPABr as the template and self-made TiO_2 as the moiety. The amount of the TiO_2 moiety has great effect on the nature of as-synthesized composite materials. The catalytic properties of TS/TiO_2 composite materials show some extra-framework titanium species may have activity in epoxidation of propylene with dilute H_2O_2.

ACKNOWLEDGMENTS

This work is financially supported by the National Science Foundation of China (No. 29792071). We wish to thank Dr. Liu L.F. for kindly help and discussions.

REFERENCES

1. M. Taramasso, G. Perego and B. Notari, US4410501.
2. B. Notari, *Catal. Today*, 1993, **18**(2): 163-172.
3. Thangaraj, A.; Eapen, M.J.; Sivasanker, S.; *et al*., *Zeolites*, 1992,**12**(8): 943-950.
4. Muller, U.; Steck, W., *Stud. Surf. Sci. Catal*., 1994, **84**: 203-2 10.
5. US5736479.
6. Fernandez, A.; Lyerer, J.; Agustin, R.; *et al*., *J. Catal*., **112**, 1988, 489.
7. Lenoc, L.; *et al*., *Stud. Surf. Sci. Catal*., 1996, **101**, 611.

4th Annual Green Chemistry &
Engineering Conference

Sustainable Technologies:
From Research to Industrial Implementation

June 27 - 29, 2000

MODELING/COMPUTATIONAL METHODS

Extended abstract not received in time for printing.
The ACS abstract is reproduced as a courtesy.

THE ROLE OF COMPUTATIONAL CHEMISTRY IN CATALYST DESIGN AND DEVELOPMENT OF GREEN PROCESSES

Matthew Neurock
Department of Chemical Engineering, University of Virginia, Charlottesville, VA 22902-2442

As we move into the 21st century, the design of environmentally-benign processes that are economically competitive on the global market will be a critical challenge for the U.S. chemical industry. Catalysis, which is at the heart of over 90% of all chemical processes will play a pivotal role. Next-generation catalysts will need to be highly active, nearly 100% selective, and stable over prolonged operation times. A fundamental understanding of the surface catalyzed chemistry will be important in enhancing our ability to design new materials. Considerable progress has been made over the past few years in advancing both *ab initio* quantum chemical methods and atomistic simulation toward understanding surface reactivity. The application of these tools in conjunction with experimental efforts should prove to be quite valuable in future catalytic materials development. This talk will focus on the advances and application of theory and simulation toward the improving the design of selective hydrogenation and oxidation catalysts.

SOLVENT SELECTION UNDER UNCERTAINTY

Ki-Joo Kim, Ph.D., Student and Urmila M. Diwekar, Professor
Environmental Institute, Carnegie Mellon University, 5000 Forbes Ave, Pittsburgh, PA 15213
Kevin G. Joback, President
Molecular Knowledge Systems, P.O. Box 10755, Bedford, NH 03110-0755

ABSTRACT
Solvent selection is an important step in process synthesis, design, or process modification. Computer aided molecular design (CAMD) techniques provide a promising tool for solvent selection. However, uncertainties inherent in these techniques and associated models are often neglected. This paper presents a new approach to solvent selection under uncertainty. A case study of acetic acid extraction demonstrates the usefulness of this approach to obtain robust decisions.

INTRODUCTION
Solvents are extensively used as process materials (e.g., extracting agent) or process fluids (e.g, CFC) in chemical process industries. Since solvents are a main source of pollution, it is desirable to use reduced amount and/or environmentally friendly solvents or solvent blends. To select new or alternative solvents, several methodologies have been developed over the years. Traditional laboratory synthesis and test methodology is a time consuming process and cannot guarantee to find best solvents. Database search methods provide a promising alternative to laboratory synthesis methods. However, these methods are limited by the accuracy and size of the databases, and the efficiency of the search engines. CAMD methods generate candidate solvents based on group contribution property prediction methods. These methods are simple and can be used to predict physical, chemical, biological, and health effect properties but their applicability is restricted by their accuracy and applicability range.

All methodologies for solvent selection are subject to uncertainties which can affect the usefulness of selected solvents. Uncertainties come from various sources such as imperfect knowledge of modeling phenomena, experimental error, and/or numerical errors. Most of the work in CAMD are mainly focused on optimization methods to guarantee a desired solvent (Sinha *et al*., 1999) neglecting or simplifying the treatment of uncertainty. This paper presents an efficient CAMD framework under uncertainty using a new and efficient optimization algorithm called stochastic annealing (Chaudhuri and Diwekar, 1996,1999). A case study of solvent

selection for a liquid-liquid extraction process demonstrates the usefulness and robustness of this approach.

SOLVENT SELECTION CRITERIA

In general the criteria used for solvent selection are based on the properties like solvent selectivity, distribution coefficient. There are numerous techniques which can predict the above property criteria with moderate to good accuracy. In this study, a simplified and effective technique based on solubility parameter (Joback, 1994) is used. The three dimensional solubility parameters, δ_d, δ_p, and δ_h, for a solvent show dispersive, polar, and hydrogen bonding forces. Similarity of solubility parameters can be measured using a Euclidean distance metric *Distance Matrix* between two liquids, A and B.

$$\textit{Distance Matrix} = \left[(\delta_d^A - \delta_d^B)^2 + (\delta_p^A - \delta_p^B)^2 + (\delta_h^A - \delta_h^B)^2 \right]^{1/2}$$

Liquids with similar solubility parameters are soluble. Hence the distance between solvent and solute (*SU*) should be small while the distance between solvent and raffinate *(SR)* should be large for better solvents.

The ratio, *SR/SU* is proportional to solvent selectivity and 1/*SU* is proportional to distribution coefficient. They may require molecular weight, molar volume, or other physical properties as correction terms. However, since *SU* and *SR* are almost linearly dependent, these terms (*SR/SU,* 1/*SU*) may not be appropriate guides for better solvent selection. In this study, we used the *Distance Matrix* itself as an objective which can be expressed as [(*SU*) + (-*SR*)]. This objective can provide candidate solvents having low *SU* and high *SR* at the same time. In addition, boiling point range is provided as the constraint to generate solvents in low or high boiling ranges. Joback's method (Reid *et al.,* 1987) is used here for this purpose, as this method uses the same groups for estimating solubility parameters as for predicting boiling points. This generality is one of the main advantages of CAMD approach based on solubility parameter. Unlike other optimization methods, we are using a new optimization method which allows us to include uncertainties in the analysis (Chaudhuri and Diwekar, 1996, 1999). The following section presents the results of the case study.

SOLVENTS FOR HOAc EXTRACTION FROM WATER

Acetic acid is a very valuable compound and hence must be recovered from waste solvents originating from various processes or industries. Ethyl acetate (B.P.=77ºC) and isoamyl acetate (B.P.=199ºC) are commonly used for this purpose and may be changed with better solvents. We demonstrate our methodology using the example of finding new and alternative solvents for acetic acid extraction from water.

First, we build each group for generating solvents and estimating solubility parameters and boiling points. For environmental friendliness we exclude aromatic, halogenated, and carboxylic groups in the group selection list. The 17 groups selected in this study are summarized in Table 1. Next step is to identify the proper constraints. In this study, we are interested in low boiling solvents. We have selected the range of boiling points as (350.3 - 30 ^{K}) to (391.1 - 10 ^{K}) where 350.3 ^{K} is the boiling point of ethyl acetate and 391.1 ^{K} is the boiling point of acetic acid.

Table 1. Groups for solvent selection

-CH_3	CH_2=CH-	-OH	>NH
-CH_2-	CH_2=C<	-O-	-CN
>CH-	-CH=CH-	>C=O	-NO_2
>C<	-CH=C<	O=CH-	
	>C=C<	-COO-	

The optimization procedure provided promising solvents for the three cases: (1) deterministic case with no uncertainties, (2) solvent selection including uncertainties in solubility and boiling point parameters as uniform distributions, and (3) solvent selection under uncertainty when uncertainties are represented by normal distributions. Table 2 shows the top 20 candidate solvents (optimal) for these three cases. It can be seen from the table that inclusion of uncertainties resulted in additional solvents which have better solvent properties like solvents such as methyl isobutyrate, isopropyl acetate, and 1,2-dimethoxy ethane. Further, weaker solvents such as ethyl vinyl ketone and trimethyl orthoformate are excluded from the list. Figure 1 shows the CDF (cumulative distribution function) and PDF (probability distribution function) of the objective function values for these 25 solvents. The CDF shows uncertainty cases cover wider ranges of molecules and the PDF shows high frequency of better solvents (minimum objective value of -23.9). Furthermore, the distributions (PDFs) for the uncertainty cases show skewed lognormal distributions having a peak in the left (better solvent property) corner and a long tail in the right (wider coverage of molecules) corner. The PDF of the deterministic case is similar to that of a uniform distribution, which means low and flat probability for generating better solvents, especially in -23.9 to -23.5, in which most of the solvents reside. The

lognormal distributions of uncertainty cases show that one can select large number of solvents from a very narrow and promising range providing robustness to the selection.

Table 2. Objectives of solvent selection for HOAc extraction from water

No	NG	Solvents	Deterministic	Uniform	Normal
1	5	Methyl isobutyrate		-24.003	-23.998
2	5	Isopropyl acetate		-24.003	-23.998
3	6	1,1-Dimethoxyethane			-23.998
4	5	Propyl acetate	-23.980	-23.921	-23.974
5	5	Methyl propyl ketone	-23.974	-23.961	-23.993
6	5	Diethyl ketone	-23.974	-23.961	-23.993
7	4	Ethyl acetate	-23.956	-23.941	-23.934
8	4	Methyl propionate	-23.956	-23.941	-23.934
9	4	Methyl ethyl ketone	-23.945	-24.006	-23.972
10	3	Methyl acetate	-23.923		-23.900
11	5	Valealdehyde	-23.901	-23.892	-23.888
12	5	Isovalealdehyde	-23.896		
13	5	Trimethyl acetaldehyde		-23.865	-23.869
14	4	Butyraldehyde	-23.855	-23.808	-23.854
15	4	Isobutyraldehyde	-23.849	-23.762	-23.831
16	4	Methyl crotonate	-23.839	-23.842	-23.760
17	4	3-Penten-2-one	-23.815	-23.952	-23.952
18	4	Ethyl vinyl ketone	-23.734		
19	7	Trimethyl orthoformate	-23.715		
20	3	Methyl acrylate	-23.709		

NG: Number of groups in a solvent

When frequency of number of groups *(NG)* in a molecule (Figure 2) is compared, molecules with *NG* of 4 has the highest frequency for all three cases. For the deterministic case with *NG* of 4, aldehyde is the most frequent group. Aldehyde has the highest δ_p and δ_h among the groups and has one free bond to construct a molecule. Hence aldehyde group can be easily constructed with alkenes or branched alkanes, and is close match to the constraints for this case study. On the other hand, for the two uncertainty cases, the frequency for ketones and esters is higher. Property prediction parameters under uncertainties are now overlapped and thus propensity for aldehyde decreases.

SUMMARY

This paper presented a new approach to CAMD under uncertainty. A case study demonstrated the usefulness of this approach. It has been found that inclusion of uncertainty in this early design stage of design can provide more promising solvents while less favorable solvents are excluded from the list. The analysis also showed that the uncertainty results provide wider selection window and robustness in solvent selection.

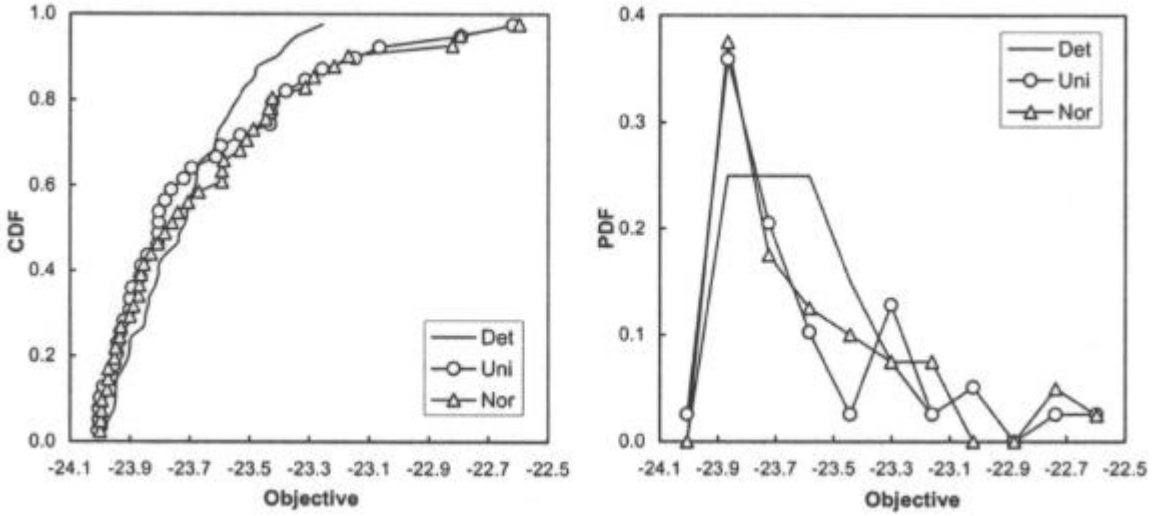

Figure 1. CDF and PDF of three solvent selection cases.

ACKNOWLEDGMENT
The authors thank the NSF and Mallinckrodt Chemicals for their funding this research (CTS-9729074).

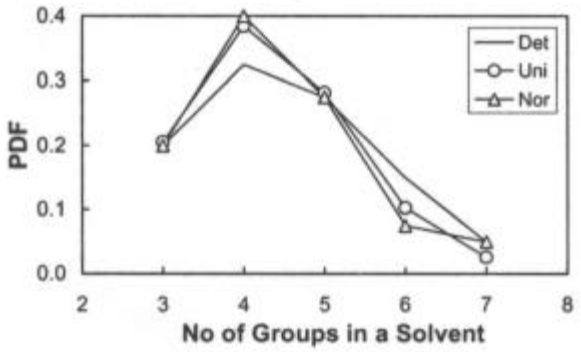

Figure 2. Number of groups (NG) in solvents.

REFERENCES

1. Chaudhuri, P. and U.M. Diwekar (1996), "Synthesis Under Uncertainty: A Penalty Function Approach", *AIChE Journal,* **42***,* 742-752
2. Chaudhuri, P. and U.M. Diwekar (1999), "Synthesis Approach to Optimal Waste Blend under Uncertainty", *AIChE Journal,* **45***,* 1671-1687
3. Joback, K.G. (1994), "Solvent Substitution For Pollution Prevention", in *AIChE Symposium Series,* **90**, No. 303, AIChE, NY
4. Reid, R.C., J.M. Prausnitz, and B.E. Poling (1987), *The Properties of Gases and Liquids,* Fourth Edition, McGraw-Hill Book Company, NY
5. Sinha, M., L.E.K. Achenie, and G.M. Ostrovsky (1999), "Environmentally Benign Solvent Design by Global Optimization", *Comp. Chem. Eng.,* **23***,* 1381-1394

MOLECULAR MODELING OF AUTOMOTIVE EXHAUST CATALYSTS

W. F. Schneider
Chemistry Department
K. C. Hass
Physics Department
Ford Research Laboratory, 2101 Village Road, Mail Drop 3083/SRL, Dearborn, MI 48124

Abstract
Lean-burn and gasoline engines offer significant fuel economy benefits over traditional stoichiometric combustion engines, but to take advantage of these benefits, new types of catalysts capable of reducing NO_x in an

oxygen-rich exhaust are required. Two strategies under investigation are a selective NO_x reduction (SCR) catalyst and a NO_x trap, but neither is able to meet the activity and durability requirements of an automobile. First principles density functional theory offers the opportunity to study the function of these two very different systems on a molecular level. In this talk, recently developed molecular models of the catalytic chemistry in the Cu-exchanged zeolite Cu-ZSM-5, the prototypical SCR catalyst, and alkaline earth oxides, the prototypical NO_x trap materials, will be described. These models provide important insights into the function of both types of systems — insights that are hoped will lead to the design of practically useful catalysts.

Introduction

The simultaneous societal demands for improved fuel economy and decreased exhaust emissions present a tremendous challenge for automobile manufacturers. While the supported precious metal "three-way" catalysts in use today are remarkably effective in simultaneously removing CO, NO_x (NO + NO_2), and hydrocarbons from the exhaust of stoichiometric internal combustion engines, they are completely ineffective for NO_x removal from more fuel-efficient lean-burn gasoline and diesel engines. In these cases, the O_2-rich exhaust interferes with the chemical reduction of NO_x. One approach to this "lean NO_x" problem is the use of a selective catalytic reduction (SCR) catalyst that preferentially promotes the reduction of NO_x in the presence of excess O_2. An alternative is the so-called NO_x trap, which stores NO_x on an oxide adsorbent during lean engine operation, and releases and reduces the NO_x to N_2 during periodic fuel-rich excursions. Fundamental deficiencies in activity and robustness prevent the adoption of either of these approaches. First-principles density functional theory (DFT) calculations allow the mechanisms of function of both systems to be probed on an atomic level, providing insights that can ultimately guide the design of superior catalytic materials.

NO_x Catalysis

Cu-exchanged ZSM-5 zeolites have amongst the highest known activities for both NO_x SCR and the direct decomposition of NO_x to the elements. Unfortunately, the maximum activity is too low, the temperature window is too narrow, and the durability and resistance to poisoning is too poor for most automotive applications. Cu-ZSM-5 is an ideal model system for studying NO_x chemistry, however. In these materials, Cu ions are atomically dispersed within the pores of ZSM-5, residing near locally anionic Al-substituted tetrahedral (T-) sites. Because the catalytic chemistry is largely localized on individual Cu ions, cluster models, constructed by extracting some small portion of the zeolite surrounding the Cu site, are well suited to studying NO_x chemistry. DFT calculations show that even a single, H-terminated T-site is satisfactory for studying adsorption and reaction at Cu ions:[1]

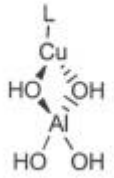

Using this model, both mono- and dinitrosyl complexes ZCuNO and $ZCu(NO)_2$ (where "Z" represents coordination to the zeolite lattice) can be identified[2]. The predicted vibrational spectra of these adsorbates are in excellent agreement with available experimental data. Because these are the only nitrosyl adsorbates identified in experimental studies, most mechanistic speculations have assumed them to be the reactive intermediates leading to N_2 production. A detailed potential energy surface search demonstrates, however, that ZCuNO and $ZCu(NO)_2$ are in fact spectators and not reactive intermediates.[3] Rather, adsorption of NO as a metastable, O-down isonitrosyl ZCuON is found to be the first step in a pathway that leads, with very small energy barrier, to N-N bond formation:[4]

$$ZCu + NO \rightarrow ZCuON \quad (1)$$

$$ZCuON + NO \rightarrow [ZCuONNO]^{\ddagger} \rightarrow ZCuO + N_2O \quad (2)$$

These initial steps are consistent with the formation of N_2O at low temperatures over NO-exposed Cu-ZSM-5. Subsequent reduction of N_2O to N_2 can be accomplished in at least two ways, the first requiring only a single Cu active site

$$ZCuO + N_2O \rightarrow [ZCuOONN]^{\ddagger} \rightarrow ZCUO_2 + N_2 \quad (3)$$
$$ZCUO_2 \rightarrow ZCU + O_2 \quad (4)$$

and the second requiring the temporary generation of a di-Cu intermediate:

$$ZCu + N_2O \rightarrow [ZCuONN]^{\ddagger} \rightarrow ZCuO + N_2 \quad (5)$$

$$2\ ZCuO \rightarrow ZCuOOCuZ \quad (6)$$

$$ZCuOOCuZ \rightarrow 2\ ZCU + O_2 \quad (7)$$

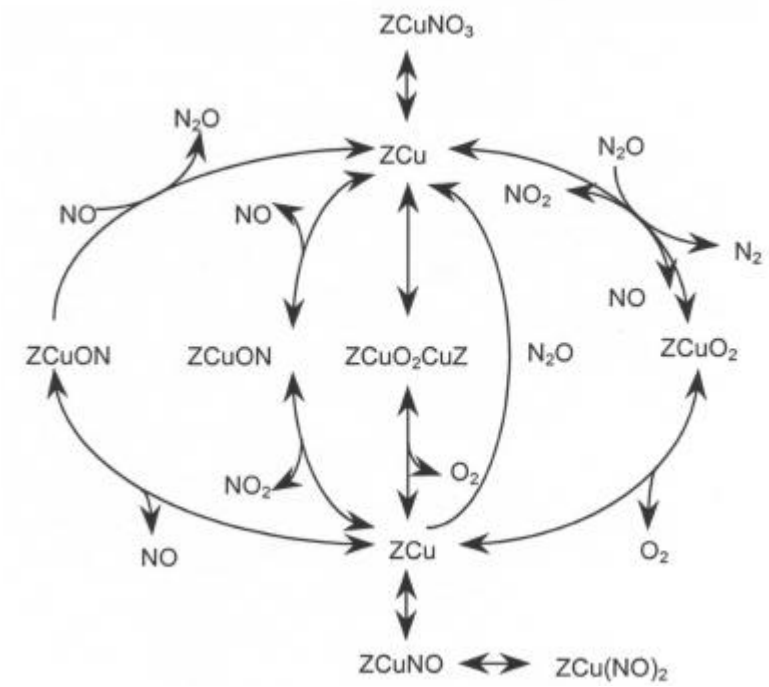

Both DFT calculations[5] and statistical models of Al distributions[6] indicate that di-Cu species should be readily formed at typical Cu exchange levels and Si:Al ratios. In either pathway, the ability of the Cu-exchanged zeolite to catalyze the desired chemistry is intimately linked to the existence of discrete Cu-oxo complexes, the ability of reduced (ZCu) sites to be regenerated by desorption of O_2, and the absence of an irreversibly oxidized Cu state.

Using these and other results, a scheme that accounts for the known NO decomposition, NO oxidation, and N_2O decomposition activity of Cu-ZSM-5 can be constructed (Fig. 1).

Figure 1. Computed NO reaction pathways in Cu-ZSM-5.

Introduction of reductant into this scheme considerably complicates the chemistry. Initial efforts have focused on the non-selective reducing ability of CO.[7] CO readily drives the ZCuO → ZCu conversion, promoting the NO to N_2 chemistry described above. In the presence of O_2, however, highly efficient CO + O_2 catalytic cycles out compete NO reduction chemistry. Future efforts will explore selective reduction chemistry, for instance employing NH_3 as a reductant.

NO_x Traps

In NO_x traps, NO_x is stored on a suitable adsorbent during lean engine operation and is then released and reduced to N_2 using conventional catalysts during periodic rich excursions. Storage is thought to occur in two steps: NO is first oxidized to NO_2 on a precious metal particle, and then is adsorbed onto an alkaline earth oxide (e.g., barium oxide, BaO) particle to form a nitrate. Unfortunately, small amounts of SO_2 in the exhaust are similarly oxidized and adsorbed to form sulfates, which block NO_2 adsorption and are difficult to remove. This sulfur-poisoning phenomenon is the primary current obstacle to NO_x trap implementation, and has been the emphasis of these computational investigations.

The alkaline earth oxides have the familiar rocksalt (NaCI) crystal structure. Here the chemistry of interest is not localized at discrete active sites but is distributed over (from an atomic perspective) an essentially infinite surface. To model the undefected (001) surface and various surface defects, such as steps, vacancies, and adatoms, a slab model is used, in which the desired surface region is treated as an infinitely repeated, periodic "supercell." Supercells containing a three-layer slab or 48 atoms per supercell are found to provide a reasonable compromise between chemical accuracy and computational efficiency.

Initial DFT supercell calculations have focused on the MgO surface. SO_2 is found to both physisorb and chemisorb on the lowest-energy (001) surface. Chemisorption occurs primarily through binding of the S atom to a surface O anion, forining a sulfite-like (SO_3^{2-}) surface species with a binding energy of 25 kcal mol^{-1}. Chemisorption at monatomic steps is approximately 20 kcal mol^{-1} stronger. SO_3 chemisorbs at terraces and steps in a

similar fashion, through the S atom to a surface 0, to form a surface-bound sulfate (SO_4^{2-}) . The SO_3 binding energy is approximately 30 kcal mol^{-1} stronger than the SO_2. The calculated vibrational spectra of the adsorbates agree well with experiment.

Similar trends are observed on BaO surfaces, but the adsorption energies in this case are greater still. SO_3 adsorbs on BaO with a binding energy exceeding 100 kcal mol^{-1}, accounting for its strong poisoning effect. While the role of BaO as an adsorbent is relatively clear, less well understood is its ability to catalyze sulfur oxide oxidations and/or reductions. Such reactions will be mediated through the generation and consumption of point surface defects — adatoms and vacancies. Preliminary calculations indicate that O adatoms are remarkably stable on BaO, and that oxidation of SO_2 to SO_3 (or equivalently, sulfite to sulfate) occurs readily through the combination of these adatoms with SO_2. Thus, pre-oxidation of SO_2 to SO_3 appears not to be a prerequisite to sulfate formation and poisoning on BaO.

References

1. Hass, K.C.; Schneider, W.F. *Phys. Chem. Chem. Phys.* **1999**, *1,* 639-648.
2. Schneider, W.F.; Hass, K.C.; Ramprasad, R.; Adams, J.B. *J. Phys. Chem. B* **1998**, *102*, 3692.
3. Ramprasad, R.; Hass, K.C.; Schneider, W.F.; Adams, J.B. *J. Phys. Chem. B* **1997**, *101*, 6903.
4. Schneider, W.F.; Hass, K.C.; Ramprasad, R.; Adams, J.B. *J.* Phys. *Chem. B* **1997**, *101*, 4353.
5. Goodman, B.R.; Hass, K.C.; Schneider, W.F.; Adams, J.B. *J. Phys. Chem. B* **1999**, *103*, 10452.
6. Goodman, B.R.; Hass, K.C.; Schneider, W.F.; Adams, J.B. *Catal. Lett.* **2000,** in press.
7. Sengupta, D.; Schneider, W.F.; Hass, K.C.; Adams, J.B. *Catal. Lett.* **1999**, *61*, 179.

DEVELOPMENT OF A COMPUTATIONAL CHEMISTRY SCREENING TOOL FOR THE PREDICTION OF ENVIRONMENTAL PROPERTIES OF HALOGENATED ORGANICS

Carlos A. Gonzalez, Florent Louis, Robert E. Huie and Michael J. Kurylo
Physical and Chemical Properties Division, National Institute of Standards and Technology
Gaithersburg, MD 20899-8381
301-975-4063, carlos.gonzalez@nist.gov

The decision to phase out the use of halons due to their role in stratospheric ozone loss resulted in a frantic search for replacements. It also unleashed the imagination of several chemists, who soon proposed a number of viable alternatives. This then led to a new crisis, as all these potential replacements had to be evaluated for environmental acceptability. This was particularly true with regard to one of the most important pieces of information relating to the atmospheric fate of volatile species: the reactivity towards the hydroxyl radical. The abstraction reaction of H-atoms by hydroxyl radicals is the determining factor in the tropospheric lifetimes of most saturated organic compounds, including halogenated species containing one or more C-H bonds. Carrying out laboratory measurements of these reactions on all the proposed replacements would be an expensive proposition, made worse by the fact that many of the compounds would have to be synthesized and provided in sufficient purity for these measurements. Clearly, screening tools are required in order to rule out those compounds which are likely to be unacceptable from an environmental standpoint.

Over the years, various structure-activity strategies have been employed in estimating rate constants for chemical reactions, including those of the hydroxyl radical. These usually require a substantial amount of data in order to provide reliable predictions. The magnitude of this task is illustrated by the results of hydrofluoroethers. Normally, it is assumed that the presence of an ether linkage decreases the bond strength of adjacent C-H bonds, increasing their reactivity. In comparing fluoroalkanes and the corresponding fluoroethers, however, both activation and deactivation are observed (Figure 1). Analyses of these results do not reveal any consistent pattern. It becomes clear that many more fluoroethers would need to be studied. From the point of view of screening halon replacements, a more serious problem was that we would need to measure rate constants for many bromofluoroethers in order to establish reactivity patterns for this class.

Rather than taking this brute force approach, we have decided to explore the possibility of applying fundamental theory to the problem of predicting reactivity. We initiated a systematic study of the application of *ab initio*

electronic structure calculations combined with transition state theory to the kinetics of hydrogen-atom abstractions by hydroxyl radicals. The objective is to develop efficient and reliable computational chemistry "screening tools" useful in predicting the fate of halon replacements once they are released into the atmosphere.

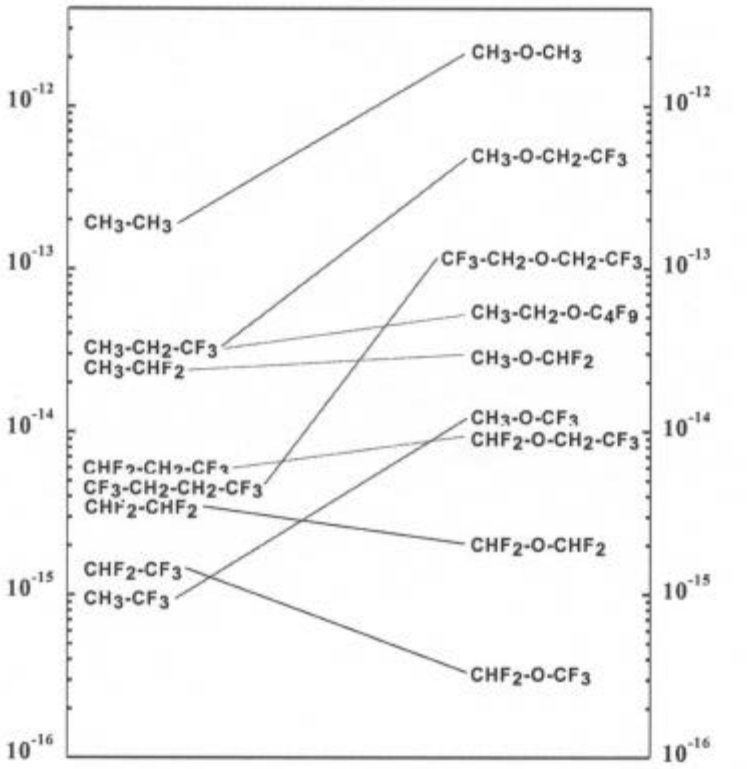

Figure 1. Graph of the relationship between the reactivity of OH towards fluoroalkanes and fluoroethers.

Our plan has been: (i) to find the minimum level of *ab initio* molecular orbital theory suitable for predicting the reactivity of a set of halocarbons whose kinetics are well known, and (ii) to apply this level of theory for the prediction of the reactivity of new species. Part (i) was done on a series of 13 halomethanes. For these compounds, the aim was to describe the reaction enthalpy, the temperature dependence of the rate constant, and to gain insight into the reactivity trends along the series of reactions OH + CHXYZ → H_2O + CXYZ (X, Y, Z = H, F, Cl, or Br). A comparison of the kinetic parameters estimated by these calculations with those derived experimentally, shows very good agreement. Step (ii) in this process involved the extension of these calculations to a series of bromine-containing halomethanes for which experimental data are not available: CH_2FBr, $CHFBr_2$, CHFClBr, $CHCl_2Br$, and $CHClBr_2$. This has been done both by the use of direct *ab initio* calculations employing transition-state theory and with an Evans-Polanyi's type relationship by utilizing the computed reaction enthalpies. The estimated uncertainties associated with these predictive tools will be presented and discussed.

As discussed in this talk, these studies have been quite successful and we have been able to demonstrate that a relatively reasonable level of theory is sufficient to predict rate constants to a degree of accuracy sufficient for a screening tool. These full transition state calculations are still difficult, however, for larger systems. Therefore, we have been exploring additional strategies for the prediction of rate constants. Since the thermodynamics are far easier to calculate than reaction kinetics, we have begun looking into applying the simple relationship between rate constant and reaction enthalpy and the rate constant embodied in the Evans-Polanyi equation. We have found that there is a simple quadratic relationship between the logarithm of the rate constant and the calculated reaction enthalpy for the halomethanes.

STRUCTURE PREDICTION IN PROTEIN FOLDING

Professor C.A. Floudas
Department of Chemical Engineering, Princeton University, Princeton, NJ 08544

The structure prediction of polypeptides and proteins from their amino acid sequence is regarded as a {\it holy

grail} in the computational chemistry, molecular and structural biology communities. During the last several decades, the quest for its solution has occupied the most brilliant minds of researchers across several disciplines. Excellent progress has been achieved and a brighter future lies ahead (Koehl and Levitt (1999), Wales and Scheraga (1999), Dill (1999)).

According to the {\it thermodynamic hypothesis} introduced by Anfinsen the native structure of a protein in a given environment corresponds to the global minimum free energy of the system. In spite of pioneering contributions and decades of effort, the *ab initio* prediction of the folded three dimensional structure of a protein remains a very challenging problem. This can be attributed to (i) the many degrees of freedom that require the development of effective conformational search algorithms to identify the global minimum, valid upper and lower bounds on the global minimum, as well as low energy conformers needed for the calculation of the entropic contributions, and (ii) the formulation of reliable potential force fields that can recognize the native state in the presence of many misfolded structures.

The approaches for the three dimensional structure prediction of polypeptides can be classified into four main categories: (a) homology or comparative modeling methods, (b) fold recognition or threading methods, (c) *ab initio* methods that utilize knowledge-based information from structural databases (e.g., secondary structure; secondary and tertiary constraints; contact residues), and (d) *ab initio* methods without the aid of knowledge-based information.

In this presentation, we will discuss recent advances for the structure refinement of oligopeptides and polypeptides. These advances are based on novel mathematical formulation of the structure refinement problem as a constrained NLP and on the principles of the deterministic global optimization approach aBB (Floudas, 2000; Adjiman *et al*., 1998) that offers theoretical guarantee of attaining the global solution of general nonlinear optimization problems, provides valid lower and upper bounds on the global solution, and identifies ensembles of low energy structures that are important in the consideration of entropic contributions. Furthermore, our recent advances introduce an approach based on torsion angle dynamics within the aBB global optimization framework. Computational results on Compstatin and BPTI will illustrate the power of the proposed approaches.

4th Annual Green Chemistry &
Engineering Conference

Sustainable Technologies:
From Research to Industrial Implementation

June 27 - 29, 2000

BIO-BASED SYNTHESIS AND PROCESSING II

THE COST OF LIGNOCELLULOSIC SUGAR FOR COMMODITY CHEMICAL PRODUCTION

Mark F. Ruth and Robert J. Wooley
National Renewable Energy Laboratory, 1617 Cole Blvd., Golden, CO 80401

ABSTRACT
Currently, some commodity chemicals are produced by microorganisms that convert sugar from corn starch to higher value products. The price of corn is one of the primary economic drivers for these processes. Research on utilization of agricultural byproducts and other types of lignocellulosic biomass as feedstocks for fuel ethanol has been on-going for the last twenty years because biomass can be obtained at a lower cost than corn. Most of the biomass-to-ethanol processes being researched consist of hydrolyzing the biomass' cellulose and hemicellulose to form sugars that are fermented to ethanol. Through the intermediate sugar, biomass can also be a feedstock for other chemicals. The economics of biomass sugar production utilizing dilute acid for hemicellulose hydrolysis and enzymes for cellulose hydrolysis have been analyzed. The analysis includes potential improvements that can reduce the hydrolysis cost making biomass an economically viable feedstock.

INTRODUCTION
A mixed sugar stream is an intermediate in biomass-to-ethanol processes and products other than ethanol could be biologically produced using similar process schemes. The transfer price of biomass sugar has been investigated and ultimately the sugar intermediate stream could compete economically with sugar streams from cornstarch because of lower feedstock costs.

BIOMASS TO ETHANOL PROCESS AND ECONOMICS
For approximately twenty years, the U.S. Department of Energy (DOE) has funded research on the development of renewable, domestically produced fuels for transportation. The biofuels program is one program in this area and it specifically targets transportation fuels made from biomass. The biofuels program is driven by a number of issues including national security, economic competitiveness in the global market, rural economic development, climate change, and air pollution. In the past the program has worked on a varied portfolio of fuel products. The current focus is on fuel grade bioethanol made from the cellulose and hemicellulose components of biomass -- agricultural wastes, trees, grasses, and other lignocellulosic materials. The abundance of biomass makes it a potential low cost feedstock for fuel ethanol and two of its three primary components (cellulose and hemicellulose) can be hydrolyzed into fermentable sugars making a relatively high mass yield (0.35-0.40 lb ethanol / lb biomass) possible. The third primary component, lignin, has other potential uses.

Engineers at the National Renewable Energy Laboratory (NREL) have rigorously analyzed biomass-to-ethanol processes during the life of the program[1,2] to predict the current and future cost of bioethanol and understand the economic impacts of proposed research. In 1999, a report[3,4] was published describing the current understanding of process design and economics of a lignocellulosic biomass to ethanol process utilizing co-current dilute acid prehydrolysis and enzymatic hydrolysis technology.

Figure 1 is a schematic of the process modeled and reported on in 1999. Hardwood sawdust enters the process and is pretreated at elevated temperatures with a sulfuric acid catalyst to hydrolyze the hemicellulose into sugars. Sugars released from the hemicellulose include xylose, arabinose, galactose, and mannose. Pretreatment not only hydrolyzes the hemicellulose sugars, but it also makes cellulose more accessible to enzymatic hydrolysis. Approximately five percent of the pretreated slurry (hydrolyzate) is pumped to enzyme production where cellulase enzymes are biologically produced by fungi in submerged culture reactors. The remaining 95% of the hydrolyzate is pumped to fermentation where the cellulase enzyme broth and ethanologens are added. This area's process scheme is called simultaneous saccharification and co-fermentation (SSCF) because cellulase enzymes are hydrolyzing cellulose into glucose and that glucose is immediately consumed by ethanologens to produce ethanol. Genetically modified ethanologens are utilized because they are capable of simultaneously converting both glucose and sugars from hemicellulose. After fermentation the ethanol broth is distilled and dehydrated to fuel grade ethanol that is stored and sold as the primary product. Lignin-rich solids from distillation are sent to the burner/boiler/turbogenerator area where they are dried and burnt to produce steam and electricity for the process. Any excess electricity is sold to the local power grid. Wastewater from the distillation area is pumped to wastewater treatment where it is mixed with flash vapor from the pretreatment area. Wastewater treatment produces a clean water stream for recycling and biogas and sludge that can be burnt to produce steam and electricity. Utility equipment to support the process is included in the model.

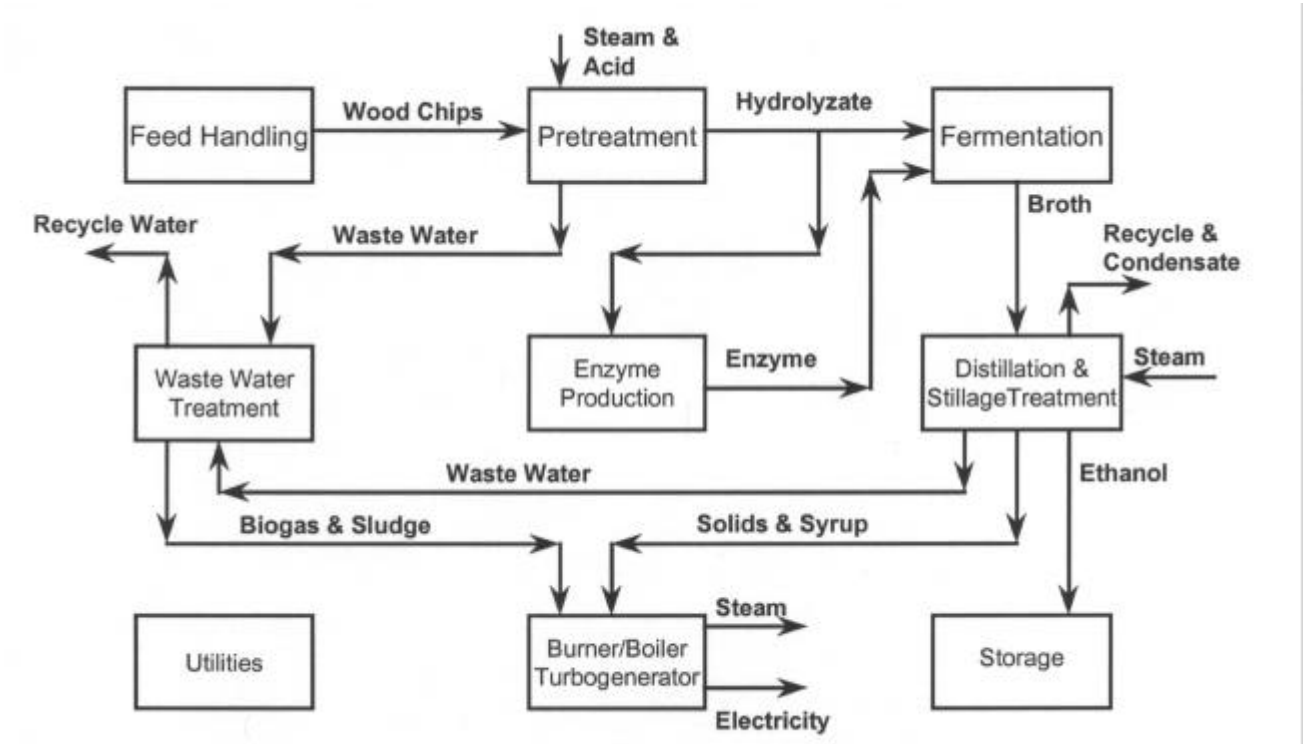

Figure 1. Schematic of One Biomass-to-Ethanol Process

To determine the economics of the above process, parameter sets were developed for different time periods ranging from technology that should be available in the near term to technology with a predicted availability of 2015 if research continues. Material and energy balances were calculated for each case and stream results were utilized for equipment sizing. Total capital investments were determined from the equipment costs (involving n^{th} plant assumptions) and operating costs were calculated from stream flow rates. Finally, minimum ethanol selling prices were calculated from the total capital investment and operating costs with a 10% post-tax discounted cash flow rate of return. The minimum ethanol selling prices range from $1.44/gal (near-term NREL technology) to $0.76/gal (2015 technology).

PRODUCTION OF BIOMASS SUGARS

Sugars are an intermediate product in the formation of ethanol. Hemicellulose is hydrolyzed to form xylose, arabinose, galactose, and mannose in the pretreatment area. Cellulase enzyme saccharifies the cellulose into glucose in the fermentation area. Two potential process schemes for other products follow: first, organisms other than ethanologens could consume the sugars and produce a desirable product or group of products simultaneously with saccharification and, second, enzymatic hydrolysis could be operated in a near sterile way producing a transferable sugar stream as its product.

To analyze the cost of the intermediate sugar stream the second scheme was chosen so the following areas were removed from the biomass-to-ethanol process model and economics: wastewater treatment (a cost was kept for treatment of the pretreatment flash vapor), distillation and stillage treatment, and storage. The fermentation area was converted to an enzymatic hydrolysis area by removing seed production of the ethanologen. Finally, a counter-current washer was added after the hydrolysis area to separate lignin for combustion in the burner from the dilute mixed sugar stream. Mass balances and capital and operating costs were determined for the sugar process and the minimum sugar transfer price was calculated.

Five cases were modeled at feedstock costs of $25/dry ton and their results are presented in Figure 2. The base case, resulting in a minimum sugar transfer price of 7.5¢/lb, is based -on parameters that are believed to be achievable soon with current research. If pretreatment yields and enzyme productivity can be improved to levels claimed possible by some researchers, the minimum transfer price will be reduced to 6.6¢/lb as shown in the potential near term case. By 2005, protein engineering is expected to result in a three-fold improvement of the

enzyme specific activity and increased thermo-tolerance. Combining the protein engineering based improvements with the potential near term parameters reduces the minimum transfer price to 5.2¢/lb. By 2010, more protein engineering is expected to result in a ten-fold improvement in the enzyme specific activity from current levels. That improvement is estimated to further reduce the minimum transfer price to 4.6¢/lb. A feedstock collection infrastructure may also be in place by 2010 allowing much larger plant sizes. By increasing the plant feed rate from 2000 dry tonne/day to 10,000 dry tonne/day, the minimum selling price is reduced from 4.6¢/lb to 3.2¢/lb.

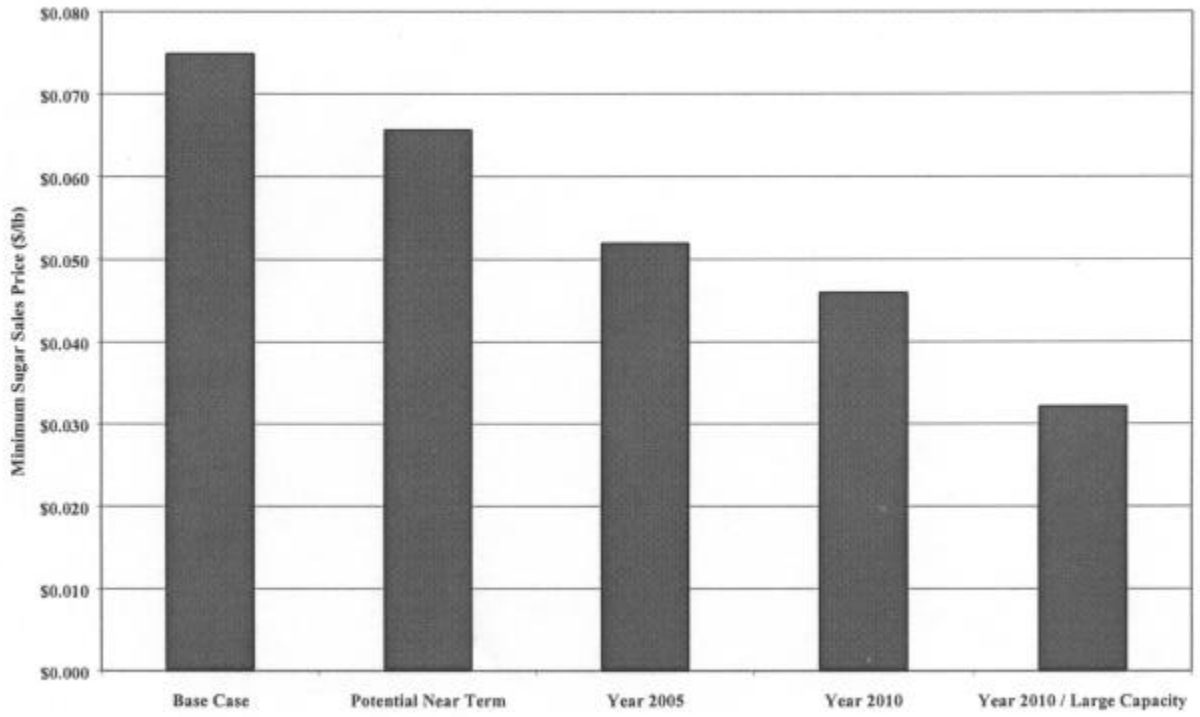

Figure 2. Estimated Biomass Sugar Transfer Prices

In some cases the lignin stream can be sold either to a nearby plant that converts lignin into higher value byproducts or a larger more cost-efficient biomass power facility. Selling the lignin at the same price as the feedstock (on a lower heating value basis) reduces the sugar price by 1.1¢/lb in the base case and 0.3¢/lb in the 2010 / Large Capacity case.

SUMMARY

By removing the ethanol specific portions of a biomass-to-ethanol process model, an economic analysis of a mixed sugar stream from biomass has been developed. The analysis shows that a dilute mixed-sugar stream from biomass is estimated to carry a required transfer price of 7.5¢/lb in the near-term and can be reduced to 3.2¢/lb with continued research and industry development. That research needs to involve improved pretreatment yields as well as increase cellulase specific activity and thermotolerance. If the lignin stream can be sold, the sugar transfer price can be reduced by 1.1¢/lb in the base case and 0.3¢/lb in the 2010 / Large Capacity case.

ACKNOWLEDGMENT

This work was funded by the Biochemical Conversion Element of the Office of Fuels Development of the U.S. Department of Energy.

REFERENCES

1. Wright, J.; D'Agincourt, C. Evaluation of Sulfuric Acid Hydrolysis Processes for Alcohol Fuel Production. *Biotechnol. Bioeng. Symp. No. 14, 1984,* 105-123.
2. Hinman, N. D.; Schell, D. J.; Riley, C. J.; Bergeron, P. W.; Walter, P. J. Preliminary Estimate of the Cost of Ethanol Production for SSF Technology. *Appl. Biochem. Biotechnol.* **1992**, *34/35,* 639-649.

3. Wooley, R.J.; Ruth, M.; Sheehan, J.; Majdeski, H.; Galvez, A. Lignocellulosic Biomass to Ethanol Process Design and Economics Utilizing Co-Current Dilute Acid Prehydrolysis and Enzymatic Hydrolysis Current and Futuristic Scenarios; Report No. NREL/TP-580-2615. National Renewable Energy Laboratory, Golden, CO, July 1999, (http://www.ott.doe.gov/biofuels/process_engineering.html).
4. Wooley, R.; Ruth, M.; Glassner, D.; Sheehan, J. Process Design and Costing of Bioethanol Technology: A Tool for Determining the Status and Direction of Research and Development. *Biotechnol. Prog.* **1999**, *15,* 794-803.

BIOLOGICAL PRODUCTION OF SUCCINIC ACID FROM GLYCEROL

Pyung-Cheon Lee, Woo-Gi Lee, Sang-Yup Lee and Ho-Nam Chang
Department of Chemical Engineering, Korea Advanced Institute of Science and Technology (KAIST),
373-1, Kusong-dong, Yusung-gu,Taejon, Korea 305-701

ABSTRACT
Fermentation of *Anaerobiospirillum succiniciproducens* was studied using glycerol as a carbon source for the production of succinic acid. When cells were anaerobically cultured in a medium containing 6.5 g/L glycerol, a high succinic acid yield (133%) was obtained while avoiding the formation of by-product acetic acid. A gram ratio of succinic acid to acetic acid was 25.8:1, which is 6.5 times higher than that obtained using glucose (ca. 4:1) as a carbon source. When glucose and glycerol were cofermented with the increasing ratio of glucose to glycerol, the grain ratio of succinic acid to acetic acid and succinic acid yield decreased, suggesting that glucose enhanced acetic acid formation irrespective of the presence of glycerol.

INTRODUCTION
Glycerol is an attractive carbon substrate for biological conversion because it is available from renewable resources in large amounts and can be utilized by a number of microorganisms[1]. Glycerol is produced as a surplus by-product in the growing oleochemical industries for the production of soaps, fatty acids, waxes and surfactants. Therefore, several environmentally friendly processes based on microbial fermentation have been proposed for glycerol utilization.

To date, however, succinic acid production from glycerol has not been reported. Succinic acid is of great interest in polymer synthesis and as an intermediate for chemical synthesis. To date, succinic acid has been produced commercially by chemical processes. Recently, however, fermentative production of succinic acid from renewable biomass by anaerobic bacteria has attracted great interest[2]. An anaerobic bacterium *Anaerobiospirillum succiniciproducens* has been considered as one of the best succinic acid producers because it can produce a significant amount of succinic acid from carbohydrates[3,4,5].

It is well known that the presence of by-product such as acetic acid can negatively affect the purification process of succinic acid. Lee *et al*.[3] reported that acetic acid was also produced as a by-product with a gram ratio of succinic acid to acetic acid of 4:1 in the fermentation of glucose by *A. succiniciproducens*. Acetic acid formation reduces succinic acid yield and makes purification of succinic acid more difficult and costly. Therefore, fermentation process for succinic acid production with reduced acetic acid formation should be developed for better fermentation performance and economical purification of succinic acid.

In this article, we report that glycerol, as an alternative substrate to glucose, provides several advantages for the production and purification of succinic acid mainly because much higher ratio of succinic acid to acetic acid can be obtained.

MATERIALS AND METHODS
Organism and growth conditions
Anaerobiospirillum succiniciproducens (ATCC 29305) was obtained from the American Type Culture Collection (Rockville, MD). Cells were grown in sealed anaerobic bottles containing 100 µL minimal salts medium1 (AnS1) containing 5 g/L glucose, 5 g/L yeast extract and 10 g/L polypeptone with CO_2 as the gas phase. The AnS1

medium contains per liter, 3 g K_2HPO_4, 1 g NaCl, 1 g $(NH_4)_2SO_4$, 0.2 $CaCl•2H_2O$, 0.2 g $MgCl_2•6H_2O$, and 1 g Na_2CO_3. The medium was heat sterilized (15 min at 121 ºC) in anaerobic bottle with nitrogen headspace and inoculated with 2.5 mL glycerol stock culture and incubated at 39 ºC for 15-16 h. Batch cultures were carried out at 39 ºC in a jar fermenter (2.5 L) containing 1 L of minimal salts medium2 (AnS2) containing 3.5-10 g glycerol, 5 g yeast extract and 10 g polypeptone. In case of cofermentation, the AnS2 medium containing glycerol, yeast extract and polypeptone were supplemented with glucose as indicated in RESULTS AND DISCUSSION. The AnS2 medium contained per liter: 3 g K_2HPO_4, 2 g NaCl, 5 g $(NH_4)_2SO_4$, 0.2 g $CaCl_2•2H_2O$, 0.4 g $MgCl_2•6H_2O$, 5 mg $FeSO_4•7H_2O$, and 3 g Na_2CO_3. The pH was controlled at 6.5 using 1.5 M Na_2CO_3. CO_2 sparging rate and agitation speed were controlled at 0.25 vvm and 200 rpm, respectively.

Enzyme assay

Glucose: PEP phosphotransferase (EC 2. 7. 1.) activity was assayed by monitoring the reduction of NADP at 340 nm. The assay mixture contained 0.1 M Tris-HCl (pH 8.4), 10 mM $MgCl_2$, 10 mM PEP, 1 mM DTT, 1 mM NADP, 15 mM glucose, 3 U glucose-6-phosphate dehydrogenase and cell extract. One unit (U) of enzyme activity represents the amount of enzyme catalyzing the conversion of 1 nmol of substrate per min into specific products.

Analytical methods

The concentrations of glucose, glycerol, succinic acid and acetic acid were measured by high-performance liquid chromatography equipped with an ion exchange column (Aminex HPX-87H) using 0.012 N H_2SO_4 as a mobile phase. Cell growth was monitored by measuring the absorbance at 660 nm (OD_{660}) using a spectrophotometer. Dry cell weight was calculated from a curve relating the absorbance at 660 nm to dry weight.

RESULTS AND DISCUSSION

When *A. succiniciproducens* was cultured using 6.5 g/L glycerol as a carbon source under anaerobic condition, the concentration and yield of succinic acid were 4.9 g/L and 133%, respectively, at the end of fermentation. The formation of by-product acetic acid was significantly avoided, which resulted in high ratio of succinic acid to acetic acid [25.8:1 (g-succinic acid/g-acetic acid)].

To study the effect of glucose on glycerol utilization, cofermentation of glycerol and glucose was carried out with varying their gram ratios. With the increasing ratio of glucose to glycerol, the gram ratio of succinic acid to acetic acid decreased from 11.0:1 to 6.5:1. Furthermore, intermittent addition of glucose reduced the ratio of succinic acid to acetic acid to 4.9:1. Succinic acid yield decreased according to the increased formation of acetic acid (Table 1). These results suggest that glucose enhances acetic acid formation irrespective of the presence of glycerol.

The reason why glucose enhances acetic acid formation compared to glycerol seems to be due to the different transport systems for glucose and glycerol. As shown in Fig. 1, if *A. succiniciproducens* uses PEP-dependent phosphotransferase system for glucose, PEP will be converted to pyruvate, which will be further metabolized to generate acetic acid, lactic acid and ethanol depending on the culture condition[6]. Therefore, when glucose is transported and metabolized in *A. succiniciproducens,* acetic acid formation will be enhanced, which results in the decrease of the ratio of succinic acid to acetic acid. *A. succiniciproducens* was found to possess glucose:PEP phosphotransferase activity for the uptake of glucose. Therefore, if glucose is mainly transported by PEP-dependent phosphotransferase system, one mole of pyruvate will be formed for every mole of glucose transported. Pyruvate will be further converted to various acids as depicted in Fig. 1. For many bacteria, glycerol is known to be transported by facilitated diffusion. If glycerol is also transported by facilitated diffusion in *A. succiniciproducens,* PEP is not consumed for the glycerol transport, and subsequently, acetic acid formation is reduced. This seems to be why higher ratio of succinic acid to acetic acid can be obtained when glycerol is used as a carbon source.

Table 1. Effect of glycerol and/or glucose on fermentation performance

	Glycerol (6.5)[a]	Glucose/ glycerol (4.2 : 8.4)	Glucose/ glycerol (4.3 : 3.6)	Glucose/ glycerol (7.3 : 3.6)	Glycerol fed with glucose (8.5)	Glucose (20)	Glycerol fed with YE[b] (12)
Maximum cell concentration (OD_{660})	0.8	2.4	2.4	2.9	4.6	3.0	1.9
Succinic acid concentration (g/L)	4.9	10.6	8.2	10.6	29.6	17.0	19.0
Succinic acid yield (%)	133	107	104	97	92	86	160
Succinic acid/acetic acid (g/g)	25.8:1	11.0:1	9.0:1	6.5:1	4.9:1	4.1:1	31.7:1

a, g/L; b, yeast extract

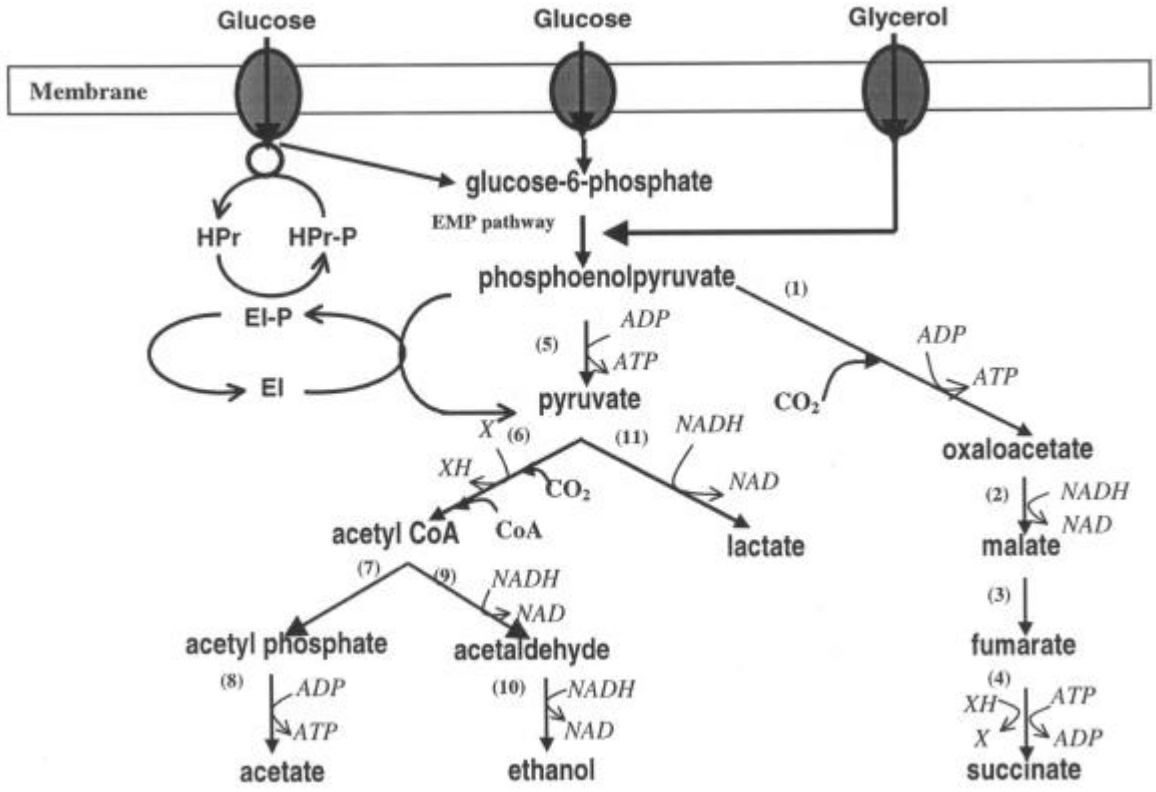

Figure 1. Proposed central metabolic pathway of *A. succiniciproducens* for the utilization of glycerol and glucose. Some of the catabolic pathways were proposed by Samuelov *et al.*[6]. In PEP-phosphotransferase transport system (PTS), EI, nonspecific protein of the PTS; HPr, nonspecific phosphoryl carrier protein of the PTS. The enzymes in catabolic pathway are: (1) PEP-carboxykinase; (2) malate dehydrogenase; (3) fumarase; (4), fumarate reductase; (5) pyruvate kinase; (6) pyruvate-ferredoxin oxidoreductase; (7) phosphotransacetylase; (8) acetate kinase; (9) aldehyde dehydrogenase; (10) alcohol dehydrogenase; (11) lactate dehydrogenase.

SUMMARY

When glycerol was used as a carbon source in the fermentation of *A. succiniciproducens,* succinic acid was produced with a high yield. Also, the formation of by-product acetic acid was avoided, which resulted in the increased ratio of succinic acid to acetic acid up to 25.8:1. This ratio is 6.5 times higher than that obtained by

batch fermentation of glucose (ca. 4:1).

ACKNOWLEDGMENT
This work was supported by Brain Korea 21 project.

REFERENCES
1. Lin, E.C.C. (1976) *Ami. Rev*. *Microbiol.* **30***:* 535-578.
2. Landucci, R.; Goodman, B. and Wyman, C. (1994) *Appl*. *Biochem. Biotechnol.* **45-46***:* 678-696.
3. Lee, P.C.; Lee WG, Kwon, S.; Lee, S.Y. and Chang, H.N. (1999) *Enzyme Microb. Technol.* **24***:* 549-554.
4. Lee, P.C.; Lee, W.G.; Lee, S.Y. and Chang, H.N. (1999) *Process Biochem.* **35***:* 49-55.
5. Lee, P.C.; Lee, W.G. Kwon, S.; Lee, S.Y. and Chang, H.N. (2000) *Appl*. *Microbiol. Biotechnol.* in press.
6. Samuclov, N.S.; Lamed, R.; Lowe, S. and Zeikus, J.G. (1991). *Appl. Environ. Microbial.* **57***:* 3013-3019.

CHITOSAN: COMMERCIAL DEVELOPMENT AND ADDING VALUE THROUGH BIOCHEMICAL MODIFICATION

C. Patrick Condon[1], Jack Cowan[2], Daniel Healey[3], Gregory F. Payne[4]
[1]ChitinWorks America, 20 Washington St., Cambridge, MD 21613
[2]Venture, P.O. Box 81892, Lafayette, LA 70598
[3]DBED, 217 E. Redwood St., Baltimore, MD 21202
[4]Center for Agricultural Biotechnology & University of Maryland Baltimore County,
Center Agric. Biotech., U. Maryland, 6139 Plant Science Bldg., College Park, MD 20740

CONVERTING WASTES INTO CHITOSAN
The motivation for producing chitosan in Maryland evolved from state efforts to reduce nutrient addition to the Chesapeake Bay. Even before *Pfiesteria* outbreaks, Maryland was investing in better methods for managing the 5,000 tons/year of wastes generated from the state's crab packing industry. To protect the Chesapeake Bay, regulations were established to limit disposal of crab chum back to the Bay. However, landfilling the chum was an expensive solution and the state sought better alternatives to the rigorous enforcement of strict environmental regulations on a marginally-profitable industry.

Several years ago the state encouraged a private company, New Earth Services (NES), to develop a composting operation to dispose of crab wastes. The composting product is a garden mulch currently marketed as "Chesapeake Blue." Although this product reduced the economic burden, the crab-packers still needed to pay to dispose their waste biomass. There remained a substantial incentive for the state to encourage the development of higher-valued byproducts from these wastes. The most obvious potential byproduct was the biopolymer chitin which is present at levels of 10 to 15 % of the crab's shell (on a dry basis). Importantly, the composting operation solved one critical problem for chitin manufacturing - the crab wastes were being centrally collected. For instance, NES was composting over 2,000 tons of crab wastes annually.

The state's Department of Business and Economic Development (DBED) recognized the opportunity to convert this centralized waste into multi-ton quantities of chitin. DBED also identified the Louisiana-based company, Venture Chemical, as a potential partner to develop chitin-based products. Venture is a twenty-year-old specialty chemical producer that markets various derivatives of cellulose and starch. DBED's analysis indicated that Venture was well-positioned to market chitin (and its derivative chitosan) as an environmentally-friendly alternative to synthetic polymers. To facilitate a business alliance between NES and Venture, DBED awarded matching investment funds for the project. In February 1997, these funds were further leveraged when NES and the University of Maryland were awarded matching state funds through a Maryland Industrial Partnership (MIPs) grants program. Through this grant, a process was developed to convert crab wastes into chitosan and lab-scale quantities of chitosan were supplied for testing. Based on promising properties of these chitosan samples the process was transferred into the University's Bioprocess Scale-Up Facility for further development and to obtain multi-kilogram quantities of material.

A preliminary economic analysis identified critical areas for process improvement and also showed the

commercial potential for large-scale production of chitosan from Maryland's crab wastes. In 1998, the two industrial partners decided to form a limited liability partnership, ChitinWorks America, to begin commercialization. ChitinWorks obtained the necessary private sector investment to establish its manufacturing plant and in October 1999 it began processing multi-ton batches of crab chum in its Cambridge, Maryland plant.

Maryland's initiative for producing chitosan was motivated by the desire to convert a waste problem into an economic opportunity — that is, to more fully "extract value" from Maryland's natural resources. For this initiative to succeed in converting large amounts of crab wastes, the chitosan must be manufactured at a low enough cost to be sold into low-value, high-volume markets. The emphasis on producing a low-cost "industrial" grade of chitosan is somewhat unique to our project as many initiatives aim to produce small amounts of chitosan for high-value, pharmaceutical opportunities. Success of our project now depends on developing the large-volume outlet markets for chitosan and/or chitosan derivatives. As a first step in commercialization, Venture plans to develop chitosan derivatives for oil drilling applications. To financially assist in their efforts Venture successfully competed for support through the National Science Foundation's Small Business Innovative Research program.

CHITIN AND CHITOSAN

Chitin is found in the outer integument (i.e. "shells") of crabs and other crustaceans. Also, chitin is found in insects and the cell walls of fungi and is considered the second (or third) most abundant natural material after cellulose (and possibly lignin). Chitosan is obtained by *N*-deacetylation of chitin. As shown in Figure 1, chitin and chitosan are structurally related to cellulose with the only differences appearing in the 2 position of the repeating sugar unit. The repeating units of cellulose, chitin, and chitosan have hydroxyl, *N*-acetyl, and primary amino groups at their 2 positions, respectively.

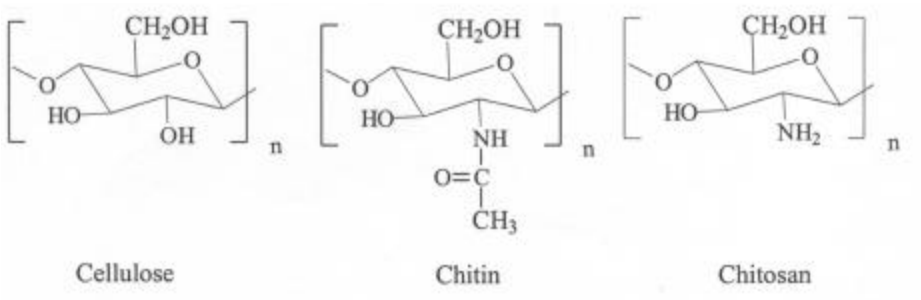

Figure 1. The β-1,4-linked polysaccharides cellulose, chitin, and chitosan.

The major advantage of chitosan over other natural, or synthetic polymers is that it is rich in amine functionality. As illustrated in Figure 2, one consequence of chitosan's amine functionality is that under moderately acidic conditions (pH<6), the amino groups of chitosan become protonated (i.e. chitosan becomes a polyelectrolyte) and chitosan can dissolve in aqueous solutions. Water-solubility is unusual for β-1,4-linked polysaccharides. For instance, cellulose is only made water-soluble by modification with hydrophilic groups such as hydroxyethyl and carboxymethyl. A second consequence of chitosan's amine functionality is that at higher pH's (pH>7) the amines are deprotonated, and have an unshared electron pair which is nucleophilic and can undergo various reactions. Thus, aldehydes, anhydrides, acid chlorides and epoxides have been used to generate chemically-modified chitosan derivatives. Importantly, the reactivity of these amines allows chitosan to be modified under facile conditions and modification is often regioselective for the 2-position. This behavior differs from that of cellulose which requires considerably harsher conditions for reaction of its hydroxyl groups, and cellulose modification is not generally regioselective (reactions occurring at hydroxyl groups at the 2, 3, and 6 positions).

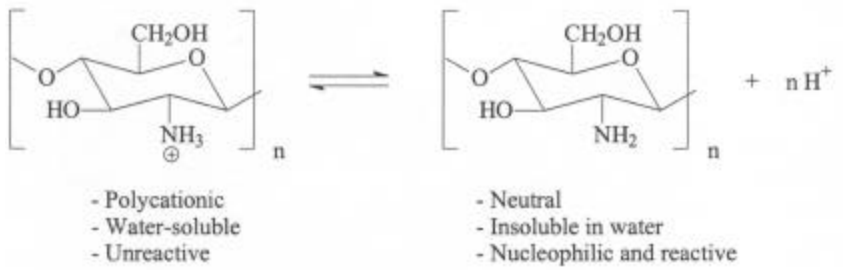

Figure 2. Chitosan acid-base behavior (pKa ≈ 6.3)

BIOCHEMICAL FUNCTIONALIZATION OF CHITOSAN

By grafting various chemical groups onto chitosan it is possible to generate derivatives that offer a wide range of functional properties. The goal of the University of Maryland's research program is to develop biochemical alternatives to standard grafting chemistries. Figure 3 shows that we are using the enzyme tyrosinase to convert phenolic substrates into reactive *ortho*-quinones. Tyrosinase uses molecular oxygen as the oxidant and has no cofactor requirements. The quinone intermediate is freely diffusible and can react with the amino groups of chitosan. Because of the broad substrate range of tyrosinases, our biochemical approach can graft a diverse range of phenols onto chitosan.

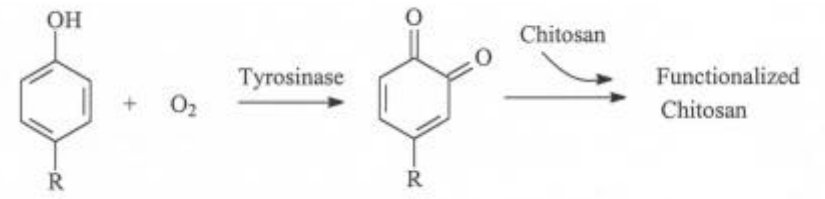

Figure 3. Biochemical grafting procedure to functionalize chitosan.

In nature, tyrosinase and the related phenol oxidase enzymes serve various functions from the hardening of insect shells (sclerotization) to the setting of mussel glues. We are attempting to mimic these functions. Initially, we demonstrated that tyrosinase-catalyzed quinones can be grafted onto chitosan.[1] In subsequent studies we demonstrated that biochemical grafting could; alter chitosan's pH-solubility behavior[2], lead to *in situ* gel formation,[3] confer water-resistant adhesive properties[4] and generate hydrophobically-modified chitosan derivatives.[5] Currently, we are attempting to create functionality using phenolic substrates that can be obtained from natural sources.

SUMMARY

A government-industry-university partnership has enabled wastes generated from Maryland's crab-packing industry to be converted into the biopolymer chitosan. Proprietary efforts are underway to introduce chitosan and chitosan derivatives into oil drilling applications. In the longer term, the partners hope to develop environmentally friendly enzymatic methods to graft natural products onto chitosan to create derivatives that offer a diverse range of functional properties.

ACKNOWLEDGMENTS

Research and development was supported by the Maryland Industrial Partnership program, the Maryland SeaGrant program, and the National Science Foundation (through DMI-9901868).

REFERENCES

1. Payne, G.F.; Chaubal, M.V.; Barbari, T.A. 1996. Enzyme-based polymer modification: Reaction of phenolic compounds with chitosan films. *Polym.,* **37**: 4643.
2. Kumar, G.; Smith, P.J.; Payne, G.F. 1999. Enzymatic grafting of a natural product onto chitosan to confer water solubility under basic conditions. *Biotechnol. Bioeng.,* **63**: 154.
3. Kumar, G.; Bristow, J.F.; Smith, P.J.; Payne, G.F. Enzymatic gelation of the natural polymer chitosan. 2000. *Polym.,* **41**: 2157.
4. Yamada, K.; Chen, T.; Kumar, G.; Vesnovsky, O.; Topoleski, L.D.T.; Payne, G.F. Chitosan based water-resistant adhesive. Analogy to mussel glue. 2000. *Biomacromol.,* In Press.
5. Chen, T.; Kumar, G.; Harris, M.T.; Smith, P.J.; Payne, G.F. 2000. Enzymatic grafting of hexyloxyphenol onto chitosan to alter surface and rheological properties. *Biotechnol. Bioeng.,* In Press.

ATTAINMENT OF THE THEORETICAL YIELD OF CARBON FROM BIOMASS

Michael Jerry Antal, Jr., Stephen G. Allen, Xiangfeng Dai, Brent Shimizu and Man Tam
Hawaii Natural Energy Institute, University of Hawaii, 2540 Dole St., Holmes Hall 246, Honolulu, HI 96822
Morten Grønli
SINTEF Energy Research, 7034 Trondheim, Norway

INTRODUCTION

Charcoal is a carbonaceous solid with a fixed carbon content of 70% or more. Charcoal is usually manufactured

from hardwoods or other dense biomass by pyrolysis in large kilns or retorts[1]. Worldwide charcoal production is estimated to lie in the range of 26[2] to 100[3] million tons per year, and is growing at an estimated rate of about 3% per year[2]. In the USA charcoal is used as a barbecue fuel, but elsewhere it is employed as a reductant for metal ores (e.g. the manufacture of ferrosilicon in Norway and iron in Brazil). A typical yield of charcoal manufactured from hardwoods in a Missouri kiln operated on a 7 to 12 day cycle is about 28 wt%[4] on a dry basis. This charcoal has a fixed carbon content of about 70 wt%; therefore the process offers a fixed carbon yield of about 20 wt% ($0.2 \approx 0.28*0.7$). Less efficient processes are widely employed in the developing world. Such processes are the principal cause of the deforestation of many tropical countries (including Thailand, Haiti, and Madagascar). Because of pollution associated with the inefficient conversion of biomass to charcoal, the charcoal fuel cycle is among the most greenhouse-gas intensive energy sources employed by mankind[5]. Simple stoichiometric arguments show that charcoal yields of 55 wt% (or more) should be possible, and thermochemical equilibrium (STANJAN) calculations indicate that a fixed carbon yield of about 30 wt% should be achieved when equilibrium is reached in a pyrolytic reactor operating at 300 ºC.

In 1986 our research led us to realize that high yields of charcoal are obtained when pyrolysis is conducted at elevated pressure wherein the vapors are held in contact with solid products of pyrolysis. A grant from the State of Hawaii enabled us to build a pilot plant, which demonstrated charcoal yields of 42 to 62 wt% with fixed carbon contents of 70% or higher on a 1 hour operating cycle[6]. In this paper we report measurements of the fixed carbon yield that result from pyrolysis of several biomass feeds at elevated pressure. We compare these values to values predicted by thermochemical equilibrium calculations. For the feeds considered, the yield of fixed carbon delivered by our equipment equals the theoretical yield.

EXPERIMENTAL

High-yield biomass charcoals were produced in two reactors with similar configurations and operating procedures. The process development unit (PDU), which is described in detail elsewhere[6], has an internal volume of 80 L and can produce as much as 10 kg of charcoal per cycle. Because the pyrolytic reactions which transform biomass to charcoal are exothermic[7,8], the pilot plant requires little heat input[6]. The laboratory reactor is a pressure vessel with an internal volume of 7.2 L. At the bottom of this reactor there are two internal 4kW Omegalux cartridge heaters that are controlled by a temperature controller (Omega CN132). Recently, we installed an ARI Industries 700 W rod heater down the central axis of the reactor to improve the uniformity of the charcoal product. To minimize heat losses the reactor walls are heated by four, external Omegalux band heaters totaling 4.4 kW. These heaters are powered by a 240V/15A transformer. In some experiments the temperature of the reaction is monitored by two type K thermocouples inserted in an annulus at the top of the reactor. The pressure within the reactor is controlled by an on-off valve. Combustible gases released by the valve are burned in a flare.

RESULTS

The thermochemical equilibrium value of the fixed-carbon yield constitutes a benchmark against which the experimental values can be compared. We refer to this value as the "theoretical" yield of carbon, which we hypothesize to be the upper limit attainable by thermal processes. We used the thermochemical equilibrium software STANJAN[9] to calculate the mass fraction of solid carbon present at equilibrium when the elements C, H, and 0 with molar ratios dictated by the composition of each feedstock (see Table 1) are mixed at 1.0 MPa and 300 ºC. Note that we neglect the presence of nitrogen and sulfur in the STANJAN calculations. This is a consequence of the fact that these two elements compose only a small fraction of the mass of the biomass feed. Moreover, STANJAN makes no provision for their presence in solid chemical compounds that could be found in the product mixture. The ash content of the feed is also neglected. In general, STANJAN predicts that solid C, and the gases CO_2, H_2O and CH_4 should be the only significant products present in equilibrium, and that the distribution of these products is not strongly dependent upon either the assumed pyrolysis temperature or the assumed pressure. The predicted thermochemical equilibrium values for the fixed-carbon yields are displayed together with the experimental values in Table 2. The measured values of the fixed-carbon yields for kukui nut shell, bamboo, and *Leucaena* effectively equal the theoretical yields within the margin of error of the data, and the yield from garlic wastes exceeds 90% of the theoretical yield.

CONCLUSIONS

The practical realization of fixed carbon yields that equal the value predicted by thermochemical equilibrium calculations suggests that further significant increases are probably not possible. In light of their high yields and reactivity, carbons derived from biomass are likely to find new markets (e.g. as reductants for metal ores). More attention should be given to biomass species (like those studied in this work) that are prone to the formation of

carbon by pyrolytic methods.

Table 1. Elemental analyses of feedstocks

	C (wt%)	H (wt%)	O (wt%)	N (wt%)	S (wt%)	Ash (wt%)
Bamboo	47.65	5.77	44.23	0.27	0.11	3.91
Garlic Waste	37.85	4.97	43.12	0.49	0.22	17.07
Kukui Nut Shell	55.76	5.60	37.99	0.34	0.03	1.45
Leucaena Wood	45.95	6.06	41.23	2.42	0.27	5.11

Table 2. Charcoal and fixed-carbon yields realized at 1.0 MPa

Feed	Proximate Analyses[1]			Average Charcoal Yield[1] (wt%)	Average Fixed C Yield[2] (wt%)	Theoretical Fixed C Yield (wt%)
	VM (wt%)	Fix-C (wt%)	Ash (wt%)			
Bamboo	27.0	67.1	5.9	45.9	32.1	33.1
Garlic Waste	27.3	49.2	23.5	42.9	25.5	27.6
Kukui Nut Shell	26.9	69.6	3.5	58.6	41.4	42.0
Leucaena Wood	27.0	69.4	3.6	44.2	32.3	32.9

[1]% of dried charcoal

[2]% of dried feed material. Fixed-C Yield = Charcoal yield * (100 - %Volatile Matter - %Char Ash) / (100 - %Feed Ash)

REFERENCES

1. W. Emrich, *Handbook of Charcoal Making* (1985), Reidel, Dordrecht.
2. F.a.A.O. FAO, *Yearbook of Forest Products 1995* (1997), FAO Forestry Series No. 30, Rome.
3. F. Rosilo-Calle, M.A.A. De Rezende, P. Furtado, D.O. Hall, *The Charcoal Dilemma* (1996), Intermediate Technologies Publications, London.
4. Charcoal: Production, Marketing, and Use (1961), USDA Forest Service Report #2213.
5. K.R. Smith, *Energy for Sustainable Development* (1995), **1**, 23-29.
6. M.J. Antal, *et al*., *Energy Fuels* (1996), **10**, 652-658.
7. W.S.L. Mok, M.J. Antal, *Thermochimica Acta* (1983), **68**, 165-186
8. W.S.L. Mok, M.J. Antal, P. Szabo, G. Varhegyi, B. Zelei, *Industrial and Engineering Chemistry Research* (1992), **31**, 1162-1166.
9. W.C. Reynolds, STANJAN *Thermochemical Equilibrium Software* (1987), Stanford University, Stanford, CA, ed. 3.91.

4th Annual Green Chemistry &
Engineering Conference

Sustainable Technologies:
From Research to Industrial Implementation

June 27 - 29, 2000

PROCESS DESIGN II

TOWARDS A GREEN CHEMISTRY AND ENGINEERING SOLUTION FOR THE U.S. ENERGY INDUSTRY: REDUCING EMISSIONS AND WASTE STREAMS

M. Mercedes Maroto-Valer, PhD, John M. Andrésen, PhD, and Harold H. Schobert, PhD
The Pennsylvania State University, The Energy Institute, 405 Academic Activities Building, University Park, Pennsylvania, PA 16802-2303
Christian A. Andrésen
Norwegian University of Science and Technology, N-7491 Trondheim, Norway

ABSTRACT
The U.S. electric power utility industry faces environmental challenges due to the emissions of nitrogen oxides (NO_x) by coal combustion furnaces and the associated increase in byproducts waste streams. This research program focuses on the development of a green chemistry and engineering solution for the U.S. energy industry, that can guarantee a sustainable source of energy for the 21st century by simultaneously reducing emissions and byproducts waste streams. This solution combines the installation of low NO_x burners, that reduce efficiently NO_x emissions, coupled with strategies that manage the associated increase in byproducts streams, mainly fly ash and unburned carbon.

INTRODUCTION
The U.S. electric power industry relies heavily on the use of coal as the main energy source, where coal-fired units generate annually over 55% of the total electricity produced in the U.S. However, the U.S. power utility industry faces environmental challenges due to the emissions of pollutants such as NO_x[1]. The implementation of Title IV of the 1990 Clean Air Act Amendment regarding NO_x emissions is mainly being addressed in coal combustion furnaces by installing low-NO_x burners. Phase II, that began last January, will achieve an additional reduction of ~ 900,000 tons of NO_x annually. Although low-NO_x burner technologies efficiently decrease NO_x emissions by lowering the temperature of combustion, they also reduce the combustion efficiency with a corresponding increase in the concentration of uncombusted coal in the fly ash, generally referred to as unburned carbon. Presently, the fate of these products is mainly disposal, due to the lack of efficient routes for their utilization. Accordingly, this research program has investigated a green chemistry and engineering solution for the U.S. energy industry, that can guarantee a sustainable source of energy for the 21st century by simultaneously reducing emissions and promoting the commercial utilization of energy related byproducts waste streams. This solution combines the installation of low-NO_x burners, that reduce efficiently NO_x emissions, coupled with strategies that manage the associated increase in byproducts streams, mainly fly ash and unburned carbon. These strategies advocate for the recovery and utilization of energy byproducts by developing two novel and cost-effective routes for the commercial utilization of unburned carbon present in fly ash as a precursor for premium carbon materials. In the first route, we have investigated the utilization of unburned carbon for the production of activated carbons. In the second route, we have developed protocols to use the unburned as a replacement for petroleum coke in the manufacture of carbon bodies. These carbon bodies, after baking, could be used for numerous applications, including brushes for electrical machines, artificial heart valves, anodes for aluminum smelting and electrodes for steel arc furnaces amongst others.

EXPERIMENTAL
Procurement of fly ash samples
The fly ashes were collected from Shawville power station Unit #4 (Bradford Township, PA) with a net capacity of 180 MW and operated by Reliant Energy. This unit has been retrofitted with low-NO_x burners. Samples were collected all the way from the economizer through the hoppers to the stack, amounting to a total of 16 samples. The carbon contents, also called loss-on-ignition or LOI, of the fly ashes were determined according to the ASTM C311 procedure. The fly ash with the highest carbon concentration was chosen as feedstock for the production of the carbon products.

Activation of fly ash carbons
The activation of the samples was carried out in an activation furnace, that consists of a stainless steel tube reactor inside a vertical tube furnace, as previously described[2]. The porosity of the samples was characterized conducting N_2 adsorption isotherms at 77K using a Quantachrome adsorption apparatus.

Manufacture of carbon bodies
The fly ashes with the highest carbon levels (40-50 wt%) were chosen as feedstocks for the beneficiaction step conducted prior to the manufacture of carbon pellets. The beneficiaction protocol reduced the inorganic content

to ~4 wt%. The carbon pellets were produced from mixtures of this concentrated fly ash carbon (CFAC), a petroleum coke (PC) and a coal tar binder pitch (CTBP). The mixtures were heated to ~130ºC and pressed into pellets. The absolute densities were measured by using a Quantachrome MVP-1 Multi Pycnometer with helium as density medium.

RESULTS AND DISCUSSION

Carbon variations between hoppers

Fly ash samples were collected from each of the hoppers and Figure I shows the configuration and gas flow for the hoppers, and the carbon values of the corresponding fly ashes. The hot-side hoppers 13-16 presented the lowest carbon contents (12-17%), while the cool-side hoppers 21-22 had the highest carbon contents (37 and 46%, respectively). This "hot-side" and "cool-side" terminology has been adopted from former studies and it is based on characteristics of the respective ashes, where fly ashes from hot-side collectors present characteristics associated with higher temperatures (lower carbon content and larger fly ash sizes) compared to those of their cool-side counterparts[3]. The cool-side bins present the highest LOI values (40-50%) and therefore they are suitable hoppers for the collection of high carbon content ashes as feed-stocks for carbon materials precursors.

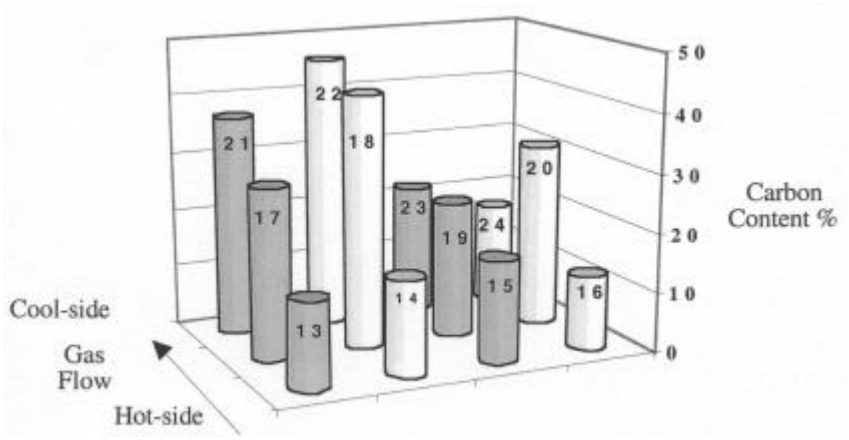

Figure 1. Variation in carbon contents of the fly ashes collected from the different hoppers. The numbers on the bars indicate the corresponding hopper number.

Activation of fly ash carbons

The N_2-77K adsorption isotherms for the three fly ash carbon samples prior to activation, designated as FAC-A, FAC-B and FAC-C are typical for nonporous or macroporous adsorbents, with surface areas between 30-40 m^2/g. Pore size distribution studies showed that the pore volume is mainly due to mesopores, that account for over 60% of the total pore volume[2]. The solid yields of the three FAC samples activated for 60 minutes are listed in Table 1. FAC-A presents higher solid yields than FAC-B (73% vs. 55%), due to their larger particle size (200 µm vs. 45 µm). The N_2-77K adsorption isotherms for the three steam activated FAC samples were Type 1, that are typical for microporous materials. The activation process promotes the development of micropores, with the micropore volume now accounting for over 60% of the total. Pore size distribution studies and CO_2 porosity measurements are in progress.

Table 1. Solid yield, BET surface area and pore volume for the activated fly ash carbons.[a]

Sample	Activation time / min	Solid yield / % weight	BET S.A. / m^2/g	V_{total} / cc/g
FAC-A-Act	60	73	332	0.15
FAC-B-Act	60	55	443	0.14
FAC-C-Act	60	79	110	0.04

[a] The solid yields and surface areas are expressed in ash free basis.

Properties of carbon pellets prepared with fly ash carbons

This study concentrated on the production of carbon pellets, where the fine fraction of petroleum coke was replaced by unburned carbon. Table 2 lists the absolute densities for the carbon pellets produced with the concentrate of fly ash carbon (CFAC), the conventional calcined petroleum coke (PC) and coal tar binder pitch (CTBP). As expected, the density of the carbon pellet A, is slightly lower than that of the petroleum coke itself (1.76 g cm^{-3} vs. 1.89 g cm^{-3}), due to the lower density of the CTBP (1.25 g cm^{-3}). For conventional carbon pellets,

the CTBP seems to mostly be filling the vacant voids between the PC particles. For pellet B, where all the fine fraction of petroleum coke has been replaced by concentrate unburned carbon, there was a difference between the observed and calculated densities (1.76 g cm^{-3} vs. 1.65 g cm^{-3}). This indicates that there is a synergistic filling effect between the unburned carbon and the coal tar binder pitch, that is reflected in a densification of the carbon pellets produced[3]. These results are very encouraging for further baking of the pellets into artifacts, that is now underway in our laboratory.

Table 2. Absolute densities of the carbon pellets prepared.

Pellet	Composition	Density / g cm^{-3}	
A	20% CTBP, 40% fine PC 40% intermediate PC	1.76[a]	1.76[b]
B	20% CTBP, 40% fine CFAC 40% intermediate PC	1.76[a]	1.65[b]

[a] Density measured by helium pycnometry. [b] Calculated density.

CONCLUSIONS

The present work has focused on the development of a green chemistry and engineering solution for the U.S. energy industry, that can guarantee a sustainable source of energy for the next century by simultaneously reducing emissions and byproducts waste streams. The detailed study of a series of fly ash hoppers has revealed that cool-side bins present the highest LOI values (50%) and therefore they could be suitable hoppers for the collection of high carbon content ashes as precursors for carbon materials. This work has demonstrated the ability of unburned carbon from coal combustion waste to generate activated carbons by 60 minutes steam activation. For the case of the carbon artifacts, the density of the carbon pellets prepared with unburned carbon is comparable to that using only petroleum coke, probably due to a strong interaction between the unburned carbon and the coal tar binder pitch.

ACKNOWLEDGMENTS

The authors wish to thank the Consortium for Premium Carbon Products from Coal (CPCPC) at The Pennsylvania State University and Reliant for financial support.

LITERATURE CITED

1. Maroto-Valer, M.M., Taulbee, D.N. and Hower, J., 1999, *Energy & Fuels*, **13**, 947.
2. Maroto-Valer, M.M., Taulbee, D.N. and Schobert, H.H., 1999, Prepr. Am. Chem. Soc. Fuel Division, 44, 101.
3. J.M. Andrésen, M.M. Maroto-Valer, C.A. Andrésen and J. Battista, 1999 International Ash Utilization Symposium, 534.

GAS LIQUID MASS TRANSFER IN HIGH PRESSURE AGITATED BUBBLE REACTOR

Maalej Samah, Ph.D. Student; Benadda Belkacem, Professor assistant
Laboratoire d'Analyse Environnementale des Procédés et des Systèmes Industriels LAEPSI INSA de Lyon,
20 av. A. Einstein 69621 Villeurbanne, France

ABSTRACT

The present study deals with the pressure effects on the mass transfer within an agitated bubble reactor operated at pressures between 10^5 and $100x10^5$ Pa. Two parameters characterizing the mass transfer are identified and investigated in respect to pressure: the gas-liquid interfacial area and the volumetric liquid side mass transfer coefficient. The chemical absorption method is used: CO_2/Na_2CO_3-$NaHCO_3$ with NaClO as catalyst. For a given superficial gas velocity, the interfacial area as well as the volumetric liquid mass transfer coefficient decrease with increasing operating pressure. However, for a given pressure, a and k_La increase with increasing superficial gas velocities. The mass transfer coefficient k_L is independent of pressure.

INTRODUCTION

Many processes of gas absorption with chemical reaction are set up at high pressures, result of technical and economical requirements. That is for example, processes of hydrocracking and hydrorefining of heavy oils, processes for gas sweetening and oxidation of liquid effluents. It exists therefore a growing need to know the phenomena involved in physical and chemical absorption under high pressures, in order to provide new chemical systems suitable for the determination of mass transfer parameters in industrial gas absorption units operating under high pressure.

In order to improve the gas-liquid contacting operation, the gas-liquid mass transfer, has to be increased. This can be achieved by optimizing the governing parameters such as the mass transfer coefficient and the interfacial area. The liquid-gas mass transfer improvement depends on: (i) the reactor type and geometry, (ii) the mass transfer parameters which can be varied with practical limits by changing the flow rates, thus, fixing the degree of turbulence, (iii) the increase in the concentration of the component being absorbed, either by increasing the partial pressure of the component or the total pressure in the reactor.

Almost all the studies[1], which have been carried out on liquid and gas mass transfer coefficients at high pressures in a bubble column or a mechanically agitated reactor, indicate that the operating pressure has no influence on the liquid-phase mass transfer coefficient, k_L. This is due to the fact that there is no influence of pressure on the liquid-phase properties. Indeed, the liquid properties such as viscosity, the density, and the diffusivity of the transferred component in the liquid phase are only affected to any extent at extremely high pressures. Furthermore, the changes with pressure in the flow regimes indicates the possibility of a pressure effect on the hydrodynamics in gas-liquid reactors. This will affect the characteristic mass transfer parameters such as film thickness and surface renewable time. Changes with pressure in the gas hold up and bubble diameters may also influence the mass transfer coefficients. In addition, as reported by some authors, a pressure influence on the surface tension may also affect the hydrodynamics of the phases. So, it can be concluded that k_L is independent of pressure if the system hydrodynamics is not affected by the pressure.

We report on mass transfer study in an agitated bubble reactor equipped with a porous plate as gas distributor. Two parameters characterizing the mass transfer are identified and investigated in respect to pressure: the gas-liquid interfacial area and volumetric liquid side mass transfer coefficient. These parameters are determined by means of the chemical reaction between carbon dioxide and "carbonate bicarbonate" aqueous solution (CO_2/Na_2CO_3-$NaHCO_3$) with NaClO as catalyst, in presence of an inert gas (N_2) at ambient temperature.

EXPERIMENTAL MASS TRANSFER STUDY

The objectives of this section are to determine experimentally the mass transfer parameters that are the interfacial area and the volumetric liquid side mass transfer coefficient for different operating conditions such as gas flow rates, velocities and pressures. A previous hydrodynamic study has demonstrated that the reactor behaves like a perfect mixed one for the conditions chosen in our experiments.

Experimental Set-up and methodology

The reactor is made of a thick stainless steel 316 material so that pressures ranging from 10^5 to $100x10^5$ Pa can be reached. The reactor height is 25 cm and has an inner diameter of about 4.6 cm. The reactor is equipped with two circular glass windows of 2 cm diameter through which flow patterns as well as the type of dispersion can be observed. The reactor works at a constant temperature of 273K (Figure 1). The gas phase is a mixture of 90 vol. % nitrogen and 10 vol. % CO_2 and it is injected at the top of the reactor through a porous perforated plate gas distributor. The reactor pressure is controlled by means of a backpressure regulator located at the reactor outlet; it is measured by a manometer. The gas flow rates are measured by a rotameter and controlled by a precise needle valve so that gas velocity up to 0.03 m/s can be fixed.

The reactor is filled with a carbonate-bicarbonate (Na_2CO_3-$NaHCO_3$) solution which is pumped in a loop circuit. NaClO is added to the solution and used as catalyst. A six ways valve is used in order to sample a known solution volume which is rinsed with pumped water deviated through the valve. This operation does not modify the pH solution. Small aliquots of the reacting solutions were sampled at different times from the feedback loop. The molar concentration of CO_2 is then determined by titration with H_2SO_4. Table 1 lists the various characteristics associated with the operating conditions used in this study.

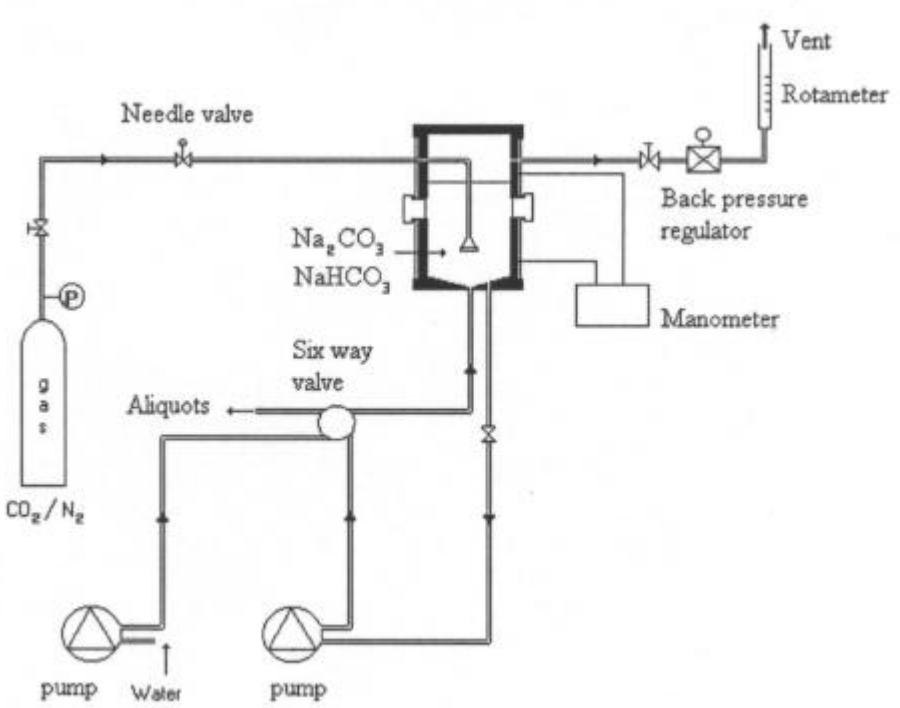

Figure 1. Experimental set-up

Table 1. Operating conditions

Operating pressure		10^5 to $50x10^5$ Pa
Temperature solution		293 K
pH of the solution	CO_2 / Na_2CO_3-$NaHCO_3$	9-10
Molar concentration of catalyst	NaClO	0.06-0.4 M
Molar concentration of reactant solution	Na_2CO_3 - $NaHCO_3$	0.4 M
Partial pressure of solute	CO_2	10%± 0.5 %
Volume of reactant		0.21
Superficial liquid velocity		$0.08x10^{-3}$ m.s^{-1}
Superficial gas velocity		0.005 - 0.03 m.s^{-1}

Kinetic Model

The following chemical system is employed: CO_2 / Na_2CO_3 - $NaHCO_3$ with NaClO as catalyst[2]. The corresponding reaction is:

$$CO_2 + CO_3^{2-} + H_2O \rightarrow 2HCO_3^-$$

Under intermediate regime (0.3<Ha<3) conditions, when the gas-side resistance may be neglected, the specific absorption flow per unit volume of the liquid phase (Φ) is given by:

$$\Phi^2 = a^2 C_A^{*2} + D_A k_1 [ClO^-] + k_L^2 a^2 C_A^{*2} \qquad (1)$$

The specific absorption flow per unit volume of the liquid phase (Φ) is the slope of the plot of $[CO_2] = f(t)$. If Φ^2 is plotted versus [CLO-], the resulting adjusted Danckwerts line allows determining the interfacial area, a, and the volumetric mass transfer coefficient k_La.

The kinetic data and physical properties of the system CO_2 / Na_2CO_3 - $NaHCO_3$ under atmospheric pressure are identical to those used in reference[3]. The diffusivity of CO_2, D_A, in carbonate and bicarbonate solutions and the

kinetic constant k_1 are assumed to be independent of pressure. Semi-empirical method have been proposed to predict the diffusion coefficient, the most used one is that of Wilke and Chang[4]

$$D_A\mu / T = D_{Ao}\mu_o / T \qquad (2)$$

where μ and μ_o are the solution and the water viscosity, respectively.

The solubility of CO_2, C^*_A, is corrected in order to take into account the pressure, neglecting the solubility of N_2 in water which is about 50 times smaller then the solubility of CO_2. The pressure dependence of the solubility of CO_2 in water can be expressed by the following relationship of Krichevsky Kasarnovsky (1935)[5]

$$\ln \frac{f_A}{X_A} = \ln H + \frac{v_\infty (P - P_v)}{RT} \qquad (3)$$

where f is the fugacity and X_A the molar fraction of CO_2 in the liquid phase. The saturated pressure of water P_v at T=293 K is equal to 0.0041 MPa. The constant v_∞, is the apparent molar volume of the gas in the liquid phase, and it can be taken to be independent of pressure. For our calculation the value of v_∞=3.3 10^{-5} m^3/mol has been taken[6]. The method used to determine the Henry's law constant is that of Van Krevelen and Hoftijzer[7], it is applied to electrolyte solutions and it is given by

$$\log(H / H_o) = \Sigma\, h_i I_i \qquad (4)$$

where the ionic I_i of salt i and the contribution h_i of different species are considered to be independent of the pressure for a given temperature. Henry's law constant H_o of CO_2 in water is obtained at atmospheric pressure[3].

Results and discussion

Figures 2 and 3 show the variations of a and k_La as a function of gas velocity, u_g, for three values of the total pressure (P = 10^5, 10x10^5 and 25x10^5 Pa). For a given pressure, it is shown that the interfacial area a and the volumetric mass transfer coefficient k_La increase with increasing superficial gas velocity. However, for a given superficial gas velocity, it is found that both a and k_La decrease with increasing pressure. Increasing the superficial gas velocities for a given pressure causes high turbulence within the liquid phase. This leads to a mass transfer enhancement that is shown by the interfacial area increase. However, while maintaining the gas velocity to a given value, the bubbles diameters and their volumes decrease with increasing pressure; this causes an interfacial area decrease with increasing operating pressures.

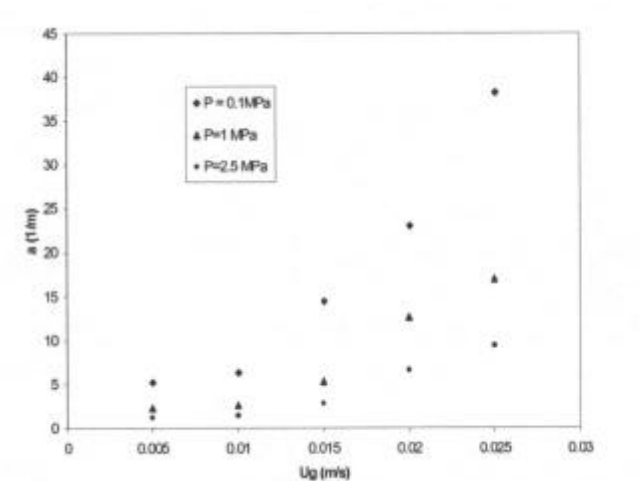

Figure 2. Interfacial area as a function of the superficial gas velocity and total pressure.

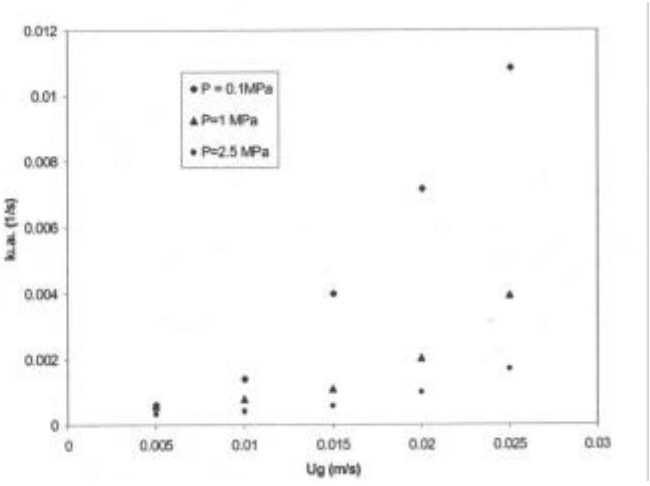

Figure 3. k_La as a function of the superficial gas velocity and pressure

Interfacial area and volumetric mass transfer coefficient variations are plotted as a function of operating pressures in logarithmic scale in Figures 4 and 5, for u_g = 0.01 m/s. As it is shown in Figure 4, the interfacial area decreases with increasing pressures below 50x10^5 Pa. As it is noticed in Figure 5, k_La decreases with increasing pressures. The operating pressure has no influence on the mass transfer coefficient k_L. This seems rather

obvious because there is no influence of pressure on the liquid phase properties.

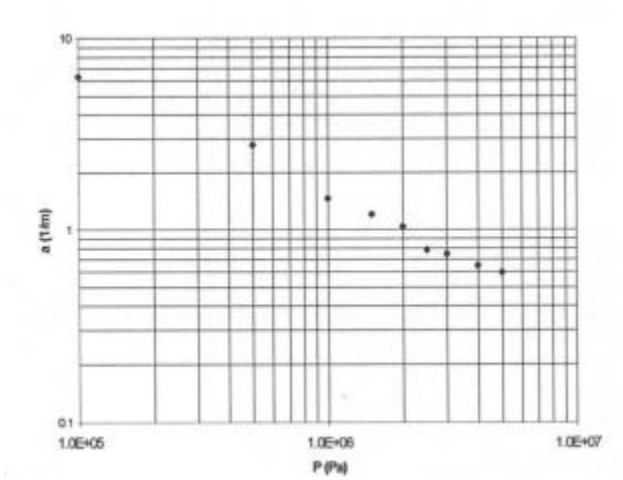

Figure 4. Variation of interfacial area with total pressure for u_g=0.01 m/s.

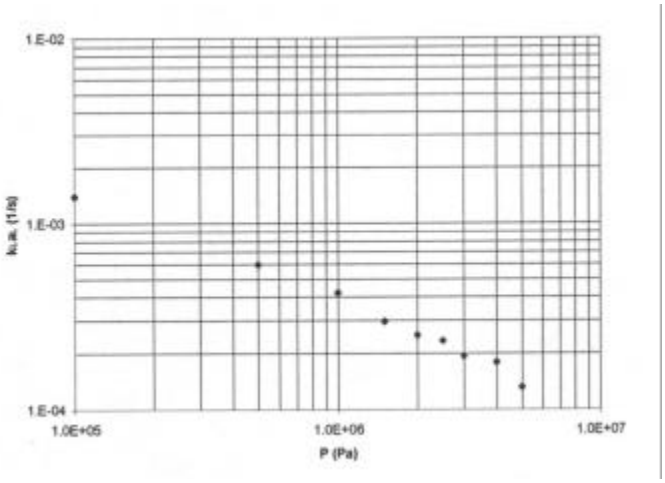

Figure 5. Variation of k_La with total pressure for u_g=0.01 m/s.

CONCLUSION

This study deals with the effects of pressure on gas-liquid mass transfer within an agitated bubble reactor. This work has succeeded in determining the interfacial area a and the liquidside volumetric mass transfer coefficient k_La, implemented in gas-liquid absorption with chemical reaction in a laboratory agitated reactor. The effect of pressure (from 10^5 to $50x10^5$ Pa) is specially studied, in addition to the influence of superficial gas velocity. Results show that a and k_La increase with superficial gas velocity whereas they decrease with increasing total pressure. k_L is independent of pressure.

This paper contributes to a knowledge of absorbers operations under pressure. As far as the influence of the chemical system is concerned, this appears important in any extrapolation of the parameters values determined for one chemical system to another.

NOMENCLATURE

a	Interfacial area [$m^2 \cdot m^{-3}$]	k_1	Kinetic constant [s
A	Gas Solute CO_2	k_La	Volumetric mass transfer coefficient [s^{-1}]
C*	Molar concentration at equilibrium [$mol \cdot m^{-3}$]	k_L	Liquid phase mass transfer coefficient [$m \cdot s^{-1}$]
D	Diffusivity of gas into the solution [$m_2 \cdot s^{-1}$]	P	Total pressure [Pa]
f	Fugacity [Pa]	P_v	Saturated vapor pressure [Pa]
Ha	Hatta number	R	Gas constant [$Pa.m^3 \cdot mol^{-1} \cdot K^{-1}$]
H	Henry law constant of CO_2 in Na_2CO_3 $NaHCO_3$ solution [$Pa.m^3 \cdot mol^{-1}$]	T	Temperature [K]
H_o	Henry law constant of CO_2 in pure water [$Pa.m^3 \cdot mol^{-1}$]	u_g	Superficial gas velocity [$m \cdot s^{-1}$]
h_i	Salt coefficient [$m^3 \cdot mol^{-1}$]	V_∞	The molar volume of the gas in the liquid phase [$m^3 \cdot mol^{-1}$]
I_i	Ionic strength [$mol \cdot m^{-3}$]	X	Liquid phase molar fraction

Greek symbols

ϕ	Specific absorption flow per unit volume of liquid phase [$mol \cdot m^{-3} \cdot s^{-1}$]
μ	Liquid viscosity [Pa.s]

REFERENCES

1. Oyevaar M.H. and Westerterp K.R. Mass transfer phenomena and hydrodynamics in agitated gas-liquid reactors and bubble columns at elevated Pressure : State of the art. *Chem. Eng. and Proc.*, **25** (1989) pp. 85-98.

2. Benadda B., Prost M., Ismaili S. and Otterbein M., Validation of gas lift bubble column as a simulation device for reactor by study of CO_2 absorption in Na_2-CO_3/$NaHCO_3$ solutions. *Chem. Eng. and Proc*., **33** (1994) P. 55.
3. Badssi A., Bugarel R., Blanc C. and Laurent A., Influence of pressure on the gas-liquid interfacial area and the gas side mass transfer coefficient of a laboratory column equipped with cross-flow sieve trays. *Chem. Eng. and Proc*., **23** (1988) pp. 89-97.
4. Wilke C.R. and Chang G.P., Correlation of diffusion coefficients in dilute solution, *AIChE J*, **1** (1955) 264-270.
5. Reid R.C., Sherwood T.K., Prausnitz J.M. The properties of gases and liquids. McGraw-Hill (1987), 741pp.
6. Caraventes A.M. Equilibre thermodynamique, transfert de matière et cinétique chimique dans un réacteur agité gaz-liquide sous pression, PhD Thesis, INPL Lorraine, 1987.
7. Van Krevelen D.W. and Hoftijzer P.J., Numéro spécial du XXIème Congr. Int. de chimie industrielle, Bruxelles, September 1948, p. 168.

ACTIVITIES ON GREEN AND SUSTAINABLE CHEMISTRY IN JAPAN

Masao Kitajima, Ph.D.
Technological Strategy and Planning Division, Japan Chemical Innovation Institute

Japan Chemical Innovation Institute

Japan Chemical Innovation Institute (JCII) was established in March 1998. So far, more than 120 Japanese companies and 9 academic and industrial societies joined JCII to support its activities. Its objective is to contribute toward the sustainable development of society and competitiveness of the Japanese industry with innovative chemical science and technology (Chemical S&T). The basic scope of JCII is that people involved in the chemical sectors of industries, academia and national institutions collaborate and share common understandings on the subjects and directions for the development of Chemical S&T in Japan.

JCII reported "Basic Concept for Advancement of Innovation in Chemical Science and Technology" in 1998, "Strategy for Chemical Science & Technology: Year 2025" in 1999, and “New Chemical ST and Road Maps" in 2000. In these reports, Sustainable Society is the keyword of all subjects.

Green & Sustainable Chemistry Network

A task force consisting of representatives from 11 Japanese chemical organizations was formed in September 1998 lead by JCII. It worked more than a year to establish a new organization dedicated to the promotion of Green and Sustainable Chemistry in Japan. Then, a workshop was held in November and the participants agreed on the concept, organization structure and framework of the activity.

Concept of Green & Sustainable Chemistry

Those who work in the area of chemistry and chemical technology shall recognize their responsibility to the society as members thereof, place the fundamental priority of their activity on Environmental and Human Health, and Safety in pursuit of the ultimate goal, and contribute to realization of a Sustainable Society, through the Innovation of Chemical Technology.

Definition of Green & Sustainable Chemistry

Green & Sustainable Chemistry is defined as "Chemical Technologies for realizing Environmental and Human Health and Safety and for the minimization of energy and resources, etc, through innovations and improvements in product and process design, selection of feedstocks, formulations and applications, and resource recycling.” The whole life cycle of chemical products should be taken into account for every step of production.

Key-factors for promoting Green & Sustainable Chemistry

1) Technologies for pollution prevention based on holistic environment impact assessment.

2) Innovative technologies with wide and practical applicability.

3) Global and international contribution

4) Conditions surrounding Japanese society, such as the environment, resources and demographic changes.

5) Planning and actions with long-term strategies, and dynamic responses to changing social and global situations.

Guidelines for practicing Green & Sustainable Chemistry

1) Pursuit of highly effective and economical product and process design and technologies in consideration of holistic life cycle assessments and environmental and human health and safety.

2) Development of products and technologies which contribute to the minimization of by-products, missive chemicals, residues and wastes, the recycling of materials back to resources, and the cleaning and mediation of the environment.

3) Development of combined multiple technological and operational systems for reduction of energy and resource consumption and cyclic utilization of materials and chemicals.

4) Reduction of dependency on non-renewable feedstocks by promoting the utilization of renewable feedstocks and by renewing technologies.

5) Promotion of collaboration and joint work among industry, academia and national institutions, other industries and various disciplines, both domestically and internationally.

6) Promotion of information exchanges dissemination and communication to enhance the reliability of chemistry among society.

7) Promotion of education and enlightening in regards to Green & Sustainable Chemistry to achieve its ultimate goal, i.e. the realization of a sustainable society.

National Projects supporting Green and Sustainable Chemistry

There have been many national projects whose objectives are to improve behaviors in environment, e.g. products and processes in relation to energy and material consumption, emission of hazardous materials, pollution safety and others.

Simple Chemistry Program is one good example. It started in 1995 as a part of New Sunshine Project with an annual budget of about 700 million yen. It supports R&D aiming at simplification of production processes to minimize energy and resource consumption.

Overview of the New Sunshine Project: Research Area

Renewable Energy
  Photo-voltaic Energy, Geothermal Energy or Wind Energy
Advanced Utilization of Fossil Fuels
  Coal Energy, Fuel Cell Power Generation, Ceramic Gas Turbine
Energy Transportation and Storage
  Superconducting Technology for Electric Power Apparatus
  Dispersed Type Battery Power Storage Technology
Environmental Technology
  Simple Chemistry Innovative Technology for the Earth
Systematization Technology
  Eco-Energy City, World Energy Network

Green Process R&D under the New Sunshine Project: Simple Chemistry

Concept

Innovative process R&D project for future chemical industry, by simplifying the production process with maximizing the energy and resources saving and minimizing emissions.

Specific programs

Catalytic Conversion of Naphtha to Lower Olefin
Novel Catalysts and Chemical Reaction Processes for the Selective Oxidation of Light Alkanes
Simple Synthetic Process using Solidified Catalyst

Other Examples of Green Chemistry R&D under the New Sunshine Project

Technologies for Recovery and Fixation of Environmentally Impacting Substances
- Biological CO_2 Fixation and Utilization
- Chemical CO_2 Fixation and Utilization

Environmentally Friendly Production Technologies
- High Performance Bio-reactor for the Production of Bio-chemicals
- Environmentally Friendly Catalysts

Other
- Biodegradable Plastics

Advanced Utilization Technology of Supercritical Fluid

Examples of Research Programs

Combined 'Reaction and Membrane Separation' Process
Development of membrane reactor combining high performance dehydrogenation oxidation catalyst with highly hydrogen-permeable membrane.

DIRECT CONVERSION OF METHANE TO C_2 HYDROCARBONS BY ELECTRIC FIELD CATALYSIS ENHANCED*

Baowei Wang, Ph. D student and Genhui Xu**, professor
School of Chemical Engineering, State Key Laboratory of C_1 Chemical Technology,
Tianjin University, P.R. China 300072
Dr. Sun Hongwei
Research Institute of Petroleum Processing, Beijing, P.R. China 100083

Abstract

Methane is one of most important greenhouse gases. A clean, low-power catalytic conversion of methane to C_2 hydrocarbons (ethane, ethylene etc.) through AC electric field enhanced plasma catalysis was studied under low temperatures that range from 50 ºC to 100 ºC, atmospheric pressure. The influence of different reaction conditions: voltage, flux of inlet methane, N_2/CH_4 (mole ratio) and catalysts were tested. The results showed the conversion of methane is 50(mole)%~60(mole)%, and the selectivity of C_2 hydrocarbons is more than 80(mole)% under the appropriate operation parameters. The reaction results are better than conventional reaction of Oxidation Coupling of methane.

Introduction

Methane is the second most important of the anthropogenic greenhouse gases (after carbon dioxide)[1]. A large proportion of methane emissions arise from anthropogenic sources, which is opposite of the situation with carbon dioxide. For the past 200 years atmospheric methane concentrations have increased from 0.8 to 1.65ppm. This change in methane concentration had been led to an estimated increase in radiative forcing of climate of 0.47 W/m^2 compared to the increase of 1.56W/m^2 due to the change in carbon dioxide concentration over a comparable time period[2] . As a greenhouse gas, methane can contribute to global warming. Within time interval 20 years 1 kg methane is equivalent to the global warming potential generated from 35kg of carbon dioxide[3], which stimulate us to talk about how to deal with the global impact of methane emissions.

In this paper a clean low-power catalytic conversion of methane to C_2 hydrocarbons (ethane, ethylene etc.) through AC electric field enhanced plasma catalysis was studied under low temperatures that range from 50 ºC to 100 ºC, atmospheric pressure.

The influence of different voltage, flux of inlet methane, N_2/CH_4 (mole ratio) and catalysts was tested under the distinct electrode form of electrical field. The results indicated that best form of the electrode was the

unsymmetry form, such as flat with point-flat; the appropriate voltage was 38V(AC); the likely range flux of inlet methane was 60ml/min~80ml/min; the suitable ratio of N_2/CH_4 (mole ratio) was 0.5~1.0 and the yield of C_2 hydrocarbon was more than 40(mole)%. Under the appropriate operation parameters the research results was gotten, the conversion of methane is 50 (mole)%~60 (mole)%, and the selectivity of C_2 hydrocarbons is more than 80(mole)%. The results are better than conventional reaction of Oxidation Coupling of methane.

Experiment

Experimental equipment

The simple experimental equipment was shown as figure 1. Pure methane or mixture of methane and inter gas came into the quartz glass tube reactor after it passed reducing value and mass flow controller. Then methane were excited to become radicals: CH^*_3, CH^*_2, CH*, H*, C* under plasma field function. In succession all kinds of radicals interacted and reacted on the catalyst surface. After reaction the gases passed mass flow controller go to the analyzer HP 5971A Gc-Ms on line.

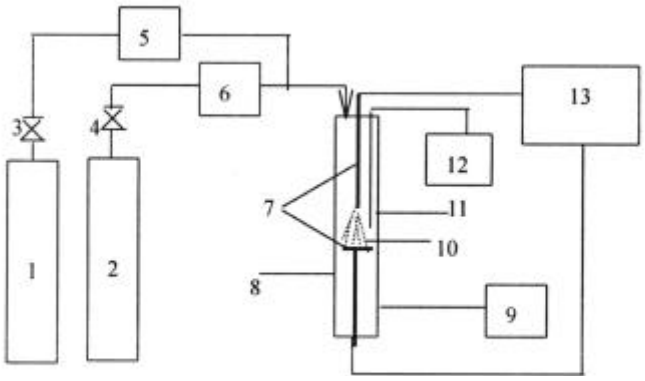

Figure 1. Simple experimental equipment
1 methane tank; 2 inter gas tank; 3, 4 reducing value; 5, 6 mass flow controller; 7 electrodes; 8 reactor; 9 Gc-Ms; 10 catalyst; 11 thermocouple; 12 temperature controller; 13 AC or DC plasma generator

Results and discussion

Effect of voltage on conversion of methane

Table 1 shows that the voltage is sensitive to the conversion of methane. If the voltage increases, the available energy of methane increases under the inlet flow of methane is constant. The amount of radicals that methane dissociates augments that lead to the conversion increases. After the conversion achieves its max 36.54%, the amount of methane dissociation radicals is too much; some radicals are incumbent on the catalyst surface and are eliminated hydrogen to carbon. The electrical energy is absorbed, the conversion of methane decreases. Therefore, the appropriate voltage is 38v under the alternate current field.

Table 1. Voltage vs. conversion of methane

Voltage(V)	34	36	38	40	42
Conversion of methane(%)	32.76	35.25	36.54	35.23	34.31

Condition: AC, temperature 24ºC, flow of methane 112.3ml/min, residence time τ=2.0 sec.

Effect of flow of methane on conversion of methane and selectivity of C_2 hydrocarbon

Fig.2 shows that that the conversion of methane increases with increasing of voltage and the selectivity of C_2 hydrocarbons decreases with increasing of the inlet flow of methane under the voltage and temperature are constant. The reason is that the residence time decreased and the available energy of methane decreased when the inlet flow of methane increases under the electrical power is constant. That leads to the radicals that was produced through methane dissociation lessen. However, methane was maybe completely eliminated hydrogen when the available energy of methane was too large if the inlet flow of methane was not too small under the voltage of electrical field was constant or the voltage was too high under the inlet flow of methane was constant. That resulted in carbon deposition. Therefore, the conversion can not too high and the appropriate inlet flow of methane is 60ml/min~80ml/min under appropriate voltage and temperature.

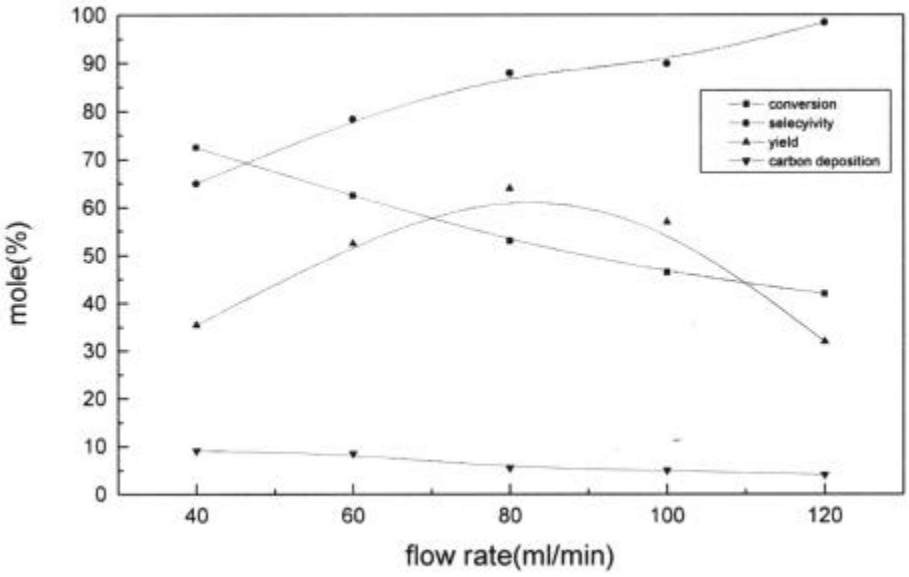

Figure 2. Flow of methane vs. selectivity of C_2 hydrocarbon, yield of C_2 hydrocarbon, and ratio of carbon deposition
Condition: AC, temperature 24ºC, voltage 38V.

Effect of inter gas

Table 2 shows that the conversion of methane and the ratio of carbon deposition decreases with increasing of the ratio of N_2/CH_4 (mole ratio) under the same other reaction conditions. The reason is that the probability of nitrogen collision with radicals increases when the ratio of N_2/CH_4 (mole ratio) increases, which causes the amount of deexcited radicals increases. The chain reaction is availably controlled because the amount of dissociative methane and the life span of radicals decreased. The conversion of methane decreases after nitrogen is added. However, it can effectively prevent carbon deposition. The ionization energy of nitrogen (1503.2kJ/mole) is more than that of methane, its radicals and C_2 hydrocarbon. Therefore, the nitrogen is not dissociated and the nitride can be produced under the supplied electrical power. If the ratio of N_2/CH_4 (mole ratio) is too small or no nitrogen , the carbon deposition occurs easily. Therefore, the appropriated ratio of N_2/CH_4 (mole ratio) is between 0.5~1.0.

Table 2. N_2/CH_4 (mole ratio) vs. conversion of methane (without catalyst)

N_2/CH_4 (mole ratio)	0.24	0.5	1.0	1.5	2.0
Conversion of methane(%)	71.6	64.9	50.6	40.0	33.3
Ratio of carbon deposition (%)	19.2	17.8	13.8	10.9	8.1

Condition: AC, voltage 38V, flow of methane 110ml/min.

Effect of catalyst

The effects of catalysts on the conversion of methane, the selectivity of C_2 hydrocarbon, the selectivity of ethylene, the yield of C_2 hydrocarbon, the yield of ethylene and the ratio of carbon deposition are shown in Table 3.

Table 3 shows that the conversion of methane is more with V_2O_5 catalyst than without catalyst and the conversion of methane is less with others than without catalyst. The selectivity of C_2 hydrocarbon is roughly more than without catalyst. The selectivity of ethylene is more with six catalysts than without catalyst. The yield of C_2 hydrocarbon is more five catalysts than without catalyst. The yield of ethylene is more five catalysts than without catalyst. The ratio of carbon deposition is less with than without catalyst. The ratio of carbon deposition is more with ten species catalyst than without catalyst. However, the deposition carbon is carbon chain fiber. This suggests that these catalyst may be the better catalysts for making carbon chain fiber. From the yield of C_2 hydrocarbon point of view, V_2O_5 are the better catalyst. From the yield of ethylene point of view, $La_{0.8}Sr_{0.2}CrO_3$ and ZnO are the better catalyst.

Summary

1. The best form of the electrode is unsymmetry form for direct conversion of methane to C_2 hydrocarbons by electric field catalysis enhanced.

Table 3. Effect of catalysts

catalyst	X%	S_2%	S_e%	Y_2%	Y_e%	CD%
without	55.08	76.31	5.79	42.02	3.18	11.59
LaBa	44.74	98.64	7.75	44.13	3.46	0.97
ZnO	43.89	85.36	8.44	37.46	3.70	6.63
$La_{0.8}Sr_{0.2}$ CrO_3	49.33	58.32	8.64	42.08	4.26	5.89
$La_{0.8}Fe_{0.3}Nb_{0.2}O_3$	51.17	87.96	7.04	45.00	3.60	4.99
$La_{0.8}Sr_{0.2}YO_{2.9}$	45.86	90.40	7.90	41.45	3.62	4.67
Ni/NaY	54.63	77.69	6.74	42.44	3.68	3.98
V_2O_5	60.90	90.87	4.91	55.33	2.99	5.70

X: the conversion of methane, S_2: the selectivity of C_2 hydrocarbon, S_e: the selectivity of ethylene, Y_2: the yield of C_2 hydrocarbon, Y_e: the yield of ethylene, CD: the ratio of carbon deposition
Condition: AC, voltage 38V, inlet flow of methane 78.55ml/min.

2. The appropriate reaction conditions was followed: voltage is 38V(AC); the likely range flux of inlet methane is 60ml/min~80ml/min (resident time: 3~4 sec), the suitable ratio of N_2/CH_4 (mole ratio) is 0.5~1.0.

3. The conversion of methane increases and the selectivity of C_2 hydrocarbons decreases with increasing of voltage under the inlet flow of methane and temperature are constant. The conversion of methane decreases and the selectivity of C_2 hydrocarbon increases with increasing of the inlet flow of methane under the voltage and temperature are constant.

4. Under the appropriate operation parameters, the conversion of methane is 50 (mole)%~60 (mole)% and the selectivity of C_2 hydrocarbons is more than 80(mole)%. The reaction results are better than conventional reaction of Oxidation Coupling of methane.

Acknowledgments
Financial support for this research was provided from National Natural Science Foundation of China (Item No-29776037).

References
1. Pierce Riemer and Paul Freund, Technologies for reducing methane emissions, Greenhouse gas control technologies, Proceeding of 4th International Conference on Greenhouse Gas Control Technologies, 30 August-2 September 1998, Interlaken, Switzerland, P755.
2. Hounghton J.T., L.G. Meiro Filho, N. Harris, A. Kattenburg and K. Maskell, eds., Climate change, 1995, The Science of Climate Change, Cambridge, UK, Cambridge University Press 996, P572.
3. O.P. Lykov and E.B. Shlikhter, Methane emission control in Russia, Greenhouse gas control technologies, Proceeding of 4th International Conference on Greenhouse Gas Control Technologies, 30 August-2 September 1998, Interlaken, Switzerland, P767.

* This was supported by the National Natural Science Foundation of China
** Author to whom correspondence should be addressed

4th Annual Green Chemistry &
Engineering Conference

Sustainable Technologies:
From Research to Industrial Implementation

June 27 - 29, 2000

BENIGN SYNTHESIS AND PROCESSING II

RECYCLING ATACTIC POLYPROPYLENE AS A MODIFIER IN POLYOLEFIN BLENDS

Holly Stretz*, Project Manager, Kenneth Pavlat, Student Chemist, Joseph H. Koo, Institute Director
Waste Minimization and Management Research Center,
Institute for Environmental and Industrial Science, Southwest Texas State University, San Marcos, TX
78666-4616
*hs05@swt.edu

ABSTRACT
Atactic polypropylene (aPP) is a tacky, low melting material that is still produced as a byproduct in the Ziegler-Natta catalyzed synthesis of crystalline isotactic polypropylene. While some aPP is used in roofing applications, a significant amount is either burned or landfilled. Blends of aPP with polystyrene and polyethylene show some interesting properties, particularly 100% enhancement of elongation, and up to 150% improvement in notched Izod toughness when compatibilized. The effect of blending on crystalline melting point and heat of fusion of HDPE was negligible.

INTRODUCTION
Atactic polypropylene (aPP) is produced as a byproduct in some commercial polypropylene reactors where certain types of Ziegler-Natta (ZN) catalysts are employed. Highly crystalline isotactic or syndiotactic polypropylene has properties suitable for structural applications, whereas atactic material is mixed with bitumen as the sticky, waxy base for roofing "tar." Atactic is solvent-washed out of the product and either landfilled or incinerated. As long as there is a market niche for the unique properties of this "washed" material, the byproduct will continue to be produced. In the complexities of the market, aPP byproduct is not always suitable for the roofing tar application, and thus we have investigated alternative market applications.

Our initial attempt to create a useful blend with polystyrene (commercial blends of isotactic polypropylene and polystyrene are common) was unsuccessful, even when compatibilized. Therefore, we are attempting the compatibilization with high density polyethylene (HDPE), a material that is currently recycled. Since aPP is a ductile material, the aim was to produce a blend with HDPE and/or recycled HDPE whose ductility would be enhanced, while maintaining most of the strength associated with the crystallinity of the raw HDPE. The initial application considered was in the toughening of HDPE geomembranes used to seal landfills. Stress crack testing is an indication of the resistance of the landfill liner to development of solvent-enhanced cracking failures in the field.

MATERIALS
All materials were used as received from material suppliers. Virgin HDPE was milk bottle grade Solvay Fortiflex A60 with a melting point of 131º C and an MI = 0. 75 g/10 min. Polyresource Recycling Inc. in Austin, TX donated the recycled HDPE with a melting point of 127º C. Eastman donated the atactic polypropylene. The EP copolymer was purchased from Acro with a melting point of 130º C.

EXPERIMENTAL METHODS
The materials were extruded twice on a Haake conical counter-rotating twin screw at 200º C and 60 rpm. A Minijector 55 injection molder, with 11 ton clamping capacity, was used for molding tensile specimens at 200º C. Tensile bars were tested with a Sintech I/D, crank grips, at 5mm/min. Izod impact testing was performed with a TMI Izod tester, a cut notch, and using a 1 lb hammer. Thermal analysis data was compiled from a Rheometrics DMTA Mark V at 1 Hz. Stress crack testing was done at Texas Research Institute (TRI) Environmental, Austin, TX.

RESULTS AND DISCUSSION
Four sets of blends were produced and tested for various mechanical properties. The initial testing was performed on compositions of recycled HDPE, i.e. ground-up milk bottles. The raw recycled HDPE contained visible bits of paper and potentially sour milk, and these contaminants as well as some potential structural degradation contributed to embrittlement of the recycled compared to virgin. Some aPP was added at 5 and 10% levels to improve ductility. Similar composition studies were then performed on virgin HDPE blends with aPP, as well as the respective recycled and virgin blends compatibilized with an ethylene-propylene block copolymer. Milk bottle grade HDPE resin was used in both cases.

For all four types of blends with aPP, the percent strain at break improved. The greatest change in extensions

were seen in virgin HDPE/aPP blends with 100% increase as 10% aPP was added, and 25% improvement for the recycled HDPE. Improvements in toughness, however, depended on the presence of the compatibilizer. Impact strength of the compatibilized blends maintained or gained toughness, with up to 150% improvement for the recycled compatibilized HDPE. The uncompatibilized blends experienced a 40% to 80% drop in toughness as measured by notched Izod. Actual values are compared in Figure 1. Stress crack testing (ASTM D5397) performed on the recycled HDPE and the recycled HDPE/5% aPP lasted 7.1 and 6.7 hours, respectively, well below the required 200 hours for a commercial landfill liner. Testing on blends more likely to meet the geomembrane requirement will be performed as funds become available.

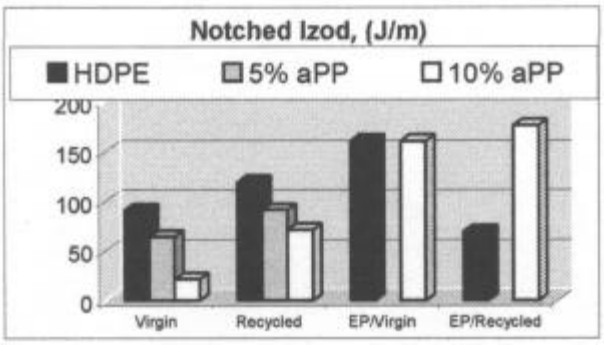

Figure 1. Notched Izod strength values for virgin versus recycled, and compatibilized versus uncompatibilized blends of HDPE and aPP.

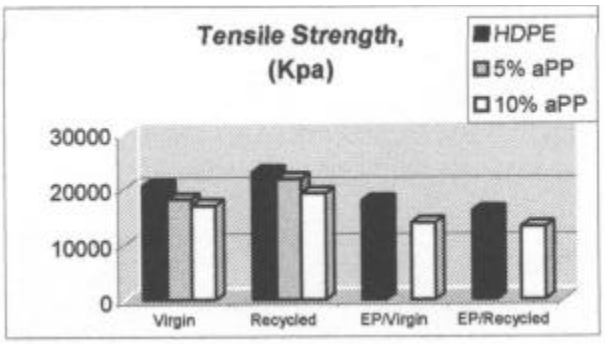

The cost in terms of tensile strength of adding this ductile aPP component is shown below in Figure 2. All blends lost approximately 20% of the raw HDPE tensile strength and 20%-40% of the unblended modulus.

Figure 2. Tensile strengths for virgin versus recycled, and compatibilized versus uncompatibilized blends of HDPE and aPP.

Blend morphology is an important consideration of some mechanical properties. We initially questioned whether the aPP was residing in the amorphous phase, whether in one or two domains (i.e. miscible or immiscible) and whether there could be some interference and intrusion into the crystalline phase of the HDPE. Crystallinity was probed using DSC thermal scans to obtain the melting point and heat of fusion. Onset melting points of the virgin materials remained in the 132 ºC range despite addition of up to 10% aPP or compatibilizer. Melting points of the recycled HDPE also maintained at 123º C despite blending plus or minus a few degrees. Heat of fusion for each set (virgin and recycled, respectively) did change, but fell by exactly the amount of the dilution factor of the particular blend. For instance, the heat of fusion of a blend with HDPE and 5% aPP fell by 5%. This only indicated dilution of the experiment, but no change in the crystals. Thus these rough measures indicated that the crystalline regions of the HDPE remained intact. The aPP must therefore reside in the amorphous phase.

The amorphous character was then probed using DMTA and observing glass transitions of the blends. The aPP itself had some crystallinity, and was not completely amorphous, so two T_g's were observed (measured by a peak in tan δ) at -115 and -8º C for the HDPE and aPP, respectively. As the percentage of aPP rose, the intensity of the tan 6 peak at -8º C rose accordingly, but no shift towards the lower temperatures was observed. Thus there were two phases (2 T_g's), but no compatibility in the absence of compatibilizer.

SUMMARY

For HDPE blends with 10% aPP added, percent strain at break and notched Izod toughness were enhanced by 100% and 150%, respectively when compatibilized. Uncompatibilized blends lost 40%-80% of their notched Izod toughness. A related measure of fracture properties is stress crack resistance, which did not improve for the recycled blend. The other blends have not yet been tested. Minimal variations in melting point and heat of fusion (some of which were due to a dilution effect) indicated that the aPP is not disrupting the HDPE crystal structure. Tensile strength and modulus, however; were lost in most blends at values 20% and 20%-40% lower, respectively. The only blend that maintained strength and modulus was the recycled compatibilized blend. The greatest potential for improvement in toughness seems to lie with the compatibilized blends. Addition of the byproduct aPP in HDPE geomembrane linings for landfills might potentially improve stress crack resistance and liner reliability.

ACKNOWLEDGMENTS
The U. S. Environmental Protection Agency (EPA) under Grant application R825505 sponsored this research. The authors would like to thank Dr. Barbara Karn, Program Officer for her valuable guidance. We also wish to thank Rick Thomas from TRI and Gene Lehane from Southwest Texas State University.

REFERENCES
1. Bartlett, D.W., Thesis, The University of Texas at Austin, (1979).
2. Collar, E.P., S. Areso, O. Laguna and J.M. Garcia-Martinez, *Journal of Polymer Materials,* **15**:355-361, (1998).
3. Collar, E.P., S. Areso, O. Laguna and J.M. Garcia-Martinez, *Journal of Polymer Materials,* **15**:363-369, (1998).
4. Da Silva, N.M. and M.B. Tavares, *Journal of Applied Polymer Science,* 60:663-667, (1996).
5. Robertson, R.E., "The Mechanical Properties of Polyolefin Blends Derived from Waste Plastics", Thesis, The University of Texas at Austin, (1972).
6. Sakurl, K., W.J. MacKnight, D.J. Lohse, D.N. Schulz, J.A. Sissano, J.S. Lin and M. Agamalyan, *Polymer,* **37.20**:4443-4453, (1996).

GREEN INTEGRATED PROCESS FOR PRODUCTION OF PROPYLENE OXIDE

Prof. Zhentao Mi, Dr. Chunyan Wang, Dr. Baoguo Wang, Dr. Wei Li, Dr. Xiangkun Meng and Dr. Xiaohui Chen
School of Chemical Engineering and Technology, Tianjin University, Tianjin, 300072, P.R. China

ABSTRACT
The process of epoxidation of propylene with H_2O_2 was widely considered as an environmentally benign process. This paper focused on the study of the process integration of epoxidation of propylene and production of H_2O_2. To make the epoxidation of propylene and the oxidation of anthrahydroquinone carry out in one reactor, a novel process was proposed by investigating the influences of the composition of the solvent mixture and other conditions on the compatibility of the two oxidation processes. It was shown that high yield and selectivity could be achieved in this process without suffering the high cost of H_2O_2.

INTRODUCTION
As a typical environmentally benign process, the epoxidation of propylene with hydrogen peroxide is of commercial interest in order to replace the traditional production method. Many researches have shown that propylene oxide can be produced with high yield and nearly complete conversion for H_2O_2 in the presence of TS-1 catalyst in a methanol based solvent system. These results, however, are penalized by the high cost of H_2O_2. Several patents have been released about the integration of the propylene epoxiation and hydrogen peroxide production to reduce the price of H_2O_2 by avoiding the purification and concentration of H_2O_2. Hydrogen peroxide is mainly manufactured by oxidation of alky-anthrahydroquinone or of isopropyl alcohol. The disadvantage of the later is the competitive oxidation of isopropanol by H_2O_2. Two integrated processes have been patented related to H_2O_2 production by anthraquinone route. In one integrated process, the solvent for epoxidation of propylene is used as the extracting agent for extracting H_2O_2 from anthraquinone working solution. In the other, both epoxidation of propylene and oxidation of anthrahydroquinone are carried out in a single reactor. In the second process, a complex solvent system must be used, which must be favorable not only to the epoxidation of propylene but also to the oxidation of alkyl-anthrahydroquinone. This paper focused on the study of the influences of the solvent system and other reaction conditions on the yield of propylene oxide, and an overall integrated process was also proposed.

EXPERIMENTAL
This study was conducted in a semi-continuous stirred-tank reactor. It consisted of a 300mL stainless steel tank, a magnetic rotator and a heating jacket. Alkyl-anthraquinone reduced solution, methanol, TS-1 catalyst and other components were fed into the reactor before reaction, while mixed gas including propylene and air flowed into the reactor continually and thus maintained the pressure as specified. Concentrations of H_2O_2 and propylene oxide were determined by iodimetry and gas chromatography analysis respectively. In comparison, a circulating flow reactor was also used. This stainless-steel reactor was composed of a riser and a downcomer with the same

diameter of 10mm. The volume of the reactor was 120 mL. It was handled continuously.

RESULTS AND DISCUSSION

In the reactor, H_2O_2 was produced by oxidation of anthrahydroquinone, then propylene was epoxidized by H_2O_2. However, several side reactions might be carried out simultaneously to deteriorate the process, which included the hydrolysis of propylene oxide to propylene glycol, open loop reaction and etherification of propylene oxide with methanol, decomposition of H_2O_2 and the deep oxidation and decomposition of anthraquinone derivatives. Many factors had influences on the selectivity and yield of the product, propylene oxide. Extensive investigation was conducted on a variety of variables to search for the optimal reaction conditions for both oxidation of anthrahydroquinone and epoxidation of propylene. Part of results is showed in Fig. 1 - Fig. 4.

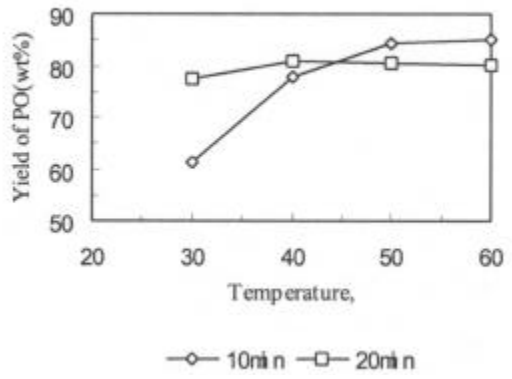

Figure 1. The influence of concentration on the coupled Reactions

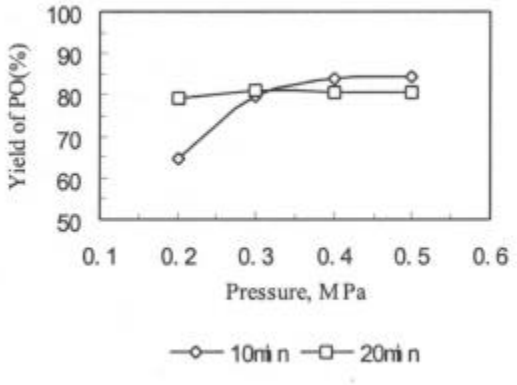

Figure 2. The influence of concentration of methanol in solvent on the process

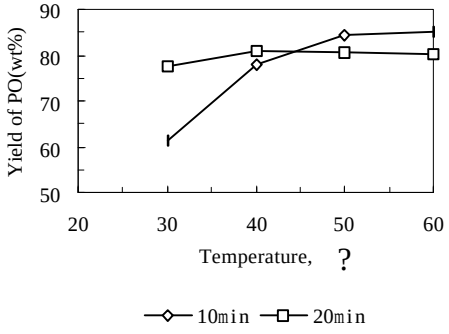

Figure 3. The influence of Temperature

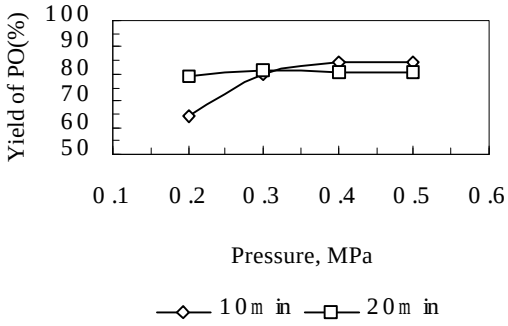

Figure 4. The influence of pressure

Composition of solvent mixture

Complex solvent was used in this reaction system. Of which, methanol functioned not only as a solvent for propylene and propylene oxide but also as a catalyst promoter. With the increase of concentration of methanol, the epoxidation of propylene was strengthened. But this could lead to the decrease of the solubility of anthrahydroquinone in solvent and then hinder the oxidation of anthrahydroquinone. It was proved that the high yield of propylene oxide could be maintained when the content of methanol is in the range of 10-20% in the tank reactor as shown in Fig. 2.

Catalyst

Anthrahyquinone could be automatically oxidized by air or oxygen without catalyst, while TS-1 molecular sieve was essential for epoxidation of propylene to achieve high selectivity and yield of propylene oxide. TS-1 had no effect on the reaction of anthrahydroquinone because of the small pore size of about 0.55nm. The proper amount of TS-1 catalyst was about 5g/L. It should be noticed, however, this catalyst was difficult to disperse in the complex solvent system in a stirred tank reactor. Experimental results indicated the reaction rate was greatly influenced by the dispersion of TS-1.

Temperature and pressure

With the high catalytic performance of TS-1 molecular sieve, the optimal reaction temperatures for the coupled oxidation reactions were very close to each other. With the increase of temperature, the yield of propylene oxide reached a maximum value and then decreased slightly. Pressure played a role in reaction by affecting the solubility of gaseous reactants, propylene and oxygen, in the liquid. Gas solubility increased with the increase of pressure, which became smaller in higher pressure range than that in lower pressure range. Considering these effects as well as the operating cost, the optimal temperature was in the range of 40-50 and the optimal pressure was about 0.4 MPa.

Composition of the feed

The feed to the reactor was composed of gaseous components and liquid mixture. Of the gaseous components, the required content of oxygen was dependent on the explosion limit of propylene, oxygen concentration in liquid and the oxidation and decomposition of anthrahydroquinone derivatives, because too much oxygen might cause deep oxidation and decomposition of anthrahydroquinone and its derivatives. The amount of propylene in gas feed affected its concentration in liquid phase and excessive propylene had to be discharged or recycled, leading to the increase of operating cost as well as environmental and safety problems. The ratio of the overall gas components to the liquid mixture in the feed had effects on the flow pattern of the three-phase flow and then affect mass transfer. Generally, the mole ratio of gaseous components to anthrahydroquinone in the feed was 8 when using air as oxidant or 4 when using oxygen as oxidant.

The improved integrated process

From the experimental research described above, it showed that mass transfer was important to carry out the two reactions in one reactor. In the production of H_2O_2 by anthraquinone route, a process intensification reactor was used to strengthen mass transfer. Here an integrated process was proposed, which uses a gas-liquid-solid three-phase circulation loop reactor and the solvent system with addition of methanol-water mixture. This process was proved to be able to improve the mass and heat transfer of the process and the yield of propylene oxide to some extent by improving the dispersion and the regeneration of TS-1 catalyst. In this improved process, the two reactions carried out in two different but close contacted liquid phases, methanol-water phase and anthraquinone working solution phase. Anthrahydroquinone was oxidized in working solution phase and produced H_2O_2, which was easier to move to the methanol-water phase, favoring the reaction of anthrahydroquinone oxidation. The epoxidation of propylene occurred in the methanol-water phase and part of the product could move to the working solution phase. In this way the two main reactions were improved and side reactions were restrained. Experimental and simulation results showed that this integrated process was an effective and economic process for the production of propylene oxide.

SUMMARY

Through the investigation of the influences of different process variables on the process performance, the operation conditions were optimized and an improved integrated process was proposed with a maximum yield of propylene oxide of 82.5% based on anthrahydroquinone. The separation and the purification of the product were simplified and the capital and operating costs of the whole process could be reduced to a large degree.

Acknowledgments

The financial support from China National Science Foundation and Sino-Petrochemical Corporation is greatly appreciated. We are grateful to Prof. Xien Xu for his special caring for this project before his death. He will be remembered forever for his contribution to the development of green chemistry and engineering development in China.

References

Clerici M G, Bellussi G. EP 526945AI, 1993
Clerici M G, Ingallina P. EP 549013AI, 1993
Meng X K. Ph.D Dissertation, Tianjin University in P. R. China, 1998.

ENVIRONMENTALLY-ATTRACTIVE SURFACE FUNCTIONALIZATION OF SELF-ASSEMBLED MESOSTRUCTURED SILICA-SURFACTANT SYSTEMS

V. Antochshuk, Graduate Student and M. Jaroniec, Professor
Department of Chemistry, Kent State University, Kent, OH 44242

ABSTRACT
A significant progress has been made in the area of self-assembled mesostructured silica-surfactant materials such as MCM-41 and MCM-48. The existing procedures for surface functionalization of these materials require template removal, which is usually done by calcination and/or extraction. Calcination leads to the complete template decomposition, whereas extraction is often not effective and requires solvents. In the proposed method a unique reactivity of self-assembled mesostructured silica-surfactant systems towards organosilanes is utilized in order to remove template and at the same time to attach desired surface functionality. This functionalization can be carried out without and with environmentally friendly solvents and does not require prior calcination and extraction. In addition, it allows for reuse of the template, thus represents an attractive way for clean preparation of mesoporous materials of tailored surface and structural properties for adsorption, catalysis and nanotechnology.

INTRODUCTION
There is a continuing interest in a clean preparation of reusable materials of tailored porous structure and desired surface functionality for heterogeneous catalysis and environmental cleanup. The discovery of ordered mesoporous silicas (OMS) and subsequent advances in their synthesis[1,2] brought a new generation of silica supports, which after suitable functionalization are very attractive from the viewpoint of green chemistry as highly selective heterogeneous catalysts for many important industrial processes[3,4] and effective adsorbents for removal of toxic ions and compounds.[5,6]

OMS are synthesized via self-assembly of suitable silica and surfactant species followed by removal of the template via extraction and/or calcination.[1,2] Further development in this area is limited to some extent by the necessity of employing the calcination and/or extraction procedures. A typical acid/alcohol extraction is not always effective for a complete removal of cationic surfactants. In contrast, the high-temperature calcination assures an effective removal of the surfactant template but simultaneously destroys potentially recoverable surfactant and often deteriorates or even disintegrates the structural ordering of OMS as well as decreases their hydrothermal stability. Conventional modification of the template-free OMS with organosilane is also limited by the necessity of employing the calcination and/or extraction procedures for the template removal.

Recent communications[7-10] demonstrated that the surfactant template can be displaced via ion exchange process[7,8] or via reaction with alkylchlorosilanes.[9,10] In the ion-exchange procedure either metal cations[7] were employed as carriers to deliver some specific ligands to the pore walls or a free-base porphyrin[8] was used. In both these cases a post-synthesis step is required to remove either metal cations[7] or residual surfactant[8]. However, the reaction of self-assembled silica-surfactant systems with chlorosilanes[9] or alkoxysilanes[10] allows one not only to attach the desired surface ligands but also to remove effectively the surfactant template, thus opens a new way for a clean and effective synthesis of functionalized materials.

The current work shows a general approach for preparation of mesoporous silicas of desired surface functionality by template displacement with organosilanes (TDS) containing at least one chloro (Cl-) or alkoxy (RO-) group. The main advantages of the TDS process are: (i) removal of the surfactant template, which could be recovered, (ii) elimination of the calcination and/or extraction steps, (iii) attachment of desired surface ligands, and (iv) relatively short reaction time, which depends on the type of silica-template interactions.[10,11] In addition, the current study provides valuable information about reactivity of self-assembled mesostructured systems towards organosilanes, which opens new opportunities for effective surface functionalization of these systems with simultaneous structure stabilization, thus providing OMS for specific applications in adsorption, catalysis and nanotechnology.

SYNTHESIS
The MCM-41 materials were prepared using a typical procedure [12], which included dissolution of silica in 1M sodium hydroxide solution at 70ºC followed by addition of surfactant solution (CTMAB). The obtained mixture was stirred for about one hour to obtain a homogeneous gel. Gels were treated under autogeneous pressure at 100ºC for four days by adjusting pH to about 10 followed by salt addition. The resulting samples were filtered and

washed with deionized water, and finally dried at 100ºC. A typical amount of the prepared sample was around 4 grams.

The one step procedure for preparation of mesoporous silicates with simultaneous surfactant removal was carried out via reaction of the appropriate silane with the uncalcined MCM-41 material.[9,10] In a typical procedure 4-12 ml of silane in the presence of 0-8 ml of heptane was added to about 0.25 g of "as-synthesized" silica-surfactant material and mixture was refluxed for 4-10 hours.[10] Organosilanes such as alkylchlorosilanes, alkylethoxysilanes, mercaptopropyltrimethoxysilane and aminopropyltriethoxysilane reacted with silanols and successfully displaced the surfactant contained inside of the self-assembled structure according to Scheme 1. The resulting white solids were filtered, washed and dried under vacuum for six hours at 90ºC. The kinetics of the TDS process was investigated for the MCM-41 sample modified with octyltriethoxysilane. The influence of heteroatoms (such as cerium) in MCM-41 on its reactivity towards organosilanes was studied too.

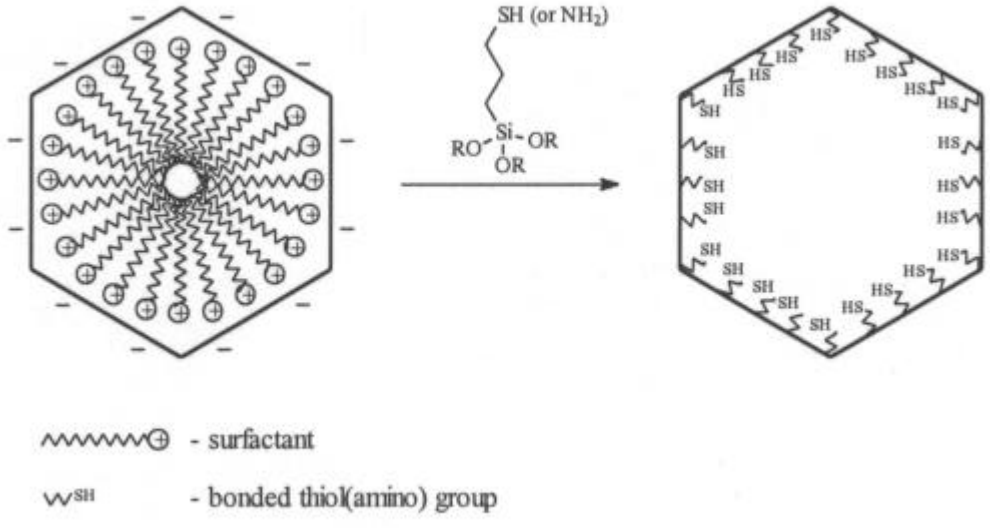

Scheme 1. Reaction pathway for preparation functionalized mesoporous materials via template displacement synthesis.

DISCUSSION

The current study shows that the self-assembled mesostructured silica-surfactant systems are stable during the template displacement synthesis (i.e., process of the simultaneous pore opening and removal of the surfactant). The TDS process consists of a direct displacement of ionic or neutral template by desired silyl group, which in fact represents the replacement of electrostatic or hydrogen bonding interactions at the organic-inorganic interface by covalent bonds. Therefore, by selecting an appropriate silane it is possible to attach almost any type of functionality to the silica surface.

"Mild" synthetic conditions preserve the structural ordering of the self-assembled mesostructured systems. A detailed study of the TDS process showed that about eight hours is required for modification of OMS synthesized under basic conditions[10] and much less time for those prepared under neutral and acidic conditions.[11] The relatively high surface area and pore volume of the samples after TDS process indicate a full accessibility of pores for various molecules. An increase in the XRD peak intensities was observed for the samples with attached aminopropyl groups, which indicates a noticeable improvement of the mesostructure ordering in comparison to that in the calcined samples. It should be noted that the TDS process could be performed with or without solvents, which gives additional options for recovery of the surfactant and makes this process attractive from the viewpoint of green chemistry.

In contrast, a typical calcination process is carried out at elevated temperatures (about 550ºC). Under these conditions the structure shrinkage occurs because the neighboring surface silanols condense with release of water and form siloxane bonds. Using the low-temperature TDS process can eliminate this "undesirable" condensation by replacing surface hydroxyls with silyl groups. Thus, the TDS process is gentler to the self-assembled mesostructured systems than high-temperature calcination because it gradually removes the source of the "future" structure collapse. Therefore, the step-by-step replacement of surfactant-silanol interactions by covalent Si-O-Si bonds results in the structure stabilization.[10]

The TDS process shows several advantages over conventional modification of calcined samples because it requires short time, makes surfactant recoverable, reduces risk of destroying nanostructure during thermal

treatment, simultaneously introduces useful functionality, and gives flexibility in attaching desirable ligands. The loading of ligands by the TDS procedure is higher than that achieved by conventional modification of calcined samples.[10]

The unique reactivity of self-assembled systems can be used to design nanostructures of tailored surface, catalytic, optical and magnetic properties. Our current research is focused on the development of novel functionalized mesoporous materials of tailored pore sizes and surface properties for advanced applications including highly efficient purification, separation and catalytic processes.

CONCLUSIONS

It is shown that the problems related to the removal of template from self-assembled silica-surfactant systems could be overcome by its displacement with functional organosilanes. This approach opens new opportunities in direction of functionalization and stabilization of self-assembled silica-surfactant systems for specific sorption and catalytic applications. The TDS process is environmentally friendly and allows for recovery and reuse of the costly surfactant template. Also, the resulting materials are of great importance for removal of various toxic substances from environment and for developing environmentally attractive catalytic processes.

ACKNOWLEDGMENTS

The donors of the Petroleum Research Fund administrated by the American Chemical Society are gratefully acknowledged for partial support of this research.

REFERENCES

1. Beck, J.S. *et. al*. *J. Am. Chem. Soc.* **1992**, *114,* 10834.
2. Huo, Q. *et. al*. *Chem. Mater.* **1994**, *6,* 1176.
3. Clark, J.H.; Macquarrie, D.J.; Wilson, K. *Stud. Surf. Sci. Catal.* **2000**, *129,* 25 1.
4. Macquarrie, D.J. *Green Chem.* **1999**, *1,* 195.
5. Feng, X. *et al*. *Science* **1997**, *276,* 923.
6. Mercier, L.; Pinnavaia, T.J. *Adv. Mater.* **1997**, *9,* 500.
7. Dal, S. *et. al*. *Adv. Mater.* **1999**, *11,* 1226.
8. Holland, B.T.; Walkup, C.; Stein, A. *J. Phys. Chem. B* **1998**, *102,* 4301.
9. Antochshuk, V.; Jaroniec, M. *Chem. Commun.* **1999**, 2373.
10. Antochshuk, V.; Jaroniec, M. *Chem. Mater.* **2000**, in press.
11. Lin, H.P. *et al*. *New J. Chem.* **2000**, *24,* 253.
12. Araujo, A.S.; Jaroniec, M. *Stud. Surf. Sci. Catal.* **2000**, *129,* 187.

4th Annual Green Chemistry &
Engineering Conference

Sustainable Technologies:
From Research to Industrial Implementation

June 27 - 29, 2000

GREENER SOLVENTS II

CO_2-SOLUBLE PHASE TRANSFER CATALYSTS FOR REACTIONS IN SUPERCRITICAL FLUIDS

Christy W. Culp, Kris N. Griffith, Charles L. Liotta and Charles A. Eckert
School of Chemical Engineering, School of Chemistry and Biochemistry, and Specialty Separations Center
Georgia Institute of Technology, Atlanta, GA 30332-0100

Phase-transfer catalysis (PTC) is a widely used technique for conducting reactions between reactants in two or more immiscible phases[1]. Such processes typically involve the use of polar organic solvents, which are often expensive and environmentally harmful. We have investigated the replacement of these solvents with supercritical fluids (SCFs) for several reactions. Supercritical fluids provide an attractive alternative not only because of the opportunity for environmentally benign processing, but also because their high solute diffusivities and low viscosities can ameliorate mass transfer limitations that are often encountered. Reactions that have been investigated include substitution[2,3], alkylation, and carboxylation reactions involving a solid salt phase and organic reactants that are dissolved in a supercritical fluid phase of either carbon dioxide or ethane.

Phase-transfer catalysts are designed such that they have the ability both to come into contact with and to react with both inorganic ionic species and organic molecules. The most common PTCs are quaternary ammonium salts, such as tetrabutylammonuim bromide, shown to the right. The catalyst is a salt, and thus it has some affinity for ionic species and can be dissolved in water. However, its long alkyl chains give it organic character as well, so that it will partition into organic solvents.

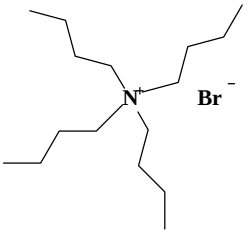

Phase-transfer catalysis follows a basic cycle that is depicted below. The reactant species are R-X and M^+Y^-, and the phase transfer catalyst is represented by Q^+X^-. The catalyst undergoes an ion-exchange reaction with the ionic reactant, picking up the reactive anion. The species Q^+Y^- then partitions into the organic phase, where the reaction with R-X takes place, both making the product R-Y and regenerating the catalyst. The catalyst then partitions back into the inorganic phase, and the cycle is completed. Note that the inorganic phase may be either an aqueous salt solution or a solid salt surface.

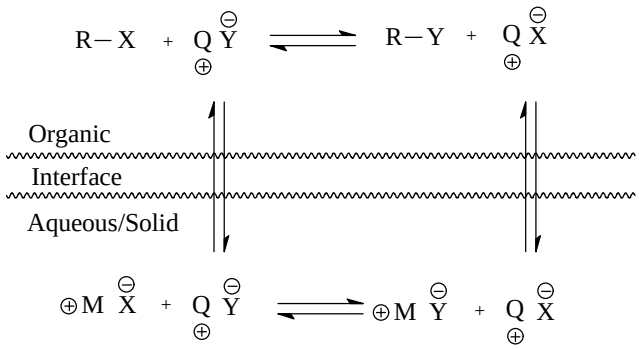

In addition to its primary purpose of shuttling reactant and product ions between phases, a phase-transfer catalyst can also act as a more traditional catalyst in that it may lower the activation energy of a chemical reaction. This is because the reacting anions are less tightly bound to the bulky catalyst cations than they are to the metal cations, allowing the reaction to take place more readily.

Because the transfer of the catalyst complex from one phase to another is integral in the PTC process, the transport properties of the solvent are important. In fact, many PTC reactions are limited by the rate of mass transfer rather than the rate of the reaction itself. Supercritical fluids provide an opportunity to alleviate these restrictions due to their low viscosities and high molecular diffusivities.

An earlier investigation of a PTC reaction in supercritical CO_2 provided insight into the nature of the reacting system. A substitution reaction was studied, that of benzyl chloride and potassium cyanide to form phenylacetonitrile[2]:

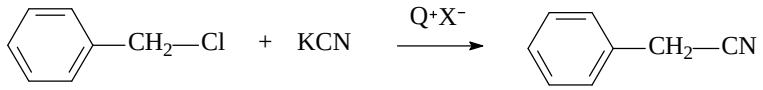

This reaction was run in carbon dioxide at 75°C and 140 bar, with tetraheptylammonium chloride as the catalyst. This reaction was found to be first-order with respect to benzyl chloride. Although the catalyst was known to be only sparingly soluble in the CO_2, the reaction rate was found to increase linearly with the amount of catalyst in the system. This evidence, as well as that found when acetone was added to the system as a cosolvent, indicates that the reaction may be taking place in a separate catalyst-rich phase on the surface of the salt particles, rather than in the supercritical fluid phase.

Because traditional phase-transfer catalysts have low solubility in CO_2, we have sought to design some that contain functional groups known to increase solubility in SCF CO_2. Two groups that are considered "CO_2-philic" are silicon-based functional groups, such as siloxanes,[4] and perfluorinated functional groups, such as perfluoroalkyl groups and perfluoroethers.[5-7]

We have thus far used perfluoroalkyl chains in our catalyst design as a means for increasing solubility in CO_2. The first catalyst we made was a pyridinium salt in which the fourth chain on the quaternized nitrogen was highly fluorinated. It is shown at left. Although we did succeed in making a quaternary pyridinium salt that was soluble in supercritical CO_2 (a mole fraction of about 2 x 10^{-3}), it did not have sufficient activity to catalyze the cyanide substitution of benzyl chloride shown before. We assume that this is due to the strong electron-withdrawing effects of the fluorines, resulting in a higher positive charge on the nitrogen such that it held the chloride so tightly that it could not be exchanged for cyanide.

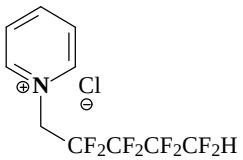

Next we looked to isolate the fluorinated chain from the reacting part of the catalyst, designing a molecule with a fluorinated ester function on one side of an aromatic ring and a quaternized amine on the other, as depicted on the right. This catalyst has been shown to catalyze the substitution reaction in CO_2 60°C and 150 bar, with reaction rates comparable to tetraheptylammonium chloride. However, its solubility in supercritical CO_2 is low, approximately 1 x 10^{-5} at 60°C and 150 bar, as measured by ultraviolet spectroscopy.

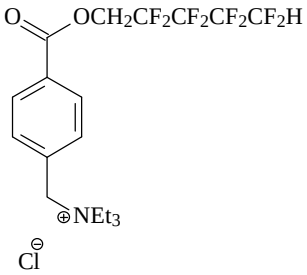

The most recent catalyst that we have synthesized and tested is very similar to the one above, but has a tail containing ten rather that four perfluoromethylene groups. Although its activity has not yet been measured, its solubility is estimated at about twice that of the previous catalyst.

In making new phase-transfer catalysts that have an affinity for supercritical carbon dioxide, we are expanding the range of processes that are available in which environmentally benign solvents and techniques can be incorporated.

References

1. Starks, C.M.; Liotta, C.L.; Halpern, M. *Phase-Transfer Catalysis*; Chapman and Hall: New York, 1994.
2. Chandler, K.; Culp, C.W.; Lamb, D.R.; Liotta, C.L.; Eckert, C.A. *Industrial and Engineering Chemistry Research* **1998**, *37*.
3. Dillow, A.K.; Yun, S.L.J.; Suleiman, D.; Boatright, D.L.; Liotta, C.L.; Eckert, C.A. *Industrial and Engineering Chemistry Research* **1996**, *35*, 1801-1806.
4. Hoefling, T.A.; Newman, D.A.; Enick, R.M.; Beckman, E.J. *Journal of Supercritical Fluids* **1993**, *6*, 165-171.
5. Hoefling, T.; Stofesky, D.; Reid, M.; Beckman, E.; Enick, R.M. *Journal of Supercritical Fluids* **1992**, *5*, 237-241.
6. Mertdogan, C.A.; Byun, H.-S.; McHugh, M.A.; Tuminello, W.H. *Macromolecules* **1996**, *29*, 6548-6555.
7. Tuminello, W.H.; Dee, G.T.; McHugh, M.A. *Macromolecules* **1995**, *28*, 1506-1510

SELF-NEUTRALIZING CATALYSIS IN NEAR-CRITICAL WATER

Heather Lesutis, Roger Gläser, Kris Griffith, Charles Liotta and Charles Eckert
Schools of Chemical Engineering and Chemistry and Specialty Separations Center
Georgia Institute of Technology, Atlanta, GA 30332-0100

The ionization constant of water at 250-300°C is about 3 orders of magnitude higher than that at room temperature, making it an effective source of both hydronium and hydroxide ions at elevated temperatures. Under these conditions water is also an excellent solvent for both ionic and organic species. Thus this near-critical water is a most advantageous solvent for a wide variety of reactions, especially those acid- and base-catalyzed reactions

which currently are run with the addition of mineral acids and bases, followed by subsequent neutralization and the need for salt disposal. For example, typical Friedel-Crafts reactions may produce 5-10 kilos of salt per kilo of product. When the dissociated near-critical water is catalytic, no neutralization or disposal is needed.

In this work we use the hydrolyses of several substituted benzoate esters and a series of substituted anisoles as probes to elucidate the activity of the two ionic species in nearcritical water. Each of these hydrolyses can run via both acid- and base-catalyzed mechanistic pathways, and the substituted anisoles can also follow an S_N2 mechanistic pathway. Analysis of Hammett plots suggests that the benzoate esters hydrolyze autocatalytically, following an acid-catalyzed mechanism, while the anisoles are hydrolyzed via the S_N2 mechanistic pathway. This work suggests that near-critical water offers significant potential, both as a benign solvent and as a self-neutralizing catalyst, for a wide variety of reactions.

ENVIRONMENTALLY BENIGN CHEMICAL PROCESSING ALTERNATIVES USING ACETIC ACID AND NEARCRITICAL WATER

James S. Brown, Charles A. Eckert*, J. Erskine Love, Institute Professor,
Charles L. Liotta, Vice Provost of Research and Dean of Graduate Studies
778 Atlantic Drive, School of Chemical Engineering, Georgia Institute of Technology, Atlanta, GA 30332-0100
e-mail: cae@che.gatech.edu
Roger Gläser
University of Stuttgart, Institute of Chemical Technology, D-70550 Stuttgart, Germany
* corresponding author

Traditional Friedel Crafts acylation reactions generally require stoichiometric quantities of $AlCl_3$ or other acid catalysts which must be neutralized to waste salts in order to recover the desired products. This results in the landfilling of several pounds of waste salt byproduct for every pound of product produced. In addition, many of these reactions are run in chlorinated organic solvents such as methylene chloride that can simultaneously dissolve the reactants as well as the reactant-catalyst complex.[1,2] In order to avoid these huge quantities of unwanted waste, polar-protic solvents at elevated temperature that simultaneously act as the solvent and catalyst can be used. Liquid water (T_c = 374ºC) in the near-critical region (250-300ºC) can act as the solvent and catalyst for certain acid-catalyzed organic reactions.[3,4] As the temperature is increased from room temperature to 275ºC, the dissociation constant of water is three orders of magnitude higher[5] making it a source of hydronium and hydroxide ions that may catalyze reactions without the need for neutralization and disposal. In addition, the dieletric constant decreases from 80 at ambient to 20 at near-critical conditions[6] making near-critical water a good solvent for both organic and ionic compounds. As the solubility of organics in water is tunable with temperature, products can be easily separated from the hot, aqueous solvent by simply cooling and decanting.

Near-critical acetic acid (T_c = 319ºC) is another polar, protic solvent that can simultaneously act as the solvent, catalyst, and reactant in some reactions. Similar to near-critical water, near-critical acetic acid readily dissolves organics, and it has a higher acid strength and dissociation constant than water. Acetic acid can also be distilled from reaction products unlike other Lewis acid catalysts, such as $AlCl_3$, that require neutralization to salts and subsequent disposal.

To demonstrate this new environmentally friendly technology, we performed some of these same reactions in aqueous and neat acetic acid at moderate temperature (250-300ºC) without producing any salt byproduct. Phenol and resorcinol were acetylated to the corresponding esters and ketones in high yield with neat acetic acid without any added acid catalyst. Avoiding these acid catalysts eliminates the high cost and environmental impact of acid neutralization and disposal.

REFERENCES

1. G.A. Olah, *Friedel-Crafts and Related Reactions,* Vol. 111, p. 1606, Interscience Publishers, New York-London-Sidney, 1964.
2. H.-J. Kabbe, A. Widdig, *Angew. Chem. Int. Ed. Engl.* 1982, **21**, 247-56.
3. K. Chandler, F. Deng, A.K. Dillow, C.L. Liotta and C.A. Eckert, *Ind. Eng. Chem. Res.,* 1997, **36**, 5175-5179.

4. B. Kuhlmann, E. Arnett and M. Siskin, *J. Org. Chem.,* 1994, **59**, 3098-3101.
5. Marshall, W.L.; Franck, E.U. *J. Phys. Chem. Ref. Data* 1981, **10**, 295 -3 04.
6. Akerlof, G.C.; Oshry, H.I. *J. Am. Chem.* Soc. 1950, **72**, 2844-2847.

AUTHOR INDEX